Modeling of Malignant Glioma and Investigations into Novel Treatments

Rutger K. Balvers

Het drukken van dit proefschrift werd mede mogelijk gemaakt door de Stichting Stop Hersentumoren, DNAtrix, ABN AMRO en het Erasmus MC Rotterdam.

Omslag: Foto van de auteur, gemaakt van een tessellatie in het Alhambra te Granada
Layout: Auteur.
Drukwerk: Ipskamp Drukkers

ISBN 978-94-6259-845-4

Modeling of Malignant Glioma and Investigations into Novel Treatments

Modelleren van het maligne glioom en onderzoek naar nieuwe behandelmethoden

Proefschrift
ter verkrijging van de graad van doctor aan de
Erasmus Universiteit Rotterdam
op gezag van de
rector magnificus

Prof.dr. H.A.P. Pols

en volgens besluit van het College voor Promoties.
De openbare verdediging zal plaatsvinden op
dinsdag 13 oktober 2015 om 09:30 uur

door

Rutger Kees Balvers

geboren te Rotterdam

Erasmus University Rotterdam

Promotiecommissie

Promotoren

Prof.dr. C.M.F. Dirven

Prof.dr. S. Leenstra

Overige leden

Prof.dr. P.A.E. Sillevis Smitt

Prof.dr. J.M. Kros

Prof.dr. P.J. van der Spek

Copromotor

Dr. M.L.M Lamfers

Table of Contents

1

Introduction and scope of the thesis

Malignant glioma comprises a spectrum of primary central nervous system tumors that are derived from glial cells. Approximately eighty percent of malignant brain tumors are diagnosed as glioma, which makes these tumors by far the most frequently occurring primary brain tumors in humans. In the Netherlands, these incidence of glioma has slightly increased over the past 2 decennia from 4.9 to 5.9 per 100.000[1]. Gliomas grow both intracranially as well as intramedullary, and are diagnosed in patients of all ages. The clinical behavior of the whole group of gliomas is heterogeneous. Many factors are associated with patient outcome such as, and not necessarily in sequence of importance, WHO-grade, tumor size, localization, patient age at presentation, clinical performance status at presentation and molecular phenotype of the tumor[2]. Although a small subgroup of patients can be cured, the majority of these tumors are incurable by current treatment regimens.

The World Health Organization classifies malignant glioma into the predominantly found glial subtype cell (e.g. astrocyte, oligodendrocytes, ependymal cells) and into four grades, which are indicative of the histological traits that are found upon pathological examination[3, 4]. Grade I gliomas are usually benign tumors that can be curatively treated by a macroscopically total resection, and if resection is not feasible due to location, usually behave indolently during radiological follow up. Grade II tumors have a propensity to occur in young adults, grow diffusely into the surrounding healthy parenchyma, and eventually will progress into higher-grade tumors. Grade III tumors, which are considered anaplastic, and as such are a step-between Grade II and IV, are tumors that demonstrate increased neovascularization upon histological examination. The separation between Grade III and IV tumors is based on two additional traits that have been demonstrated indicative of poor prognosis namely intratumoral necrosis and high mitotic index. Grade IV gliomas are termed GlioBlastoma Multiforme (GBM), a name derived from the undifferentiated and pleiomorphic histological presentation between and within individual cases of these tumors. Unfortunately, GBM are the most prevalently diagnosed gliomas of these four grades and have the worst prognosis. Newly diagnosed GBM patients are expected to live another 12-15 months (median survival) provided that a gross-total surgical resection is followed up by concomitant chemo-irradiation[5]. Actual survival numbers tend to be lower due to factors that influence the eligibility to undergo this optimal treatment, such as age and clinical condition[1]. Median survival for low-grade glioma is between 55-84 months, with a large variety between subtypes. Similar to GBM, for low-grade glioma surgery followed at some point by radiation and or chemotherapy is the currently applied standard therapy. With regard to neurosurgery for glial tumors, the objective is to obtain a tissue diagnosis and achieve a maximally safe (and gross total) resection of the tumor[6, 7]. Since glial tumors (especially low grades) are diffusely infiltrative growing tumors, the borders of the tumor are impossible to discern from non-invaded healthy brain parenchyma. The adage to do no harm to the patient is especially imperative in the treatment of glial tumors since too aggressive approaches can have devastating clinical consequences. As a result, even in a gross total resection, the margins of the resection cavity should always be considered populated by residual tumor cells that must be adjuvantly treated at some point. In aggressive tumors (GBM and some LGG) this is directly following resection if feasible, and for true low grades at the moment of the eventual recurrence of disease[8]. To predict which patients are better off treated aggressively rather than a wait and see approach, molecular markers can be utilized to predict the clinical course up to some level. At the moment of writing this thesis, the field of molecular characterization of gliomas is vibrant and the definitive conclusions based on large cohort studies are pending. It is expected, that histological examination will more and more be supplemented by testing for molecular markers that may prove indicative for clinical outcome and response to treatment.

Due to the dismal current (!) prognosis of the majority of gliomas, improved treatment modalities are warranted. To ensure these options will surface, a better appreciation of the molecular phenomena that drive glioma initiation, treatment response and recurrence is needed. Especially the last two decades, with the advent of multiple techniques to interrogate the molecular blueprint of tumors, have brought the scientific community paramount information on glioma fundamentals. However, in remembrance of one of the propositions posed in this thesis; the measure of an education is that one acquires some idea of the extent of ones own ignorance. Ergo, the increased knowledge derived from multiplatform molecular characterization studies has also lead to a dazzling amount of information that points at the complexity of this disease and the limitations of our experiments to test for potential treatments. Therefore the last two decades of scientific research on glioma, especially GBM, have delivered very little with respect to better treatment outcome for patients. Several explanations can be brought forward to account for the lack of clinical translation of the positive preclinical results provided by researchers in the recent past. For one, the complexity of the disease was until recently only to a limited extent recapitulated in preclinical models. The cure of xenografted mice does not translate into a cured patient, since the xenografted cells do not recapitulate the human condition in mice in several aspects. This holds true for the invasive growth pattern, the function of the blood brain barrier and the role of the systemic and local immune system on therapeutic outcome.

Secondly, the molecular characterization studies published to date have delivered ample evidence that the Multiforme part of the disease is probably responsible (at least in part) for the lack of recapitulation of preclinical evidence. Since malignant glioma may actually be comprised of 3-6 (dependent of which publication one chooses to follow[9-12]) different subtypes that have a distinct genetic etiology and therefore probably also a separate response profile to targeted agents. An example of this is the predictive value of 1p19q deletions and MGMT gene methylation in the context of alkylating chemotherapy efficacy, which seems to code for a specific entity of predominately oligodendroglial, IDH1 mutated tumors[3, 13]. As a result of the hindsight provided by the latter example, the stratification of clinical trials in the past may have been biased by therapeutic response in only a subgroup of patients. With the continued advancement of the aforementioned insight into disease classification, the evolution of the models to test potential drugs is even more warranted.

The aim of this thesis is to contribute a little to the body of scientific evidence that will one day bring fruition to patients in the form of better treat-

ment outcome. The scope of this thesis was designed around two major topics, which are further elaborated on in the next paragraphs.

The first pillar of the thesis is structured around the utilization of so-called glioma stem-like cells (GSCs) that can be derived from patient tumors by selective propagation techniques in vitro. The concept of GSCs is driven by the hypothesis that tumors harbor poorly differentiated initiating cells that give rise to sub-clones or subpopulations that form the bulk tumor. In line with this concept, it is postulated that these initiating cells could be the driving population behind tumor proliferation, recurrence and resistance. As a result, scientific interest grew in selectively culturing these cells for fundamental and translational studies. This lead to several publications indicating GSCs to; 1) more adequately mimic human disease in vitro and in xenografts when compared to conventionally used cell lines[14], 2) retain hallmark features of the tumor on a molecular level when compared to conventionally serum-supplemented primary cultures[14, 15].

The aim of our studies was to investigate the distribution of reported molecular alterations within and between GSCs derived from patient samples in our hospital (Chapter 2). Off specific interest was the ability to investigate inter-individual heterogeneity to adequately define response profiles for potentially interesting compounds (Chapter 3, 6 and 8). These studies would potentially result in clinical trials that stratify patients based on these response profiles.

The second pillar of the thesis is structured around the utilization of the aforementioned GSCs to improve feasibility studies for a particularly interesting alternative treatment for GBM, namely oncolytic virotherapy. Oncolytic virotherapy (OV) capitalizes on the ability of viral vectors to selectively infect and lyse malignant cells. The rationale behind this strategy was first observed in the 1950s and has become of renewed interest with the advent of gene therapy in the 1990s[16]. A thorough review of the concept for oncolytic adenovirus based OV for GBM is provided in Chapter 5. In short, OV for GBM has been demonstrated by numerous studies, both preclinical and clinical, to be an interesting alternative since viruses are programmed by nature to effectively kill cells by hijacking similar molecular machinery as cancer cells utilize for subverting apoptosis/immunological clearance. In addition, GBM only very rarely metastasize to other organs, which renders these tumors an optimal candidate for localized administration in order to circumvent systemic barriers (such as circulating antibodies, complement system and immune cells).

The studies described within this thesis are based on the GSC model and address the feasibility of combination strategies that potentially improve the oncolytic capacities of Delta24-RGD, an adenovirus based viral vector. In addition, reovirus based OV was tested in GSCs to address inter-individual heterogeneity with regard to infectivity, viral progeny production and overall oncolytic capacity. Lastly, we addressed a novel administration strategy for Delta24-RGD based on cellular vehicles (Chapter 8).

The common ground for these studies is the circumvention of (more recently) discovered hurdles (i.e. inadequate models, the need for combination strategies, lack of efficient intratumoral delivery) and potential research strategies to that may have direct impact in the form of augmented therapeutic effect when successful. Hence, the title of the thesis; ***Modeling of malignant glioma and investigations into novel treatments***

References

1. Ho, V.K., et al., Changing incidence and improved survival of gliomas. Eur J Cancer, 2014. 50(13): p. 2309-18.

2. Huse, J.T. and E.C. Holland, Targeting brain cancer: advances in the molecular pathology of malignant glioma and medulloblastoma. Nat Rev Cancer, 2010. 10(5): p. 319-31.

3. Louis, D.N., et al., International Society Of Neuropathology--Haarlem consensus guidelines for nervous system tumor classification and grading. Brain Pathol, 2014. 24(5): p. 429-35.

4. Louis, D.N., et al., The 2007 WHO classification of tumours of the central nervous system. Acta Neuropathol, 2007. 114(2): p. 97-109.

5. Stupp, R., et al., Radiotherapy plus concomitant and adjuvant temozolomide for glioblastoma. N Engl J Med, 2005. 352(10): p. 987-96.

6. Lacroix, M., et al., A multivariate analysis of 416 patients with glioblastoma multiforme: prognosis, extent of resection, and survival. J Neurosurg, 2001. 95(2): p. 190-8.

7. Marko, N.F., et al., Extent of resection of glioblastoma revisited: personalized survival modeling facilitates more accurate survival prediction and supports a maximum-safe-resection approach to surgery. J Clin Oncol, 2014. 32(8): p. 774-82.

8. Weller, M., et al., EANO guideline for the diagnosis and treatment of anaplastic gliomas and glioblastoma. Lancet Oncol, 2014. 15(9): p. e395-403.

9. Verhaak, R.G., et al., Integrated genomic analysis identifies clinically relevant subtypes of glioblastoma characterized by abnormalities in PDGFRA, IDH1, EGFR, and NF1. Cancer Cell, 2010. 17(1): p. 98-110.

10. Gravendeel, L.A., et al., Intrinsic gene expression profiles of gliomas are a better predictor of survival than histology. Cancer Res, 2009. 69(23): p. 9065-72.

11. Sturm, D., et al., Paediatric and adult glioblastoma: multiform (epi)genomic culprits emerge. Nat Rev Cancer, 2014. 14(2): p. 92-107.

12. Sturm, D., et al., Hotspot mutations in H3F3A and IDH1 define distinct epigenetic and biological subgroups of glioblastoma. Cancer Cell, 2012. 22(4): p. 425-37.

13. Erdem-Eraslan, L., et al., Intrinsic molecular subtypes of glioma are prognostic and predict benefit from adjuvant procarbazine, lomustine, and vincristine chemotherapy in combination with other prognostic factors in anaplastic oligodendroglial brain tumors: a report from EORTC study 26951. J Clin Oncol, 2013. 31(3): p. 328-36.

14. Lee, J., et al., Tumor stem cells derived from glioblastomas cultured in bFGF and EGF more closely mirror the phenotype and genotype of primary tumors than do serum-cultured cell lines. Cancer Cell, 2006. 9(5): p. 391-403.

15. Li, A., et al., Genomic changes and gene expression profiles reveal that established glioma cell lines are poorly representative of primary human gliomas. Mol Cancer Res, 2008. 6(1): p. 21-30.

16. Chiocca, E.A., Oncolytic viruses. Nat Rev Cancer, 2002. 2(12): p. 938-50.

2

Serum-free culture success of glial tumors is related to specific

Chapter was published as;

Serum-free culture success of glial tumors is related to specific molecular profiles and expression of extracellular matrix–associated gene modules. *Rutger K. Balvers, Anne Kleijn, Jenneke J. Kloezeman, Pim J. French, Andreas Kremer, Martin J. van den Bent, Clemens M. F. Dirven, Sieger Leenstra and Martine L. M. Lamfers*

Neuro Oncology (2013) 15 (12): 1684-1695. doi: 10.1093/neuonc/not116.

First published online: September 17, 2013

Abstract

Background. Recent molecular characterization studies have identified clinically relevant molecular subtypes to coexist within the same histological entities of glioma. Comparative studies between serum-supplemented and serum-free (SF) culture conditions have demonstrated that SF conditions select for glioma stem-like cells, which superiorly conserve genomic alterations. However, neither the representation of molecular subtypes within SF culture assays nor the molecular distinctions between successful and nonsuccessful attempts have been elucidated. **Methods.** A cohort of 261 glioma samples from varying histological grades was documented for SF culture success and clinical outcome. Gene expression and single nucleotide polymorphism arrays were interrogated on a panel of tumors for comparative analysis of SF+ (successful cul- tures) and SF2 (unsuccessful cultures). **Results.** SF culture outcome was correlated with tumor grade, while no relation was found between SF+ and patient overall survival. Copy number – based hierarchical clustering revealed an absolute separation between SF+ and SF2 parental tumors. All SF+ cultures are derived from tumors that are isocitrate dehydrogenase 1 (IDH1) wild type, chromosome 7 amplified, and chromosome 10q deleted. SF2 cultures derived from IDH1 mutant tumors demonstrated a fade-out of mutated cells during the first passages. SF+ tumors were enriched for The Cancer Genome Atlas Classical subtype and intrinsic glioma subtype-18. Comparative gene ontology analysis between SF+ and SF2 tumors demonstrated enrichment for modules associated with extracellular matrix composition, Hox-gene signaling, and inflammation. **Conclusion**. SF cultures are derived from a subset of parental tumors with a shared molecular background including enrichment for extracellular matrix – associated gene modules. These results provide leads to develop enhanced culture protocols for glioma samples not propagatable under current SF conditions.

Introduction

Glial tumors consist of a heterogeneous group of primary CNS neoplasms. While the clinical outcome of these tumors varies substantially between different grades (World Health Organization [WHO] grades I – IV), only grade I tumors can be treated curatively.1 In the last decade, substantial effort has been put into characterizing the pathogenic mechanisms underlying this complex group of glial cell– derived tumors. These efforts have led to the establishment of several molecular subclasses of glioma, which differentiate types of gliomas based on their intrinsic molecular distinctions and similarities, rather than the conventional characteristics used for histology-based grading.2 – 5 Indeed, gene expression – based clustering of glioma from several grades within the WHO grading system proved more predictive of survival than the histo- logical classification.4, 6 Thus far, however, this gain of insight has not led to improved clinical outcome for patients, since there are no specific treatment strategies designed to target specific subtypes of glioma as of yet. Consequently, the development of preclinical models that accurately reflect the molecular heterogeneity of glioma is imperative for both translationally relevant drug screening programs and the advancement of patient-tailored treatment options.

Commercially available cell cultures of glioma have been demonstrated to poorly mimic the molecular aberrations found in patient samples.7,8 Furthermore, the xenograft models derived from these cultures do not sufficiently recapitulate the histological hallmarks of glioma.9 With the advent of the cancer stem cell hypothesis, several groups have implemented serum-free (SF) cell culture regimens, originally developed for neural stem cell propagation, to establish glioma stem-like cell (GSC) cultures from fresh tumor tissue.10,11 By analyzing gene expression profiles of GSCs and serum supplemented (SS) cultures, a distinct separation between the aforementioned and the parental tumors was revealed by unsupervised clustering.7 Several groups have reported GSC cultures to be superior with regard to retaining the original patient gene expression signature and histological phenotype in xenografts.7,11,12 This has led to a wide variety of applications for these cell culture assays, ranging from inquiries into fundamental hypotheses13,14 to preclinical testing of novel agents.15 – 17

Several contradicting publications have since been published on the optimal cell culture methodology,18,19 mandatory molecular aberrations for successful propagation,20 – 22 and positive selection for gene expression signatures related to specific molecular subtypes in vitro.14, 23 Most of these previous publications have focused on the characterization of successfully propagated specimens of glioblastoma multiforme (GBM; WHO grade IV) from adults. Reports on the culture success of grade II and grade III gliomas are sparse.20,24 Therefore, we undertook a characterization study of a large cohort (N 1⁄4 261), which addresses the distribution of glioma from all histological entities for the outcome of GSC culture attempt. Within equal WHO grades, correlations between cell culture outcome and patient overall survival were assessed. Tumor samples of both successful and unsuccessful cultures (n 1⁄4 46 in total) were also subjected to molecular analysis, and a number of molecular traits that influence cell culture success rate were identified, as well as genes that may play a role in this process. These results emphasize the need for, and provide leads to, the development of im- proved culture protocols supporting growth of all subtypes of glioma. This is essential for implementation of this model in drug screening programs for personalized treatment strategies.

Material and Methods

Glial Stem-like Cell Cultures and Serum-supplemented Cultures From Glioma Resection Specimens

A detailed protocol for SS and SF culture establishment from primary glioma samples is included in the supplementary information (Supplementary Methods and Materials).

In short, tumor specimens were handled within 2 h postresection. Dissociated tumor cells were plated in Dulbecco's modified Eagle's medium (DMEM) – F12 with 1% penicil- lin/streptomycin, B27 (Invitrogen), human epidermal growth factor (EGF; 5 mg/mL), human basic fibroblast growth factor (FGF; 5 mg/mL) (both from Tebu-Bio), and heparin (5 mg/mL; Sigma-Aldrich). Passaging of proliferating GSC cultures was performed on growth factor reduced extracellular matrix (ECM) – coated plates (BD

Biosciences). Tumor sphere formation was tested regularly by plating passaged cell cultures from coated to noncoated flasks. SS cultures were established in parallel with GSC cultures from 25% – 50% of the total yield of cell pellet derived from the dissociation process, depending on total volume after visual inspection. For all samples, the use of patient tumor material was acquired with informed consent from patients as approved by the institutional review board of the Erasmus Medical Center, Rotterdam. Cell culture images were acquired on the Incucyte-FLR system (Essen Bioscience).

Nucleic Acid Isolation, cDNA Synthesis, and Array Hybridization From Tumor and Cell Culture Specimens

Samples were selected based on volume (for isolation of both DNA and RNA) and tissue viability (as verified by histological examination using conventional hematoxylin and eosin staining). Total RNA and genomic DNA were isolated from cell culture pellets or from fresh frozen tissue samples (DNeasy or RNeasy isolation kits [Qiagen]). DNA and RNA concentration thresholds were 25 ng/mL and 50 ng/mL, respectively. RNA quality was assessed on a Bioanalyzer (Agilent). RNA integrity numbers .6.5 were used for our experiments. Sample labeling, DNA amplification, and array hybridization for SNP6.0 arrays were performed at AROS Applied Biotechnology, according to standard array manufacturer's protocol (Affymetrix) with 100–500 ng total DNA per sample.

The whole-genome expression cDNA-mediated annealing, selection, extension, and ligation (DASL) assay, HumanHT-12 v4 beadchip (Illumina), was performed at AROS Applied Biotechnology, according to Illumina instructions with a minimum of 400 ng total RNA per sample.

Copy Number Analysis on Tumor and Cell Culture Samples

After quality control inspection, raw data files in the .CEL format were loaded into Partek Genomics Suite vv6.5 and 6.6 and annotated for sample identification. Before allele intensities and copy number ratios were calculated, batch effects of separately run cohorts were removed by algorithms distributed by the software manufacturer. Samples were normalized and log2 transformed, and subsequently copy number intensities were calculated against the SNP6.0 hapmap reference file. Histograms were plotted for detected segments for both the SF+ and the SF2/SFnp groups. Unsupervised hierarchical clustering was performed on copy number intensities on Euclidian based algorithms developed by the manufacturer.

Loss of heterozygosity for 1p19q information was attained from microsatellite analysis or copy number intensity measurements on SNP6.0 arrays. Microsatellite analysis was performed as described previously.25 Direct sequencing of isocitrate dehydrogenase 1 (IDH1) exon 4 mutations was performed as described previously.4

Gene Expression Profiling

For comparative analysis, raw probe calls were log2 trans- formed and quantile normalized before processing. Differentially expressed genes were detected through 1-way ANOVAs with the SF result as the discriminating factor. Genes with a P-value ,.05 and that were 2-fold higher or lower in the SF+ group were used for gene set enrichment studies. Gene ontology libraries used were supplied through DAVID.26 Biological function and cel- lular component libraries were checked for at least 3 genes per module and a P-value ,.05.

Statistics

Apart from molecular characterization data, all clinical data statistical analysis was performed in SPSS Statistics v19 (IBM). P-values are provided in the legends or the text. Group proportion statistics are based on univariate analysis based on Fishers exact test. Survival statistics are based on Wilcoxon log-rank pairwise comparisons.

Results

Malignant Gliomas of All Histological Grades Can Be Propagated in Serum-free Medium

To evaluate the success rate of primary glioma in SF cultures, we set up a tissue handling routine for a systematic and reproducible throughput of

Table 1. SF culture results related to histological WHO grade

Histology	SF+	SF−	SFnp	Total, %
A	1	9	10***	8
OA	1	0	4	2
OD	1	10	8	7
Grade II, *n* (%)	3	19	22	44 (17%)
AA	3	10	7	8
AOA	3	4	4	4
AOD	3	7	7	7
Grade III, *n* (%)	9	21	18	48 (18%)
GBM	54**	51	41	56
GBM-r	7	4	5	6
GBM-s	0	2	5	3
Grade IV, *n* (%)	61*	57	51	169 (65%)
Total (%)	73 (28%)	97 (37%)	91 (35%)	261

SF culture results in relation to histopathological diagnosis. Abbreviations: SF−, failed to form tumor spheres under SF conditions; SFnp, failed to proliferate for more than 5 passages under SF conditions; SF+, thrived past 5 passages under SF conditions; A, astrocytoma (WHO II); AA, anaplastic astrocytoma (WHO III); OD, oligodendroglioma (WHO II); AOD, anaplastic oligodendroglioma (WHO III); OA, oligoastrocytoma (WHO II); AOA, anaplastic oligoastrocytoma (WHO III); GBM-r, recurrence of primary GBM (WHO IV); GBM-s, GBM secondary to known grades II–III glioma. *$P < .05$ compared with SF+ grade 2 and grade 3. **$P < .05$ compared with GBM SF− and SFnp, ***$P < .05$ compared with A SF+.

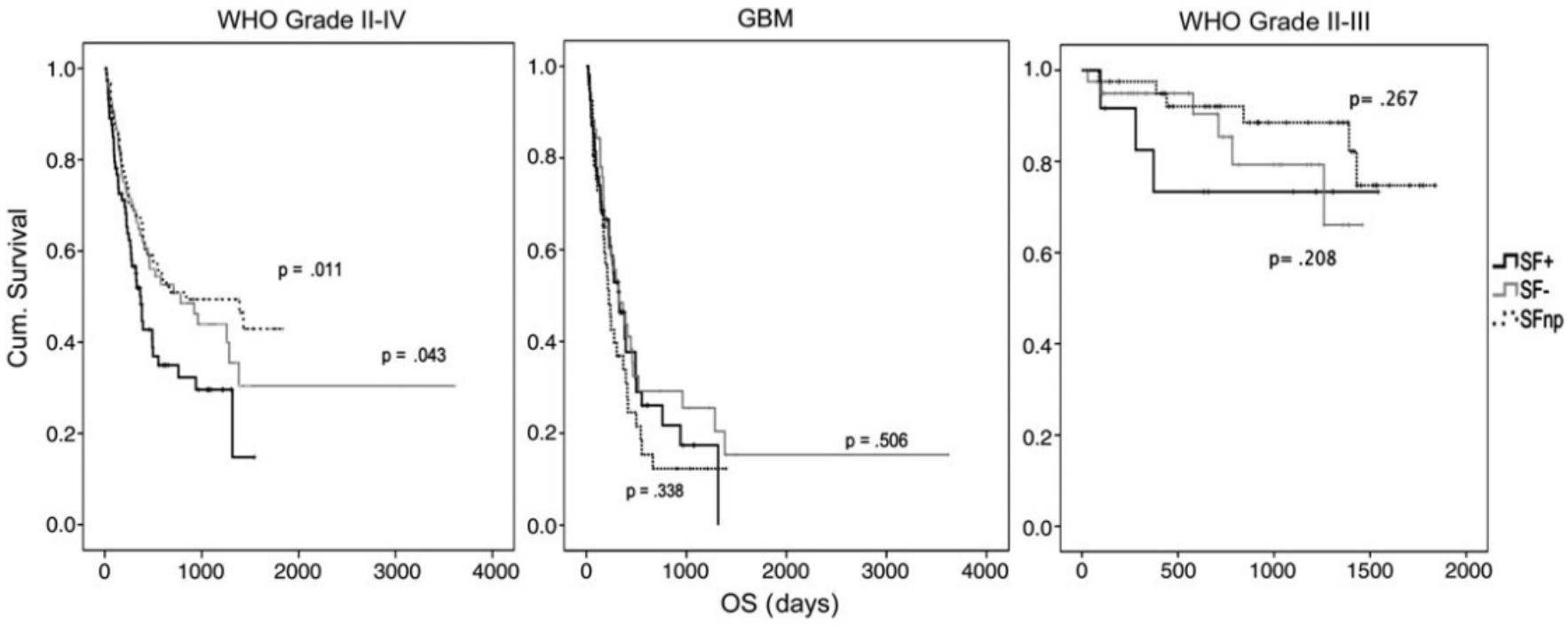

Fig. 1. SF culture outcome is not associated with worse clinical outcome in GBM. Kaplan–Meier-based overall survival (OS) curves for SF culture results for indicated histological entities of malignant glioma. SF+ (black), SF− (gray), and SFnp (dotted). Log-rank (Mantel–Cox) *P*-values are based on SF+ vs SF− or SF+ vs SFnp. Note a trend in decreased OS for SF+ grades II–III samples, while GBM samples show no difference.

primary tumor samples. After ruling out technical or contaminating sources for failure, we analyzed a panel of 261 individual specimens, covering the complete spectrum of histological grades of malignant glioma (Table 1). The ability to form tumor spheres after dissociation (n 1⁄4 165, 63%) was merely indicative for initial selection of glioma-initiating cells. SF culture outcome was not unambiguous, since a subset of cases (35%, termed SFnp) did initially yield spheres, but these would senesce or expire within 5 passages. The SF+ group (28%) represents cultures that proliferated 6 passages or more, exhibiting long-term expansion suit- able for reproducible experiments. The majority of these cultures were kept in culture past p10 (n 1⁄4 55, 75%), demonstrating the capacity of a (sub)population of these cultures to drive self-renewal. The SF2 group (37%) consisted of tumors that did not form any spheres after dissociation. These cultures failed in p0, despite transferring floating aggregates onto ECM coating.

As expected, the yield of SF+ within grades II and III glioma is substantially lower (n 1⁄4 12 of 92 attempts [13%]) compared with grade IV (n 1⁄4 61 of 169 [36%], P , .05). Grade II astrocytoma was significantly associated with SFnp (P,.05). As anticipated, for primary GBM, 37% were successfully cultured under SF conditions, which is in great contrast to secondary GBM (0/7). The proportion was even larger in recurrent GBM, where 7/16 (44%) succeeded. Taken together, SF culture media are suitable for propagation of all histological subtypes of glioma, except secondary GBM. However, in general, the probability of SF culture success increases with WHO grade.

Serum-free Culture Success Is Not Prognostic of Clinical Outcome

Other studies have suggested that sphere formation is prognostic for clinical outcome in both adult and pediatric glial tumors.24,27,28 Therefore, we compared overall survival of the 261 patients in this study with regard to SF culture outcome of patient-derived tumor tissue. Overall survival of SF+ (median 1⁄4 373 days, 95% confidence interval [CI] 1⁄4 301 – 445), SF2 (median 1⁄4 783 days, 95% CI 1⁄4 SFnp (median 1⁄4 841 days, 95% CI 1⁄4 301 – 1265), and48 – 1634) was significantly different for SF+ versus SFnp samples (Wilcoxon log-rank P 1⁄4 .011) and for SF+ versus SF2 (P 1⁄4 .043) (Fig. 1). However, comparison of these groups within the same histology demonstrated that the differences in overall survival were related mainly to tumor grade. Indeed, differences within the GBM samples were found to be nonsignificant for SF+ versus SF2 (P 1⁄4 .506) and SF+ versus SFnp (P 1⁄4 .338). Within the grades II – III tumors, a trend was observed for dismal survival in the SF+ group. At the time of writing, a significant difference was not reached, since the majority of grades II–III patients are a live to date (SF+vsSF2[P1⁄4 .208] and SF+ vs SFnp [P 1⁄4 .267]).

SF+ Cultures Recapitulate TCGA-Defined Genotypic Hallmarks of Parental Tumor Tissue

The ability to retain driver mutations in vitro is crucial for the implementation of SF cultures for drug screening assays. To address the genotypic similarity of parental tumors and the derived in vitro progeny, a panel of SF+, SF2, and SFnp tumor samples (n 1⁄4 27) was interrogated on single nucleotide polymorphism (SNP) whole-genome arrays. Samples were selected for being representative of SF culture outcome with regard to proliferation, morphology, and pattern of extinction in vitro. Frequently occurring copy number alterations (CNAs), as previously reported in The Cancer Genome Atlas (TCGA),29 were ob- served in both SF+ and SF2/SFnp parental tumors. Specifically, we found focal amplifications on segments containing EGF receptor (EGFR), cyclin-dependent kinase CDK)4, and murine double minute (MDM) 2, but not in platelet derived growth factor receptor–a (Supplementary data, Table S1). For 10 individual cases, we added early (before p4) and late passages (past p4, before

p12) to evaluate genotypic stability in vitro under SF conditions (Supplementary data, Fig. S1). Copy number intensity analysis revealed that both early and late passages of SF+ cultures retain hallmark somatic CNAs.

Serum Cultures of SFnp Tumors, but Not SF- Tumors, Retain Parental Copy Number Alterations for a Number of Passages

Since a considerable number of SFnp/SF2 samples do proliferate under SS conditions, we investigated whether this platform could serve as an alternative culture model for this specific subgroup of tumors. It has been reported that serum cultures tend to drift from the original genotypic profile by either the emergence of de novo mutations or the total loss of cancer cells due to overgrowth by non-neoplastic cells.12 Indeed, for all SF2 (n 1⁄4 5) samples cultured under serum conditions, we noticed a loss of parental CNAs (Fig. 2), coinciding with morphological changes of the tumor cells from a heterogeneous and polarized phenotype to a more fibroblastic phenotype. On the contrary, parallel-established early passages of both SF and serum cultures derived from SFnp tumors (n 1⁄4 4) were found to harbor mutations analogous to the parental tumor (Fig. 2). We therefore conclude that SS culture does not offer an alternative for culture of SF2 tumors; however, it may support low passage drug screening experiments on SFnp samples, since these samples retain (at least for a limited number of passages) their genomic profile. In addition, there is an apparent molecular distinction between SF2 and SFnp tumors with regard to the ability to proliferate as SS cultures.

Molecular Characterization Based on Copy Number Alterations Identifies an Absolute Separation Between SF+ and SF2/SFnp Tumors

The distinction between SF+ versus SFnp/SF2 tumors with regard to CNA conservation in vitro led us to hypothesize that a specific molecular mechanism dictates SF culture outcome. We therefore investigated differences in CNAs occurring between the 3 SF outcome groups, by copy number intensity–based unsupervised hierarchical genome clustering on patient tissue (n 1⁄4 27). Strikingly, SF+ separated completely from SF2 and SFnp tumors on the cluster dendrogram (Fig. 3). Furthermore, SF2 and SFnp intermixed within the cluster dendrogram, illustrating less genomic variation between these groups individually than between the combined SF2/SFnp group and SF+ samples. Moreover, a principal component analysis of SNP allele intensities between SF+ and SF2/SFnp samples revealed a similar clear separation between the 2 groups (Supplementary data, Fig. S2).

Detailed analysis showed that all SF+ tumors (n 1⁄4 11) demonstrated gains of chromosome 7 (7p+) and loss of heterozygosity of chromosome 10q or the entire chromo- some 10 (SF2 P 1⁄4 .0009 and SFnp P 1⁄4 .0027) (Fig. 3, Table 2). These 2 arms harbor the EGFR (chr.7p11.2) and phosphatase and tensin homolog (PTEN) (chr.10q23.31) loci, respectively, which were both found to be significantly discriminating between SF+ and SF2/ SFnp cohorts (P , .001 in an ANOVA based on SNP allele intensity). However, Fishers exact tests based on EGFR amplification status demonstrated no significant difference between SF+ and SF2/ SFnp cohorts. Although CNAs on CDKN2A/B were more frequently found in SF+ tumors, there was no significant difference between SF+ and SF2 or SFnp. Other differentially affected segments were found on chr1p, 12q, and 15q, which do not harbor focal somatic mutations, as reported by TCGA, but may carry drivers of SF culture results because these segments are frequently affected in both low-grade and high-grade glioma.30

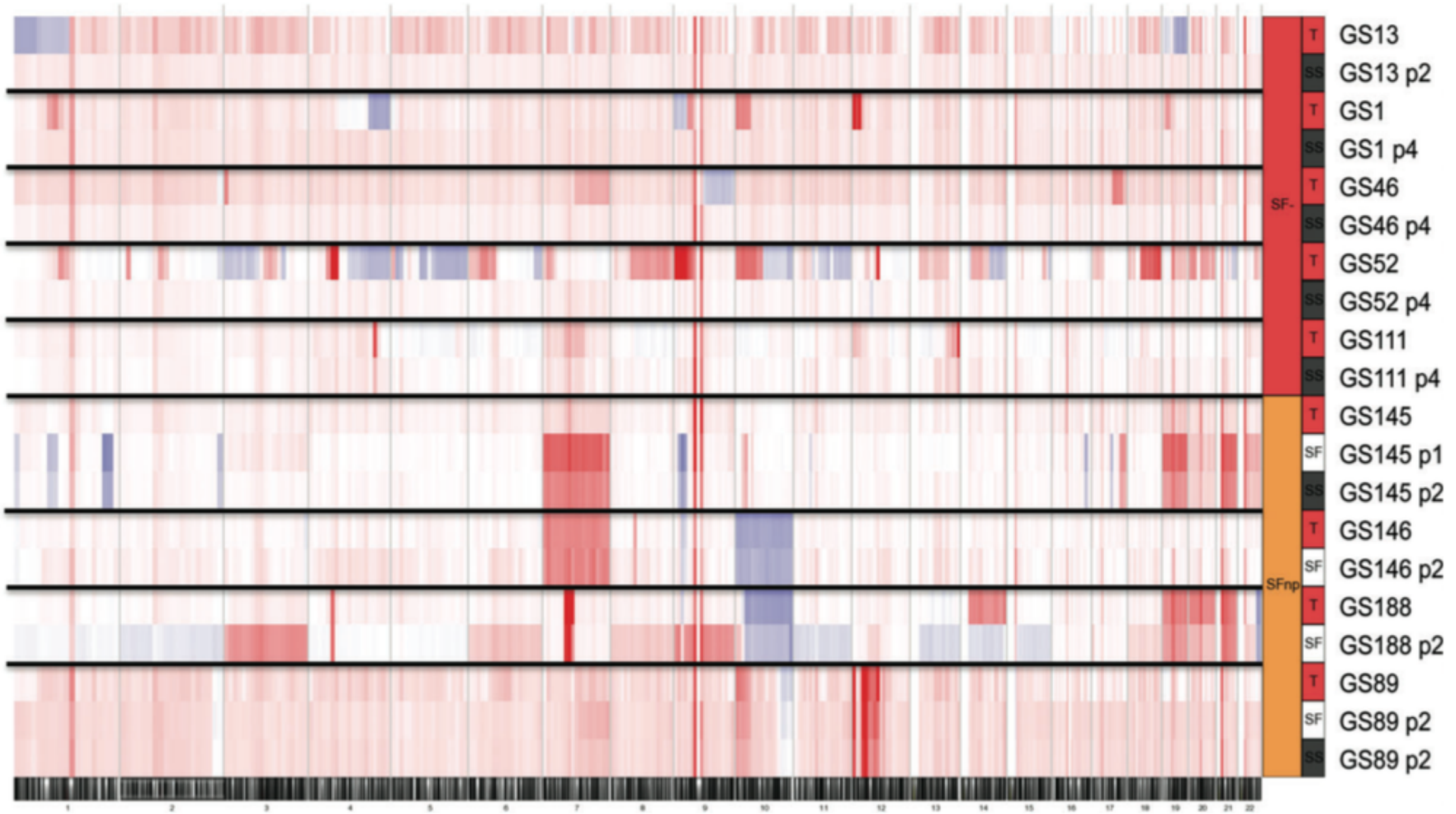

Fig. 2. Low passage cultures from SFnp tumors retain CNAs as found in parental tumors, while SS cultures from SF− tumors are overgrown by nonneoplastic cells. Heat map plots of copy number analysis results demonstrated loss of aberrations in SS cultures derived from SF− tumors. Each band is composed of the genomic data of 1 sample, as indicated in the legend on the right. Color-coding indicates blue for losses, red for gains, and white for nonaffected. Numbers below indicate chromosome number.

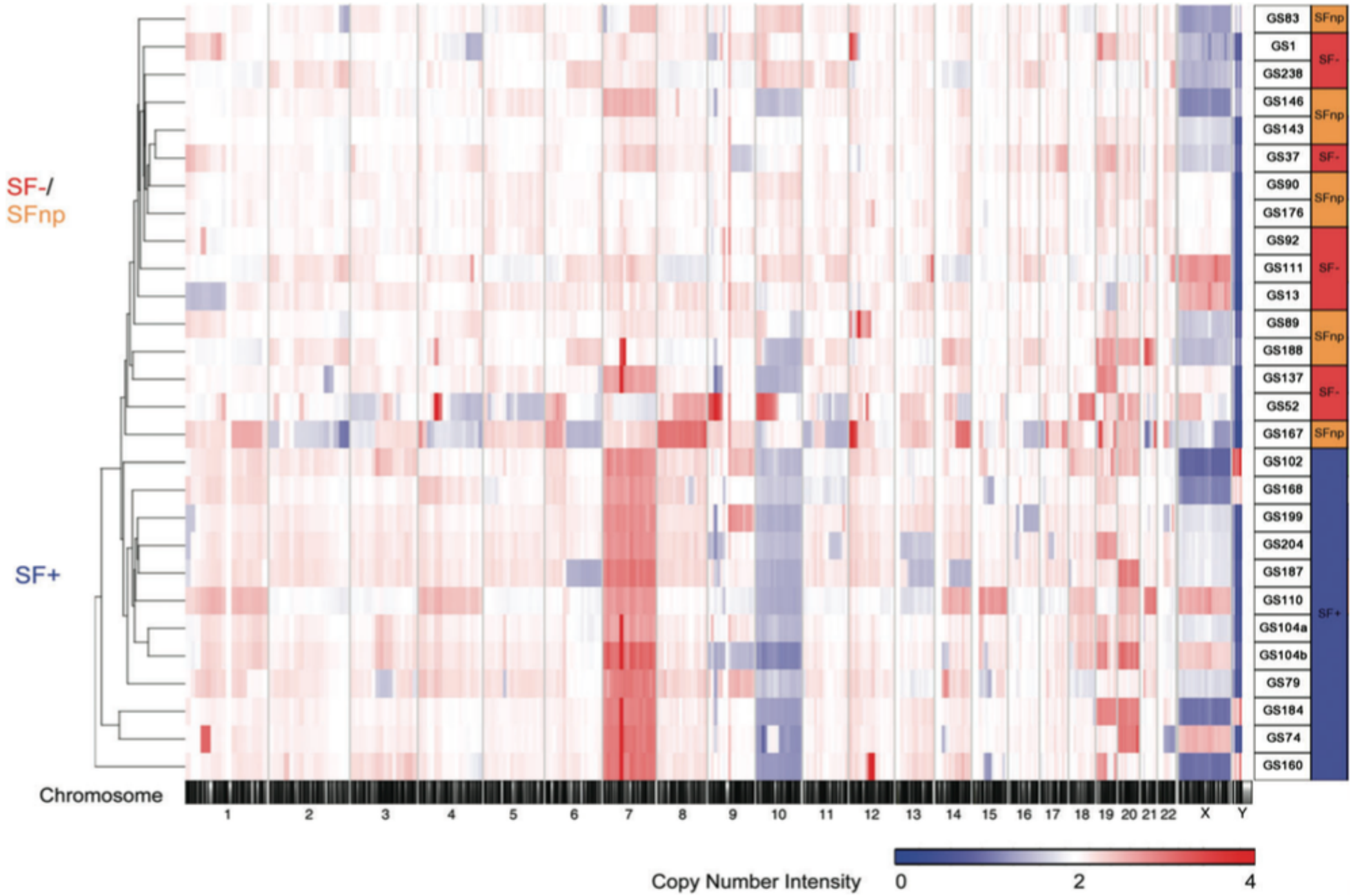

Fig. 3. Genomic analysis of parental tumors reveals complete separation of SF+ and SF− /SFnp samples. Copy number intensity–based unsupervised hierarchical clustering of SF+ and SF− /SFnp tumors. Heat map intensities are coded between copy number intensity varying 0–4n. Note the similarity between SF− /SFnp samples as indicated by the integration of the samples within the same cluster dendrogram tree.

Gene Expression Profiling of SF+ Tumors Reveals Enrichment for the TCGA Classical and Intrinsic Glioma–18 Subtypes

Gene expression–based molecular subtyping has been reported to correlate with specific CNA profiles in GBM and to have prognostic and predictive value.4,5,31 We therefore assessed whether the spectrum of reported subtypes was represented within the SF+ tumors. Gene signatures from 2 previously published molecular classifiers based on WHO grade IV glial tumors (referred to as the TCGA classifier)5 and WHO grades I – IV glial tumors (here referred to as the intrinsic glioma subtype [IGS] classifier4) were determined in parental tissue. We expanded the previously described cohort of samples used for SNP profiling with a selection of SF+, SF2, and SFnp samples (n 1⁄4 41) (Supplementary data, Table S2). All TCGA subtypes were represented in the SF+ group, although a significant enrichment for the Classical (CLA) subtype was revealed (64% vs 27% incidence in the TCGA dataset). The SF2/ SFnp cohort was enriched for PRO tumors, while the only SF+ PRO samples were histologically grade II-III samples (Fig. 4A and Supplementary data, Table S2).

As our cohort contains tumors from all WHO grades, we also evaluated the distribution of the IGS classifier set within our SF+ cohort. This classifier has been reported to be prognostic of clinical outcome in gliomas of all WHO grades. Considerable overlap was demonstrated between IGS and TCGA subtypes,4 which is recapitulated within our cohort (Table 2). For instance, IGS-18 was found to be overrepresented in the SF+ group (58%) compared with the original IGS dataset (22.5%), which is con- gruent with the fact that this subtype resembles the TCGA CLA subtype. Additionally, the TCGA PRO subtype is associated with 2 separate IGSs, which were coined IGS-9 and IGS-17. Despite the fact that both subtypes are enriched for IDH1 mutated and cytosine–phosphate–guanine island methylator phenotype (CIMP) tumors, median survival between the 2 subtypes differed almost 2-fold (6.06 y in IGS-9 vs 3.3 y in IGS-17). Interestingly, IGS-9 tumors were not represented in our SF+ cohort, whereas IGS-17 samples were (n 1⁄4 3), and both of these IGSs were overrepresented in our SF2/SFnp cohort (Fig. 4A, Supplementary data, Table S2).

Culture Success Is Not Solely Dependent on EGFR Copy Number or Expression Level

With the demonstrated enrichment for molecular sub- types enriched for EGFR gains and amplifications (TCGA CLA-mesenchymal-neuronal and IGS-18-23- 16) in culture medium supplemented with a surfeit of ligand (EGF), we hypothesized that one of the driving mechanisms might originate from the dependency that EGFR-expressing cells have under EGF supplemented medium. However, when EGF was omitted from the medium of established SF+ cultures, no effect on proliferation or viability was found in 9 out of 12 SF+ cultures (Supplementary data, Fig. S3A-B). From these 12 cultures, 2 samples (GS184 and GS184rec), with known EGFR mutation in tissue, even demonstrated enhanced proliferation on fibroblast growth factor – only medium, which could be in line with an

Table 2. SF+ samples are positively corrected with CNA 7p10q, CLA and IGS-18 subtype and IDH1-WT tumors

	Group			
	SF− *n* = 12	**SFnp *n* = 15**	**SF+ *n* = 19**	***P***
TCGA				
ND	1	2	2	
CLA	2	3	11	.0086
MES	2	2	2	
NEU	1	2	2	
PRO	6	6	2	.0183
IGS				
ND	1	2	2	
16	0	0	1	
17	3	6	3	.296
18	3	1	10	.0078
22	1	0	0	
23	1	3	3	
9	3	3	0	.032
IDH				
MUT	7	6	0	.00021
WT	5	9	19	
1p19q loss				
ND	4	2	8	
Loss	4	3	0	.066
NC	4	10	11	
Chr7p10q				
ND	6	10	8	
Normal	5	4	0	
Present	1	1	11	.00022
EGFR				
ND	6	10	8	
$n < 4$	5	3	7	
$n > 4$	1	2	4	
CDKN2A/B				
ND	6	10	8	
NC	3	3	2	
$n < 2$	3	2	9	.18

Table illustrates an overview of the distribution of previously identified driver alterations and subtypes associated with glioma. Significance levels are derived from Fishers exact test–based comparison between SF+ vs SF−/SFnp combined cohort. Abbreviations (for group names similar to Table 1): ND, not determined; NC, no change; MES, mesenchymal; NEU, neuronal; PRO, proneural; CLA, classical. 1p19q signifies the combined loss of chromosome 1p and 19q. Chr7p10q, the combined gain of 7p and loss of 10q.

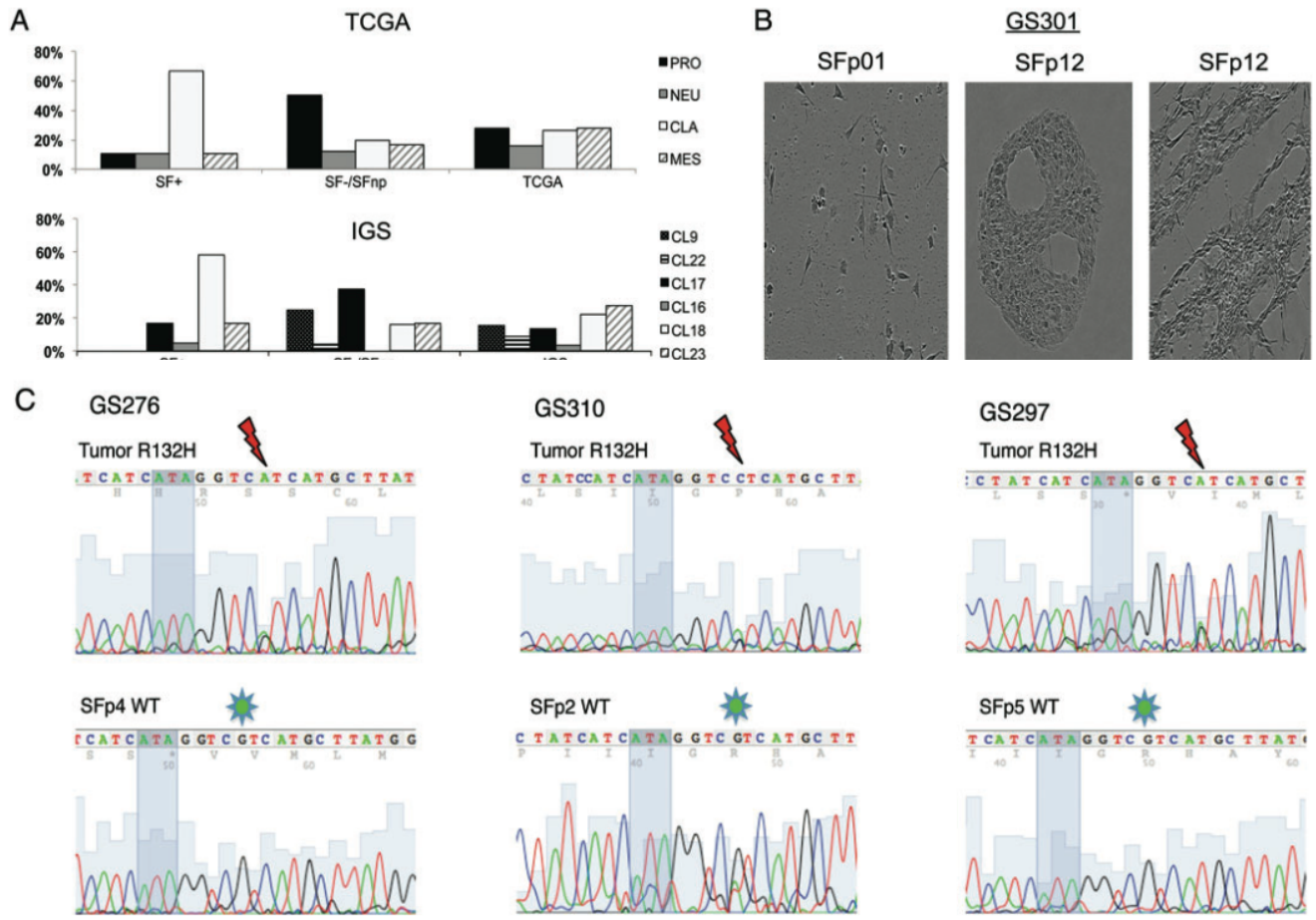

Fig. 4. Gene expression profiling and IDH1 sequencing data demonstrates SF culture selects for TCGA CLA/IGS-18 and IDH1 wild-type tumors. (A) Distribution of SF+ and SF− samples across the previously published TCGA and IGS classifiers. Samples were assigned according to the centroids as published in the original reports, on the right. Proneural samples are spread between IGS-9, -17, and -22. Noteworthy is the lack of IGS-9 and -22 in the SF+ group, as well as the overrepresentation of IGS-18/CLA samples in the SF+ population compared with the incidences reported in the original publications. (B) Sequencing illustrations of IDH1 codons 130 (ATA in shadow) through 134. Thundermarks indicate G to A or C mutation in codon R132, indicative of R132H. Note the loss of this mutation in GS276 and GS297 SF passages. In GS310 SFp2 the sequence reveals a minor A peak, demonstrating an ambiguous mutation pattern, indicative of mixed populations of mutated tumor cells and (nonneoplastic) IDH-WT cells. (C) Microscopic images of GS301 SS/SF cultures demonstrate loss of neoplastic cells. SF culture retains original morphology as found in p0 for a longer duration than SS; however, eventually (p12) proliferation of nonneoplastic stromal cells is abundant with typical accumulation of bands and halos suggestive for fibroblasts.

inhibitory effect of EGF on EGFR amplified GSCs as described by others.32

Together with the lack of a significant difference between the occurrence of EGFR amplifications (Table 2 and Supplementary data, Table S1) between the SF+ and SF2/SFnp cohorts, we conclude that the EGFR copy number is unlikely to dictate SF culture outcome.

Current Culture Protocols Select Against Propagation of IDH1-mutant Cells

Since grades II and III samples, and specifically IGS-9/ PRO tumors, were found to be less prone to SF culture propagation, we looked into other characteristics of these subtypes in relation to SF success. As both IGS-9/ 17 and PRO subtypes are enriched for tumors that harbor IDH1/2 mutations (IDH-MUT),25,33 we investigated the IDH1 status of tumors and cultures.

None of the SF+ tumors we investigated (n 1⁄4 19) were IDH-MUT, while 12 of 24 SF2/SFnp tumors were mutated (Supplementary data, Table S5). IDH1 mutation status was also assessed in early passages of SFnp as well as SS cultures from SF2 tumors and revealed a gradual decrease or instant loss of the IDH-MUT sequencing peak, invariably resulting in cultures that contained solely IDH1 wild-type (IDH-WT) cells (Fig. 4B and C, Supplementary data, Table S5). SNP array – based karyograms and 1p19q loss of heterozygosity analysis of these cultures also revealed a loss of CNAs present in parental tumor (exemplified in Supplementary data, Fig. S4). We therefore conclude that current SF and SS culture protocols select against and do not sustain long-term proliferation of IDH-MUT cells.

Comparative Gene Expression Analysis of SF+ Versus SF2 Tumors Identifies Enrichment for Extracellular Matrix–Associated Gene Modules in SF+ Tumors

Identification of genes or pathways that dictate SF culture outcome may perhaps provide leads to defining culture conditions for the SF2/SFnp tumors. We therefore analyzed DASL probe intensities of parental tumors from a cohort of 17 SF+ tumors and 24 SF2/ SFnp tumors and performed an ANOVA-based statistical analysis for SF culture outcome. As a result, 999 genes were identified that differentiated between SF+ and SF2/SFnp on a 2-fold expression level (P , .05). Gene Ontology (GO) analysis revealed that Hox genes, cell cycling and division, inflammatory, chemotaxis, and migration clusters are upregulated, whereas neuronal development and adhesion clusters are downregulated in SF+ tumors (Supplementary data, Table S3– 4). Kyoto Encyclopedia of Genes and Genomes (KEGG) pathway analysis demonstrated SF+ tumors to be upregulated for cytokine-cytokine interaction, ECM and focal adhesion pathways, nucleotide-binding oligomerization domain – like receptor, and Janus kinase/signal transducers and activators of transcription signaling, among others. Downregulated modules in SF+ tumors compared with SF2 tumors are neuroactive ligand receptor interaction genes, calcium signaling and a “cancer specific” module containing genes such as PI3KR1, RET, BCL2, BMP2, CTNNA3, and CDKN2B (Table 3). Altogether these results suggest that SF+ tumors share molecular features oriented around ECM interaction, which may drive SF outcome.

Discussion

Serum-free cultures of patient-derived GSCs have become a preferred platform for in vitro drug screening studies. The validity of this approach depends, however, on the representation of the whole spectrum of glioma subtypes within the SF culture assay. In order to address this issue, we examined the distribution of glioma subtypes within SF cultures based on histology and expression profiles, as well as on the presence of hallmark molecular characteristics described for grades II – IV glioma. To our knowledge, the presented series of 261 low- and high-grade gliomas is unique in its variation in histological diagnoses and cohort size.

Retrospective analysis of SF culture outcome within this cohort leads us to conclude that tumor sphere formation by itself is not a valid parameter to designate a culture as successful (SF+). The relatively high incidence of tumor spheres that cease to proliferate within a few pas- sages (as reported by others before18) advocates for the introduction of a threshold differentiating between SF+ and samples that do not render practically useful cultures. One argument for the separation of SF+ and SF2/SFnp samples was provided by our genomic analysis, which demonstrated a separation of SFnp/SF2 collectively from the SF+ samples. In addition, the enrichment of molecular subtypes between SF2/SFnp and SF+ samples suggests that these groups have distinct molecular backgrounds that drive SF culture outcome.

Within our investigated cohort, SF culture outcome was directly correlated with WHO tumor grade. Others have reported a correlation between the ability of patient- derived glioma cultures to form tumor spheres on SF culture medium and dismal clinical outcome.24,27,28 In accordance with these authors, we find the incidence of SF+ to increase

Table 3. SF+ tumors with increased expression of genes implicating ECM signaling

Term	Count	Genes
SF+ downregulated pathways		
hsa04080: Neuroactive ligand-receptor interaction	22	*GABRD, GABRG2, PARD3, GABRA1, GABRB3, GRIK2, GRIN1, PTH1R, GRIK4, HTR4, GRIA4, VIPR2, GRM4, GRM3, SSTR2, HRH3, GRIN2C, SSTR1, CHRM1, PRSS3, ADRA1A, GRID1*
hsa04020: Calcium signaling pathway	13	*SLC8A3, SLC8A2, ERBB3, GRIN1, HTR4, PRKCB, GNAL, ATP2B3, GRIN2C, CHRM1, RYR1, ADRA1A, CACNA1A*
hsa05200: Pathways in cancer	15	*FGF8, BMP2, RET, HSP90AA1, BCR, FGF12, ZBTB16, CTNNA3, PRKCB, WNT7B, CDKN2B, NTRK1, BCL2, PTCH1, PIK3R1*
hsa05412: Arrhythmogenic right ventricular cardiomyopathy	6	*CACNG6, SGCD, CACNG3, CACNG2, SGCA, CTNNA3*
hsa04144: Endocytosis	10	*SH3GL3, RET, RAB11FIP2, PARD3, CLTA, CLTB, ERBB3, NTRK1, AGAP2, EPN2*
hsa05410: Hypertrophic cardiomyopathy	6	*MYL3, CACNG6, SGCD, CACNG3, CACNG2, SGCA*
hsa05414: Dilated cardiomyopathy	6	*MYL3, CACNG6, SGCD, CACNG3, CACNG2, SGCA*
SF+ upregulated pathways		
hsa04060: Cytokine-cytokine receptor interaction	18	*CSF3, CCL2, TNFRSF12A, IL7, IL21R, MET, CXCL2, CCL8, CD70, IL15, CCL27, TNFRSF11A, IL12RB1, CXCL14, CCL20, IL1RAP, VEGFA, IL1B*
hsa04512: ECM-receptor interaction	7	*IBSP, COL6A3, ITGA11, LAMC1, COL5A1, HMMR, FN1*
hsa04621: NOD-like receptor signaling pathway	6	*CCL2, CXCL2, CCL8, IL1B, TNFAIP3, BIRC3*
hsa00360: Phenylalanine metabolism	4	*ALDH1A3, ALDH3B1, ALDH3A1, HPD*
hsa00350: Tyrosine metabolism	5	*ALDH1A3, METTL2B, ALDH3B1, ALDH3A1, HPD*
hsa00340: Histidine metabolism	4	*ALDH1A3, METTL2B, ALDH3B1, ALDH3A1*
hsa04510: Focal adhesion	10	*IBSP, RAC2, MET, VEGFA, COL6A3, ITGA11, LAMC1, BIRC3, COL5A1, FN1*
hsa04630: JAK-STAT signaling pathway	8	*CSF3, SPRY1, IL12RB1, IL7, SOCS1, IL21R, IL15, IL13RA2*
hsa04114: Oocyte meiosis	6	*INS, PLK1, SGOL1, CAMK2D, CDC20, AURKA*
hsa04950: Maturity onset diabetes of the young	3	*BHLHA15, INS, HNF4G*
hsa04612: Antigen processing and presentation	5	*CIITA, PDIA3, HSPA7, KIR2DL1, HLA-C*

Abbreviations: NOD, nucleotide-binding oligomerization domain; JAK-STAT, Janus kinase/signal transducers and activators of transcription.
Overview of pathways differentially expressed between SF+ and SF−/SFnp tumors. KEGG pathway analysis on ANOVA-derived gene lists comparing SF+ with SF−/SFnp tumors were uploaded and mapped according to the KEGG annotation tool in DAVID. Significant pathways and associated genes are depicted by official gene symbol.

with WHO grade and we see a significant decrease in overall survival for the SF+ group. However, within tumors of equal grade, we found no significant reduction in overall survival for SF+ compared with SF2 or SFnp. Therefore, we have not been able to confirm the results of earlier publications in our large cohort. As for the grades II–III SF+ tumors, the observed tendency for dismal outcome may suggest a reflection of shared molecular features as found in SF+ GBM, resulting in a propensity to proliferate under these selective in vitro conditions.

The driving CNAs found in parental tumors are conserved in vitro under multiple passages on SF conditions, which has been demonstrated before.12,15 For SF2 samples, we demonstrated that SS parallel cultures are rapidly overgrown with nonneoplastic cells, indicating that short-term serum cultures do not offer an alternative for in vitro propagation of these tumors. On the contrary, the apparent conservation of CNAs in low passages of SFnp cultures suggests that SS medium may serve as a suit- able alternative for low-passage, high-throughput screening in selected cases; however, this warrants further study.

To date, 3 publications have reported propagation of IDH1-MUT patient-derived glioma cells under SF conditions.34 – 36 Of these, 2 groups of researchers published data suggestive of the loss of proliferative capacity in IDH-MUT cells during long-term in vitro propagation, which could be circumvented by serial passaging in xenografts.34,35 Recently, Rohle et al36 reported an anaplastic oligodendroglioma SF culture that sufficiently propagated to perform viability assays for drug screening, although data with regard to the longevity and passage numbers of this culture in vitro were not provided. Taking this into account, we conclude that IDH-MUT cell cultures are selected against, under the current SF and SS culture protocols applied within this study, for the derivation of reproducible and long-term expanding in vitro models.

Identifying biological drivers of SF culture may provide leads to adjustments in culture protocols that increase SF culture yield. By interrogating genomic and expression- based differences between samples of SF+ and SF2/ SFnp groups, we identified a distinct molecular profile associated with SF propagation. Genomic profiling demonstrated the characteristic combination of chr7p gain and chr10q loss in all SF+ tumors. Loss of functional phosphatase and tensin homolog, which resides on chr10q, has been reported mandatory for successful SF cultures by Chen and colleagues14; however, these authors did not in- vestigate the coincidence of chr7p gains. Gene expression profiling of parental tumors demonstrated that the SF+ population was significantly enriched for TCGA CLA subtype tumors and decreased for the PRO subtype. In accordance with these data, the 7p10q CNA combination has been demonstrated to be associated with the TCGA CLA subtype by Verhaak et al.5 Interestingly, Schulte et al23 reported superior conservation of PRO-related gene expression in GSC's compared with adherent SF or SS cultures. This phenomenon may be attributed to the neurosphere culture medium composition, which was initially developed to facilitate propagation of nonneoplastic neural stem cells and suggests that transcriptomal changes occur in vitro. In addition, we have found a molecular IGS (IGS-9) that is exclusively incompatible with in vitro propagation. This subtype is correlated with 1p19q codeletion, CIMP, and IDH1-MUT tumors.

Our gene expression–based ontology analysis revealed several discriminatory pathways for SF+ tumors (Table 3). Given the enrichment for genes that modulate the ECM (such as inflammation, neovascularization, etc), we hypothesize that the driving substrates of SF culture outcome are related to these modules. Further support for this assumption is provided by the differential expression of several tumor-associated ECM molecules and cell adhesion genes between SF+ and SF2/SFnp. The interplay between ECM and cancer stem cells has been demonstrated to play a crucial role in the switch between cell survival and programmed cell death,37,38 suggesting a possible link in the ability to proliferate as (floating) spheres. We speculate that this signature renders the GSCs in these tumors less susceptible to the activation of programmed cell death in the absence of components of the ECM that are mandatory for survival. In addition, the leading GO-module upregulated in SF+ tumors was highly enriched for Hox genes, which have recently been implicated in SF+ culture proliferation and maintenance.39 Future research into these differentially expressed gene modules is expected to provide insight into the underlying mechanisms involved in GSC survival under SF conditions.

In sum, we conclude that SF culture medium selects for a subgroup of grades II – IV gliomas that share a CNA trait consisting of chr7p10q alterations as well as gene expression modules that dictate the interaction between GSCs and the ECM. Follow-up studies are under way to validate genes identified in this study. These may ultimately provide leads to improve the yield and subtype distribution of glial tumors in SF culture assays. A next aim is the development of improved culture protocols based on a better understanding of the requirements of these tumors and may include alternative (combinations of) growth factors and ECM substrates, which better recapitulate the intratumoral environment. With regard to the testing of novel drugs and inquiries into canonical pathways driving glial tumors, we suggest that caution is warranted with conclusions drawn from SF culture models, as current protocols support only the cultures of glioma of the described subtypes.

Funding

Part of this work was funded by Foundation STOPBraintumors.org, Netherlands.

Acknowledgment

We thank Dr W.N.M. Dinjens from the Erasmus MC Department of Pathology for 1p19q LOH analysis.

References

1. Huse JT, Holland EC. Targeting brain cancer: advances in the molecular pathology of malignant glioma and medulloblastoma. Nat Rev Cancer. 2010;10(5):319 – 331.

2. Liang Y, Diehn M, Watson N, et al. Gene expression profiling reveals molecularly and clinically distinct subtypes of glioblastoma multiforme. Proc Natl Acad Sci U S A. 2005;102(16):5814 – 5819.

3. Phillips HS, Kharbanda S, Chen R, et al. Molecular subclasses of high- grade glioma predict prognosis, delineate a pattern of disease progression, and resemble stages in neurogenesis. Cancer Cell. 2006;9(3):157 – 173.

4. Gravendeel LA, Kouwenhoven MC, Gevaert O, et al. Intrinsic gene expres- sion profiles of gliomas are a better predictor of survival than histology. Cancer Res. 2009;69(23):9065 – 9072.

5. Verhaak RG, Hoadley KA, Purdom E, et al. Integrated genomic analysis identifies clinically relevant subtypes of glioblastoma characterized by abnormalities in PDGFRA, IDH1, EGFR, and NF1. Cancer Cell. 2010; 17(1):98 – 110.

6. Nutt CL, Mani DR, Betensky RA, et al. Gene expression-based classifica- tion of malignant gliomas correlates better with survival than histological classification. Cancer Res. 2003;63(7):1602 – 1607.

7. Lee J, Kotliarova S, Kotliarov Y, et al. Tumor stem cells derived from glio- blastomas cultured in bFGF and EGF more closely mirror the phenotype and genotype of primary tumors than do serum-cultured cell lines. Cancer Cell. 2006;9(5):391 – 403.

8. Li A, Walling J, Kotliarov Y, et al. Genomic changes and gene expression profiles reveal that established glioma cell lines are poorly representative of primary human gliomas. Mol Cancer Res. 2008;6(1):21 – 30.

9. Huszthy PC, Daphu I, Niclou SP, et al. In vivo models of primary brain tumors: pitfalls and perspectives. Neuro Oncol. 2012.

10. Singh SK, Clarke ID, Terasaki M, et al. Identification of a cancer stem cell in human brain tumors. Cancer Res. 2003;63(18):5821–5828.

11. Galli R, Binda E, Orfanelli U, et al. Isolation and characterization of tumor- igenic, stem-like neural precursors from human glioblastoma. Cancer Res. 2004;64(19):7011 – 7021.

12. Ernst A, Hofmann S, Ahmadi R, et al. Genomic and expression profiling of glioblastoma stem cell-like spheroid cultures identifies novel tumor- relevant genes associated with survival. Clin Cancer Res. 2009;15(21): 6541 – 6550.

13. Ikushima H, Todo T, Ino Y, Takahashi M, Miyazawa K, Miyazono K. Autocrine TGF-beta signaling maintains tumorigenicity of glioma- initiating cells through Sry-related HMG-box factors. Cell Stem Cell. 2009;5(5):504 – 514.

14. Chen R, Nishimura MC, Bumbaca SM, et al. A hierarchy of self-renewing tumor-initiating cell types in glioblastoma. Cancer Cell. 2010;17(4): 362 – 375.

15. Pollard SM, Yoshikawa K, Clarke ID, et al. Glioma stem cell lines expanded in adherent culture have tumor-specific phenotypes and are suitable for chemical and genetic screens. Cell Stem Cell. 2009;4(6): 568 – 580.

16. Wakimoto H, Kesari S, Farrell CJ, et al. Human glioblastoma-derived cancer stem cells: establishment of invasive glioma models and treatment with oncolytic herpes simplex virus vectors. Cancer Res. 2009;69(8): 3472 – 3481.

17. Visnyei K, Onodera H, Damoiseaux R, et al. A molecular screening ap- proach to identify and characterize inhibitors of glioblastoma stem cells. Mol Cancer Ther. 2011;10(10):1818 – 1828.

18. Pollard S, Clarke ID, Smith A, Dirks P. Brain cancer stem cells: a level playing field. Cell Stem Cell. 2009;5(5):468 – 469.

19. Reynolds BA, Vescovi AL. Brain cancer stem cells: think twice before going flat. Cell Stem Cell. 2009;5(5):466 – 467. author reply 468 – 9.

20. Patru C, Romao L, Varlet P, et al. CD133, CD15/SSEA-1, CD34 or side populations do not resume tumor-initiating properties of long-term cultured cancer stem cells from human malignant glio-neuronal tumors. BMC Cancer. 2010;10:66.

21. Wan F, Zhang S, Xie R, et al. The utility and limitations of neurosphere assay, CD133 immunophenotyping and side population assay in glioma stem cell research. Brain Pathol. 2010;20(5):877 – 889.

22. Beier D, Hau P, Proescholdt M, et al. CD133(+) and CD133(–) glioblastoma-derived cancer stem cells show differential growth charac- teristics and molecular profiles. Cancer Res. 2007;67(9):4010 – 4015.

23. Schulte A, Gunther HS, Phillips HS, et al. A distinct subset of glioma cell lines with stem cell-like properties reflects the transcriptional phenotype of glioblastomas and overexpresses CXCR4 as therapeutic target. Glia. 2011;59(4):590 – 602.

24. Panosyan EH, Laks DR, Masterman-Smith M, et al. Clinical outcome in pediatric glial and embryonal brain tumors correlates with in vitro multi-passageable neurosphere formation. Pediatr Blood Cancer.

2010;55(4):644 – 651.

25. van den Bent MJ, Gravendeel LA, Gorlia T, et al. A hypermethylated phenotype is a better predictor of survival than MGMT methylation in an- aplastic oligodendroglial brain tumors: a report from EORTC study 26951.

Clin Cancer Res. 2011;17(22):7148 – 7155.

26. Dennis G, Jr., Sherman BT, Hosack DA, et al. DAVID: Database for Annotation, Visualization, and Integrated Discovery. Genome Biol. 2003;4(5):P3.

27. Laks DR, Masterman-Smith M, Visnyei K, et al. Neurosphere formation is an independent predictor of clinical outcome in malignant glioma. Stem Cells. 2009;27(4):980 – 987.

28. Pallini R, Ricci-Vitiani L, Banna GL, et al. Cancer stem cell analysis and clinical outcome in patients with glioblastoma multiforme. Clin Cancer Res. 2008;14(24):8205 – 8212.

29. Cancer Genome Atlas Research Network. Comprehensive genomic char- acterization defines human glioblastoma genes and core pathways. Nature. 2008;455(7216):1061 – 1068.

30. Bredel M, Scholtens DM, Harsh GR, et al. A network model of a coopera- tive genetic landscape in brain tumors. JAMA. 2009;302(3):261 – 275.

31. Erdem-Eraslan L, Gravendeel LA, de Rooi J, et al. Intrinsic molecular sub- types of glioma are prognostic and predict benefit from adjuvant procar- bazine, lomustine, and vincristine chemotherapy in combination with other prognostic factors in anaplastic oligodendroglial brain tumors: a report from EORTC study 26951. J Clin Oncol. 2013;31(3):328 – 336.

32. Schulte A, Gunther HS, Martens T, et al. Glioblastoma stem-like cell lines with either maintenance or loss of high-level EGFR amplification, generat- ed via modulation of ligand concentration. Clin Cancer Res. 2012;18(7):1901 – 1913.

33. Noushmehr H, Weisenberger DJ, Diefes K, et al. Identification of a CpG island methylator phenotype that defines a distinct subgroup of glioma. Cancer Cell. 2010;17(5):510 – 522.

34. Klink B, Miletic H, Stieber D, et al. A novel, diffusely infiltrative xenograft model of human anaplastic oligodendroglioma with mutations in FUBP1, CIC, and IDH1. PLoS One. 2013;8(3):e59773.

35. Luchman HA, Stechishin OD, Dang NH, et al. An in vivo patient-derived model of endogenous IDH1-mutant glioma. Neuro Oncol. 2012;14(2): 184 – 191.

36. Rohle D, Popovici-Muller J, Palaskas N, et al. An inhibitor of mutant IDH1 delays growth and promotes differentiation of glioma cells. Science. 2013;340(6132):626 – 630.

37. Chrenek MA, Wong P, Weaver VM. Tumour-stromal interactions. Integrins and cell adhesions as modulators of mammary cell survival and transformation. Breast Cancer Res. 2001;3(4):224 – 229.

38. Lathia JD, Li M, Hall PE, et al. Laminin alpha 2 enables glioblastoma stem cell growth. Ann Neurol. 2012;72(5):766 – 778.

39. Gallo M, Ho J, Coutinho FJ, et al. A tumorigenic MLL-homeobox network in human glioblastoma stem cells. Cancer Res. 2013;73(1): 417 – 427.

Supplementary materials

Tissue handling and in vitro culture assays

Primary tumor tissue samples are collected from patients for which informed consent was obtained, guided by the Institutional Review Board of the Erasmus Medical Center Rotterdam.

Fresh resected tumor biopsies are collected in culture medium (DMEM supplemented with fetal calf serum (10%), penicillin and streptomycin (1%)). Within 2 hours post resection, samples are minced with surgical blades, into lumps with a volume that can be easily aspirated into conventional 5ml cell culture pipettes without flow-obstruction. These lumps are chemically dissociated in a cocktail of culture medium supplemented with DNAse (1%) and Collagenase A (5%) for 1,5 hours in a 37”C shaking water-bath.

Subsequently the dissociated cells are rinsed through a 70um cell strainer and centrifuged. Pellet is subsequently treated with erythrocyte lysis buffer (1ml 0.75M NH_4Cl, 1mM EDTA, 0.1 $KHCO_3$), for 8-10 minutes on ice, and re-dissolved in culture medium.

Next, the solution is spun once more to remove all debris from lysed erythrocytes. These (white) pellets are plated out to establish cultures on serum supplemented (SS) and serum free (SF) medium. SS medium consists of the same components as mentioned for the biopsy collection medium. SF medium constitutes DMEM-F12 with 1% penicillin/streptomycin, B27 (Invitrogen), human EGF (5ug/ml), human basic FGF (5ug/ml) (both Tebu-Bio) and heparin (5mg/ml) (Sigma-Aldrich).

The seeding concentration is based on viability inspection after erythrocyte lysis supernatant is discarded. On average we would start a culture with approximately 1x10*6 viable cells per 5ml in T25 or T75 culture flasks. For every sample, parallel SS cultures are started with 25-50% of the total pellet, depending on the assessment of total yield and viability after dissociation. Since the main objective is to start SF cultures, seeding concentration of SS cultures is adjusted in favor of increasing the yield of SF cultures. In our experience, there is virtually no threshold to establishing SS cultures when proper adjustments are made with regard to culture flask volume.

Next day, cells are inspected for viability once more. If apparent, abundant cellular debris is removed by centrifugation and cells are resuspended in fresh medium. On day 3 and 7 cells are inspected again for the formation and size of tumor-spheres. Cultures that contain a sufficient number of tumor-spheres of adequate volume (100um size) are dissociated for re-proliferation assessment. If no sphere formation is apparent, but cells adhere to the bottom of the flask, cells are left to proliferate since these adherent cells will often form spheres within a couple of days. If a culture does not form spheres at all, our experience is that usually these cultures will stop proliferating under SF conditions.

In order to perform the assay in a reproducible manner we have a standardized protocol to harvest pellets and cryovials at early passages. This is done in order to guarantee the ability to re-start cultures at low passages and perform profiling studies. This means that on average, a culture must form spheres in p0 and p1, proliferate in p2 through p5 to be able to store cell pellets for profiling studies. Furthermore, the ability to initialize sphere formation over multiple passages is a good indicator of prolonged and reproducible in vitro usage. In our experience, from p5 onwards SF cultures rarely senesce before p20. This leaves enough room to perform reproducible experiments with translationally relevant SF cultures.

Classification of SF culture groups

SF+ cultures Successfully propagated samples are able to proliferate for at least 5 passages post dissociation. These cultures form spheres when plated under SF conditions and usually harbor very heterogeneous intercellular morphological aspects when plated in ECM coated wells. We continue to store cryovials of these cultures at low passages to ensure tissue banking of these cultures for drug screening and other experimental procedures. Routine profiling studies of these SF+ cultures further more enables us to work with well-characterized GSC’s.

SFnp cultures SFnp samples are able to form spheroids under SF condition after dissociation. However, after passaging, these spheroids do not proliferate for at least 5 passages. Usually, within 1 or 2 passages these spheroids senesce, or the sphere formation is merely based on aggregation of cells rather than expansion of the culture. This leads to a decay of the proportion of viable cells over the first 4 passages, which renders the culture unsuitable for reproducible experiments.

SF- cultures SF- cultures are not forming spheroids in the first week under SF conditions. At inspection, it is our experience that these cultures merely have floating debris with sometimes some adherent stromal cells. The floating debris can be easily distinguished from sphere formation by its aspect, which is typically devoid of intact nuclear cellular morphology, which can be found in spheroids. In addition, the amount of viable cells only decreases over time, while this is not the case for SFnp or SF+ samples. These samples usually enrich for viable cells after centrifugation steps in the first week after dissociation.

We have excluded samples that were not proliferating due to lack of sample volume. Other obvious procedural flaws and contamination were excluded as well.

Importantly, the majority of SF- samples yielded very large volume pellets after dissociation, which rapidly deceased after seeding, regardless of seeding concentration or culture medium. This holds true especially for grade II and grade III samples. However, fine-tuning the seeding concentration to higher or lower thresholds does not alter outcome in our experience. Therefore, the above-mentioned seeding concentration of 1x106 cells is in our experience suited for initial seeding in all grades.

Supplementary Tables and Figures

GS ID	SF Outcome	Histology	TCGA	IGS	EGFR	CDK4	PDGFRA	MDM2	CDKN2A/B	PTEN	NF1	RB1
GS110	SF+	GBM	MES	23								
GS79	SF+	GBM	CLA	18								
GS74	SF+	GBM	CLA	18								
GS184	SF+	GBM	CLA	18								
GS160	SF+	GBM	CLA	18								
GS204	SF+	GBM	ND	ND								
GS199	SF+	GBM	CLA	18								
GS187	SF+	GBM	MES	23								
GS168	SF+	GBM	ND	ND								
GS104a	SF+	GBM	CLA	18								
GS104b	SF+	GBM	CLA	18								
GS102	SF+	GBM	NEU	16								
GS111	SF-	GBM	MES	23								
GS92	SF-	GBM	CLA	18								
GS137	SF-	GBM	CLA	18								
GS238	SF-	GBM	NEU	17								
GS52	SF-	GBM	PRO	22								
GS1	SF-	AOD	PRO	17								
GS137	SF-	OD	PRO	9								
GS46	SF-	AOD	PRO	17								
GS83	SFnp	GBM	ND	ND								
GS146	SFnp	GBM	NEU	17								
GS176	SFnp	GBM	PRO	17								
GS167	SFnp	GBM	MES	23								
GS188	SFnp	GBM	CLA	18								
GS90	SFnp	GBM	CLA	23								
GS89	SFnp	AA	PRO	17								
GS143	SFnp	GBM	ND	ND								

Table S1) Distribution of frequently occurring CNA's in GBM amongst the SF+ and SF- tumors. Frequently occurring CNA's as found in the TCGA cohort were scored for in SF+ and SF-/SFnp parental tumors. Abbreviations for histology are as found in legend Fig1. Red indicates copy number ≧ 4n. Blue indicates copy number ≦ 1. Integration of gene-signature according to TCGA and IGS classifiers is depicted as well. Note the enrichment of 7p+10q- combined CNA's in the SF+ group. CDK6 and MET focal amplifications were not found in our cohort.

GS	Diagnosis	Localization	Group	TCGA	IGS	IDH
GS79	GBM	Frontal-R	SF+	CLA	18	WT
GS102	GBM	Occipital-L	SF+	NEU	16	WT
GS104	GBM	Parieto-Occipital-R	SF+	CLA	18	WT
GS187	GBM-r	Parieto-Occipital-R	SF+	MES	23	WT
GS184	GBM	Temporal-R	SF+	CLA	18	WT
GS160	GBM	Temporal-R	SF+	CLA	18	WT
GS74	GBM	Parietal-R	SF+	CLA	18	WT
GS110	GBM	Fronto-Parietal-L	SF+	MES	23	WT
GS199	GBM	Occipital-R	SF+	CLA	18	WT
GS257	GBM	Occipital-R	SF+	CLA	18	WT
GS224	GBM-r	Fronto-Temporal-L	SF+	CLA	23	WT
GS245	GBM	Temporal-R	SF+	NEU	17	WT
GS261	GBM	Occipital-L	SF+	CLA	18	WT
GS289	GBM	Temporal-R	SF+	CLA	18	WT
GS254	A	Frontal-R	SF+	PRO	17	WT
GS284	AOA	Frontal-R	SF+	CLA	18	WT
GS286	OD	Frontal-R	SF+	PRO	17	WT
GS276	AOD	Frontal-R	SFnp	PRO	9	R132H
GS153	AA	Frontal-R	SFnp	PRO	17	R132H
GS297	AOD	Frontal-R	SFnp	PRO	9	R132H
GS301	AA	Frontal-R	SFnp	PRO	17	R132G
GS310	AOD	Frontal-R	SFnp	PRO	9	R132H
GS137	GBM	Parieto-Occipital-L	SF-	CLA	18	WT
GS146	GBM	Temporal-R	SFnp	NEU	17	WT
GS176	GBM	Frontotemporal-L	SFnp	NEU	17	WT
GS238	GBM	Occipital-L	SF-	NEU	17	WT
GS167	GBM	Parietal-R	SFnp	MES	23	WT
GS188	GBM	Parieto-temporal-L	SFnp	CLA	18	WT
GS90	GBM	Frontal-R	SFnp	CLA	23	WT
GS89	AA	Frontal-L	SFnp	PRO	17	R132H
GS1	AOD	Frontal-L	SF-	PRO	17	R132H
GS46	AOD	Fronto-Parietal-L	SF-	PRO	17	R132S
GS189	AOD	Frontal-R	SF-	PRO	9	R132H
GS108	AOD	Frontal-R	SF-	PRO	9	R132H
GS206	GBM	Temporal-R	SF-	CLA	18	WT
GS252	GBM	Temporal-L	SFnp	MES	23	WT
GS158	AOD	Frontal-L	SF-	PRO	9	R132H
GS185	OA	Temporal-R	SFnp	CLA	17	WT
GS52	GBM	Frontal-L	SF-	PRO	22	R132H
GS111	GBM	Frontal-R	SF-	MES	23	WT
GS92	GBM	Parieto-Occipital-R	SF-	MES	18	WT

Table S2) Overview of samples selected for DASL based gene expression analysis. Molecular subtype, IDH-1 mutation status and LOH of 1p19q are scored for. NC = no change. N.D. = not determined.

Annotation Cluster 1	Enrichment Score: 5.49	Count	%	PValue	Genes
Development	GO:0048598~embryonic morphogenesis	23	6.14973262	6.49E-07	TWSG1, PAX3, HOXD10, HOXB3, HOXA1, HOXB4, HOXA2, HOXB2, DKK1, SALL4, HOXC9, CHRNA9, HOXB7, HOXA5, HOXB8, ALDH1A3, HOXB5, HOXC4, GFPT1, HOXA10, HOXA9, ROR2, IFT88
Annotation Cluster 2	Enrichment Score: 4.85				
Cell Cycle	GO:0022403~cell cycle phase	26	6.95187166	2.60E-06	NEK2, LRRCC1, AURKA, CEP55, RCC1, GTSE1, KIF2C, NIPBL, KRT7, CAMK2D, ASPM, EXO1, DLGAP5, SGOL1, NUF2, MND1, CENPF, CDC20, BIRC5, CDKN3, HMGA2, WEE1, SMC4, PLK1, SPAG5, KPNA2
Annotation Cluster 3	Enrichment Score: 4.08				
Inflammation and Wound Healing	GO:0009611~response to wounding	30	8.02139037	2.88E-06	F2RL2, CCL2, S100A8, TLR1, F2RL1, CXCL2, CCL8, HOXB13, IL15, ELK3, CASP6, CCL20, SAA2, SAA1, INS, IL1RAP, SERPINE1, TICAM2, IL1B, SCNN1B, PTX3, FN1, CIITA, LY75, PDPN, COL5A1, PLAUR, TNFAIP6, TFPI, PLAU
Annotation Cluster 4	Enrichment Score: 3.45				
Chemotaxis and Behavior	GO:0007610~behavior	21	5.61497326	0.00245749	HCRT, CCL2, MET, CXCL2, CCL8, ESR2, NTSR1, HOXD10, CCL27, PLAUR, CXCL14, RAC2, SAA2, CCL20, SAA1, HOXB8, NHLH2, IL1B, FOSL1, CHRNA3, PLAU
Annotation Cluster 5	Enrichment Score: 1.95				
Cell Migration	GO:0016477~cell migration	14	3.74331551	0.00602053	CCL2, TNFRSF12A, MET, ITGA11, ESR2, PAX3, COL5A1, SAA2, SAA1, IL1B, LAMC1, SCNN1B, PLAU, FN1

Annotation Cluster 1	Enrichment Score: 10.42	Count	%	PValue	Genes
Neurological System processes	GO:0007267~cell-cell signaling	50	9.96015936	2.71E-13	EDN3, SYT1, GABRB3, GRIK2, LTBP4, SNCA, GRIK4, FGF12, GJA4, VIPR2, GRIN2C, SLC22A3, CHRNA4, GABRG2, KIF5A, PDYN, GRM4, SSTR2, GRM3, SSTR1, CHRM1, CPLX3, CPLX1, GRAP, RIMS1, ADCYAP1, AMPH, GAD2, ECE2, SYN1, HRH3, CRB1, SYN3, SYN2, TEK, APBA2, PRIMA1, GABRD, HCN2, BMP2, SLC12A5, GRIN1, GRIA4, ACCN1, WNT7B, PNOC, KCNN3, ADRA1A, SST, CACNA1A
Annotation Cluster 2	Enrichment Score: 5.22				
Adhesion	GO:0007155~cell adhesion	40	7.96812749	2.95E-06	PPFIA2, PARD3, PCDHA2, CLDN5, DSCAML1, VTN, PCDHGA4, MMRN1, PCDHGA2, PCDHGA1, CDH20, TNR, BCL2, DGCR6, TEK, CNTNAP2, KIRREL2, NEGR1, DSCAM, FLRT1, RET, TNXB, NRXN2, ICAM5, PCDH11Y, ICAM2, PTPRT, AJAP1, CTNNA3, CDH12, CDH13, HAS1, CD209, CDH18, RELN, CNTN4, MADCAM1, CNTN3, OMG, NTM
Annotation Cluster 3	Enrichment Score: 4.69				
Ion transporting	GO:0006811~ion transport	48	9.56175299	1.47E-08	SLC8A3, JPH4, JPH3, GABRB3, KCNAB2, KCNAB1, GRIK2, SLC22A14, GRIK4, GJA4, KCNJ11, KCNJ3, ATP2B3, GRIN2C, SLC22A3, CHRNA4, SLC22A6, NALCN, GRID1, HCN1, GABRD, GABRG2, HCN2, SVOP, SLC8A2, GABRA1, KCNB1, SLC12A5, GRIN1, CACNG6, ATP1A3, CACNG3, GRIA4, CACNG2, PRKCB, CNNM1, ACCN1, ATP2C2, ACCN4, KCNT1, KCNN3, KCNN2, RYR1, KCNH8, SLC13A4, ABCC8, CACNA1A, CLCN4
Annotation Cluster 4	Enrichment Score: 4.14				
Neurotransmitter transport	GO:0006836~neurotransmitter transport	15	2.98804781	1.83E-08	SYT1, CPLX3, CPLX2, CPLX1, SLC6A15, SLC6A17, RIMS1, SLC32A1, GRM4, HRH3, SYN1, SYN3, SYN2, SLC22A3, CACNA1A
Annotation Cluster 5	Enrichment Score: 3.38				
Neuron differentiation	GO:0030182~neuron differentiation	29	5.77689243	6.56E-06	EDN3, PARD3, CCK, NDN, ERBB3, DSCAML1, RTN1, CRB1, ANK3, BCL11B, BCL2, TNR, CNTNAP2, LGI4, DSCAM, RET, GNAO1, EMX1, STMN2, NTNG2, NTRK3, SLITRK4, NRL, NTRK1, CNTN4, RELN, NTM, CACNA1A, KALRN

Table S3-4) Overview of gene modules upregulated en downregulated in SF+ tumors. Individual genes are depicted by gene symbol. The percentages indicate the amount of positive genes within the entire module.

GS	Diagnosis	Localization	Group	TCGA	IGS	IDH	1p19q	Sex	Age at OR	Alive?	OS	IDH-MUT conserved in vitro	IDH-MUT lost in vitro
GS276	AOD	Frontal-R	SFnp	PRO	9	R132H	Loss	f	73	N	12	SF: ambigous in p2	SF: p4
GS153	AA	Frontal-R	SFnp	PRO	17	R132H	NC	f	31	Y	26	N.A	SF : p1
GS297	AOD	Frontal-R	SFnp	PRO	9	R132H	Loss	f	54	Y	5	SF : p1	SF : p5
GS301	AA	Frontal-R	SFnp	PRO	17	R132G	NC	m	35	Y	5	SF: p1	p3
GS310	AOD	Frontal-R	SFnp	PRO	9	R132H	Loss	m	66	Y	4	SF: p0	SF: ambiguous in p2, stopped proliferating
GS89	AA	Frontal-L	SFnp	PRO	17	R132H	NC	m	20	Y	47	N.A	SF: p2, SS : p1
GS1	AOD	Frontal-L	SF-	PRO	17	R132H	NC	m	44	N	47	N.A	SS p4
GS13	OD	Temporal-R	SF-	PRO	9	R132H	Loss	f	43	Y	39	N.A	SS p2
GS46	AOD	Fronto-Parietal-L	SF-	PRO	17	R132S	NC	m	28	Y	44	N.A	SS p4
GS189	AOD	Frontal-R	SF-	PRO	9	R132H	Loss	f	38	Y	20	N.A	N.A
GS108	AOD	Frontal-R	SF-	PRO	9	R132H	Loss	f	45	Y	30	N.A	N.A
GS158	AOD	Frontal-L	SF-	PRO	9	R132H	Loss	m	38	Y	13	N.A	N.A
GS52	GBM 2nd	Frontal-L	SF-	PRO	22	R132H	NC	f	62	Y	35	N.A	SS p3
GS4	OD	Frontal-R	SF-	ND	ND	R132H	Loss	f	48	Y	55	N.A	SSp3
GS5	A	Temporal-L	SF-	ND	ND	R132H	ND	f	27	Y	55	N.A	SSp3
GS8	A	Frontal-L	SF-	ND	ND	R132H	ND	m	47	Y	42	N.A	SSp6
GS20	OD	Frontal-R	SF-	ND	ND	R132H	Loss	m	33	Y	49	N.A	SSp3
GS22	A	Temporal-L	SF-	ND	ND	R132H	ND	f	39	Y	48	N.A	SSp3
GS27	OA	Parietal-R	SF-	ND	ND	R132H	NC	m	29	Y	46	N.A	SSp2
GS26	AA	Frontal-R	SF-	ND	ND	R132H	NC	f	42	Y	46	N.A	SSp3
GS14	GBM 2nd	Frontal-R	SF-	ND	ND	R132H	ND	f	35	Y	51	N.A	SSp3

Table S5) Negative selection against IDH-MUT tumor cells in SF culture conditions results in non-neoplastic cultures. Cell cultures from IDH-1 mutated tumors were sequenced for mutational status at indicated passage numbers. Abbreviations; ND= Not determined, NC = No Change, N.A. = not available. For loss of IDH-MUT in vitro, the earliest sample available that was assessed for IDH-MUT status is depicted.

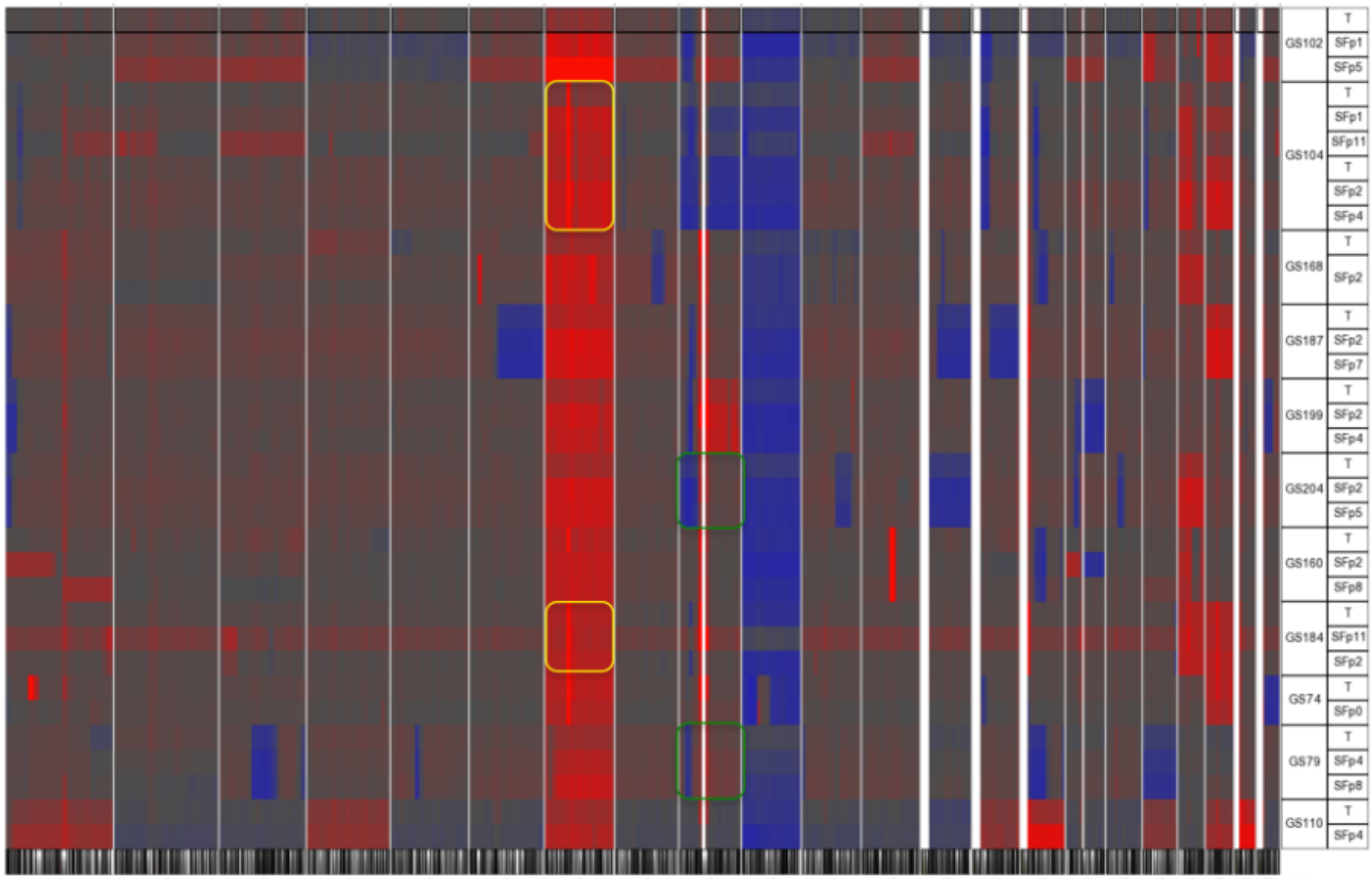

Fig.S1) SF cultures from SF+ tumors retain copy number alterations as found in the parental tissue. Heatmap profile of cultures from indicated passages of SF+ samples genotyped on SNP6.0 array platform. Color coding indicates genomic gains (red) and losses (blue). Numbers below indicate the chromosome depicted above. Note the retained EGFR amplification found on chromosome 7p, as indicated by intense red band in the yellow boxes. Similarly, CDKN2A/B deletions are retained on chromosome 9p, as indicated by the blue bands in the green boxes.

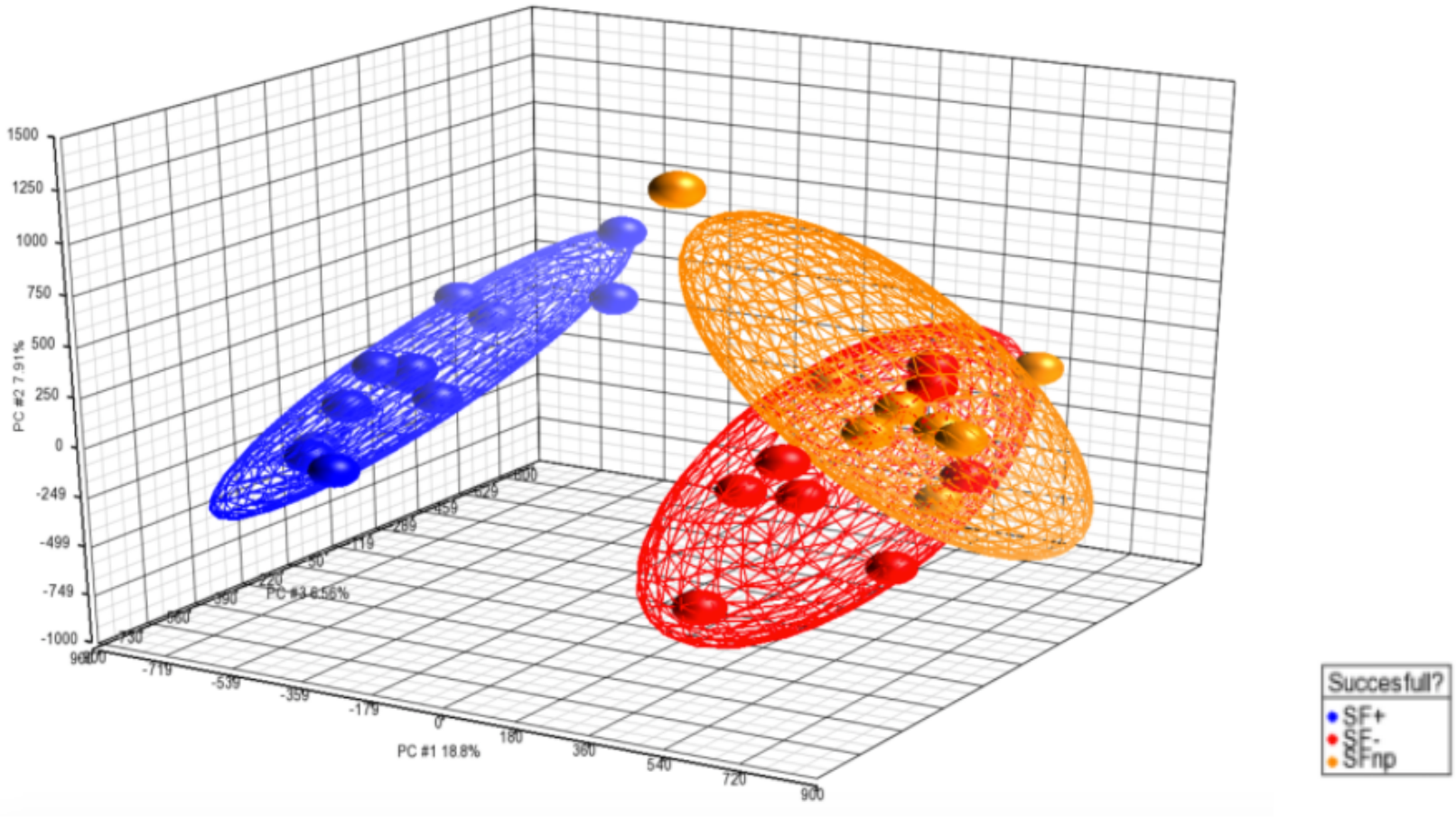

Fig.S2) Principal Component Analysis of Genotyping (SNP calls) results of patient tumors from which GS cultures were derived. Color coding is applied for the 3 different culture outcomes. Note the genotypic segregation of SF+ tumors from SF-/SFnp tumors. Data was retrieved after correcting for batch effect.

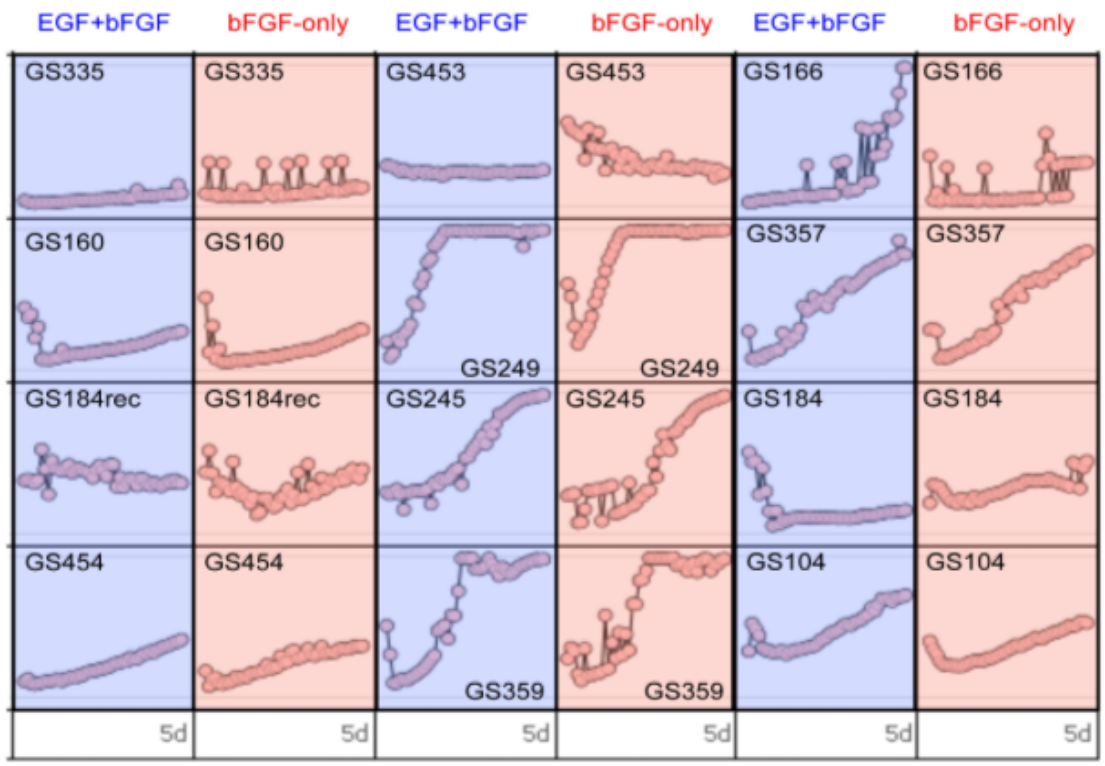

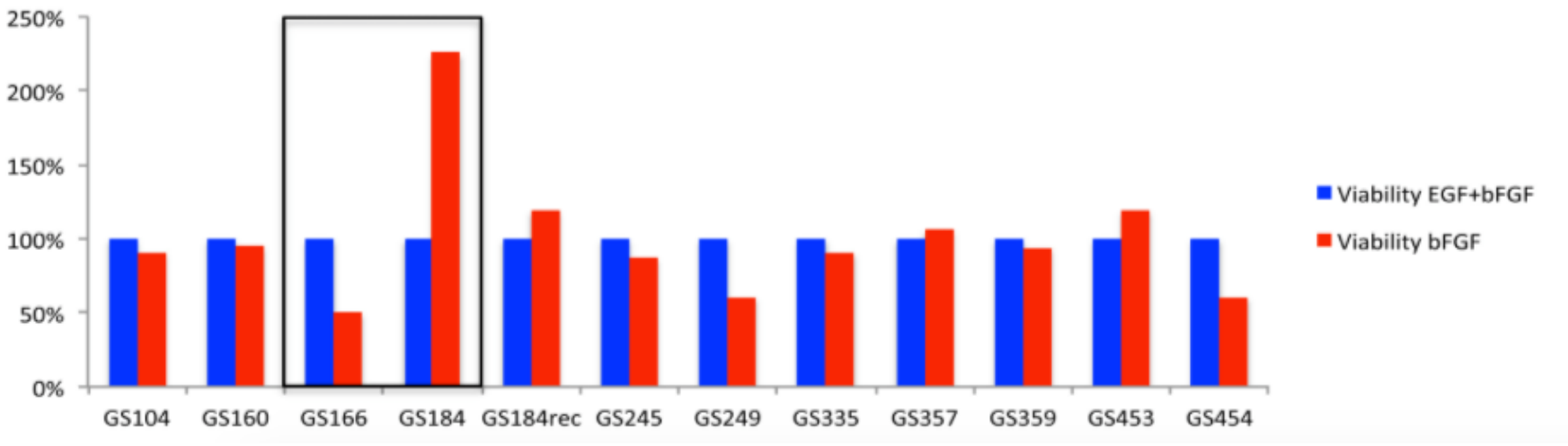

Fig.S3) EGF addition to SF medium does not alter SF culture proliferation and viability. A) Panel of 12 previously established SF+ cultures are monitored for 5 days on SF medium with EGF and bFGF or SF medium with bFGF supplementation only. Graphs are depictions of Incucyte standardized confluency measurements from 4 square microscopic localizations within a 24-well format. Note that, with the exception of GS166, all culture have comparable growth patterns between the two conditions. B) Viability data of the same experiment as described in A), with bar charts depicting Cell Titer GLO based read-out at 5 days of the same panel. Note the increase in viability of GS184 and GS184rec plus decrease viability of GS166. For the other cultures, there is overlap between the results of the confluency measurements which overall show no significant difference between the two conditions.

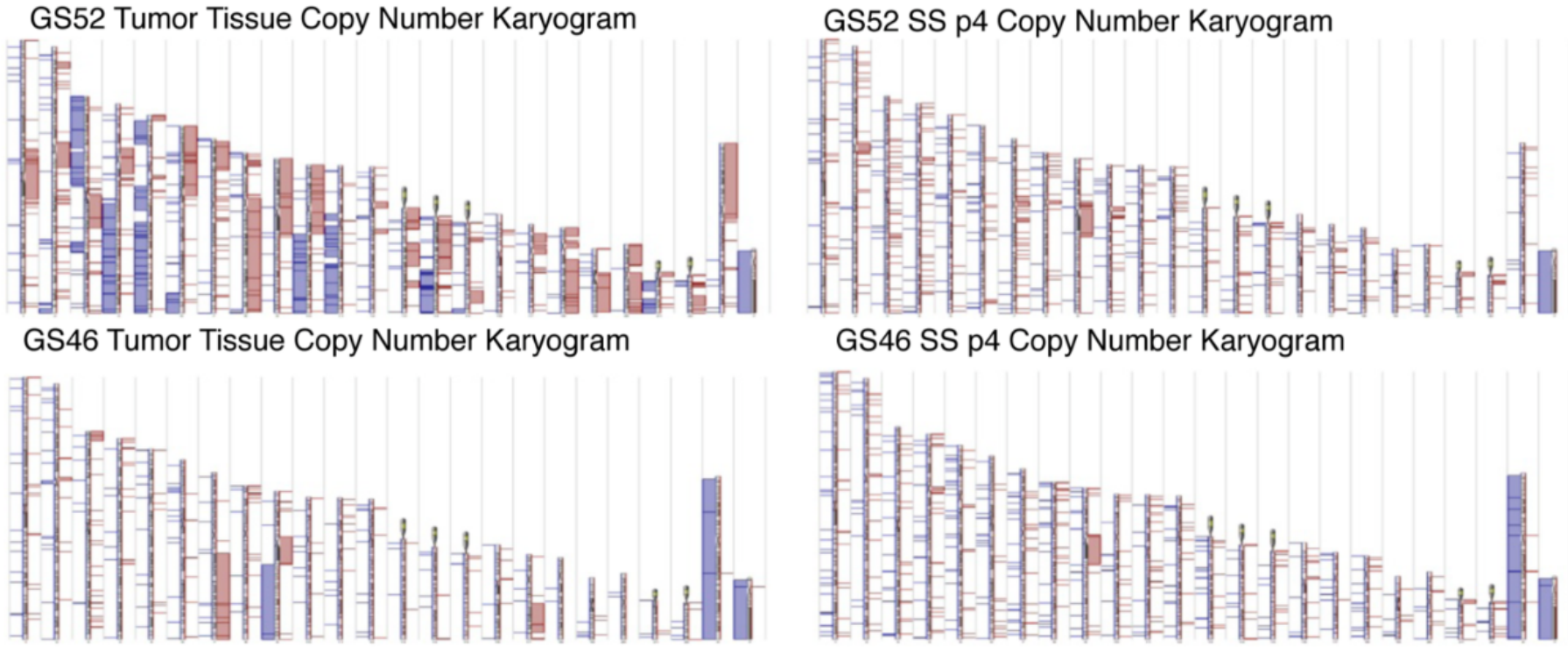

Fig.S4) Comparative SNP karyogram analysis reveals loss of copy number alterations. Chromosomes are depicted in numerical sequence with chromosome 1 on the far left, and the Y chromosome on the far right. Red and blue bands indicative of gains and losses in the tumor karyotype are lost in the SS cultures derived from these tumors, illustrating nonneoplastic overgrowth

3

ABT-888 enhances cytotoxic effects of temozolomide independent of MGMT status in serum free cultured glioma cells

Chapter was published as;

ABT-888 enhances cytotoxic effects of temozolomide independent of MGMT status in serum free cultured glioma cells.
Rutger K Balvers, Martine LM Lamfers, Jenneke J Kloezeman, Anne Kleijn, Lotte ME Berghauser Pont, Clemens MF Dirven and Sieger Leenstra,

Journal of Translational Medicine (2015) 13:74 DOI 10.1186/s12967-015-0427-y

Published online 26th february 2015

Abstract

Background: The current standard of care for Glioblastoma Multiforme (GBM) consists of fractionated focal irradiation with concomitant temozolomide (TMZ) chemotherapy. A promising strategy to increase the efficacy of TMZ is through interference with the DNA damage repair machinery, by poly(ADP-ribose) polymerase protein inhibition(PARPi). The objective of the present study was to investigate the therapeutic benefit of combination therapy in patient-derived glioma stem-like cells (GSC). **Methods:** Combination therapy feasibility was tested on established GBM cell lines U373 and T98. We developed an in vitro drug-screening assay based on GSC cultures derived from a panel of primary patient tissue samples (n = 20) to evaluate the effect of PARPi (ABT-888) monotherapy and combination therapy with TMZ. Therapeutic effect was assessed by viability, double stranded breaks, apoptosis and autophagy assays and longitudinal microscopic cell monitoring was performed. O-6-methylguanine-DNA methyltransferase (MGMT) status was determined by methylation assay and protein expression by western blots. **Results:** PARPi monotherapy was found to decrease viability by more than 25% in 4 of the 20 GSCs (20%) at 10 μM. TMZ monotherapy at 50 μM and 100 μM was effective in 12 and 14 of the 20 GSCs, respectively. TMZ resistance to 100 μM was found in 7 of 8 MGMT protein positive cultures. Potentiation of TMZ therapy through PARPi was found in 90% (n = 20) of GSCs, of which 6 were initially resistant and 7 were sensitive to TMZ monotherapy. Increased induction of double stranded breaks and apoptosis were noted in responsive GSCs. There was a trend noted, albeit statistically insignificant, of increased autophagy both in western blots and accumulation of autophagosomes. **Conclusion:** PARPi mediated potentiation of TMZ is independent of TMZ sensitivity and can override MGMT(-) mediated resistance when administered simultaneously. Response to combination therapy was associated with increased double strand breaks induction, and coincided by increased apoptosis and autophagy. PARPi addition potentiates TMZ treatment in primary GSCs. PARPi could potentially enhance the therapeutic efficacy of the standard of care in GBM.

Introduction

Glioblastoma Multiforme (GBM) is the most common primary brain tumor for which there is no curative therapeutic option [1]. First-line treatment of GBM consists of tumor resection, followed by fractionated focal irradiation (IR) in combination with concomitant and adjuvant administration of the alkylating agent temozolomide (TMZ). Despite recent advances in understanding the molecular biology of GBM, the clinical perspective for newly diagnosed patients remains poor. The addition of TMZ to surgery followed by radiation has increased median survival from 12 to 15 months compared with IR monotherapy [2]. Hence, the need for therapeutic agents that can augment current treatment outcome is urgent.

It has been demonstrated that therapeutic efficacy of this chemoradiation regimen, apart from clinical factors, depends on intrinsic molecular features of the tumor [3,4] such as methylation of the O6-methylguanine- DNA methyltransferase (MGMT) promoter gene and the subsequent lack of expression of the MGMT protein within GBM cells [5].

Several mechanisms have been identified that lead to the repair of alkylation-induced damage, such as base-excision repair (BER), mismatch repair (MMR) and homologous recombination (HR) repair [6,7]. The addition of DNA-repair system interfering agents may therefore potentiate the efficacy of TMZ treatment. Poly ADP Ribose Polymerase (PARP) proteins share the ability to transfer an ADP-ribose moïety from nicotinamide adenine dinucleotide (NAD+) to an acceptor protein and facilitate the accumulation of multiple sequential (poly) ADP-ribose units to the preceding one(s), a process termed PARylation. These proteins have been demonstrated to be essential in BER, after DNA damage induced by cytotoxic agents. PARP protein inhibitors (PARPi) were demonstrated to enhance therapeutic efficacy of several conventional cytotoxic agents, such as alkylating chemotherapy. One such agent, ABT-888 (Veliparib®), has been demonstrated to primarily bind to PARP-1and PARP-2, and infer- iorly to PARP-3 and PARP-4 [8]. In humans, PARP-1 activity is responsible for 85-90% of PAR production with the remainder primarily attributable to PARP-2. Therefore, we will reference PARPi function from here on as dimin- ished activity of PARP-1 and PARP-2.

Low passage glioma stem cell (GSC) cultures have been demonstrated to superiorly recapitulate genomic and gene-expression profiles, when compared with GBM cell lines and serum supplemented primary cultures [9,10]. The investigation of therapeutic effect of combined agents in patient derived material provides the ability to identify predictors of responsiveness in vitro. In the present study we investigated the sensitivity of a large panel of patient derived GSCs to monotherapy with both TMZ and PARPi. Additionally, we evaluated the ability of PARPi to potentiate TMZ cytotoxicity at varying clinically relevant doses. The ability of PARPi to overcome TMZ resistance is addressed in the context of MGMT expression in GSCs.

Methods

Cell cultures

All GSC primary cultures were derived from tumors of operated patients from the Erasmus Medical Center Rotterdam, The Netherlands. Prior to surgery, patients sign informed consent as approved by the Institutional Review Board of the Erasmus Medical Center Rotterdam. Tumor grading was performed by the local pathologist according to guidelines of the WHO grading of primary brain tumors. Freshly resected tumor samples were dissociated to establish primary cultures as described earlier [11]. Serum free medium constitutes DMEM-F12 with 1% penicillin/streptomycin, B27 (Invitrogen, Bleiswijk, The Netherlands), human EGF (5 ug/ml), human basic FGF (5 ug/ml) (both Tebu-Bio, Heerhugowaard, The Netherlands) and heparin (5 mg/ml) (Sigma-Aldrich, Zwijndrecht, The Netherlands). Tumor spheres were dissociated and passaged regularly for experiments or to derive material for characterization studies. T98 and U373MG conventional cell cultures were acquired from the American Type Culture Collection (ATCC, Manassas, VA) and propagated on DMEM supplemented with 10% fetal bovine serum and 1% penicillin + streptomycin.

Viability and proliferation assays

Patient-derived tumor spheres were dissociated with AccutaseTM (Invitrogen, Bleijswijk, The Netherlands), and cell lines T98 and U373 with trypsin. Cells were seeded at 1000 cells per well in 96 wells plates. For GSCs, wells were coated with extracellular matrix coating (BD Bioscience, Breda, The Netherlands). After 24 hours, cells were treated with TMZ (Sun Pharmaceutical Indus- tries, Mumbai, India), or ABT-888 (Selleckchem, Huissen, The Netherlands), at indicated doses that have been demonstrated clinically relevant [12,13]. Combination therapy reagents were prepared by adding a mixed reagent in culture medium at equal volumes to monotherapy. Vehicle controls constituted of equal DMSO concentrations as needed for the dilution of TMZ therapy. After 5 days, viability was measured by performing the Cell Titer GLOTM assay according to the manufacturer's instructions (Promega, Leiden, The Netherlands). All experiments were carried out in triplicate. T98 and U373 were used as positive and negative internal controls during GSC-based drug-screening experiments. Read-out was performed in a plate reader by measuring lumines- cence (Tecan Infinite 200, Tecan Benelux, Giessen, NL). Proliferation assays consisted of longitudinal imaging of cell confluency in the Incucyte HD Live Cell imaging incubator. Cells were seeded in 96 wellsplates and placed into the Incucyte incubator. Phase contrast images were acquired at 1-3hr intervals and confluence per well was calculated using a software platform supplied by the manufacturer (Essen Bioscience, Hertfordshire, UK).

Combination indexes of PARPi and TMZ combination therapy were obtained through Cell Titer GLO read-out, and calculated according to the Chou-Talalay procedure [14]. In short, serial dilution experiments with TMZ and ABT-888 monotherapy were carried out in order to determine the IC50 of each drug separately. Based on the Y-intercept and the slope of the curve derived from linearization of the viability data, the IC50 was calculated. Subsequently, ABT-888 and TMZ combination experiments were dosed by combining 3 stepwise derivatives (with 3 fold increases or decreases) of the IC50 value of both drugs in T98 and U373 respectively. Based on these experiments, standardized log derivatives of the dosages needed to elicit a decrease of viability (fraction affected, Fa) at a specific dose of each (combination of) agent(s) can be calculated. Subsequently the dose reduction index (DRI) of combination therapy is the ratio between the monotherapy dose and the combination therapy dose for a given Fa. The combination index is thus provided as the combined 1/DRI of both agents (1/DRItmz + 1/DRIabt-888), which should remain below 1 in order to demonstrate synergy.

Double stranded breaks assays

To determine the induction of DSBs in GSCs, cells were seeded at a concentration of 2.5x104 cells per well in matrigel coated 96 wells plates. Experiments were carried out as instructed by the manufacturer of the OxiSlect DNA Double Strand Break Staining Kit (Cell Bio Labs Inc, San Diego, CA, USA). In short, cells were incubated overnight and treated next day with 100 uM TMZ, 10 uM ABT-888 or combination therapy with both agents. Positive controls consisted of etoposide (0.1 mM) treated cells, whereas for negative controls we used non-treated controls. Read-out was performed 16 hours post-treatment. Cells were fixed in 4%PFA/PBS, washed and stained according to manufacturer's protocol with primary antiγH2Ax antibody solution (1:100) and counterstained with secondary FITC conjugated anti- body solution (1:100). After washing, cells were incu- bated in the Incucyte and yH2Ax positive cells were counted per well with software as provided by the Incucyte manufacturer.

Apoptosis and autophagy assays

To determine the induction of apoptosis or autophagy by mono- or combination-therapy GSCs were plated out in similar conditions with regard to culture conditions, drug dosing and preparations, and cell seeding, as de- scribed for the viability assays. The Cell Player Caspase 3/7 reagent (Essen Bioscience, Hertfordshire, UK) was added in a 1:1000 dilution to the culture medium at the time of treatment administration (according to manufacturers instructions). Read-out was performed after 48 hrs post-treatment by counting the ratio between apoptotic cells and total cells per well, using algorithms provided within the software of the Incucyte FLR.

For autophagy experiments, cells were seeded, treated and cultured as described above for previous in vitro ex- periments. To determine the induction of autophagy, we used the Cyto-ID Autophagy detection kit (Enzo Life Sciences, Raamsdonksveer, The Netherlands). This kit provides a monodansylcadaverine based dye that specif- ically stains autophagosomes [15]. To this end, cells were washed 16hrs post-treatment with assay buffer provided by the manufacturer. Next, cells were stained with the Cyto-ID green detection reagent for 30 minutes and subsequently washed twice more with assay buffer and cells were imaged in the Incucyte FLR for the detection of autophagosomes. Incucyte software was used to process imaging data. First a threshold was set for circumference and fluorescence intensity to identify autop- hagosomes. Next the autophagosomes per well were calculated using algorithms provided by the Incucyte manufacturer.

MGMT methylation assay and western blotting

All samples used were derived from GS cultures passaged no more than 7 times. DNA and protein extraction was derived from fresh frozen pellets. Quantitative PCR on MGMT promoter methylation was assessed as previously decribed [16]. The following methylation specific primers were used F: TTTCGACGTTCGTAG GTTTTCGC and R: GCACTCTTCCGAAAACGAAA CG. The un-methylated specific primers were F: TTTGTGTTTTGATGTTTGTAGGTTTTTGT and R: AACTCCACACTCTTCCAAAAACAAAACAQ. Western blots for MGMT protein expression were performed as follows. Samples were cultured, treated as indicated, and sequentially pelleted, washed twice in ice-cold PBS, and lysed in RIPA buffer with proteinase inhibitor (1%). Protein concentration was measured by performing the Bradford assay. The samples were diluted in Laemli buffer and run on 10% SDS-PAGE gel for electrophoresis. After running the gel, proteins were transferred to PVDF membranes in a BIO-RAD transfer system. Membranes were blocked with 5% milk in TBS-Tween (0.2%) and stained with primary antibodies at 4°C over night. After washing, secondary antibodies were applied for 1 hour with subsequent washing steps. Protein detection was achieved by using ECL chemiluminescent detection reagent (Pierce, Thermo Scientific Etten-

Leur,NL). Antibodies used are anti-MGMT (Abcam, Cambridge MA, USA), LC3B (Cell Signaling, Danvers, MA, USA) and anti-β-actin (Clone C4, Millipore Amsterdam, The Netherlands).

Statistical analysis

Data are presented as averages ± standard deviations as compared to non-treated controls. Statistical analysis was performed using the paired two-tailed Student's t-test. Statistical significance was defined as $p < 0.05$. Enhancement factors were determined as the ratio between the most effective single agent (between ABT-888 and TMZ) and the effect of combination therapy.

Results

PARP inhibition potentiates TMZ in sensitive and resistant conventional celllines

The addition of PARPi to TMZ treatment was tested in two conventionally used GBM cell lines, T98 and U373 respectively, for which the MGMT gene methylation and protein status have been previously reported [17]. Quantification of cytotoxicity was assessed by cell viability as well as monolayer confluency (Figure 1A and B). In ac- cordance with previous reports [18], U373 was sensitive to TMZ monotherapy, whereas T98 was resistant ($p>0.05$ for both dosages compared to non-treated control).

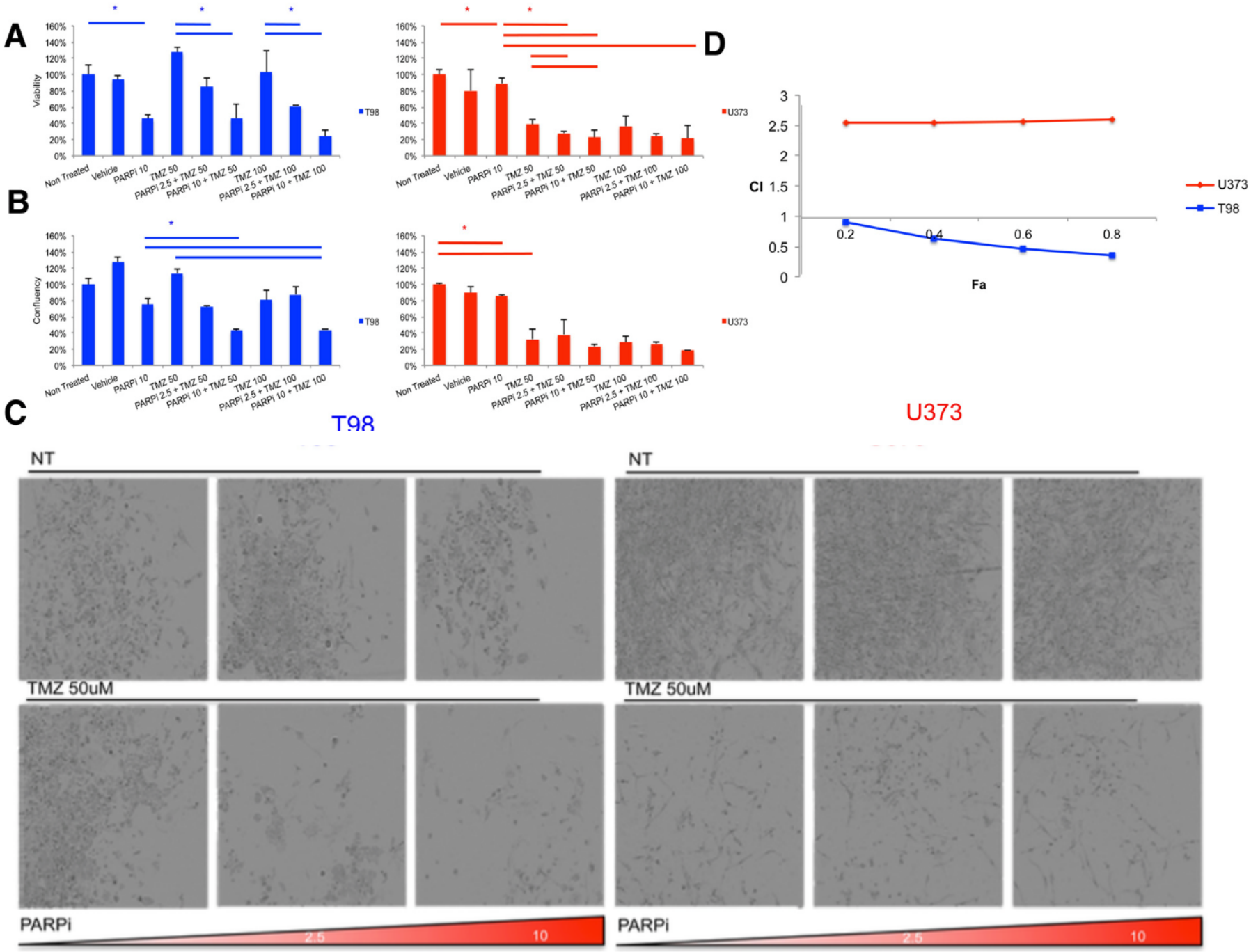

Figure 1 PARPi potentiates TMZ therapy in conventional GBM cell lines on serum-supplemented medium. A) Viability of T98 and U373 cell lines treated at the indicated doses with TMZ and PARPi. Viability is indicated as a measure of ATP conversion into luminescence. Lines above columns indicate significance between two conditions with a p-value <0.05. If monotherapy with TMZ is significant when compared to non-treated controls, the significance of combination therapy when compared to non-treated controls is related and therefore not defined as such in the figure. **B)** Viability as a measure of confluence per well as measured by microscopy. Read out is performed at 5 days post treatment. **C)** Microscopic images of U373 and T98. From left to right the PARPi dosage increases from 0 to 10 uM. Lower panel depicts combination therapy with TMZ at indicated dosages. Note the differential effect of PARPi monotherapy between T98 and U373. **D)** Combination Index (CI) plotted against Fraction affected (Fa) for T98 and U373. PARPi with TMZ combination therapy is synergistic in T98 but not in U373. CI < 1 demonstrates synergistic interaction of combination therapy with TMZ and PARPi at the indicated Fa. CI > 1 demonstrates antagonistic effect of combination therapy at the indicated Fa.

Conversely, T98 was sensitive to PARPi monother- apy whereas U373 was not. Comparative analysis of confluency and ATP-based viability generally correlated well. However, T98 susceptibility for ABT-888 monotherapy appeared more pronounced when assessed for viability than the confluency results suggest. Microscopic examination (Figure 1C) revealed fewer viable cells and drifting debris suggestive of cytotoxic effect of ABT-888 at 10 uM in T98 cells, which was not apparent in U373.

PARPi potentiated TMZ therapy in case of TMZ 50 μM in T98. Adding PARPi resulted in a dose dependent decrease of viability by 42% ±11% (2.5 μM PARPi) and 82% ±16% (10 μM PARPi). Similar results were found for the combination of TMZ at 100 μM with PARPi at 10 μM in T98 ($p<0.001$). In U373, combination treatment of TMZ 50 μM with 2.5 uM PARPi was more effective than mono-treatment, however, the net decrease was small (10% ±2.6%, $p<0.05$), while not signifi- cant for TMZ 100 μM/10 uM PARPi.

To evaluate synergy between the two agents in a systematic manner, the Chou-Talalay combination index (CI) was determined for both agents in these two cell-lines [14]. T98 was comparatively resistant to TMZ with an IC50 at 5 days of 415.5 μM (R2 = 0.97), while the IC50 of U373 was 66.8 uM (R2 = 0.94) at 5 days. T98 was relatively sensitive to PARPi with an IC50 of 16.46 μM (R2 = 0.98) compared to an IC50 of 58.6 uM (R2 = 0.97) for U373. Next, the combination index (the ratio between dose reduction of combined treatment and monotherapy with either agents individually) was plotted. For T98 the combination of PARPi and TMZ was found synergistic with a CI below 1 for all Fa (fraction affected) (Figure 1D). In contrast, the CI U373 consistently demonstrated a CI>1, suggestive of antagonized cytotoxicity of ABT-888 when combined with TMZ in this cell line.

PARPi and TMZ monotherapy screening experiments in GSCs

Molecular characteristics as found in primary GBM tissue, are inferiorly recapitulated in conventional cell lines such as T98 and U373, when compared to early passages of serum-free patient-derived cultures [10,19]. Therefore, we tested 20 GSC cultures from high-grade malignant glioma for the PARPi ABT-888 and TMZ sensitivity (overview of clinically relevant information in Table 1). GSC cultures were labeled sensitive if more than 25% reduction in viability was measured as compared to non- treated controls. For PARPi monotherapy at 10μM, this was found in 4/20 cultures (20%), (Figure 2A).

Sensitivity to TMZ was tested at two standard concentrations of 50 μM (low dose) and 100 μM (high dose). These concentrations are derived from experiments with T98 and U373 as the optimal concentrations to detect additional effect by combination therapy in both TMZ sensitive and resistant cultures, within physiological ranges as found in plasma

Table 1 Overview of GSC panel drug screening results

GS ID	Histology	Age	OS	MGMT Blot/Methyl	PARPi	TMZ	Enhancement factor TMZ 50	p-value	Enhancement factor TMZ 100	p-value
GS249	GBM	53	215	- / ND	0.30	0.66	3.06	0.01	2.92	0.03
GS187	GBM	73	394	- / UM	0.12	0.55	2.22	0.00	2.31	0
GS41	AOD	64	1316	ND	0.11	0.61	1.74	0.08	0.92	0.19
GS125	GBM	75	234	+ / UM	0.21	0.71	1.59	0.17	1.78	0.06
GS203	GBM	64	554	- / M	0.39	0.61	1.68	0.01	1.71	0.01
GS184	GBM	50	833	- / M	0.16	0.74	1.40	0.10	1.66	0.01
GS186	GBM	49	792	- / M	0.21	0.74	1.30	0.03	1.49	0
GS224	GBM	58	101	- / M	0.17	0.73	1.15	0.20	1.20	0.03
GS177	GBM	63	843	- / M	0.20	0.76	1.14	0.01	1.15	0.2
GS182	GBM	70	835	- / M	0.38	0.51	1.14	0.02	1.31	0.05
GS200	GBM	57	321	- / ND	0.48	0.35	1.16	0.02	1.18	0.08
GS143	GBM	54	395	- / ND	0.60	0.32	1.17	0.40	1.32	0.09
GS126	GBM	41	962	+ / M	0.27	0.06	1.68	0.02	1.69	0.01
GS79	GBM	71	384	+ / UM	0.11	0.23	2.11	0.00	2.48	0
GS124	GBM	71	1033	+ / ND	0.22	−0.11	1.19	0.40	1.19	0.06
GS148	AOD	82	97	+ / UM	0.20	−0.07	1.15	0.80	1.15	0.06
GS173	GBM	68	138	+ / ND	−0.05	0.14	1.24	0.07	1.73	0.01
GS204	GBM	50	18	+ / UM	0.07	0.02	1.17	0.03	1.17	0.04
GS161	GBM	62	264	+ / M	0.17	−0.02	0.80	0.04	0.80	0.2
GS160	GBM	46	46	+ / UM	0.07	0.16	0.83	0.03	0.75	0

The separation between TMZ sensitive and resistant groups is based on monotherapy results for TMZ 100 μM results. Significance is depicted as a p-value derived Student's *T*-test of the most effective single agent compared to combination therapy. For OS, boxes without shading depict patients that were alive at the moment of composing this article. Abbreviations as followed; AOD = Anaplastic Oligodendroglioma, GBM = Glioblastoma Multiforme, OS = Overall Survival in days, MGMT = O6-methylguanine-DNA methyltransferase, Blot = Western blotting results which can be positive (+) or negatieve (−), Methyl = Methylation assay which can be Methylated or UnMethylated). ND = Not determined.

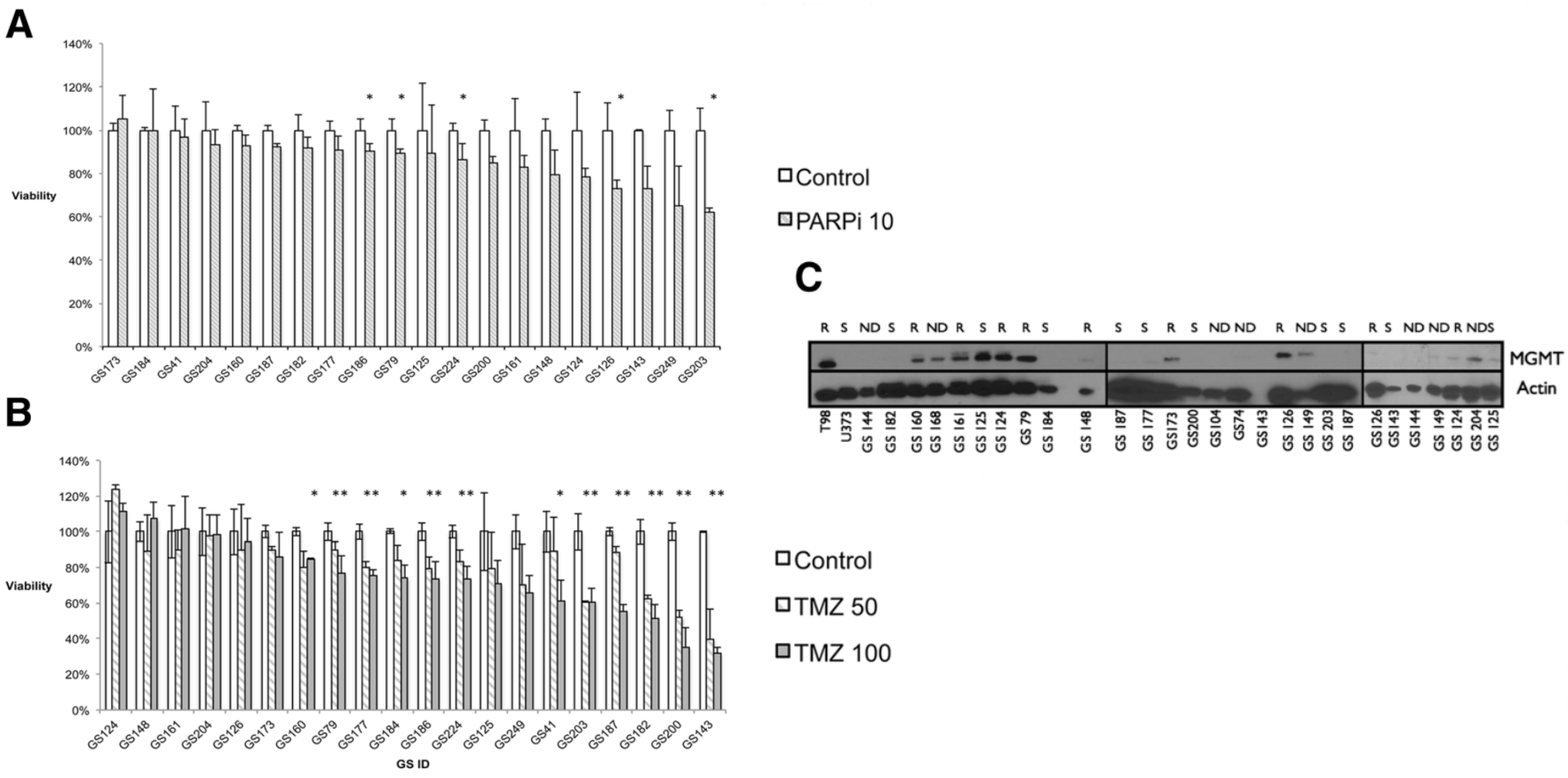

Figure 2 PARPi and TMZ monotherapy efficacy in GS cultures. A) Panel of GS cultures tested for sensitivity to PARPi at 10 uM. Readout of viability was performed at day 5 and is depicted as a percentage when compared to non-treated controls. * Illustrates a p-value <0.05. **B)** GS culture panel tested against indicated concentrations in uM of TMZ monotherapy. Viability at day 5 is indicated as percentages when compared to paired non-treated controls. * indicates $p < 0.05$ as compared to non treated controls. **C)** Overview of western blotting results derived from GS cultures. MGMT protein expression is indicated with actin protein expression used as a loading control. TMZ sensitivity is indicated with an S (sensitive), R (resistant) and ND (TMZ sensitivity not determined in monotherapy screen). For several GSCs protein isolates were loaded in separate runs as technical controls.

and CSF of patients treated with TMZ [20]. Low dose TMZ induced more than 25% viability loss in 5/20 cultures (25%) (Figure 2B). High dose TMZ treatment had therapeutic effect in 12/20 cultures (55%). Based on these results we categorized the 20 GSC cultures into PARPi and TMZ resistant and sensitive cultures based on the initial monotherapy screen (Table 1). Six of the 20 cultures were tested at least three times for reproducibility of the results, which demonstrated consistent TMZ and PARPi therapeutic efficacy profiles over multiple pas- sages (data not shown).

Since therapeutic response of malignant glioma to TMZ is known to be highly correlated with MGMT promoter methylation and a subsequent decrease in MGMT protein expression [5,21], we performed Western blotting of MGMT protein in 19 out 20 cell cultures tested in our initial drug screening (Figure 2C). MGMT was expressed in 9 GSC cultures (MGMT(+)), of which 8 were found to be resistant to 100 μM of TMZ. Conversely, all 11 MGMT negative (MGMT(-)) cultures were found sensitive to TMZ therapy. Together, TMZ sensitivity was highly correlated to MGMT expression ($p=0.007$). In addition we determined the promotor methylation status, which generally correlated well with protein expression (n = 11/14, 78%). Interestingly, the sensitivity to ABT-888 was also correlated to MGMT expression, since MGMT expressing GSCs were significantly more resistant to ABT-888 10 uM monotherapy compared to MGMT negative GSCs ($p=0.01$).

PARPi addition potentiates TMZ treatment in primary GSCs

To determine the ability of the PARPi ABT-888 to potentiate TMZ efficacy, we evaluated the therapeutic effect of combination therapy in the aforementioned GSC cultures (n=20). Enhancement factors were calculated as the ratio between the most effective drug in monotherapy and the effect of combination therapy. Efficacy enhancement by combination therapy was determined as an enhancement factor >1. As shown in Table 1, enhancement of 50 μM TMZ by10 uM PARPi was found in 18 of 20 cultures (90%) of which 10 cultures had a p-value of <0.05. Average and median decrease of viability as compared to TMZ monotherapy was 22.8% and 21.9%, respectively. For high dose TMZ monotherapy, 17 out of 20 (65%) cases were potentiated of which 11 had a p-value <0.05. In this group the average and median reduction in viability was 23% and 28.8% (Table 1). Except for GS41, enrichment factors between high and low dose TMZ were similar or increased with the higher dosing of TMZ, suggesting a dose response effect of combination therapy. In conclusion, 18 out of 20 GSC cultures were coined responders to combination therapy (R), and two MGMT(+) cultures were coined non-responders (NR).

We found that PARPi potentiated four of the MGMT(+) GSC cultures ($p<0.05$); at both low and high dose TMZ. Similarly, in 4 out of 8 MGMT negative cultures we dis- covered additive effect of combination therapy ($p<0.05$). Student's t-test revealed no significant difference between MGMT(+) or MGMT(-) GSCs with regard to ABT-888 potentiation of TMZ-

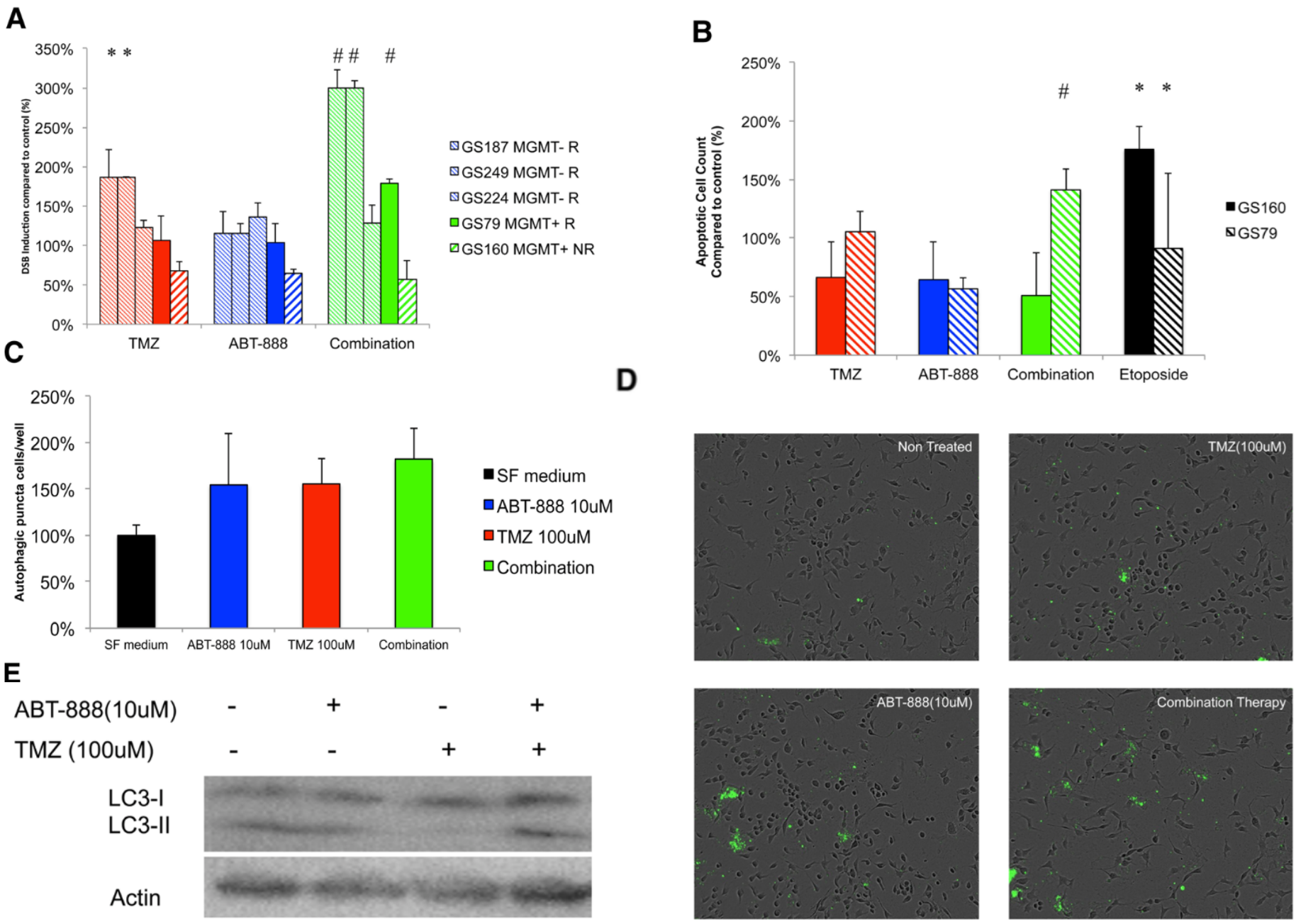

Figure 3 PARP inhibition increases TMZ induced double stranded breaks, autophagy and apoptosis in GSCs. A) DSB induction is significantly enhanced by combination therapy. GSCs, MGMT(+) and MGMT(-) were scored for γH2Ax positive cells, as an indicator for DSB induction,16 hrs post-treatment. GS160 results are all significant as compared to non-treated controls. For the other cultures, significance is indicated as described in the following; * indicates $p < 0,05$ as compared to non-treated controls. # indicates $p < 0.05$ as compared to monotherapy. R = combination therapy responder, NR = non-responder. **B)** Apoptosis induction is significantly enhanced by combination therapy in responder GSCs but not in non-responders. Wells were scored for apoptosis positive cells by live imaging. Read out was performed at 48 hrs post-treatment. Apoptotic cells were significantly ($p < 0.05$) increased after combination therapy as compared to monontherapy in GSC79. For GS160 cells were not affected by TMZ/ABT-888 combination therapy while the positive control (etoposide 0.1 mM) was successfully inducing apoptosis. **C)** TMZ and ABT-888 induce autophagy in GS79, which is augmented by combination therapy. Autophagosomes were counted per well and compared to non-treated controls. Readout was performed 16 hrs post-treatment. Compared to controls, all treatment conditions were significantly increased $p < 0.05$. However, combination therapy vs. monotherapy with ABT-888 or TMZ was found not significantly increased ($p = 0.3$ and $p = 0.4$). **D)** Representative images acquired by the Incucyte FLR of GS79 stained for autophagosomes at indicated treatment conditions. Note the accumulation of speckled dots in treated cells, specifically localized in enlarged cytopathic cells. **E)** Combination therapy enhances autophagic flux as compared to monotherapy in GS79. Western blot 24 hrs post-treatment indicates the accumulation of LC3-II (lipidated isoform) that is indicative for increased autophagic flux. Actin blots serve as loading controls.

therapy (p=0.71 low dose, and p=0.50 high dose respectively). Similarly, TMZ sensitivity as deter- mined by monotherapy screening was not correlated to ABT-888 potentiation (p=0.24 low dose TMZ, p=0.42 high dose TMZ, respectively). In the single culture (GS173) for which the lack of MGMT expression was not correlated to TMZ sensitivity, we found PARPi mediated potentiation of TMZ as well. Thus, PARPi can potentiate TMZ efficacy regardless of the sensitivity to TMZ or MGMT status.

PARP inhibition increases TMZ induced double stranded breaks, autophagy and apoptosis in GSCs

The progression of alkylation based single stranded breaks (SSBs) to double stranded breaks (DSBs) has been proposed to be fatal in cancer cells. While MGMT can facilitate repair of SSBs, the rationale behind the addition of ABT-888 to TMZ is to comprise the DNA- repair cascade

needed to prevent the induction of DSBs after alkylation induced SSB formation. To address this proposed role of DSB induction as an outcome of therapeutic efficacy in our GSC panel, three MGMT(-) and two MGMT(+) GSCs were tested for DSB induction when treated with TMZ, ABT-888 or combination therapy. The induction of DSBs by TMZ monotherapy was significant ($p < 0.01$) in 2 out of 3 MGMT(-) GSCs (Figure 3A). Monotherapy with ABT-888 did not yield a significant increase in DSB induction. Interestingly, DSB induction was not apparent in one non-responder GS160 (MGMT(+)), suggestive of the premise that DSB induction is needed for combination therapy to potentiate TMZ-monotherapy.

Next we assessed the induction of apoptosis and autophagy, two pathways implicated to be upregulated in response to both TMZ and PARP inhibitor treatment [22-24]. We found that, in GS79 (MGMT(+), R), apoptosis was significantly ($p<0.05$) increased by combination therapy as compared to monotherapy (Figure 3B). The resistance to apoptosis induction following drug administration in GS160 further substantiated the hypothesis that DSB induction is mandatory for cell death after combination therapy. Autophagy has been implicated both in the induction of senescence after cytotoxic insult to facilitate DNA repair, as well as the induction of caspase dependent cell death (apoptosis). The induction of autophagy by therapeutic agents can be monitored through the accumulation of autophagic vacuoles by fluorescent microscopy or the conversion of LC3B-I into the lipidated LC3B-II [25]. We found that both TMZ and ABT-888 induced autophagy in GS79 (Figure 3C) through a fluorescence based autophagy induction monitoring kit. In addition, combination therapy was found that have an additive effect with regard to the induction of autophagosomes on microscopic imaging (Figure 3C-D). Furthermore, the conversion of LC3B-I to LC3B-II, a golden standard for the assessment of autophagic flux [26], demonstrated to be increased in combination therapy on western blot (Figure 3E).

Discussion

We here report the potential of ABT-888 as an additive to TMZ chemotherapy for the treatment of GBM. ABT- 888 is a selective inhibitor of both PARP-1 and PARP-2 protein function, which are together responsible for the majority of PAR activity [8]. The results presented here, demonstrate that PARPi decreases proliferation and viability of the glioma cell line T98 and of a substantial subset of patient-derived GSCs. Furthermore, combined treatment with PARPi and TMZ leads to significant potentiation of therapeutic efficacy in the majority of GSCs, irrespective of MGMT protein expression. In addition, we found that MGMT+ GSCs are also significantly more resistant to ABT-888 monotherapy, as compared to MGMT(-) GSCs. We have found evidence that the potentiation of TMZ therapy by ABT-888 is dependent on the induction of DSBs, which coincides with increased apoptosis and autophagy in responsive cells.

Several studies have demonstrated the feasibility of PARPi as an adjuvant in the treatment of malignancies [27]. PARP activity has been implicated in both single stranded break (SSB) repair and double stranded break (DSB) repair [28]. Indeed, PARPi increased the efficacy of both TMZ and other alkylating agents in preclinical models of GBM and other solid tumors [29,30]. Although previous studies have demonstrated the feasibility of this strategy in preclinical models based on serum supplemented conventional cell lines [29,31,32], we here address this form of combination therapy in a panel of patient-derived GSCs. This is important since conventional cell lines have been demonstrated to poorly mimic the genomic and transcriptomic landscape of GBM [19]. In addition, GSCs have been postulated to play an important role in therapy resistance to current standard of care for patients [33-36]. The results for TMZ mono- therapy in our GSC panel are in congruence with previous publications [37-40] and reproduce MGMT protein expression and subsequent TMZ resistance as found in parental tumors [41]. Therefore, this study also confirms that GSC panels are a suitable platform for assessing the potential of TMZ combination therapy with other promising agents.

Although it is expected for most GBM samples to be resistant to monotherapy with PARPi, since most GBM have intact DNA-repair-signaling pathways, testing for ABT-888 monotherapy effect demonstrated that a substantial (20%) part of our panel was sensitive to clinically relevant dosages of ABT-888. This has not been demonstrated in patient derived glioma samples with ABT-888 before, although other PARPi have had similar effects in conventional cell lines [32]. Therefore, we conclude that PARPi could be beneficial to therapeutic efficacy in GBM, apart from interacting synergistically with TMZ. Previous studies have demonstrated phosphatase and tensin homologue (PTEN) deficient cells to be particularly vulnerable to PARPi monotherapy through compromised homologous recombination repair [7]. For T98, susceptibility to PARPi could be related to a mutation in the PTEN gene, as reported for this cell line [42]. In GBM tissue profiling studies, PTEN signaling has been demonstrated to be dysfunctional in 40-65% of GBM cases [43,44]. However, other genes have also been implicated in the efficacy of PARPi in vitro as well, such as BRCA-1/2 or CDK5 [45,46]. Future research on PARPi therapy may therefore benefit from focused research on the identification of predictive molecular signatures for the susceptibility to PARPi mono- or combination therapy in malignant glioma.

Our study shows that PARPi enhances TMZ chemo- therapy in 18 out of 20 cultures at varying doses (90%). The potentiating effect of PARPi to TMZ is found in both TMZ resistant and sensitive cultures. Combination therapy was effective in 6 out of 8 MGMT expressing GSC cultures, suggesting that the additive effect is independent of MGMT status. At the time of finalizing this manuscript, Tentori and colleagues, published a similar study that demonstrated synergistic effect of combined PARPi (inhibitor GPI-15427) and TMZ therapy in a panel of 10 GSCs, data which are largely analogous with our findings [47]. These results indicate that PARPi has the potential to improve therapeutic efficacy of TMZ in both responders and non-responders to TMZ monotherapy.

Since the current chemo-irradiation treatment regimen has considerable side-effects, the possible potentiation of TMZ by PARPi may also be considered in the context of TMZ dose reduction, leading to reduced side-effects, and prolonged therapeutic dosing in patients undergoing chemo-irradiation. As combination therapy efficacy may be unrelated to MGMT status, this may provide for an interesting alternative to patients with a

recurrence after TMZ treatment. As such, other alkylating agents (e.g CCNU in the context of PCV, which is frequently used for recurrent oligodendroglioma) may be of considerable interest to study in combination with PARPi [48].

The mechanisms through which PARPi enhances TMZ induced cytotoxicity may be ambiguous. For one, after the induction of SSBs by TMZ, PARPi prevents the binding of PARP1-2 to damaged DNA foci to facilitate BER. The PARPi mediated prevention of BER enhances the formation of DSBs, which would eventually be lethal. Our DSB and apoptosis induction assays provide compelling evidence that this hypothesis holds truth in combination therapy responder GSCs. Next to that, the induction of autophagy after TMZ or ABT-888 might provide an alternative mode of programmed cell death that is induced after combination therapy. Whereas monotherapy might induce autophagy as a mode of cellular adaptation to the cytotoxic event, the cumulative stress elicited by combination therapy might induce autophagic cell death, which has been described as a context dependent mode of programmed cell death induced after a tipping point of autophagic flux is reached [49].

Conclusion

This study underscores the potential of PARPi as an enhancer of TMZ treatment of patients with GBM. Furthermore, in select cases PARPi could elicit therapeutic effect as a single agent. We have demonstrated the efficacy of PARPi in GSCs, which are a more relevant in vitro model for GBM than the conventional cell lines used previously. PARPi-mediated potentiation of TMZ therapy is independent of TMZ monotherapy sensitivity or MGMT protein expression, which makes PARPi a promising drug for addition to the current standard of care chemo-irradiation regime.

Acknowledgements

Part of this work was funded by the Foundation STOPbraintumors.

References

1. Huse JT, Holland EC. Targeting brain cancer: advances in the molecular pathology of malignant glioma and medulloblastoma. Nat Rev Cancer. 2010;10(5):319–31.

2. Stupp R, Mason WP, van den Bent MJ, Weller M, Fisher B, Taphoorn MJ, et al. Radiotherapy plus concomitant and adjuvant temozolomide for glioblastoma. N Engl J Med. 2005;352(10):987–96.

3. Noushmehr H, Weisenberger DJ, Diefes K, Phillips HS, Pujara K, Berman BP, et al. Identification of a CpG island methylator phenotype that defines a distinct subgroup of glioma. Cancer Cell. 2010;17(5):510–22.

4. Weller M, Stupp R, Reifenberger G, Brandes AA, van den Bent MJ, Wick W, et al. MGMT promoter methylation in malignant gliomas: ready for personalized medicine? Nat Rev Neurol. 2010;6(1):39–51.

5. Hegi ME, Diserens AC, Gorlia T, Hamou MF, de Tribolet N, Weller M, et al. MGMT gene silencing and benefit from temozolomide in glioblastoma. N Engl J Med. 2005;352(10):997–1003.

6. Agnihotri S, Gajadhar AS, Ternamian C, Gorlia T, Diefes KL, Mischel PS, et al. Alkylpurine-DNA-N-glycosylase confers resistance to temozolomide in xenograft models of glioblastoma multiforme and is associated with poor survival in patients. J Clin Invest. 2012;122(1):253–66.

7. McEllin B, Camacho CV, Mukherjee B, Hahm B, Tomimatsu N, Bachoo RM,
et al. PTEN loss compromises homologous recombination repair in astrocytes: implications for glioblastoma therapy with temozolomide or poly (ADP-ribose) polymerase inhibitors. Cancer Res. 2010;70(13):5457–64.

8. Wahlberg E, Karlberg T, Kouznetsova E, Markova N, Macchiarulo A, Thorsell AG, et al. Family-wide chemical profiling and structural analysis of PARP and tankyrase inhibitors. Nat Biotechnol. 2012;30(3):283–8.

9. Pollard SM, Yoshikawa K, Clarke ID, Danovi D, Stricker S, Russell R, et al. Glioma stem cell lines expanded in adherent culture have tumor-specific phenotypes and are suitable for chemical and genetic screens. Cell Stem Cell. 2009;4(6):568–80.

10. Lee J, Kotliarova S, Kotliarov Y, Li A, Su Q, Donin NM, et al. Tumor stem cells derived from glioblastomas cultured in bFGF and EGF more closely mirror the phenotype and genotype of primary tumors than do serum-cultured cell lines. Cancer Cell. 2006;9(5):391–403.

11. Balvers RK, Kleijn A, Kloezeman JJ, French PJ, Kremer A, van den Bent MJ, et al. Serum-free culture success of glial tumors is related to specific molecular profiles and expression of extracellular matrix-associated gene modules. Neuro Oncol. 2013;15(12):1684–95.

12. Muscal JA, Thompson PA, Giranda VL, Dayton BD, Bauch J, Horton T, et al. Plasma and cerebrospinal fluid pharmacokinetics of ABT-888 after oral administration in non-human primates. Cancer Chemother Pharmacol. 2010;65(3):419–25.

13. Rosso L, Brock CS, Gallo JM, Saleem A, Price PM, Turkheimer FE, et al. A new model for prediction of drug distribution in tumor and normal tissues: pharmacokinetics of temozolomide in glioma patients. Cancer Res. 2009;69(1):120–7.

14. Chou TC. Drug combination studies and their synergy quantification using the Chou-Talalay method. Cancer Res. 2010;70(2):440–6.

15. Biederbick A, Kern HF, Elsasser HP. Monodansylcadaverine (MDC) is a specific in vivo marker for autophagic vacuoles. Eur J Cell Biol. 1995;66(1):3–14.

16. Berghauser Pont LM, Spoor JK, Venkatesan S, Swagemakers S, Kloezeman JJ, Dirven CM, et al. The Bcl-2 inhibitor Obatoclax over-

comes resistance to histone deacetylase inhibitors SAHA and LBH589 as radiosensitizers in patient-derived glioblastoma stem-like cells. Genes Cancer. 2014;5(11–12):445–59.

17. Costello JF, Futscher BW, Tano K, Graunke DM, Pieper RO. Graded methylation in the promoter and body of the O6-methylguanine DNA methyltransferase (MGMT) gene correlates with MGMT expression in human glioma cells. J Biol Chem. 1994;269(25):17228–37.

18. van Nifterik KA, van den Berg J, van der Meide WF, Ameziane N, Wedekind LE, Steenbergen RD, et al. Absence of the MGMT protein as well as methylation of the MGMT promoter predict the sensitivity for temozolomide. Br J Cancer. 2010;103(1):29–35.

19. Li A, Walling J, Kotliarov Y, Center A, Steed ME, Ahn SJ, et al. Genomic changes and gene expression profiles reveal that established glioma cell lines are poorly representative of primary human gliomas. Mol Cancer Res. 2008;6(1):21–30.

20. Ostermann S, Csajka C, Buclin T, Leyvraz S, Lejeune F, Decosterd LA, et al. Plasma and cerebrospinal fluid population pharmacokinetics of temozolomide in malignant glioma patients. Clin Cancer Res. 2004;10(11):3728–36.

21. Lalezari S, Chou AP, Tran A, Solis OE, Khanlou N, Chen W, et al. Combined analysis of O6-methylguanine-DNA methyltransferase protein expression and promoter methylation provides optimized prognostication of glioblastoma outcome. Neuro Oncol. 2013;15(3):370–81.

22. Barazzuol L, Jena R, Burnet NG, Meira LB, Jeynes JC, Kirkby KJ, et al. Evaluation of poly (ADP-ribose) polymerase inhibitor ABT-888 combined with radiotherapy and temozolomide in glioblastoma. Radiat Oncol. 2013;8:65.

23. Albert JM, Cao C, Kim KW, Willey CD, Geng L, Xiao D, et al. Inhibition of poly (ADP-ribose) polymerase enhances cell death and improves tumor growth delay in irradiated lung cancer models. Clin Cancer Res. 2007;13(10):3033–42.

24. Ethier C, Tardif M, Arul L, Poirier GG. PARP-1 modulation of mTOR signaling in response to a DNA alkylating agent. PLoS One. 2012;7(10):e47978.

25. Jiang H, White EJ, Conrad C, Gomez-Manzano C, Fueyo J. Autophagy pathways in glioblastoma. Methods Enzymol. 2009;453:273–86.

26. Klionsky DJ, Abdalla FC, Abeliovich H, Abraham RT, Acevedo-Arozena A, Adeli K, et al. Guidelines for the use and interpretation of assays for monitoring autophagy. Autophagy. 2012;8(4):445–544.

27. Kummar S, Chen A, Parchment RE, Kinders RJ, Ji J, Tomaszewski JE, et al. Advances in using PARP inhibitors to treat cancer. BMC Med. 2012;10:25.

28. Krishnakumar R, Kraus WL. The PARP side of the nucleus: molecular actions, physiological outcomes, and clinical targets. Mol Cell. 2010;39(1):8–24.

29. Tentori L, Portarena I, Torino F, Scerrati M, Navarra P, Graziani G. Poly(ADP-ribose)
polymerase inhibitor increases growth inhibition and reduces G(2)/M cell accumulation induced by temozolomide in malignant glioma cells. Glia. 2002;40(1):44–54.

30. Donawho CK, Luo Y, Penning TD, Bauch JL, Bouska JJ, Bontcheva-Diaz VD, et al. ABT-888, an orally active poly(ADP-ribose) polymerase inhibitor that potentiates DNA-damaging agents in preclinical tumor models. Clin Cancer Res. 2007;13(9):2728–37.

31. Palma JP, Wang YC, Rodriguez LE, Montgomery D, Ellis PA, Bukofzer G, et al. ABT-888 confers broad in vivo activity in combination with temozolomide in diverse tumors. Clin Cancer Res. 2009;15(23):7277–90.

32. Tentori L, Leonetti C, Scarsella M, D'Amati G, Vergati M, Portarena I, et al. Systemic administration of GPI 15427, a novel poly(ADP-ribose) polymerase-1 inhibitor, increases the antitumor activity of temozolomide against intracranial melanoma, glioma, lymphoma. Clin Cancer Res. 2003;9(14):5370–9.

33. Bao S, Wu Q, McLendon RE, Hao Y, Shi Q, Hjelmeland AB, et al. Glioma stem cells promote radioresistance by preferential acti-

vation of the DNA damage response. Nature. 2006;444(7120):756–60.

34. Beier D, Schriefer B, Brawanski K, Hau P, Weis J, Schulz JB, et al. Efficacy of clinically relevant temozolomide dosing schemes in glioblastoma cancer stem cell lines. J Neurooncol. 2012;109(1):45–52.

35. Beier D, Schulz JB, Beier CP. Chemoresistance of glioblastoma cancer stem cells–much more complex than expected. Mol Cancer. 2011;10:128.

36. Liu G, Yuan X, Zeng Z, Tunici P, Ng H, Abdulkadir IR, et al. Analysis of gene expression and chemoresistance of CD133+ cancer stem cells in glioblastoma. Mol Cancer. 2006;5:67.

37. Glas M, Rath BH, Simon M, Reinartz R, Schramme A, Trageser D, et al. Residual tumor cells are unique cellular targets in glioblastoma. Ann Neurol. 2010;68(2):264–9.

38. Clement V, Sanchez P, de Tribolet N, Radovanovic I, Ruiz I, Altaba A. HEDGEHOG-GLI1 signaling regulates human glioma growth, cancer stem cell self-renewal, and tumorigenicity. Curr Biol. 2007;17(2):165–72.

39. Beier D, Rohrl S, Pillai DR, Schwarz S, Kunz-Schughart LA, Leukel P, et al. Temozolomide preferentially depletes cancer stem cells in glioblastoma. Cancer Res. 2008;68(14):5706–15.

40. Blough MD, Westgate MR, Beauchamp D, Kelly JJ, Stechishin O, Ramirez AL, et al. Sensitivity to temozolomide in brain tumor initiating cells. Neuro Oncol. 2010;12(7):756–60.

41. Villalva C, Cortes U, Wager M, Tourani JM, Rivet P, Marquant C, et al. O6-Methylguanine-Methyltransferase (MGMT) promoter methylation status in glioma stem-like cells is correlated to temozolomide sensitivity under differentiation-promoting conditions. Int J Mol Sci. 2012;13(6):6983–94.

42. Ishii N, Maier D, Merlo A, Tada M, Sawamura Y, Diserens AC, et al. Frequent co-alterations of TP53, p16/CDKN2A, p14ARF, PTEN tumor suppressor genes in human glioma cell lines. Brain Pathol. 1999;9(3):469–79.

43. Ohgaki H, Kleihues P. Genetic alterations and signaling pathways in the evolution of gliomas. Cancer Sci. 2009;100(12):2235–41.

44. Cancer Genome Atlas Research, N. Comprehensive genomic characterization defines human glioblastoma genes and core pathways. Nature. 2008;455(7216):1061–8.

45. Turner NC, Lord CJ, Iorns E, Brough R, Swift S, Elliott R, et al. A synthetic lethal siRNA screen identifying genes mediating sensitivity to a PARP inhibitor. EMBO J. 2008;27(9):1368–77.

46. Dedes KJ, Wilkerson PM, Wetterskog D, Weigelt B, Ashworth A, Reis-Filho JS. Synthetic lethality of PARP inhibition in cancers lacking BRCA1 and BRCA2 mutations. Cell Cycle. 2011;10(8):1192–9.

47. Tentori L, Ricci-Vitiani L, Muzi A, Ciccarone F, Pelacchi F, Calabrese R, et al. Pharmacological inhibition of poly(ADP-ribose) polymerase-1 modulates resistance of human glioblastoma stem cells to temozolomide. BMC Cancer. 2014;14(1):151.

48. van den Bent MJ, Carpentier AF, Brandes AA, Sanson M, Taphoorn MJ, Bernsen HJ, et al. Adjuvant procarbazine, lomustine, and vincristine improves progression-free survival but not overall survival in newly diagnosed anaplastic oligodendrogliomas and oligoastrocytomas: a randomized European Organisation for Research and Treatment of Cancer phase III trial. J Clin Oncol. 2006;24(18):2715–22.

49. Galluzzi L, Vitale I, Abrams JM, Alnemri ES, Baehrecke EH, Blagosklonny MV, et al. Molecular definitions of cell death subroutines: recommendations of the Nomenclature Committee on Cell Death 2012. Cell Death Differ. 2012;19(1):107–20.

4

Malignant glioma in vitro models: on the utilization of stem-like cells

Chapter was accepted for publication as

Malignant glioma in vitro models: on the utilization of stem-like cells and the recapitulation of molecular subtypes *Rutger K Balvers, Clemens MF Dirven, Sieger Leenstra and Martine LM Lamfers*

Current Cancer Drug Therapeutics; Glioblastoma Multiforme

ABSTRACT

Recent publications on the molecular characterization of malignant glioma have had profound impact on the appreciation of tumoral heterogeneity within and between patients. Both these phenomena are implicated in the variability in clinical outcome between patients, as well as the inevitable recurrence of these tumors after conventional treatment. The advent of selective cell culture protocols for the propagation of patient-derived glioma stem-like cells (GSCs) provides researchers the ability to selectively study the cells that could be at the root of tumor proliferation and resistance to therapy. As these techniques are widely applied in contemporary studies and becoming the preferred in vitro model, molecular characterization of GSCs is considered pivotal for the identification and advancement of novel therapies for this devastating disease.

This review aims to provide an overview of canonical molecular alterations defining subtypes of malignant glioma as derived from genotypic, transcriptomic and epigenetic profiling in relation to their representation in GSC models. The distribution of these hallmark alterations as found in characterization studies of GSCs is compared between publications. Finally, conclusions of these studies with respect to coverage of driving alterations and translational relevance are provided. By doing so, we provide a contemporary overview of scientific results derived from GSC models and hopefully create appreciation of the advantages and caveats of utilizing these models for studying malignant glioma.

1. INTRODUCTION

Malignant glioma comprises a clinically and molecularly heterogeneous group of central nervous system (CNS) malignancies that are currently incurable. Histological examination of malignant glioma, differentiates tumors by the glial cell lineage that is most abundantly represented within tissue biopsies (astrocytic, oligodendroglial, and mixed oligo-astrocytic tumors[1]. The aggressiveness of the tumor is graded by signs of proliferation and neovascularization. Glioblastoma (GBM), the end-stage of the tumor, is characterized by an abundance of mitotic cells and necrosis. The optimal treatment regime for GBM is gross total resection followed by intensive chemo-irradiation, resulting in a median survival of 15 months after the initial diagnosis[2].

Recent publications, in which large collections of GBM tissue were molecularly characterized on both genotypic, transcriptomic and epigenetic profiling platforms, revealed discriminative molecular signatures by which tumors can be subtyped into several clusters based on molecular similarity. Attempts to establish a parallel grading system with molecular predictors for malignant glioma are ongoing and are expected to eventually solve several discrepancies (e.g. inter-observer heterogeneity and large variation in clinical outcome within histological entities) that occur using histopathological classification of tumors[3-6].

Similar to other malignancies, promising in vitro discoveries with regard to GBM biology have been numerous, while the translation of these successes into clinical application remains rare[7, 8]. Amongst several explanations, the lack of translational success lies partly within the experimental design of preclinical studies. To adequately predict therapeutic response in patients, disease models (whether in vitro or in vivo) are utilized on the premise that they recapitulate features of the disease as accurate as possible.

For GBM, as for other malignancies, the widespread use of previously available clonal cell lines and derived xenografts may have hampered the translation of promising agents since these lacked several crucial factors (e.g. intratumoral heterogeneity, diffuse infiltrative growth, acquired resistance to therapy, and the interplay with the host immune system) that are now understood to dictate disease resistance to therapy[9]. With the advent of stem cell research, and the subsequently proposed cancer stem cell theory, the field of GBM research has embraced a variety of culture assays that may offer a more accurate representation of GBM biology and therefore be more predictive of the therapeutic efficacy of promising (combination) therapies. What these assays generally have in common is the omittance of serum from the culture medium, combined with the addition of several supplements with nutrients and mitogens that favor neuronal proliferation (of which EGF and bFGF are the most commonly used)[10]. Expansion of spheroid bodies or aggregates of freshly dissociated patient derived tissue under these conditions leads to neurospheres (or tumorspheres or gliomaspheres). For practical reasons with regard to drug screening purposes, others have demonstrated matrix-protein based coatings to allow the culture of similar cells retaining GSC marker expression and xenograft-initiating capacity[11-13].

Based on patient-derived GBM tissue, various groups have reported on the establishment of heterogeneous populations of primary cultures in specified media designed to select for glioma-initiating (or stem) cells (from here on referred to as GSCs)[14-17]. These culture assays potentially provide the opportunity to investigate a form of personalized medicine since patients' debulked tumor specimens can be propagated as GSC lines that may be individually tested using in vitro compound libraries. Promising and intriguing as this may sound, to date several questions remain unanswered with regard to the applicability and translational value of these GSC selective culturing methods. For instance, since there are no stringent rules in culture establishment or propagation protocols, nor in techniques applied for validation, there can be quite some variability in applied GSC culture methods between laboratories[18]. In addition, the yield of tumor samples that can be successfully propagated under these serum free conditions is limited (40-67%), which hints at a selection bias [17, 19, 20]. Furthermore, the ability to derive GSC cultures from a GBM has been proposed as a prognostic factor for overall survival[19, 21], although this could not be reproduced in larger data sets[17]. To date, no studies have been published that validate GSC derived evidence of potentially efficacious therapies through randomized controlled trials in humans.

These are just a few of many caveats, which are relevant to the interpretation of GSC based studies. Current review of the literature is intended to provide a comprehensive overview of recently published cell culture characterization efforts and discuss the advantages and short

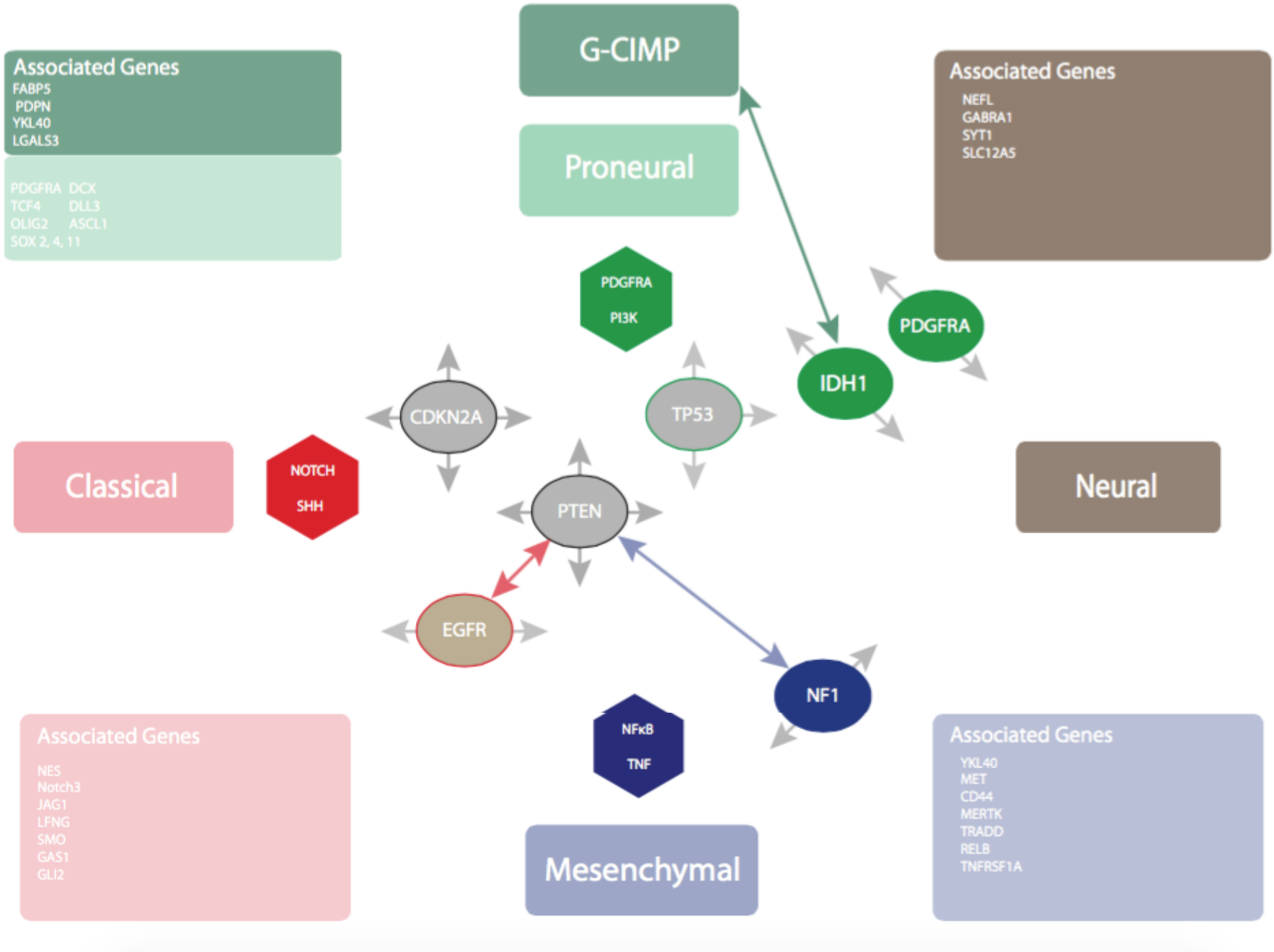

Figure 1) Overview of the TCGA coined molecular subtypes of GBM and the respective canonical somatic mutations and significantly differentiating genes within the boxes. The driving somatic alterations are depicted in the center. Color coding demonstrates significant relation to the defined subtype found in the square boxes. Gray coding suggests that the genes have shared distribution between the subtypes. The presence of arrows around a gene indicates that the alteration is shared between the subtypes that the arrow points towards.

comings of GSC culture methodology. At last, we summarize the implications of these publications for GBM research in the near future.

2. Molecular profiling studies of GBM

Molecular analysis of GBM has been performed over the last 30 years[22], however, only as of the last 10 years have large multi-institutional cohorts of GB tissue, been molecularly analyzed in an integrative way using high throughput platforms. From 2008 through 2013 The Cancer Genome Atlas (TCGA) initiative published, in serial, the largest cohort of GBM tissue samples that have been analyzed on a multi-platform basis, integrating genomic, expression profiling and epigenetic data[23-25]. These studies confirmed some of earlier findings of other groups with regard to expression profiling and genotyping of GBM [26-29]. While the TCGA glioma dataset originally included GBM samples only, others have included low-grade gliomas as well [28, 30-33].

As of yet, there is no consensus regarding the number of gene expression-based clusters for malignant glioma. However, for GBM, the four clusters that were coined in the TCGA studies (Proneural, Neural, Mesenchymal and Classical; PN, NEU, MES and CLA, respectively) have been applied to characterize cell cultures most frequently [17, 20, 34-37]. Others have reported these subgroups to be relevant to low grade gliomas as well [38, 39], however, a caveat resides in the fact that the TCGA subtypes were consensus clustered and validated on GBM tissue, which therefore constitutes a bias towards signifier genes that may not discriminate between subgroups of low grades. In line with this, it cannot be deemed coincidental that most LGGs are therefore coined proneural in TCGA, while more diverse outcome of molecular subtyping has been described in cohorts based on WHO grade II-IV glioma[29, 31].

Although there is overlap between the four TCGA clusters at the level of involved signaling pathways and distribution of genetic mutations, it is possible to distill segregating features for each cluster. Proneural tumors are correlated to oligodendroglial and proneural marker expression and have activated PI3K and PDGFRA signaling pathway related gene expression. There is a higher frequency of somatic mutations and copy number changes in PDGFRA, TP53, PI3KCA or PI3KR1 and IDH1. The classical subtype is characterized by upregulated Notch and Hedgehog pathway signaling. Combined EGFR focal amplifications and PTEN alterations (either deletions or somatic mutations) are also characteristic for CLA tumors. Furthermore, TP53 mutations are generally not found within CLA subtype tumors. The lack of TP53 mutations is also the main segregator between CLA and NEU tumors. The Neural subtype is most resemblant of non-neoplastic (control) brain expression profiles and is segregated from the other clusters by enriched neural expression markers such as NEFL, GABRA1, SYT1 and SLC12A5. While EGFR mutations are abundant in each cluster, EGFR and TP53 co-mutations are only found in PN and NEU tumors, whereas TP53-PTEN and TP53-NF1 co-mutations are more suggestive for mesenchymal tumors. The MES expression profile is characterized by NFκB and TNF signaling pathway genes and mesenchymal differentiation associated markers such as YKL-40 (also known as CHI3L1), MET and CD44. In relation to TNF signaling, CD68 and other microglial markers are overexpressed compared to other tumors suggesting a more pronounced interaction with the immune system when compared to other GBM subtypes. Somatic mutations of NF1 and RB are overrepresented in MES when compared to other subtypes, and co-mutations with PTEN or TP53 are even more suggestive of MES tumors.

Epigenetic profiling of GBM has segregated six separated groups for which the so-called Glioma-CPG-Island-Methylation Profile (GCIMP) cluster stands out most distinctly based on prolonged survival and enrichment of segregating somatic mutations (IDH-1, p53 and ATRX)[25]. Expression profiling combined with methylation profiling demonstrated that the prognostically favorable PN subtype is enriched for hypermethylated (GCIMP) samples, which appears to confound the survival advantage of PN tumors. Strikingly, the PN tumors that were not GCIMP, were demonstrated to share an equally poor prognosis as the non-hypermethylated samples in the other expression profiling clusters (CLA, MES and NEU)[24].

In addition, GCIMP tumors were enriched for MGMT promoter methylation, which by itself is an established marker for therapeutic response (addressed in paragraph 3.1). Intriguingly, the large retrospective analysis of treated samples in the TCGA cohort recapitulated the value of MGMT promoter methylation as a predictor of therapeutic response solely in the CL subtype[25]. In the next paragraphs we will discuss the recapitulation of these driving molecular alterations within the GSCs that have been characterized on these platforms to date.

2.1 Distribution of GBM gene expression profiles amongst GSC cultures compared to serum supplemented cultures.

With the advent of the cancer stem cell hypothesis, the culture assays for propagating stem cells were repurposed to facilitate selective propagation of tumor stem-like cells. When this was demonstrated to be successful, malignant stem cell markers where sought after to specifically identify and propagate the “ driver” cells within tumor bulk[18]. For GBM, a number of GSC markers were established which can be selected for by flow-cytometry such as CD133, CD15, CD44, A2B5, Sox2 and many others. However, none of these markers have been consistently proven selective for GSC’s when compared to non-neoplastic or non-GSC tumor cells. Nor does the lack of expression rule out stem cell like behavior of tumor cells with regard to clonal expansion or xenografts derivation[20, 40].

Although several groups had already reported on the isolation of GSCs through establishing cell cultures from GBM specimens under serum free (SF) culture conditions, it was not until 2006 that a large scale multiplatform study, comparing molecular characteristics of SF cultures to serum supplemented (SS) counterparts, was published by Lee et al.[23]. Serum-based cell cultures were shown to lose the transcriptomic profile found in the original tumor as well as their tumorigenic capacity in mice, whereas SF cultures retained these features. The superior recapitulation of gene expression signatures by SF compared to SS cultures was later reproduced by several other groups[17, 37, 41, 42].

These first studies also found that SF cultures had increased expression of several neuronal development related genes, such as NOTCH, Patched and SOX genes. In addition, OLIG2, NES and DLL3 were found to be overexpressed in comparison to cell lines. Comparative gene ontology analysis between SF and SS cultured clones, from the same parental tumor specimen, reported enrichment for genes annotated to be involved in (nervous system) development, cell to cell signaling, morphology, and neurological diseases in the SF clones. In contrast, serum cultured cells were enriched for proliferation, cell death and cancer-specific annotated genes[42].

Next the distribution of TCGA subtypes in GSC culture models was assessed by a number of groups. Several groups have established that tumors from all different transcriptomic subtypes of GBM can be propagated in vitro[20, 34]. However, the distribution of successfully propagated cases was not equal between subtypes[17].

2.2 Distribution of hallmark genomic alterations in GBM amongst SF cultures

Several groups have investigated whether propagation under SF conditions selects for genomic alterations. The frequent copy number events that have been reported in GBM have all been recapitulated in serum-free cultured GSCs (Table 1). Strikingly, it was also demonstrated in a number of publications that all GSCs harbor the frequently found amplification of chromosome 7(p) and deletion of chromosome 10(q) (or focally of PTEN). In addition, deletions of the CDKN2a/b fragment on 9(p) are frequently found. As such, these CNAs appear to confer a selective advantage for the survival of GBM cells under defined serum-free conditions. To a lesser frequency, just as seen in the entire patient population, copy number alterations are found on segments containing NF1, RB, PDGFR, CDK4, CDK6 and Myc are found.

The most frequently reported somatic focal mutations in GBM are recapitulated in GSCs as well, with the exception of IDH, ATRX and telomerase promoter mutations. The presence of the IDH-1 mutation is related to notorious difficulties in the propagation of these tumors in vitro. Reports on successful propagation and establishment of IDH1-mutant GBM models are scarce and appear to depend on propagation in xenograft models[43, 44]. We previously demonstrated that attempts to establish long-term GSC cultures from IDH-1 mutant gliomas (n=21), did not yield a single successful culture. The short-term SF and SS cultures all demonstrated loss of the mutation within five passages[17, 43, 45, 46]. The ATRX and (mutually exclusive) TERT promoter mutations have not yet been reported in the literature in the context of cell culture models at the time of writing this manuscript.

As the successful propagation of GSCs may be a reflection of a biological phenotype, several publications investigated the requisite molecular constitution of tumors for successful serum free propagation. At the moment of drafting this review, definitive evidence of the molecular phenotype mandatory for SF propagation is not available. The most consistently reported trait of GSCs is the co-appearance of Chr.7p/10q alterations, which may coincide with EGFR and PTEN function.

Chen et al, who meticulously analyzed multiple common CNA's, and other predispositions of the parent tumor that could influence successful propagation (TP53, p16, PDGFRA, CD133) exclusively found PTEN to be significantly associated[20]. Retrospective analysis of previous publications suggests that this is in line with data of other publications in which 10q deletions or PTEN mutations were frequently discovered with SRY/FISH and aCGH/SNP analysis (Table 1). In addition, others have reproduced these findings in later studies as well[17]. On the contrary, karyotyping studies have demonstrated polyploidy for chromosome 10 in parental tumor tissue of GSCs[47]. It was found, however, that this does not guarantee wild-type PTEN function since other mechanisms of PTEN inactivation (such as epigenetic silencing, focal mutations or post-translational inhibition[48]) have been demonstrated to occur in frequently in such tumors. This finding, rules out a mandatory loss of chromosome 10(q) for successful in vitro propagation under serum free conditions [47, 49], however definitive evidence as to the mandatory dysfunction of the PTEN gene remains to be published. In line with this subject; for NSCs it was demonstrated that a selection of rapidly proliferating cells are induced as the result of knockout studies in the PI3K-AKT-FOXO pathway where PTEN acts as an important checkpoint, advocating for an advantage for PTEN loss for cell proliferation in SF assays[50, 51]. In line with this, PI3KR1 and PI3KCA mutations or decreased protein expression have been found in GSCs as well[17].

An additional interesting observation is the gradual loss of focal amplifications of the EGFR locus over serial passaging of cultures [52, 53]. This is surprising since virtually all SF propagated cultures have gains on chromosome 7, which harbors the EGFR gene, and retain these over multiple passages. This may suggest that a clonal population of cells containing high focal amplifications lose their selective advantage when there is an abundance of EGF. This loss of focal amplifications can be prevented by omitting EGF from the culture medium[52]. In addition, it was demonstrated that these high focal amplifications of EGFR and/or its EGFRvIII mutant, contribute to the aggressiveness of the tumor in xenografts[52].

While both above-discussed CNA's (del 10q, amp 7p) are frequent events in GBM (80% of adult GBM), a substantial group of tumors do not propagate (10-40%) on SF medium [17, 19, 20]. In this regard, it is interesting to note a recent publication by Ozawa and colleagues that demonstrated non-GCIMP tumors to originate from a common precursor with Chr7p-10q alterations as a shared early event[54]. Intriguingly the causal driver alteration attained from Chr7p gains was deemed to be increased PDGFA signaling, instead of the widely assumed EGFR amplifications that co-occurs so frequently, but is demonstrated to be a later event.

Taken together, GSCs selectively cover the majority of non-GCIMP GBM, which is congruent with the distribution of the TCGA subtypes in GSCs.

2.3 Methylation-profiling of GSCs

With the advent of high-throughput methylation profiling, several papers have indicated the relevance of epigenetic subgroups to clinical

behavior (prognosis, localization and possible therapeutic response) of malignant gliomas with similar histology and grading[24, 25, 55, 56]. As such, the interest for the driving epigenetic signatures in GBM, and the recapitulation hereof in GSCs, has led to a number of publications investigating epigenetic status of in vitro GBM cells[34, 48, 57, 58].

Stricker et al reported GSCs to share epigenetic anomalies as found in 67 TCGA profiled patients; however, a paired analysis of cultures and primary tumors was not performed. Evidence is provided that the epigenetic state of these cells can be influenced by known stem cell transcription factors and cytokines, suggestive of adaptation based on microenvironmental cues[59]. Baronchelli et al noted that the methylation profile in three GSCs was similar to fetal forebrain neural stem cell and (non-paired) GBM controls. These authors discerned a panel of 10 GSC specific methylated promoter regions, however, the lack of paired controls makes these results difficult to interpret in the context of recapitulation of epigenetic phenotype in SF culture[48]. Bhat et al reported a drift of the epigenetic state in vitro under SF conditions. When testing for a panel of GCIMP associated promoters, the authors demonstrated a GCIMP profile in GSCs derived from MES subtyped tumors after serial passaging under SF conditions [34]. This suggests a selective advantage (or medium based induction) of a GCIMP epigenetic signature under SF culturing conditions. This is remarkable since GCIMP tumors did not proliferate under SF conditions. Whether this drift towards a GCIMP state is driven by the medium or relates to selective advantage for incidental GCIMP clones in an otherwise MES tumor was not elucidated. The therapeutic response to radiation therapy was related to PN or MES transcriptomic and epigenetic state, with the latter being more resistant. This is relevant especially since epigenetic drift to CIMP status was already observed in low passages ($p<2$). The described epigenetic drift of GSCs from the primary tumor was reproduced in a report by Baysan and co-authors [58]. Contrary to Bhat et al, these authors did find evidence of reconstitution of MES epigenetic condition in xenografts, suggesting once more a role for the microenvironment in dictating the epigenetic state. The up regulation of the PRMT5 gene under SF condition was identified as a possible driving event for hypermethylation in GSCs. This literature on epigenetics in GSCs, albeit sparse compared to transcriptomic and genetic characterization, provides some intriguing evidence with regard to the possible limitations of the GSC model for in vitro studies. Additional studies are warranted to further inquire into the epigenetic drift towards a PN methylation profile and its relevance in tumor behavior including drug response.

3.0 Translational relevance of SF cultures with regard to drug screening assays

Since most of these studies have been set-up to interrogate hypotheses built around the cell of origin, and the canonical pathways discriminating between bulk tumor cells and initiating tumor cells, very little is published on the predictive value of SF cultures in drug screening experiments. A sound estimate of translational value can only be made after evaluation of clinical trials based on preclinical models that utilized GSCs and GSC-based xenografts. At the time of writing this manuscript, we are not aware of any of such trials being finished. We therefore chose to elaborate on evaluating the prognostic value of SF models by weighing them against molecular markers used for predicting clinical response.

3.1 Treatment response characteristics to temozolomide in GSCs

As mentioned before, the clinical outcome and response to temozolomide (TMZ), the current golden standard chemotherapeutic in the treatment of newly diagnosed GBM, is related to the MGMT protein status in the tumor [60]. Since most of the therapeutic alternatives to the current regimen will probably first be implemented after, or concurrent with, TMZ the manner of MGMT promoter status recapitulation in vitro is of pivotal importance to translational relevance of GSCs. Numerous groups have investigated GSC response to TMZ, and the expression of MGMT protein and promoter methylation, with varying results [61-67]. While initial reports suggested GSCs to be more resistant to TMZ than the non-GSC/serum cultured counterparts[67], this was not reproduced by others[61, 68]. In most GSCs the overall promoter methylation status of MGMT appears to be congruent between GSCs and parental tumors[69]. As in patients, MGMT gene transcript and protein expression seem to predict in vitro TMZ response [65, 70]. Furthermore, the MGMT expression in GSCs was shown to correlate to patient survival in at least the majority of samples in one study[71]. As the interindividual variability to TMZ therapy is recapitulated in panels of GSC, it may be expected that GSCs serve as a proper tool for predicting therapeutic response to TMZ in patients.

3.2. GSC models for GCIMP glioma

With regard to the molecular heterogeneity between individuals observed with malignant glioma, GSCs seem to recapitulate most subtypes, as described earlier. However, in vitro models for the clinically more favorable subtypes of the disease (IDH-1 mutant, GCIMP and 1p19q deletion harboring tumors) are to date only sparsely available as patient-derived cell culture models. To date, no publications exist that have demonstrated successfully derived GSCs from GCIMP determined tumors. While the GCIMP epigenetic signature is induced by SF medium in cultures that are non-GCIMP[34], intriguingly, the GCIMP status of the tumors appears incompatible with the establishment of cultures under SF conditions[17]. The underlying mechanism of this presumed discrepancy is at the moment of writing unclear. Possible explanations may be sought for instance in intolerance to dissociation procedures, mandatory stromal interactions for tumor propagation [58], or induced senescence by agents in the SF medium[72]. Since a large proportion of low grade glioma (LGG) patients are GCIMP[38], the decreased propensity of LGG to proliferate under SF conditions[17], may be related to this problem. The GCIMP tumors, together with tumors bearing the previously mentioned Ch7p10q CNA trait, cover whole spectrum of malignant glioma subtypes in adults. Therefore, the lack of GCIMP tumor proliferation, irrespective of IDH1-mutation, argues for a selection bias in GSC culture for a specific subgroup of the more aggressive phenotype. Whilst one could argue that the unfavorable traits of the higher grades of this disease deserve to be addressed more urgently, the potential clinical impact of new therapeutic options for LGG patients may be much larger. Therefore, the

development of adequate LGG models is urgently needed to develop targeted therapies for this disease as early in its course as possible.

3.3 Intratumoral heterogeneity and its implications for GSC based drug screening

A difficult problem regarding the translational relevance of GSCs is the heterogeneity of canonical molecular alterations observed between and within tumors. This intratumoral heterogeneity is not limited to distinct clonal populations in the perspective of copy number alterations and somatic mutations[73, 74], but may also be a dynamic phenomenon with regard to the transcriptional state of cancer cells[75]. For instance, the clonal variation of CNAs may be much more profound in GBM than previously appreciated. Individual tumors contain a mosaic distribution of TCGA subtypes within the bulk tumor. [36, 75]. Single cell RNA-seq experiments of 430 GBM cells derived from five individual tumors revealed a mosaic-reminiscent cell-to-cell variability with regard to surface receptor genes (e.g. PGFR, EGFR, ERBB2, etc)[75]. The regional heterogeneity could be driven by the microenvironment in order to provide a survival advantage within different niches. Indeed, there may be a specific set of transcriptional programs warranted for survival of tumor cells in a necrotic core, which may hold no advantage in the diffuse infiltrative periphery of the tumor and vice versa[35, 75, 76]. In line with this, the intratumoral heterogeneity provides an escape during chemotherapy for treatment resistant clones that cause eventual disease relapse. This daunting problem was elegantly demonstrated by Meyer et al, who interrogated 6-8 single cell derived clones from 3 individual parental tumors for drug response in vitro by screening the NCI oncology compound library[77]. Indeed, clone-to-clone variability was demonstrated for a multitude of compounds in the library (including TMZ), providing compelling evidence for the contribution of intratumoral heterogeneity to therapeutic resistance.

The aforementioned holds grave implications for the testing of drugs since the derivation of GSCs, and the resultant epigenetic, genetic and transcriptomal state confirmed through profiling, may be primarily dependent on the localization selected for biopsy. This advocates for thorough validation experiments with each GSC specimen derived from biopsies with respect to the characterization of subtype specific molecular alterations. Off note, the referred intrinsic resistance derived from intratumoral variability is distinct from the reported ability of clones to develop resistance during treatment. This process is thought to occur through acquisition of molecular traits that provide an escape to cytotoxic effects of chemotherapy, a phenomenon coined acquired resistance and well described for TMZ therapy [78-80].

3.4 Biopsy localization based variability of molecular phenotype and consequences to therapy response

In addition, researchers should bear in mind that the cells used for in vitro experiments are usually from a localization that the neurosurgeon deemed as non-eloquent tissue. The subsequent recidive of the tumor after treatment is organized from cells invading into the surrounding tissue not amenable for resection. This enigma has been addressed in a number of studies to date by investigating the molecular and therapeutic response differences between bulk samples and peripheral margin cells defined by either surgeons estimate of macroscopic total resection, fluorescence identification peri-operatively, or planning based on MRI-enhancement pre- and perioperatively [35, 76, 81]. As such, it is intriguing to note that the majority of biopsies (17 out of 27, 63%) obtained from these infiltrative regions were found to be comprised of the NEU molecular subtype, which in the TCGA population of bulk samples is rare (83 out 542 samples, 15%)[35]. While this may be influenced by a relatively increased proportion of the sample being derived from non-neoplastic cells when compared to bulk tumor, histological validation confirmed necrosis, mitosis and tumor markers within the selected samples.

This is clinically relevant since diffuse invading cells may respond differently to therapy when compared to the core (bulk removed) sampled cells. Glas et al demonstrated in five paired core and peripheral cultures that the therapeutic response to radiation and chemotherapy (lomustine and TMZ) was significantly different in more than half (64%) of tested conditions[76]. In practice, the establishment of GSCs from the invading margin of the resection cavity of tumors may be challenging, as reported by Piccirillo et al, who found that these samples senesce under serum free conditions, and are less likely (but not unable) to proliferate as xenografts in orthotopic immunocompromised mice[81].

4.0 Conclusions and recommendations

In conclusion, we propose the use of GSCs as a convenient and reliable tool for the investigation of drug responses in vitro. As summarized in Table 3, the advantages of GSCs over serum supplemented cultures with regard to recapitulation of driving molecular alterations between parental tumor, xenograft and cell cultures has led researchers worldwide to implement these methods to investigate GBM in vitro. As a model of the disease, there will always be limitations to the application and interpretation of the data to the human condition. Based on the presented overview of these limitations we would like to stress the importance of further development of the GSC-based models to address some of these shortcomings.

First, clinical studies are required to interrogate prospectively the predictive value of drug response for agents tested both in patients and their resection tissue derived GSCs. If positive, these studies would make a crucial contribution to the advancement of personalized medicine in GBM. With the increased knowledge of intratumoral heterogeneity, we advocate for precise tracking of sample biopsy records, and the validation of molecular characteristics of parental tissue(s) and subsequently derived clones to adequately interpret derived data.

With exception of the epigenetic condition of these cells, the transcriptome and the copy number profile are adequately recapitulated for at least for the first five passages of the derived cultures. Future studies are expected to shed light on this phenomenon as well as the epigenetic drift and the profound implications of the interplay between GSCs and the microenvironment in which these cells subside. In addition, the improved derivation of tumor cells from the residing margin of the resection

cavity, may lead to better understanding of the biology that drives invasion, recurrence and interplay between stromal cells. With regard to recurrence, and the increasing tendency to reoperate patients with recurrent disease, studies will focus on the temporal molecular dynamics with regard to driving events in drug resistance and tumor relapse. At last, we hope to see clinical trials capitalizing on the enhanced insight derived from GSC models to improve clinical outcome of GBM patients in the near future.

	Method	Tissue and/or Cultures	(n)	Gains	Losses	EGFR	PTEN	PDGFRA	TP53	IDH-1	NF1	Message
Singh et al (2003) [15]	K	SF Cultures	1	Chr. 7	Chr. 10	Yes	ND	ND	ND	ND	ND	CD133+ cells are brain tumor initiating cells
Galli (2004)[47]	K	SF Cultures	2	Chr. 7, 20, 19, 22, 3, 21	Chr 1,2,13,14, 22	ND	ND	ND	ND	ND	ND	GB contains tumor initiating neural progenitor cells
Lee (2006) [14]	aCGH, K	Tumor and cultures (paired)	2	Chr. 7	Chr. 9, 10	Yes	ND	ND	ND	ND	Yes (SS)	SF cultures are superior to SS cultures as GB models for in vitro and in vivo experiments
Tso (2006) [32]	aCGH, K	SS cultures	4	Chr. 7	Chr. 10, 17	ND	ND	ND	ND	ND	ND	Primary SS GB cultures express mesenchymal like properties
DeWitt Hamer (2008)[82]	aCGH, K	Tumor, SS Culture and Organotypic spheroids	8	Chr. 7, 8,12,	Chr. 1,9,10,13, 14							Organotypic cultures retain tumor specific CNA's superior to SS cultures.
Gunther (2008)[42]	SNP, K	Tumor	9	Chr. 4, 7	Chr 9,10, 17	Yes	Yes	Yes	Yes	ND	ND	GSC's form distinct subtypes based on molecular and phenotypic characterization
Piccirillo (2009)[83]	SNP, K	SF Cultures	1	Chr. 7, 12, 14, 15	Chr. 1, 9, 18, 19	Yes	ND	ND	Yes	ND	ND	Distinct pools of GSC co-exist in GB
Ernst (2009)[41]	aCGH	SF tumor spheroids	20	7 .19, .20	6q, 10, 14q, 22q	Yes	Yes	Yes	ND	ND	ND	SF spheroids have a superior correlation to parental tumor compared to SS cultures
Al Fael (2009)[12]	aCGH, K	Tumor and SF cultures	6	7 (all)	Chr. 9, 10, 13	No	ND	ND	ND	ND	ND	SF cultures, on extracellular matrix coating, conserve genotypic features with superior yield compared to neurosphere assay
Pollard (2009)[11]	aCGH, K	Tumor and SF cultures	2	Chr 1, 7, 10,12	Chr. 10	Yes	Yes	ND	ND	ND	ND	SF cultures on laminin conserve genotypic features with superior yield compared to neurosphere assay
Chen (2010)[20]	SNP	Tumor and SF cultures	16	7(all)	10 (93 %)	Yes	Yes	Yes	Yes	ND	ND	PTEN is mandatory for SF culture propagation.
Kelly (2010)[44]	aCGH, K	Tumor and paired cultures	2	ND	1p, 19q	ND	ND	ND	ND	Yes	ND	Establishment of 2 LGG cultures of which 1 harbors the IDH1 R132G mutation.
Vik-Mo (2010)[84]	SNP, K	Tumor and cultures (paired)	5	Chr. 1, 6, 7,11, 15, 16 .19, .20	Chr 4, 9, 10, 11, 14,15 21	Yes	Yes	No	ND	ND	ND	Brain tumor stem cells maintain overall molecular phenotype and tumorogenicity after in vitro culturing

	Method	Tissue and/or Cultures	(n)	Gains	Losses	EGFR	PTEN	PDGFRA	TP53	IDH-1	NF1	Message
Wakimoto (2012)[85]	aCGH, K	Tumor and cultures (paired)	5	Chr. 1, 4, 7, 10, 19, 20, 21, 22	Chr. 1,9,10,13, 14	Yes	Yes	Yes	ND	ND	No	Brain tumor stem cells maintain overall molecular phenotype and tumorigenicity after in vitro culturing
Balvers (2013)[17]	SNP	Tumor and paired cultures	27	Chr. 1, 4, 7, 10, 19, 20, 21, 22	Chr1, 9, 10, 11, 14, 15, 21	Yes	Yes	Yes	Yes	No	Yes	SF cultures are all Chr7p10q, IDH1-WT, with all TCGA subtypes represented but with enrichment for CLA subtypes
Bhat (2013)[34]	Microsatellite analysis, sequencing	Tumor and paired cultures	14	ND	LOH chr 10	Yes	Yes	ND	ND	No	ND	Proneural and mesenchymal transcriptome are recapitulated in vitro, however epigenetic drift is observed towards a GCIMP transcriptome over serial passaging
Baronchelli (2013) [48]	SNP, FISH, microsatellite analysis	Tumor and nonpaired cultures	6	chr 4, 7,10,19,20 ,X	Chr1, 9, 10, 11, 14, 15, 21	Yes	Yes	Yes	Yes	ND	ND	GSC recapitulate canonical genetic alterations as found in patient samples
Baysan (2014)[58]	SNP	Tumor and paired cultures	5	Chr 4,7,19,20	Chr 1,3,9 ,10,13	Yes	Yes	ND	ND	NO	ND	GSC recapitulate canonical genetic alterations as found in patient samples, although epigenetic drift occurs

Legend Table 1)

Overview of literature regarding genotyping of primary glioma culturing studies. Abbreviations: K = Karyotyping, FISH = Fluorescent In Situ Hybridization, SNP = Single Nucleotide Polymorphism array based comparative genomic hybridization, aCGH, array based Comparative Genomic Hybridization, ND = not determined.

Table 2; overview of advantages and disadvantages of the GSC model for contemporary translational studies in GBM

GBM hallmarks and relevant traits to experimental studies	Advantages of GSC model	Disadvantages of of GSC model
Methodological considerations	Compatible with many standardized assays. Coating based assays are more convenient in handling than tumorspheres[11, 13]. Vitrification needed for biobanking does not influence expression of genotypic profile[86].	Expensive medium and coating preparation, laborious handling compared to conventional cell lines
Histological recapitulation of disease hallmarks in xenografts	Invasive growth pattern, (pseudo-palisading) necrosis[85]. Variability between samples in growth pattern and survival	Xenografts usually have extended overall survival when compared to conventional cell lines leading to longer experiment turnover
Copy number alterations and somatic mutations stability	Stable and adequate recapitulation of canonical genomic events. nonGCIMP tumors (80% population) are covered.	IDH-1 mutations appear incompatible with SF-culture conditions[17]. EGFR mutations have a selective disadvantage[52] could be similar for other RTKs.
Gene expression subtype stability	Recapitulation of tumor subtype in vitro, stable for at least 5 passages[11, 17]	GCIMP tumors do not proliferate under SF conditions[34].
Epigenetic phenotype stability	Adequate model for addressing epigenetic remodeling of cancer cells in vitro[59]	Epigenetic drift from original tumor profile in vitro[34, 58]
Treatment response to conventional therapy and acquired resistance studies	Recapitulation of parental tumor MGMT status in GSCs has been demonstrated[64, 70]. Acquired resistance can be studied.	Blood brain barrier interaction cannot be addressed.
Drug screening studies	Suitable for combination strategies, addressing intratumoral heterogeneity, compound libraries, shRNA libraries and relating response to specific molecular features. High throughput screening of inter-tumoral heterogeneity for drug response. High throughput screening of intratumoral heterogeneity with regard to clonal diversity to drug response	Tumorspheres usually inconvenient for reproducible plating. Low passages of GSCs sometimes have considerable variability with regard to proliferation speed.

5

Advances in Oncolytic Virotherapy for Brain Tumors

Book chapter published as:

Advances in Oncolytic Virotherapy for Brain Tumors. *Rutger K. Balvers, Candelaria Gomez-Manzano, Hong Jiang, Sujan Piya, Sarah R. Klein, Martine L.M. Lamfers, Clemens M.F. Dirven and Juan Fueyo*
Gene Therapy of Cancer. Edition: 3rd, Chapter: 10, Publisher: Elsevier, Editors: E.C. Lattime, S.L. Gerson, pp.137-15

ISBN-13: 978-0123942951, DOI: http://dx.doi.org/10.1016/B978-0-12-394295-1.00010-X

First publication October 3th, 2013

Abstract

Lessons from the history of cancer therapy inform that a multi- modal approach offers the best potential to eradicate the tumor mass and prevent the recurrence after therapy. One of the most promising experimental therapies for cancer is the use of oncolytic adenoviruses as therapeutic agents. These biologic agents exert their function by directly infecting and killing tumor cells. The new progeny generated after the first infection round will spread, generating a therapeutic wave that will optimally eliminate every cancer cell. Recently, modifications in the virus genome have allowed for the designing of viruses that infect with more potency than wild-type adenoviruses, replicate exclusively in tumor cells, selectively target cellular receptors or molecular defects in the cancer cells, and deliver prodrug genes. In addition, these last-generation viruses can be combined with chemotherapy and other forms of cancer therapies to enhance the tumor killing capability. With the steady and fast pace of the progress in our knowledge of the genetics of tumors, we may soon fulfill our hope of reaching the final objective of an adenovirus-based personalized medicine for cancer.

INTRODUCTION

Oncolytic virotherapy utilizes the ability of replicating viruses to selectively infect malignant cells, replicate within them, and subsequently lyse these cells to reinfect neighboring cells with the newly produced progeny. Various case reports in the previous century showed this paradigm to be a feasible alternative therapy for the treatment of cancer [1], and results from preclinical experiments for malignant gliomas using genetically modified tumor-specific oncolytic adenoviruses have been very promising [2].

The rationale for treating malignant gliomas with oncolytic adenoviruses is based on several aspects of the disease. First, no curative treatment options currently exist for patients diagnosed with malignant gliomas, and the potential for rapid recurrence after primary treatment necessitates the development of more efficient alternatives. Glioblastoma (grade IV glioma) has the most dismal prognosis, with a median survival of only 15 months after initial diagnosis despite the use of aggressive chemoradiotherapy regiments [3]. Second, although oncolytic virotherapy for disseminated disease in several other cancer types is hampered by the physiologic boundaries of the circulatory and innate immune systems, metastasis is very uncommon in malignant gliomas; therefore, these tumors might be targeted using local delivery of oncolytic viruses. Last, molecular aberrations in several signaling pathways render malignant gliomas vulnerable to oncolytic adenoviruses and offer targets for the immune system.

Adenoviruses are double-stranded DNA viruses that can cause (usually mild) respiratory, digestive, and ocular infections in humans. Adenoviruses have long been used to deliver genes and are generally considered to be safe [4], easy to genetically manipulate [5], and researchers are capable of generating high-stock titers for clinical administration. However, adenoviral vectors were originally constructed to be replication deficient; thus, the therapeutic success depended on the efficacy of the first round of infection. This strategy later proved to be insufficiently potent for achieving a relevant anticancer efficacy [6], which led researchers to develop conditionally replication-competent adenoviruses as oncolytic therapy. Although the concept of inducing oncolysis by replicating vectors was not entirely new [7], the ability to modify the viral genome to increase safety, specificity, and modify infectivity led to a shift from gene therapy to oncolytic virotherapy.

Indeed, replication-competent adenoviruses proved to be more effective than replication-incompetent vectors for the treatment of solid tumors, thereby resulting in multiple clinical trials for several different tumor types [8]. It is important to note that although 55 different human adenoviruses exist, all the current clinical trials (n 5 87) of adenovirus-based therapy utilize (at least the backbone of) human adenovirus serotype 5 (Ad5) [9]. This tendency is predominantly attributed to the commercial availability of convenient molecular tools for genetically modifying Ad5 and the extensive knowledge of this species genome. Although the basic genomic makeup of human adenovirus species is relatively well conserved, considerable interspecies variation exists at both ends of the genome in the E1 and E4 regions [10]. The E1 region drives the replication of the virus, whereas the E4 region contains a variety of late genes that are, among other functions, involved in the capsid and binding motifs of the virus. Therefore, E4 variations may also account for the diversity between species in the tropism for specific cellular receptors for facilitating viral entry. Comparative studies have assessed the oncolytic efficiency of several human adenoviruses for treating animal models of melanoma, ovarian carcinoma, and lung carcinoma, and the oncolytic potential of Ad35 [11], Ad6, and Ad11 [9] was shown to be similar to that of Ad5. Furthermore, chimeric vectors that utilize the Ad3 or Ad35 fiber for enhanced tumor tropism have been developed and used in glioma models and other malignancies. These chimeric viruses still depend on the Ad5 genes for nuclear trafficking, replication, and lysis; therefore, we focus on the Ad5 viral mechanisms.

Because viruses continuously adapt to manipulate and evade core cellular stress"response pathways to maintain their survival and reproduction, they can teach us important lessons about reverting the resistance of cancer cells to current cytostatic drugs. Furthermore, studying the ability of oncolytic viruses to subvert intracellular and systemic antiviral response can improve our understanding of the delicate inter- play between tumor cells and their microenvironment.

The purpose of this chapter is to provide a basic understanding of the potential, caveats, and future directions of adenovirus-based virotherapy for malignant glioma.

HURDLES FOR ADENOVIRUS-BASED ONCOLYTIC VIROTHERAPY

The use of adenovirus for oncolytic virotherapy has been shown to have several pitfalls, many of which were identified during the testing of viral vectors designed for gene therapy. Prior to treatment, approximately 50% of the human population has been in contact with adenoviruses, with the generation of neutralizing antibodies that activate adaptive immune responses to the oncolytic adenoviruses soon after administration

[12]. The peripheral circulation forms a very effective barrier for adenoviruses because coagulation factors bind with high affinity to the capsid protein hexon [13]. In addition, erythrocytes bind to adenoviruses through their coxsackievirus and adenovirus receptor (CAR) [14]. Both phenomena result in an efficient sequestration of viral complexes into the liver and subsequent clearance. Although adenoviral clearance from the circulation is very effective, and therefore detrimental to an effective oncolysis, intratumoral delivery and its associated local immunogenicity may have ambivalent effects. In addition, the viral entry receptor CAR is highly expressed in a variety of off-target organs, whereas several tumors have been shown to have low or absent expression of CAR [15]. In malignant gliomas, the expression levels of CAR and integrins are heterogeneous

TABLE 10.1 Genetic Modifications of Adenoviral Vectors and Oncolytic Adenoviruses

Backbones	Agent	Tumor-Specific Promoter	Fiber Modification	Inserted Transgene	Additional Modification	References
Ad5	Ad5-WT	VEGFR-1	RGD	IL-24		Kaliberova *et al.* [61]
		Midkine				Kohno *et al.* [57]
			pk7			Zheng *et al.* [107]
			CAV1 knob			Zheng *et al.* [107]
			MAV-1 knob			Paul *et al.* [27]
			CAV2 knob			Paul *et al.* [27]
			Ad7 fiber			Paul *et al.* [27]
		CXCR4	Ad3 knob			Ulasov *et al.* [86]
		Survivin	Ad3 knob			Ulasov *et al.* [86]
		GFAP	Ad35		E4 under E2F promoter	Hoffman *et al.* [63]
		COX-2	Ad35		E4 under Ki67 promoter	Hoffman *et al.* [63]
		h-TERT				Ito *et al.* [55]
		HIF response element			dE3	Post *et al.* [52]
		HIF response element		IL-4		Cherry *et al.* [54]
dE1A-E1B	Ad5-IR		Ad35	TRAIL		Wohlfart *et al.* [108]
	CB1					Gomez-Manzano *et al.* [109]
Delta-24 (dl922-947)	Delta-24					Fueyo *et al.* [41]
			RGD			Suzuki *et al.* [110], Fueyo *et al.* [17]
			EGFRvIII ScFv		Y477A (abrogated CAR binding)	Piao *et al.* [23]
				TIMP3		Lamfers *et al.* [45]
				hyCD		Conrad *et al.* [43]
				p53		Geoerger *et al.* [79]
		Tyrosinase	Ad3 knob		E4 under tyrosinase promoter	Ulasov *et al.* [60]
		E2F	RGD			Alonso *et al.* [56]
dE1B55k (dl1520)	ONYX-015					Geoerger *et al.* [111]
			Fk/20			Shinoura *et al.* [112]
Delo3 (dl520)			RGD		E1B19K	Holzmuller *et al.* [113]

among and within individual patient samples [16] and in conventional glioma cell lines [17], which were found to be predictive for the oncolytic efficacy. This aspect of CAR expression might limit both the specificity and the efficacy of oncolytic adenoviruses. Intriguingly, CAR has been shown to act as a tumor suppressor when introduced into the U118 glioma cell line in vitro and in flank tumors [18]. Furthermore, recent publications have related CAR expression to α-catenin-induced migration and proliferation in colon cancer [19] and have related the loss of CAR expression to chemotherapy-induced senescence [20].

MODIFYING ONCOLYTIC ADENOVIRUSES TO TREAT MALIGNANT GLIOMAS

To overcome the previously described hurdles, researchers have evaluated alternative targeting strategies for redirecting oncolytic adenoviruses specifically to tumor cells while attenuating their ability to replicate and lyse healthy cells (Table 10.1). Native adenoviral tropism is mediated by the fiber knob (attachment) and penton base (internalization) proteins in the capsid of the virus, which facilitate bind- ing to CAR and integrin αVβ3/β5, respectively. The following strategies for enhancing the tumor cell specificity of oncolytic adenoviruses have been explored: modification of the structural capsid to increase tumor tropism, deletion of viral early genes that are required for viral replication in off-target cells, and introduction of tumor tissue-specific promoters for viral replication [21]. In the subsequent sections, we discuss the results of studies of oncolytic adenovirus for malignant glioma that have implemented these strategies.

Redirecting Adenoviruses Toward Glioma- Specific Receptors

Several strategies for caspid modification have been explored [5]. Two of these were tested in the setting of malignant gliomas with varying success. The first strategy is based on the incorporation of ligands into the fiber protein, such as Arg-Gly-Asp (RGD) motif (binds to integrins), single-chain Fv fragment (scFV) antibodies (bind to tumor-specific receptors), or poly- lysine (binds to heparin receptors). The second strat- egy involves the creation of chimeric fiber-based vectors, which utilize the entry receptors of adenoviruses that naturally infect nonhuman species. A myriad of xenofibers have been reported (Table 10.1).

Probably the most frequently and most extensively characterized approach for fiber modification in the context of malignant gliomas is the incorporation of an RGD motif into the HI loop of the fiber protein [16,17,22]. This strategy was shown to enhance infectivity drastically in both conventional cell lines lacking CAR expression and primary patient-derived mono- layers and organotypic spheroids [22]. Retargeting oncolytic adenoviruses to the tumor-specific mutant epidermal growth factor receptor (EGFRvIII) also proved feasible in vitro and in vivo for targeting tumor cells expressing this receptor [23].

In an interesting comparative study of the infectivity of several fiber-modified vectors [24], the authors reported increased infectivity of vectors targeted toward the CD46 receptor, which is the preferred entry receptor for many type B adenoviral species (e.g., Ad35 but not Ad3). This receptor facilitates the cleavage of complement factors C3b and C4b to prevent the activation of the complement system against the host cell [25]. Although it was first discovered in monocytes, expression of the CD46 receptor is more or less ubiquitous; the CD46 receptor is shared among numerous pathogens as an entry receptor, and its role in oncolytic measles virus cell entry has been studied extensively [26]. CD46 expression in malignant gliomas is still somewhat controversial [27], although most studies have confirmed that chimeric fibers that supposedly utilize this receptor displayed and enhanced infectivity in a subset of malignant gliomas cultures. Particularly, the infectivity in early passage primary glioblastoma cell cultures was markedly improved for the chimeric Ad5/35 vector compared to the wild-type Ad5 [28].

Unlike Ad5/35, Ad5/3 chimeric vectors have been shown to utilize the CD80/86 receptor and similarly enhance infectivity compared to wild-type Ad5. Furthermore, these vectors were found to be less cytotoxic in normal human astrocyte cultures [29,30]. Xenofiber chimeric vectors based on several different adenoviral species were tested in both conventional glioma cell lines and patient-derived glioblastoma cultures [27]. The authors of that study could not confirm the success of Ad5/3 vector infectivity in primary glioblastoma samples; however, they did find striking increases in the infectivity by canine- and porcine-derived xenotype fiber vectors. Taken together, all these studies confirm the feasibility of increasing the therapeutic efficacy of Ad5 backbone-based vectors by modifying the method of cell entry.

One important caveat has been reported in one study, in which the authors were unable to reproduce the in vitro beneficial effects of a panel of capsid- modified viruses when tested in xenograft glioblastoma models with either low- or high-CAR expression [31]. By measuring transduction of a luciferase imaging system as derivative for infectivity, the authors found that the modified adenoviral vectors were not superior to the unmodified adenoviral vector in D54-derived xenografts (high CAR) or U87-derived xenografts (low CAR). This study underscores the limitations of in vitro models for predicting infectivity of adenoviruses, and it suggests that the role of the extracellular matrix and hypoxia should be considered as relevant factors that contribute to therapeutic success (or the lack thereof) in xenografts. In addition, none of these studies tested these vectors in glioma stem cell (GSC)- based models. In approximately the past decade, GSCs have been established as a superior model for studying glioblastoma drug response—compared to conventional cell lines such as U251, U87, and U373—in regard to the maintenance of glioblastoma gene expression signatures and recapitulation of glioblastoma hallmarks in murine xenograft models [32]. One study did examine CAR expression in a panel of four GSC cultures and found that 60"95% of cells in these cultures were positive, thereby leading to effective oncolysis with Delta-24-RGD and a prolongation of survival from 38.5 to 66.3 days in a GSC-derived xenograft model [33]. Nonetheless, the infectivity of GSCs remains to be interrogated for CD46-, CD80-, and CD86-targeted vectors.

Targeting Cancer Genetic Pathways

The second well-established strategy for creating tumor specificity is the implementation of genetic modifications that attenuate the replication of oncolytic adenoviruses in nonmalignant cells. Adenoviruses hijack the function of several tumor-suppressive path- ways, which are inactivated in cells in the G0 cell cycle phase, to facilitate the efficient transcription of viral genes. This viral manipulation of the cellular machinery is facilitated by the adenoviral E1A gene, and it is performed in concert with the prevention by the adenoviral E1B genes of the subsequent cellular activation of apoptosis signaling pathways [34]. In malignant gliomas, both cell cycling and apoptosis pathways are frequently dysfunctional [35] and are thereby putative candidates for adenoviral replication. The suggested paradigm here would be the modification of the viral genome targeting a neoplastic pathway.

Indeed, the first oncolytic adenovirus tested in the context of malignant gliomas was the E1B-55K-deleted (dl1520) ONYX-15 virus. E1B-55K binds to p53 in the early stage of infection, thereby effectively blocking apoptotic signaling induced by the transduction of the viral E1A gene [36]. Approximately 35% of glioblastomas harbor somatic mutations in the p53 gene, whereas 87% have altered signaling within the p53 cascade [37]. Because binding to p53 is not the only function of E1B-55K, other (at least equally) important factors are likely contributing to the tumor selectivity of ONYX-15 [38,39]. ONYX-15 was the first oncolytic adenovirus to be tested in a clinical trial, which demonstrated a favorable toxicity profile for both intratumoral and intravascular administration. Imaging studies and lymphocytic infiltration suggested ONYX- 15 had biological activity; however, the clinical benefit to patients was not significant [40]. The lack of clinical evidence for ONYX-15 as an effective agent was recently countered by the approval of the Chinese Food and Drug Administration for the treatment of refractory head and neck cancer in combination with cisplatin after a successful phase III trial. These results warrant the exploration of multimodal treatment strategies, which we discuss later in this chapter.

The cell cycle-targeted variant of this strategy is successfully capitalized by a 24-bp deletion in the CR2 of E1A coined Delta-24 [41], and a similar vector was reported as dl922-947 [42]. This deletion results in the inability of E1A to bind to the retinoblastoma protein, a protein essential for cell growth arrest in the G1 phase, by blocking the transcription factor E2F1. By doing so, E1A is causing the release of the transcriptional activity of E2F; as a consequence of the release of E2F, there will be activation of cellular pathways that are critical for viral replication [17]. The retinoblastoma-related network is altered in approximately 78% of glioblastomas, and homozygous deletions of retinoblastoma gene are found in 11% of them, according to The Cancer Genome Atlas (TCGA) data set [37]. The Delta-24 mutation has been implemented in several vectors investigated in preclinical studies of malignant gliomas [43"45]. Mechanistically, the small 24-bp alteration does not affect the maximum evolutionarily conserved adenoviral machinery, therefore maintaining the oncolytic potency of the agent while leaving room for the insertion of potentiating transgenes. This biological agent is being clinically evaluated for the first time in a phase I trial investigating the biosafety of intratumoral injection (opened December 2008; ClinicalTrials.gov ID No NCT00805376). A second independent trial was initiated to investigate convection-enhanced delivery via 48 hr of continuous infusion (EudraCT No. 2007-001104-21). At the time of writing of this chapter, both trials were still accruing patients.

Another vector that has been studied for treating malignant gliomas is Ad5-YB1 (also termed dl520). This oncolytic adenovirus depends on the nuclear accumulation of the transcription factor YB-1 for efficient replication. Adenoviral DNA replication is facilitated by the interplay between E1A-E2F and the E2 viral promoters. E2 expression is regulated by E1 and E2 late promoters. The nuclear accumulation of YB-1 facilitated by E1B-55k (which can be transcribed independent of E1A after high viral dosing) has been demonstrated to induce the expression of the E2 late promoters, thereby facilitating viral DNA replication [46]. Ad5-YB1 can therefore be used as an oncolytic adenovirus to facilitate E1A-independent viral replication and, consequently, oncolysis [47]. Elevated nuclear YB-1 expression was demonstrated in glioblastomas [48]. Furthermore, YB-1 expression was particularly high in glioblastoma vasculature [49], and Ad5-YB-1 seemed to repress vascular endothelial growth factor levels in glioblastoma cell lines in vitro [50]. Ad5-YB1 can therefore be used as an oncolytic adenovirus to facilitate E1A-independent viral replication and, consequently, oncolysis [47].

Tumor-Specific Promoter-Driven Oncolytic Adenoviruses

Similar to the previously described strategy, the tumor-specific promoter (TSP)-driven oncolytic adenoviruses mainly derive their specificity from withhold- ing the ability to replicate in nonmalignant cells. All the oncolytic adenoviruses that have been evaluated in studies of glioblastoma models have linked E1A function to a promoter that is active in tissue and/or tissue vasculature (Table 10.1). For oncolytic adenoviruses, the TSP should be homogeneously expressed and at a higher rate in tumor tissue than in normal brain tissue and in other organs such as the liver in order to minimize toxicity and facilitate the efficient replication of the viral genome. Unfortunately, the number of promoters that fulfill these requirements is limited. Therefore, combinations of safety strategies are implemented, such as using the backbone Delta-24 vector with the E2F response element as applied in the oncolytic adenoviruses named ICOVIR [51].

Hypoxia/hypoxia-inducible factor (HIF)-dependent replicative adenoviruses (HYPR-Ads) are controlled by hypoxia-inducible response elements, leading to transcription of E1A in hypoxic cells [52], resulting in specific lysis of glioblastoma, medulloblastoma, and normal cells under hypoxic conditions in vitro. Although the ability of oncolytic adenoviruses to replicate in hypoxic tumors seems to be problematic, both wild-type adenovirus and the HYPR-Ads were able to replicate under hypoxic conditions. HYPR-Ads were also shown to replicate in hypoxic tumor areas in a xenograft flank model of the LN229 glioblastoma cell line [53]. Novel improved oncolytic adenoviruses based on the same principle with augmented replicative ability (HIF-Ad) have been combined with interleukin-4 (IL-4) to boost adaptive immune response [54].

Another specific feature of tumor cells is telomerase expression; therefore, the human telomerase reverse transcriptase (hTERT) promoter is

specifically active in malignant cells. The use of the hTERT promoter to direct E1A transcription was first reported in glioblastomas by Ito et al. [55]. Other promoters that have been utilized in glioblastomas are the E2F [56], midkine [57], survivin [58], CXCR4 [59], tyrosinase [60], and vascular endothelial growth factor [61] promoters. One of the few comparative studies of TSP-driven oncolytic adenoviruses showed that survivin was superior to CXCR4 and midkine with regard to both tumor- specific expression and oncolytic efficacy in vitro [59].

The true specificity of promoter-driven E1A transcription is debatable because only very few copies of E1A can lead to viral replication and subsequent E1A accumulation [62]. To circumvent this problem, researchers have developed double-promoter systems that lock the transcription of E4 under a second specific promoter. This strategy was applied to glioblastoma in a study by Hoffmann et al. [24], in which two vector systems were shown to work particularly well. These authors used a combined system that was designed using the Delta-24 background with E1A transcription regulated by the GFAP/COX-2 (cyclooxy- genase-2) tissue-specific promoter, followed by a proliferation-specific E4 transcription (using E2F/Ki67 promoter [63]). This double heterologous system proved to be selective and effective in a panel of cell lines. Moreover, in combination with a chimeric fiber (Ad5/35), the use of this system rendered significantly longer survival times compared to the homologous Ad5-based counterparts in a subcutaneous glioblastoma xenograft model [24].

In summary, the safety and specificity of oncolytic adenoviruses in vivo have been favorable thus far. This does not imply that incorporating extra safety mechanisms, without hampering therapeutic effect, is futile. Combining the aforementioned three strategies should accommodate the development of clinically secure vectors. Of note, in other solid tumors, the use of tissue- specific microRNAs has proven to be a useful strategy for targeting oncolytic adenoviruses to tumor cells efficiently [64,65]. This strategy has not yet been tested in glioblastomas, although miRNAs have been suggested to play an important role in the development of the dis- ease, which would facilitate the development of glioblastoma subtype-specific oncolytic adenoviruses [66].

SYSTEMIC DELIVERY OF ONCOLYTIC ADENOVIRUSES BY CELLULAR VEHICLES

The first trials with replication-incompetent adenoviruses revealed only limited spread of these vectors from the site of administration [67]. Therefore, the paradigm of reinfection after efficient lysis by replication- competent adenoviruses was thought to improve the dissemination of the oncolytic adenoviruses. This notion seemed to hold true in animal models, but it remains to be confirmed in clinical trials. Because oncolytic adenoviruses are administered intratumorally, the blood"brain barrier is less relevant than when agents are intravenously administered. However, it remains to be discerned how efficiently oncolytic adenoviruses can disperse through the tumor parenchyma and infect invasive tumor cells in patients. Factors such as (altered) extracellular matrix, hypoxia, necrosis, and perturbed intratumoral perfusion have all been described to negatively influence viral spread [68]. Furthermore, intratumoral administration limits the dosing frequency of oncolytic adenoviruses to a singular or once-repeated event, which should ideally take place after tumor debulking.

Several strategies have been explored to circumvent this potentially limiting factor. The carrier cell (or Trojan horse) strategy [69] has been applied in the con- text of oncolytic adenoviruses by infecting neural [70], mesenchymal [71], and adipose stem cells [72] for systemic or intratumoral delivery. For other oncolytic adenoviruses, leukocytes have been successfully employed as well [73]. Once infected, carrier cells have (1) the capability to shield viral particles from the peripheral immune barriers, (2) tropism toward the tumor microenvironment, and (3) the ability to produce progeny to facilitate the amplification of viral release into the tumor microenvironment. This strategy potentially switches the administration of virus from locally to systemically, allowing for more frequent and timed dosing.

Other enhanced features of vehicles that have been explored include the ability to contribute to an antitumor immune response and the secretion of therapeutic agents. Stem cells can be manipulated to deliver several therapeutic agents (e.g., miRNAs, cytokines, and prodrugs); however, they are thought to have some potential disadvantages, such as malignant degeneration after grafting and negative contributions to the immune-suppressive or angiogenic tumor environment [74]. Loading stem cells with oncolytic adenoviruses resolves these problems because the vehicle cell will succumb to the infection. The tropism of carrier cells in general, before and after being loaded with oncolytic adenoviruses, demands special attention because not every in vivo model seems to be equally well attractive for homing purposes. The feasibility of this strategy was first demonstrated by the observation that neural stem cells had the capability of migrating from the contralateral hemisphere to the ipsilateral hemisphere harboring a xenograft tumor [75].

Several studies have demonstrated that once these vehicles get into the tumor, the delivery of oncolytic adenovirus is accomplished, resulting in therapeutic efficacy [76]. Doucette et al. demonstrated the homing capacities of murine mesenchymal stem cells (MSCs) delivered via intracarotid injection toward a PDGF-B- induced RCAS/NTVa model [77]. These MSCs were not infected with virus, and therefore the results have no predictive value with regard to addressing the ability of these cells to shield the virus from the circulation. Other researchers have reported that the delivery of MSCs via intravenous injection may yield lower intratumoral delivery than delivery via intracarotid injection [35]. In a different comparative study, the efficiency of neural stem cells to deliver oncolytic adenoviruses was found to be superior to that of MSCs in U87-derived xenografts [78]. More mechanistic studies are needed to elucidate the molecular factors that contribute to the homing of stem cells toward glioblastoma models.

COMBINING ONCOLYTIC ADENOVIRUSES WITH APPROVED CYTOSTATIC MODALITIES

TABLE 10.2 Combined Therapies Using Oncolytic Adenoviruses

Drug	Vectors Tested	Models	Results	References
Irradiation	ONYX-015	Subcutaneous xenografts of primary GB cultures	Potentiation of *in vivo* therapeutic effect through increased fibrosis. No increased replication or infectivity *in vitro*.	Geoerger *et al.* [79]
	Delta-24 and Delta-24-p53	Cell lines, spheroids, subcutaneous xenografts	Delta-24 and Delta-24-p53 were equally potent *in vivo* when combined with IR.	Idema *et al.* [114]
	Delta-24-RGD	Cell lines, primary cultures, subcutaneous and orthotopic xenografts	Potentiation of Delta-24-RGD by IR differed in orthotopic xenografts and subcutaneous models. Nonsignificant result in orthotopic xenografts underscores the importance of the selected model.	Lamfers *et al.* [22,80]
	dl520	Cell lines, s.c. xenograft	Nuclear YB-1 upregulation, improved viral replication, and *in vivo* growth inhibition.	Bieler *et al.* [115]
	CRAd-S-pk7	Cell lines, brain tumor stem cells, subcutaneous xenograft	Survivin promoter is IR-inducible. IR potentiates CRAd-S-pk7 *in vitro* and *in vivo*.	Nandi *et al.* [82]
	Ad-MDA-7/IL-24	GB primary cell cultures on SS medium, orthotopic xenografts	JNK-ERK-dependent cell death resulting in *in vitro* and *in vivo* potentiation of combination therapy.	Yacoub *et al.* [81]
TMZ	Delta-24-RGD	Cell lines and orthotopic xenografts	Synergy in combination therapy *in vitro* and *in vivo*. Prevention of p300 recruitment to the MGMT promoter, which leads to reduced expression.	Alonso *et al.* [85]
	ICOVIR-5	Cell lines and orthotopic xenografts	Synergy in combination therapy *in vitro* and *in vivo*. No significant effect on replication.	Alonso *et al.* [116]
	OBP-405 (hTERT TSP)	Cell lines and orthotopic xenografts	Autophagy-dependent lysis *in vitro* and *in vivo*. TMZ-induced autophagy potentiates oncolytic adenovirus-mediated survival *in vivo*.	Yokoyama *et al.* [87]
	CRAd-RGDflt-Mda7/IL-24	Cell lines and orthotopic xenografts	Prolonged survival and *in vitro* potentiation	Kaliberova *et al.* [61]
	CRAD-S-pk7	Cell lines and orthotopic xenografts	Induction of autophagy and apoptotic cell death. Additive effect *in vitro* and *in vivo*.	Ulasov *et al.* [86]
	Ad5-Delo-RGD	Cell lines and subcutaneous xenografts	*In vitro* enhanced viral replication, decreased VEGF expression, and prolonged survival *in vivo*.	Holzmuller *et al.* [50]
RAD-001	Delta-24-RGD	Cell lines and orthotopic xenografts	Synergy in combination therapy *in vitro* and *in vivo*.	Alonso *et al.* [89]
	OBP-405 (hTERT TSP)	Cell lines and orthotopic xenografts	Autophagy-dependent lysis *in vitro* and *in vivo*. RAD001-induced autophagy potentiates CRAd-mediated survival *in vivo*.	Yokoyama *et al.* [87]

Cyclophosphamide	Delta-24	Cell lines and orthotopic xenografts	Attenuated loss of transgene expression and reduced infiltration of immune cells.	Lamfers *et al.* [88]
Trichostatin-A	Ad5-Delo-RGD	Cell lines	Increased expression of CAR receptor.	Bieler *et al.* [47]
Cisplatin	Ad5-Delo-RGD	Cell lines	Potentiation of *in vitro* therapeutic effect.	Holzmuller *et al.* [50]
Daunorubicin	Ad5-Delo-RGD	Cell lines	Potentiation of *in vitro* therapeutic effect.	Bieler *et al.* [47], Holzmuller *et al.* [50]
Docetaxel	Ad5-Delo-RGD	Cell lines	Potentiation of *in vitro* therapeutic effect.	Bieler *et al.* [47]
Irinotecan	Delta-24-RGD	Cell lines and orthotopic xenografts	Potentiation of *in vitro* therapeutic effect, no impact on replication, and prolonged survival.	Gomez-Manzano *et al.* [90]
	Ad5-Delo-RGD	Cell lines	Potentiation of *in vitro* therapeutic effect, no impact on replication, and especially successful when combined with virus and TSA.	Bieler *et al.* [47]

The shared molecular mechanisms of tumor cell immortality and malignant transformation by adenovirus prompted researchers to investigate combinatorial regimens with established agents to boost therapeutic efficacy. Apart from the insertion of oncostatic transgenes in viral vectors, several cytostatic agents were demonstrated to have synergistic effects when combined with oncolytic adenoviruses (Table 10.2). Because all patients with glioblastomas receive ionizing radiation (IR) and (if in good clinical condition) the alkylating agent temozolomide (TMZ), these modalities were evaluated to determine their effect when combined with oncolytic adenoviruses.

Geoerger et al. reported that radiation therapy potentiated when subsequent ONYX-15 oncolytic adenovirus was administered in a p53-mutant xenograft model derived from a primary patient culture [79]. Lamfers et al. found striking differences between in vitro and in vivo regimens in which Delta-24-RGD was combined with IR. Although the addition of IR did not increase the expression levels of adenoviral entry receptors in glioma cultures, the transgene expression of luciferase-carrying vectors did increase when Delta-24-RGD and IR were combined. These authors found that survival was prolonged in both subcutaneous and orthotopic U87-derived xenografts, although the difference was not significant in orthotopic xenografts. Intriguingly, the difference between using total body irradiation and whole-brain irradiation was very strikingly in favor of whole-brain irradiation [80]. Similar results were reported in studies using other oncolytic adenovirus, such as Ad-MDA7- IL24 [81] and CRAd-S-pk7 [82]. These findings support the feasibility of combining IR with oncolytic adenoviruses in clinical trials.

The other standard clinical agent prescribed for glioblastomas is TMZ, which, via alkylation, induces single-strand breaks that can be repaired by the DNA- repair enzyme MGMT. The methylation of the MGMT promoter has predictive significance on therapeutic outcome with alkylating agents in (at least) subsets of glioblastomas [83]. The E1A protein is known to be a binding partner of p300/CBP that strongly represses MGMT promoter activity [84]. Indeed, several oncolytic adenoviruses are potentiated when administered in combination with TMZ: Delta-24-RGD [85], ICOVIR-5 [85], CRAd-Survivin-Pk7 [86], Ad5-Delo3-RGD [50], OBP-405 [87], and CRADRGD-flt-IL24 [61].

Other drugs that have been combined with oncoly- tic adenoviruses in glioblastoma models include cyclophosphamide (CP) [88], everolimus [89], irinotecan [90], and daunorubicin, docetaxel, and trichostatin A (TSA) [47]. CP has been administered in combination with several oncolytic viruses. Recent clinical evidence showed that CP induced a beneficial immune- modulatory phenotype for adaptive immune responses. A clinical trial of low-dose CP and oncolytic adenoviruses in patients with chemotherapy-refractory metastatic malignancies revealed a reduction of tumor- infiltrating Tregs, an increase in the presence of CD8 T cells, and a favorable effect on disease control and survival in a subset of patients [91]. Because of the myriad of viruses used and the tumor types treated in this study, the clinical results should be interpreted cautiously. However, the role of CP on the effect of oncolytic adenoviruses in humans is encouraging.

TSA is a potent histone deacetylase inhibitor (HDACi) that has been shown to increase CAR expression, in turn leading to enhanced infectivity. Other oncolytic viruses benefited from the induction of transcriptional downregulation of antiviral response genes, thereby resulting in higher viral yield in glioblastoma cultures pretreated with HDACi [92]. Of note, TSA can induce the expression of MGMT, which would render TSA detrimental in combination with TMZ [84].

The chemotherapeutics that inhibit DNA repair or the induction of DNA damage have complementary effects with the virus due to the modulation of the cell cycle by the E1 genes. Specifically, the deregulation of cell cycling could be detrimental to DNA damage repair systems (as in the MGMT example), thereby leading to enhanced cytotoxicity of the chemotherapeutic agents. Importantly, none of these drugs have been found to negatively impact viral replication.

ONCOLYTIC ADENOVIRUSES AND AUTOPHAGY-MEDIATED LYSIS

Autophagy is a cellular maintenance system that has been implicated to play canonical roles in diseases such as cancer, (auto)immune diseases, neurodegenerative diseases, and developmental disorders [93]. Stressful conditions such as starvation, infection, or cytotoxic damage result in a phenomenon that is described as macroautophagy (henceforth referred to as “autophagy”), in which large vesicular structures engulf cytoplasmic content. These structures, the so- called autophagosomes, are subsequently processed to fuse in the lysosomal pathway and form autophagolysosomes, in which the intravesicular content is degraded and processed for several purposes. For instance, antigen presentation through MHC-II complexes is autophagy dependent, as is the adoptive immune response to viral pathogens. The role of autophagy in disease is regarded to be context and outcome dependent, meaning that in some circumstances, autophagy seems to prevent cell death, whereas in others it facilitates cell death [94]. Autophagic cell death is considered to be a programmed cell death pathway in which morphological examination of cells reveals extensive vacuolization of the cytoplasm while key features of apoptosis and necrosis are non-apparent [95]. The term autophagic cell death suggests that autophagy is the key executer of cell demise, but this proposal is rather controversial [96]. However, in tissue development, cell death might be prevented via inhibitory interventions in the molecular processes underlying autophagy [97].

The role of autophagy and autophagic cell death in the infectious cycle of oncolytic adenoviruses was published by Kondo’s group [55]. These authors described autophagic features in hTERT-Ad-infected cells, plus a partial rescue of oncolysis in cells that were treated with the autophagy inhibitor 3-methyladenine. Follow-up research revealed the upregulation of ATG5"ATG12 expression during infection and co-localization with adenovirus fiber in a brain tumor stem cell-derived xenograft model [33]. The manipulation of autophagy can be achieved via several inducing and inhibiting drugs. Everolimus, a mammalian target of rapamycin inhibitor, efficiently induces autophagy and was indeed found to synergize with Delta-24-RGD in vitro and in vivo in orthotopic U87 models [89]. Other cytostatic drugs known to induce autophagy that have been reported to

potentiate oncolytic adenovirus therapeutic effect are TMZ [86] and OSU-03012 (a PDK-1 inhibitor [98]).

The role of autophagy in adenovirus-induced oncolysis has not been clarified. As previously mentioned, the prevention of autophagy results in an almost complete rescue of oncolysis by adenoviruses. However, the prevention of autophagosomal fusion with lysosomes, described as the completion of autophagic flux, was shown to not prevent oncolysis significantly [99]. This finding suggests that the induction of autophagy, rather than the degradation of autophagosomal content, is mandatory for a successful adenoviral infectious cycle. Indeed, the activation of caspase-8, an initiator caspase in the extrinsic apoptotic signaling pathway, has been shown to depend on the initiation of autophagy during the adenoviral infectious cycle. Furthermore, caspase-8 processing and subsequent activation have been shown to depend on the autophagy-related proteins p62 and LC3B. Knockdown or mutation protein experiments of LC3B revealed that caspase-8 activation, and thereby cell death, is substantially diminished after TRAIL or MG- 132 (proteasome inhibitor) treatment [100,101].

The theory that autophagy would provide a platform for caspase-mediated cell death has been previously postulated [102]. Just as caspase-8-mediated apoptosis can be activated in autophagosomes, so can the regulated necrosis pathway. The activation of programmed death pathway machinery via death receptor-induced signaling complex (DISC) assembly in autophagosomes can be influenced by several drugs and relates to the immunogenicity of the death pathway of choice. The ability to activate multiple pathways on the same scaffold formed by autophagosomes is in line with the inability of caspase inhibitors to completely rescue cells from lysis once autophagy is induced [99]. With regard to caspase-8-mediated cell death, it is noteworthy that caspase-8 is heterogeneously expressed in malignant gliomas, and a substantial proportion of these tumors lacks protein expression [103,104].

MOLECULAR PROFILING OF MALIGNANT GLIOMAS AND ONCOLYTIC ADENOVIRUSES

During the past decade, an enormous effort has been made to profile malignant gliomas on several molecular platforms. Molecular characterization studies hold promise for deciphering the biological basis of patient heterogeneity in drug response and could therefore be relevant for predicting which patients might benefit from oncolytic virotherapy or which patients should be treated with a different alternative. Furthermore, these large data catalogs could provide insight into tumor-tailored strategies to combine therapeutic agents with maximal cytotoxic effect. To date, TCGA has provided the largest catalog of samples and combined multiple platforms (histology gene expression, copy number alterations, and methylation status) to eventually segregate at least four different subtypes [104]. These four subtypes (proneural, neural, classical, and mesenchymal) were coined to describe the characteristics of the biological function of the genes overrepresented in each cluster.

Retrospective analysis of glioblastomas with regard to median survival did not reveal significant differences among the four clusters, although classical and mesenchymal tumors seemed to benefit more from aggressive therapy than did proneural and neural tumors [104]. Second, the subtypes seemed to coincide with several copy number alterations (CNAs), although none of the more frequent CNAs seemed to be exclusive to the subclasses defined by TCGA. The two most distinct subtypes with regard to both CNAs and gene expression profiles are the proneural and mesenchymal. The proneural signature coincides with IDH1 mutations, PDGFR-α amplifications, and the overexpression of genes involved in central nervous system development. Mesenchymal tumors are typified by the overexpression of genes related to nuclear factor-κB and tumor necrosis factor-α signaling. Furthermore, these mesenchymal tumors are more closely associated with intratumoral necrosis and signs of inflammation, typified by a higher intratumoral infiltration of microglial cells and lymphocytes.

This evident inflammatory component of mesenchymal tumors could be of interest in oncolytic virotherapy for multiple reasons. First, the immune surveillance within solid tumors correlates with the presence of immune cell infiltrates in vaccine therapy for melanoma, pancreatic cancer, and colon cancer. The presence of a proinflammatory microenvironment, increased signaling of inflammation-associated path- ways within cancer cells, and the secretion of proangiogenic cytokines predisposes the tumor to an effective antitumor response after vaccination [105].

The first evidence of this paradigm was presented in a phase I trial by Prins et al. that showed that tumors with a mesenchymal phenotype were more susceptible to dendritic cell vaccines based on autologous tumor lysates with adjunctive TLR3 or TLR7 agonists [106].

PERSPECTIVE

The purpose of this chapter is to provide basic and updated information about the science supporting the design and utilization of oncolytic adenoviruses for the treatment of cancer at preclinical and clinical levels. Several lines of progress were discussed in sufficient detail to present the advantages and disadvantages of this approach. Moreover, the progress in our under- standing of the genetics of tumors is providing investigators with new conceptual tools to improve the potency and tumor selectivity of the virotherapy approaches. In the near future, the armamentarium of anticancer therapeutic strategies will surely include replication-competent adenoviruses. These constructs will probably be administered in combination with targeted small molecules, conventional therapies including chemo- and radiotherapy, and other biological approaches, such as immunotherapy. It is now the moment for the oncolytic virus approach to move from the stage of repeatedly demonstrating its safety to show for the first time its much expected anticancer efficacy.

References

[1] Bluming AZ, Ziegler JL. Regression of Burkitt's lymphoma in association with measles infection. Lancet 1971;2(7715):105"6.
[2] Zemp FJ, Corredor JC, Lun X, Muruve DA, Forsyth PA.

Oncolytic viruses as experimental treatments for malignant gliomas: using a scourge to treat a devil. Cytokine Growth Factor Rev 2010;21(2-3):103"17.

[3] Huse JT, Holland EC. Targeting brain cancer: advances in the molecular pathology of malignant glioma and medulloblastoma. Nat Rev Cancer 2010;10(5):319"31.

[4] Chuah MK, Collen D, VandenDriessche T. Biosafety of adenoviral vectors. Curr Gene Ther 2003;3(6):527"43.

[5] Mathis JM, Stoff-Khalili MA, Curiel DT. Oncolytic adenoviruses: selective retargeting to tumor cells. Oncogene 2005;24(52):7775"91.

[6] Lang FF, Yung WK, Sawaya R, Tofilon PJ. Adenovirus-mediated p53 gene therapy for human gliomas. Neurosurgery 1999; 45(5):1093"104.

[7] Sinkovics J, Horvath J. New developments in the virus therapy of cancer: a historical review. Intervirology 1993;36(4):193"214. II. ONCOLYTIC VIRUSES

[8] Liu TC, Galanis E, Kirn D. Clinical trial results with oncolytic virotherapy: a century of promise, a decade of progress. Nat Clin Pract Oncol 2007;4(2):101"17.

[9] Chen CY, Weaver EA, Khare R, May SM, Barry MA. Mining the adenovirus virome for oncolytics against multiple solid tumor types. Cancer Gene Ther 2011;18(10):744"50.

[10] Davison AJ, Benko M, Harrach B. Genetic content and evolution of adenoviruses. J Gen Virol 2003;84(Pt 11):2895"908.

[11] Hoffmann D, Bayer W, Heim A, Potthoff A, Nettelbeck DM, Wildner O. Evaluation of twenty-one human adenovirus types and one infectivity-enhanced adenovirus for the treatment of malignant melanoma. J Invest Dermatol 2008;128(4):988"98.

. [12] Nwanegbo E, Vardas E, Gao W, Whittle H, Sun H, Rowe D, et al. Prevalence of neutralizing antibodies to adenoviral serotypes 5 and 35 in the adult populations of the Gambia, South Africa, and the United States. Clin Diagn Lab Immunol 2004;11(2):351"7.

. [13] Parker AL, Waddington SN, Nicol CG, Shayakhmetov DM, Buckley SM, Denby L, et al. Multiple vitamin K-dependent coagulation zymogens promote adenovirus-mediated gene delivery to hepatocytes. Blood 2006;108(8):2554"61.

. [14] Carlisle RC, Di Y, Cerny AM, Sonnen AF, Sim RB, Green NK, et al. Human erythrocytes bind and inactivate type 5 adenovirus by presenting Coxsackie virus-adenovirus receptor and complement receptor 1. Blood 2009;113(9):1909"18.

. [15] Miller CR, Buchsbaum DJ, Reynolds PN, Douglas JT, Gillespie GY, Mayo MS, et al. Differential susceptibility of primary and established human glioma cells to adenovirus infection: target- ing via the epidermal growth factor receptor achieves fiber receptor-independent gene transfer. Cancer Res 1998;58 (24):5738"48.

. [16] Grill J, Van Beusechem VW, Van Der Valk P, Dirven CM, Leonhart A, Pherai DS, et al. Combined targeting of adenoviruses to integrins and epidermal growth factor receptors increases gene transfer into primary glioma cells and spheroids. Clin Cancer Res 2001;7(3):641"50.

. [17] Fueyo J, Alemany R, Gomez-Manzano C, Fuller GN, Khan A, Conrad CA, et al. Preclinical characterization of the antiglioma activity of a tropism-enhanced adenovirus targeted to the retinoblastoma pathway. J Natl Cancer Inst 2003;95(9):652"60.

. [18] Kim M, Sumerel LA, Belousova N, Lyons GR, Carey DE, Krasnykh V, et al. The coxsackievirus and adenovirus receptor acts as a tumour suppressor in malignant glioma cells. Br J Cancer 2003;88(9):1411"6.

. [19] Stecker K, Koschel A, Wiedenmann B, Anders M. Loss of Coxsackie and adenovirus receptor downregulates alpha- catenin expression. Br J Cancer 2009;101(9):1574"9.

. [20] Wu PC, Wang Q, Dong ZM, Chu E, Roberson RS, Ivanova IC, et al. Expression of coxsackie and adenovirus receptor distinguishes transitional cancer states in therapy-induced cellular senescence. Cell Death Dis 2010;1:e70.

. [21] Chiocca EA. Oncolytic viruses. Nat Rev Cancer 2002;2(12):938"50.

. [22] Lamfers ML, Grill J, Dirven CM, Van Beusechem VW, Geoerger B, Van Den Berg J, et al. Potential of the conditionally replicative adenovirus Ad5-Delta24RGD in the treatment of malignant gliomas and its enhanced effect with radiotherapy. Cancer Res 2002;62(20):5736"42.

. [23] Piao Y, Jiang H, Alemany R, Krasnykh V, Marini FC, Xu J, et al.
Oncolytic adenovirus retargeted to Delta-EGFR induces selective antiglioma activity. Cancer Gene Ther 2009;16(3):256"65.

. [24] Hoffmann D, Meyer B, Wildner O. Improved glioblastoma treatment with Ad5/35 fiber chimeric conditionally replicating adenoviruses. J Gene Med 2007;9(9):764"78.

. [25] Riley-Vargas RC, Gill DB, Kemper C, Liszewski MK, Atkinson JP. CD46: expanding beyond complement regulation. Trends Immunol 2004;25(9):496"503.

[26] Phuong LK, Allen C, Peng KW, Giannini C, Greiner S, TenEyck CJ, et al. Use of a vaccine strain of measles virus genetically engineered to produce carcinoembryonic antigen as a novel therapeutic agent against glioblastoma multiforme. Cancer Res 2003;63(10):2462"9.

[27] Paul CP, Everts M, Glasgow JN, Dent P, Fisher PB, Ulasov IV, et al. Characterization of infectivity of knob-modified adenoviral vectors in glioma. Cancer Biol Ther 2008;7(5):786"93.

[28] Hoffmann D, Heim A, Nettelbeck DM, Steinstraesser L, Wildner O. Evaluation of twenty human adenoviral types and one infectivity-enhanced adenovirus for the therapy of soft tis- sue sarcoma. Hum Gene Ther 2007;18(1):51"62.

[29] Ulasov IV, Rivera AA, Han Y, Curiel DT, Zhu ZB, Lesniak MS. Targeting adenovirus to CD80 and CD86 receptors increases gene transfer efficiency to malignant glioma cells. J Neurosurg 2007;107(3):617"27.

[30] Ulasov IV, Tyler MA, Zheng S, Han Y, Lesniak MS. CD46 represents a target for adenoviral gene therapy of malignant glioma. Hum Gene Ther 2006;17(5):556"64.

[31] Van Houdt WJ, Wu H, Glasgow JN, Lamfers ML, Dirven CM, Gillespie GY, et al. Gene delivery into malignant glioma by infectivity-enhanced adenovirus: in vivo versus in vitro models. Neuro Oncol 2007;9(3):280"90.

[32] Lee J, Kotliarova S, Kotliarov Y, Li A, Su Q, Donin NM, et al. Tumor stem cells derived from glioblastomas cultured in bFGF and EGF more closely mirror the phenotype and genotype of primary tumors than do serum-cultured cell lines. Cancer Cell 2006;9(5):391"403.

[33] Jiang H, Gomez-Manzano C, Aoki H, Alonso MM, Kondo S, McCormick F, et al. Examination of the therapeutic potential of Delta-24-RGD in brain tumor stem cells: role of autophagic cell death. J Natl Cancer Inst 2007;99(18):1410"4.

[34] Berk AJ. Recent lessons in gene expression, cell cycle control, and cell biology from adenovirus. Oncogene 2005;24 (52):7673"85.

[35] Nakamizo A, Marini F, Amano T, Khan A, Studeny M, Gumin J, et al. Human bone marrow-derived mesenchymal stem cells in the treatment of gliomas. Cancer Res 2005;65(8):3307"18.

[36] Kirn D. Oncolytic virotherapy for cancer with the adenovirus dl1520 (Onyx-015): results of phase I and II trials. Expert Opin Biol Ther 2001;1(3):525"38.

[37] TCGA Network. Comprehensive genomic characterization defines human glioblastoma genes and core pathways. Nature 2008;455(7216):1061"8.

[38] Harada JN, Berk AJ. p53-Independent and -dependent requirements for E1B-55K in adenovirus type 5 replication. J Virol 1999;73(7):5333"44.

[39] O'Shea CC, Johnson L, Bagus B, Choi S, Nicholas C, Shen A, et al. Late viral RNA export, rather than p53 inactivation, determines ONYX-015 tumor selectivity. Cancer Cell 2004;6(6):611"23.

[40] Chiocca EA, Abbed KM, Tatter S, Louis DN, Hochberg FH, Barker F, et al. A phase I open-label, dose-escalation, multi-institutional trial of injection with an E1B-attenuated adenovirus, ONYX-015, into the peritumoral region of recurrent malignant gliomas, in the adjuvant setting. Mol Ther 2004;10 (5):958"66.

[41] Fueyo J, Gomez-Manzano C, Alemany R, Lee PS, McDonnell TJ, Mitlianga P, et al. A mutant oncolytic adenovirus targeting the Rb pathway produces anti-glioma effect in vivo. Oncogene 2000;19(1):2"12.

[42] Botta G, Perruolo G, Libertini S, Cassese A, Abagnale A, Beguinot F, et al. PED/PEA-15 modulates coxsackievirus- adenovirus receptor expression and adenoviral infectivity via ERK-mediated signals in glioma cells. Hum Gene Ther 2010; 21(9):1067"76.

[43] Conrad C, Miller CR, Ji Y, Gomez-Manzano C, Bharara S, McMurray JS, et al. Delta24-hyCD adenovirus suppresses glioma growth in vivo by combining oncolysis and chemosensitization. Cancer Gene Ther 2005;12(3):284"94.

. [44] Geoerger B, Vassal G, Opolon P, Dirven CM, Morizet J, Laudani L, et al. Oncolytic activity of p53-expressing conditionally replicative adenovirus AdDelta24-p53 against human malignant glioma. Cancer Res 2004;64(16):5753"9.

. [45] Lamfers ML, Gianni D, Tung CH, Idema S, Schagen FH, Carette JE, et al. Tissue inhibitor of metalloproteinase-3 expres- sion from an oncolytic adenovirus inhibits matrix metalloproteinase activity in

vivo without affecting antitumor efficacy in malignant glioma. Cancer Res 2005;65(20):9398"405.

. [46] Holm PS, Bergmann S, Jurchott K, Lage H, Brand K, Ladhoff A, et al. YB-1 relocates to the nucleus in adenovirus-infected cells and facilitates viral replication by inducing E2 gene expression through the E2 late promoter. J Biol Chem 2002;277(12):10427"34.

. [47] Bieler A, Mantwill K, Dravits T, Bernshausen A, Glockzin G, Kohler-Vargas N, et al. Novel three-pronged strategy to enhance cancer cell killing in glioblastoma cell lines: histone deacetylase inhibitor, chemotherapy, and oncolytic adenovirus dl520. Hum Gene Ther 2006;17(1):55"70.

. [48] Faury D, Nantel A, Dunn SE, Guiot MC, Haque T, Hauser P, et al. Molecular profiling identifies prognostic subgroups of pediatric glioblastoma and shows increased YB-1 expression in tumors. J Clin Oncol 2007;25(10):1196"208.

. [49] Takahashi M, Shimajiri S, Izumi H, Hirano G, Kashiwagi E, Yasuniwa Y, et al. Y-box binding protein-1 is a novel molecular target for tumor vessels. Cancer Sci 2010;101(6):1367"73.

. [50] Holzmuller R, Mantwill K, Haczek C, Rognoni E, Anton M, Kasajima A, et al. YB-1 dependent virotherapy in combination with temozolomide as a multimodal therapy approach to eradicate malignant glioma. Int J Cancer 2011;129(5):1265"76.

. [51] Cascallo M, Alonso MM, Rojas JJ, Perez-Gimenez A, Fueyo J, Alemany R. Systemic toxicity-efficacy profile of ICOVIR-5, a potent and selective oncolytic adenovirus based on the pRB pathway. Mol Ther 2007;15(9):1607"15.

. [52] Post DE, Van Meir EG. A novel hypoxia-inducible factor (HIF) activated oncolytic adenovirus for cancer therapy. Oncogene 2003;22(14):2065"72.

. [53] Post DE, Devi NS, Li Z, Brat DJ, Kaur B, Nicholson A, et al. Cancer therapy with a replicating oncolytic adenovirus targeting the hypoxic microenvironment of tumors. Clin Cancer Res 2004;10(24):8603"12.

. [54] Cherry T, Longo SL, Tovar-Spinoza Z, Post DE. Second- generation HIF-activated oncolytic adenoviruses with improved replication, oncolytic, and antitumor efficacy. Gene Ther 2010;17(12):1430"41.

. [55] Ito H, Aoki H, Kuhnel F, Kondo Y, Kubicka S, Wirth T, et al. Autophagic cell death of malignant glioma cells induced by a conditionally replicating adenovirus. J Natl Cancer Inst 2006;98 (9):625"36.

. [56] Alonso MM, Cascallo M, Gomez-Manzano C, Jiang H, Bekele BN, Perez-Gimenez A, et al. ICOVIR-5 shows E2F1 addiction and potent antiglioma effect in vivo. Cancer Res 2007;67(17):8255"63.

. [57] Kohno S, Nakagawa K, Hamada K, Harada H, Yamasaki K, Hashimoto K, et al. Midkine promoter-based conditionally replicative adenovirus for malignant glioma therapy. Oncol Rep 2004;12(1):73"8.

. [58] Van Houdt WJ, Haviv YS, Lu B, Wang M, Rivera AA, Ulasov IV, et al. The human survivin promoter: a novel transcriptional targeting strategy for treatment of glioma. J Neurosurg 2006; 104(4):583"92.

. [59] Ulasov IV, Rivera AA, Sonabend AM, Rivera LB, Wang M, Zhu ZB, et al. Comparative evaluation of survivin, midkine and CXCR4 promoters for transcriptional targeting of glioma gene therapy. Cancer Biol Ther 2007;6(5):679"85.

. [60] Ulasov IV, Rivera AA, Nettelbeck DM, Rivera LB, Mathis JM,
Sonabend AM, et al. An oncolytic adenoviral vector carrying the tyrosinase promoter for glioma gene therapy. Int J Oncol 2007;31(5):1177"85.

. [61] Kaliberova LN, Krendelchtchikova V, Harmon DK, Stockard CR, Petersen AS, Markert JM, et al. CRAdRGDflt-IL24 virotherapy in combination with chemotherapy of experimental glioma. Cancer Gene Ther 2009;16(10):794"805.

. [62] Hitt MM, Graham FL. Adenovirus E1A under the control of heterologous promoters: wide variation in E1A expression levels has little effect on virus replication. Virology 1990; 179(2):667"78.

. [63] Hoffmann D, Wildner O. Efficient generation of double heterologous promoter controlled oncolytic adenovirus vectors by a single homologous recombination step in Escherichia coli. BMC Biotechnol 2006;6:36.

. [64] Bell JC, Kirn D. MicroRNAs fine-tune oncolytic viruses. Nat Biotechnol 2008;26(12):1346"8.

. [65] Ylosmaki E, Hakkarainen T, Hemminki A, Visakorpi T, Andino R, Saksela K. Generation of a conditionally replicating adenovirus based on targeted destruction of E1A mRNA by a cell type-specific MicroRNA. J Virol 2008;82(22):11009"15.

. [66] Kim TM, Huang W, Park R, Park PJ, Johnson MD. A develop- mental taxonomy of glioblastoma defined and maintained by microRNAs. Cancer Res 2011;71(9):3387"99.

. [67] Lang FF, Bruner JM, Fuller GN, Aldape K, Prados MD, Chang S, et al. Phase I trial of adenovirus-mediated p53 gene therapy for recurrent glioma: biological and clinical results. J Clin Oncol 2003;21(13):2508"18.

. [68] Kaur B, Cripe TP, Chiocca EA. “Buy one get one free”: armed viruses for the treatment of cancer cells and their microenvironment. Curr Gene Ther 2009;9(5):341"55.

. [69] Willmon C, Harrington K, Kottke T, Prestwich R, Melcher A, Vile R. Cell carriers for oncolytic viruses: fed ex for cancer therapy. Mol Ther 2009;17(10):1667"76.

. [70] Ahmed AU, Thaci B, Alexiades NG, Han Y, Qian S, Liu F, et al. Neural stem cell-based cell carriers enhance therapeutic efficacy of an oncolytic adenovirus in an orthotopic mouse model of human glioblastoma. Mol Ther 2011;19(9):1714"26.

. [71] Komarova S, Kawakami Y, Stoff-Khalili MA, Curiel DT, Pereboeva L. Mesenchymal progenitor cells as cellular vehicles for delivery of oncolytic adenoviruses. Mol Cancer Ther 2006; 5(3):755"66.

. [72] Lamfers M, Idema S, van Milligen F, Schouten T, van der Valk P, Vandertop P, et al. Homing properties of adipose-derived stem cells to intracerebral glioma and the effects of adenovirus infection. Cancer Lett 2009;274(1):78"87.

. [73] Russell SJ, Peng KW. The utility of cells as vehicles for oncolytic virus therapies. Curr Opin Mol Ther 2008;10(4):380"6.

. [74] Tabatabai G, Wick W, Weller M. Stem cell-mediated gene therapies for malignant gliomas: a promising targeted therapeutic approach? Discov Med 2011;11(61):529"36.

. [75] Aboody KS, Brown A, Rainov NG, Bower KA, Liu S, Yang W, et al. Neural stem cells display extensive tropism for pathology in adult brain: evidence from intracranial gliomas. Proc Natl Acad Sci USA 2000;97(23):12846"51.

. [76] Yong RL, Shinojima N, Fueyo J, Gumin J, Vecil GG, Marini FC, et al. Human bone marrow-derived mesenchymal stem cells for intravascular delivery of oncolytic adenovirus Delta24-RGD to human gliomas. Cancer Res 2009;69(23):8932"40.

. [77] Doucette T, Rao G, Yang Y, Gumin J, Shinojima N, Bekele BN, et al. Mesenchymal stem cells display tumor-specific tropism in an RCAS/Ntv—A glioma model. Neoplasia 2011;13(8):716"25.

[78] Ahmed AU, Tyler MA, Thaci B, Alexiades NG, Han Y, Ulasov IV, et al. A comparative study of neural and mesenchymal stem cell-based carriers for oncolytic adenovirus in a model of malignant glioma. Mol Pharm 2011;8(5):1559"72.

. [79] Geoerger B, Grill J, Opolon P, Morizet J, Aubert G, Lecluse Y, et al. Potentiation of radiation therapy by the oncolytic adenovirus dl1520 (ONYX-015) in human malignant glioma xenografts. Br J Cancer 2003;89(3):577"84.

. [80] Lamfers ML, Idema S, Bosscher L, Heukelom S, Moeniralm S, van der Meulen-Muileman IH, et al. Differential effects of combined Ad5-delta 24RGD and radiation therapy in in vitro versus in vivo models of malignant glioma. Clin Cancer Res 2007;13(24):7451"8.

. [81] Yacoub A, Hamed H, Emdad L, Dos Santos W, Gupta P, Broaddus WC, et al. MDA-7/IL-24 plus radiation enhance survival in animals with intracranial primary human GBM tumors. Cancer Biol Ther 2008;7(6):917"33.

. [82] Nandi S, Ulasov IV, Rolle CE, Han Y, Lesniak MS. A chimeric adenovirus with an Ad 3 fiber knob modification augments glioma virotherapy. J Gene Med 2009;11(11):1005"11.

. [83] Weller M, Stupp R, Reifenberger G, Brandes AA, van den Bent MJ, Wick W, et al. MGMT promoter methylation in malig-

nant gliomas: ready for personalized medicine? Nat Rev Neurol 2010;6(1):39"51.

. [84] Bhakat KK, Mitra S. Regulation of the human O(6)-methylgua- nine-DNA methyltransferase gene by transcriptional coactiva- tors cAMP response element-binding protein-binding protein and p300. J Biol Chem 2000;275(44):34197"204.

. [85] Alonso MM, Gomez-Manzano C, Bekele BN, Yung WK, Fueyo J. Adenovirus-based strategies overcome temozolomide resis- tance by silencing the O6-methylguanine-DNA methyltransfer- ase promoter. Cancer Res 2007;67(24):11499"504.

. [86] Ulasov IV, Sonabend AM, Nandi S, Khramtsov A, Han Y, Lesniak MS. Combination of adenoviral virotherapy and temozolomide chemotherapy eradicates malignant glioma through autophagic and apoptotic cell death in vivo. Br J Cancer 2009;100(7):1154"64.

. [87] Yokoyama T, Iwado E, Kondo Y, Aoki H, Hayashi Y, Georgescu MM, et al. Autophagy-inducing agents augment the antitumor effect of telerase-selve oncolytic adenovirus OBP-405 on glioblastoma cells. Gene Ther 2008;15(17):1233"9.

. [88] Lamfers ML, Fulci G, Gianni D, Tang Y, Kurozumi K, Kaur B, et al. Cyclophosphamide increases transgene expression mediated by an oncolytic adenovirus in glioma-bearing mice monitored by bioluminescence imaging. Mol Ther 2006; 14(6):779"88.

. [89] Alonso MM, Jiang H, Yokoyama T, Xu J, Bekele NB, Lang FF, et al. Delta-24-RGD in combination with RAD001 induces enhanced anti-glioma effect via autophagic cell death. Mol Ther 2008;16(3):487"93.

. [90] Gomez-Manzano C, Alonso MM, Yung WK, McCormick F, Curiel DT, Lang FF, et al. Delta-24 increases the expression and activity of topoisomerase I and enhances the antiglioma effect of irinotecan. Clin Cancer Res 2006;12(2):556"62.

. [91] Cerullo V, Diaconu I, Kangasniemi L, Rajecki M, Escutenaire S, Koski A, et al. Immunological effects of low-dose cyclophosphamide in cancer patients treated with oncolytic adenovirus. Mol Ther 2011;19(9):1737"46.

. [92] Otsuki A, Patel A, Kasai K, Suzuki M, Kurozumi K, Chiocca EA, et al. Histone deacetylase inhibitors augment antitumor efficacy of herpes-based oncolytic viruses. Mol Ther 2008; 16(9):1546"55.

. [93] Mizushima N, Levine B, Cuervo AM, Klionsky DJ. Autophagy fights disease through cellular self-digestion. Nature 2008; 451(7182):1069"75.

[94] Eisenberg-Lerner A, Bialik S, Simon HU, Kimchi A. Life and death partners: apoptosis, autophagy and the cross-talk between them. Cell Death Differ 2009;16(7):966"75.

[95] Galluzzi L, Vitale I, Abrams JM, Alnemri ES, Baehrecke EH, Blagosklonny MV, et al. Molecular definitions of cell death subroutines: recommendations of the nomenclature committee on cell death 2012. Cell Death Differ 2011;19:107"20.

[96] Kroemer G, Levine B. Autophagic cell death: the story of a misnomer. Nat Rev Mol Cell Biol 2008;9(12):1004"10.

[97] Berry DL, Baehrecke EH. Growth arrest and autophagy are required for salivary gland cell degradation in Drosophila. Cell 2007;131(6):1137"48.

[98] Hamed HA, Yacoub A, Park MA, Eulitt P, Sarkar D, Dimitrie IP, et al. OSU-03012 enhances Ad.7-induced GBM cell killing via ER stress and autophagy and by decreasing expression of mitochondrial protective proteins. Cancer Biol Ther 2010;9 (7):526"36.

[99] Jiang H, White EJ, Rios-Vicil CI, Xu J, Gomez-Manzano C, Fueyo J. Human adenovirus type 5 induces cell lysis through autophagy and autophagy-triggered caspase activity. J Virol 2011;85(10):4720"9.

[100] Jin Z, Li Y, Pitti R, Lawrence D, Pham VC, Lill JR, et al. Cullin3-based polyubiquitination and p62-dependent aggregation of caspase-8 mediate extrinsic apoptosis signaling. Cell 2009;137(4):721"35.

[101] Pan JA, Ullman E, Dou Z, Zong WX. Inhibition of protein deg- radation induces apoptosis through a microtubule-associated protein 1 light chain 3-mediated activation of caspase-8 at intracellular membranes. Mol Cell Biol 2011;31(15):3158"70.

[102] Walsh CM, Edinger AL. The complex interplay between autophagy, apoptosis, and necrotic signals promotes T-cell homeostasis. Immunol Rev 2010;236:95"109.

[103] Ashley DM, Riffkin CD, Muscat AM, Knight MJ, Kaye AH, Novak U, et al. Caspase 8 is absent or low in many ex vivo gliomas. Cancer 2005;104(7):1487"96.

[104] Verhaak RG, Hoadley KA, Purdom E, Wang V, Qi Y, Wilkerson MD, et al. Integrated genomic analysis identifies clinically relevant subtypes of glioblastoma characterized by abnormalities in PDGFRA, IDH1, EGFR, and NF1. Cancer Cell 2010;17(1):98"110.

[105] Bedognetti D, Wang E, Sertoli MR, Marincola FM. Gene- expression profiling in vaccine therapy and immunotherapy for cancer. Expert Rev Vaccines 2010;9(6):555"65.

[106] Prins RM, Soto H, Konkankit V, Odesa SK, Eskin A, Yong WH, et al. Gene expression profile correlates with T-cell infiltration and relative survival in glioblastoma patients vaccinated with dendritic cell immunotherapy. Clin Cancer Res 2011;17(6):1603"15.

[107] Zheng S, Ulasov IV, Han Y, Tyler MA, Zhu ZB, Lesniak MS. Fiber-knob modifications enhance adenoviral tropism and gene transfer in malignant glioma. J Gene Med 2007;9(3):151"60.

[108] Wohlfahrt ME, Beard BC, Lieber A, Kiem HP. A capsid-modi- fied, conditionally replicating oncolytic adenovirus vector expressing TRAIL leads to enhanced cancer cell killing in human glioblastoma models. Cancer Res 2007;67(18):8783"90.

[109] Gomez-Manzano C, Balague C, Alemany R, Lemoine MG, Mitlianga P, Jiang H, et al. A novel E1A-E1B mutant adenovirus induces glioma regression in vivo. Oncogene 2004; 23(10):1821"8.

[110] Suzuki K, Fueyo J, Krasnykh V, Reynolds PN, Curiel DT, Alemany R. A conditionally replicative adenovirus with enhanced infectivity shows improved oncolytic potency. Clin Cancer Res 2001;7(1):120"6.

[111] Geoerger B, Grill J, Opolon P, Morizet J, Aubert G, Terrier- Lacombe MJ, et al. Oncolytic activity of the E1B-55 kDa-deleted adenovirus ONYX-015 is independent of cellular p53 status in human malignant glioma xenografts. Cancer Res 2002;62(3):764"72.

. [112] Shinoura N, Yoshida Y, Tsunoda R, Ohashi M, Zhang W, Asai A, et al. Highly augmented cytopathic effect of a fiber-mutant E1B-defective adenovirus for gene therapy of gliomas. Cancer Res 1999;59(14):3411"6.

. [113] Holzmu¨ller R, Mantwill K, Haczek C, Rognoni E, Anton M, Kasajima A, et al. YB-1 dependent virotherapy in combination with temozolomide as a multimodal therapy approach to eradicate malignant glioma. Int J Cancer 2011;129(5):1265"76.

. [114] Idema S, Lamfers ML, van Beusechem VW, Noske DP, Heukelom S, Moeniralm S, et al. AdDelta24 and the p53- expressing variant AdDelta24-p53 achieve potent anti-tumor activity in glioma when combined with radiotherapy. J Gene Med 2007;9(12):1046"56.

[115] Bieler A, Mantwill K, Holzmu¨ ller R, Ju¨ rchott K, Kaszubiak A, Sta ¨rk S, et al. Impact of radiation therapy on the oncolytic adenovirus dl520: implications on the treatment of glioblastoma. Radiother Oncol 2008;86(3):419"27.

[116] Alonso MM, Gomez-Manzano C, Jiang H, Bekele NB, Piao Y, Yung WK, et al. Combination of the oncolytic adenovirus ICOVIR-5 with chemotherapy provides enhanced anti-glioma effect in vivo. Cancer Gene Ther 2007;14(8):756"61.

6

In vitro screening of clinical drugs identifies sensitizers of oncolytic

Chapter was published as:

In vitro screening of clinical drugs identifies sensitizers of oncolytic viral therapy in glioblastoma stem-like cells. *Lotte M.E. Berghauser Pont, Rutger K. Balvers, Jenneke J. Kloezeman, Michal O. Nowicki, Wouter van den Bossche, Andreas Kremer, Hiroaki Wakimoto, Bernadette G. van den Hoogen, Sieger Leenstra, Clemens M.F. Dirven, E. Antonio Chiocca, Sean E. Lawler, Martine L.M. Lamfers*

Gene therapy 07/2015; DOI:10.1038/gt.2015.72

Abstract

Oncolytic viruses (OV) have broad potential as an adjuvant for the treatment of solid tumors. The present study addresses the feasibility of clinically applicable drugs to enhance the oncolytic potential of the OV Delta24-RGD in glioblastoma. In total, 446 drugs were screened for their viral sensitizing properties in glioblastoma stem-like cells (GSCs) in vitro. Validation was done for ten drugs to determine synergy based on the Chou Talalay assay. Mechanistic studies were undertaken to assess viability, replication efficacy, viral infection enhancement and cell death pathway induction in a selected panel of drugs. Four viral sensitizers (fluphenazine, indirubin, lofepramine and ranolazine) were demonstrated to reproducibly synergize with Delta24-RGD in multiple assays. After validation we underscored general applicability by testing candidate drugs in a broader context of a panel of different GSCs, various solid tumor models and multiple OVs.Overall this study identified four viral sensitizers which synergize with Delta24-RGD and two other strains of oncolytic viruses. The viral sensitizers interact with infection, replication and cell death pathways to enhance efficacy of the OV.

Introduction

Patients newly diagnosed with glioblastoma have a median survival of 14.7 months despite surgery and radiation combined with adjuvant chemotherapy using temozolomide.1, 2 Hence, studies into more effective alternatives are warranted. An approach which is currently under phase-I/II clinical investigation is the use of the oncolytic adenovirus Delta24-RGD.3 Treatment with Delta24-RGD has shown promising results in preclinical models4 and has demonstrated therapeutic responses in a subset of patients.3 This is similar to results of other oncolytic virus (OV) trials.5 Delta24-RGD was engineered to specifically target and replicate in cancer cells deficient in the Rb pathway by means of a 24-base pair deletion in the viral E1A gene. Insertion of the RGD-peptide into the fiber-knob enhances viral entry by attachment to αvβ3/αvβ5 integrins.6 Delta24-RGD is therefore not dependent on entry via the coxsackie adenovirus receptor (CAR), which is usually sparsely expressed in glioblastoma.7

In OV therapy heterogeneous responses have been shown both in preclinical models as well as in patients.3, 8, 9 Therefore such treatment strategies require enhancement of OV efficacy in order to be potentially curative. This can be achieved by enhancing replication, attenuating cellular defense mechanisms to infection, enhancing viral lysis or altering the immune response.

The current study is aimed at the identification of sensitizers of oncolysis mediated by Delta24-RGD using the National Institutes of Health (NIH) clinical collection.10 One of the advantages of this drug library is the favorable toxicity profile of the drugs as these agents are routinely prescribed for a wide spectrum of clinical indications. Also, the pharmacological properties are known for most of these agents. These factors make these drugs suitable for rapid translation into clinical trials after in vitro confirmation. Potential heterogeneity in response to the newly identified combination therapies was studied utilizing a well-characterized panel of patient-derived glioblastoma stem-like cell cultures (GSCs).11, 12 This model is known to preserve the original phenotypic and genotypic tumor characteristics.11, 12 We characterize the identified viral sensitizers with regard to important aspects in glioblastoma treatment, including synergistic interactions and viral mechanistic enhancement such as viral infectivity, protein production, expression and replication. Moreover, we study the cellular induction of apoptosis and necrosis.

In addition, we present data on the general applicability of the identified drugs as viral sensitizers in other types of neoplasms and in combination with other types of OVs. The effects of Delta24-RGD are also enhanced by the identified viral sensitizers in triple negative breast cancer, ovarian carcinoma and colon carcinoma. Finally, the identified viral sensitizers enhanced the efficacy of both the HSV-1-based OV G47Δ-mcherry13 as well as the naturally occurring oncolytic Newcastle disease virus (NDV)14 in the GSC model.

Materials and methods

Clinical drugs

The NIH clinical collection which contains 446 drugs was obtained from the NCI/DTP Open Chemical Repository (http://dtp.cancer.gov). All drugs were dissolved in DMSO at 10mM. For validation, the hereafter named drugs were purchased individually, dissolved in DMSO and stored at -20°C. Anagrelide (37.5mM), rabeprazole (250mM) and Amlodipine (500mM) were obtained from Sequoia Research Products Ltd. (UK). Ebselen (50mM), fenoldopam mesylate (100mM), fluphenazine diHCl (100mM), indirubin (37.5mM), lofepramine (50mM), stiripentol (400mM), sumatriptan succinate (100mM), ranolazine diHCl (100mM) from Sigma-Aldrich (MO, USA).

Viruses

The oncolytic virus Delta24-RGD was used for the viability experiments and the titration experiments. This virus has been described previously 6 and includes both a 24-base pair deletion (E1A region) for selective replication in Rb-pathway deregulated tumor cells, and an RGD peptide insertion for cell binding and entry using αv integrins.59 The replication-deficient adenoviral vector Ad.luc.RGD was used for assessment of infectivity and was kindly provided by Dr. D.T. Curiel, (University of Alabama, Birmingham, Al, USA). The Delta24-RGD-GFP was constructed for monitoring viral replication using fluorescent imaging and contains a GFP expression cassette under the E3-promotor. This virus was produced, purified and titrated as previously described.60 The Newcastle disease virus (NDV) has been described previously.14 The Herpes Simplex Virus-1 based OV G47Δ-mCherry was constructed as described previously.13

Patient-derived serum-free cultured glioblastoma stem-like cells

The patient-derived GSCs used for the experiments included a panel of cultures that were established and maintained under serum-free conditions. The tumor specimens were acquired with patients' informed consent and with approval of the institutional review board of the Eras-

musMC. The fresh resection material was dissociated mechanically and enzymatically as described previously.11 The applied method has been demonstrated to 1) retain genetic stability after passaging 11, 61; 2) to recapitulate the phenotypic characteristics of the original tumor 11, 12 and 3) to preserve markers of stemness in glioblastoma cells.62 The cells were maintained under serum-free conditions in DMEM/F12 medium supplemented with 1% penicillin/streptomycin, 2% B27, 20ng/ml bFGF, 20ng/ml EGF (Life Technologies, Paisley, UK), and 5µg/ml heparin (Sigma-Aldrich), at 37°C in a humid 95% air/5% CO2 chamber. The parental tumors and the cell cultures were molecularly characterized as has been described previously.11 The GSCs were classified as glioma World Health Organization (WHO) guidelines grade IV by histopathological assessment of the parental tumor. The passages used were between p8 – p22.

Cell lines

The A549 lung adenocarcinoma cell line and SKOV3 ovarian carcinoma cells were obtained from ATCC (VA, USA). The HCT-116 colon carcinoma cells were obtained from Sigma-Aldrich. The triple negative breast carcinoma cell lines MB-MDA-231 was kindly provided by K. Naipal, MD, of the Department of Genetics, ErasmusMC, Rotterdam, The Netherlands. The cells were cultured in DMEM medium conditions with 10% FBS and 1% penicillin/streptomycin. The cell lines were maintained at 37 °C in a humid 95% air/5% CO2 chamber.

Viability assays and screening method

Patient-derived GSCs and the cell lines of the other tumor types were seeded at 1x103 cells/well in 96-well plates. After 24 hours of incubation the cells were treated with the drugs at a concentration of 100µM, and combined with Delta24-RGD (MOI 50). Cell viability was measured using the CellTiter-Glo assay (Promega, WI, USA) after five days of incubation. For all drugs the combination drug effects were compared to single agent effects, with DMSO as controls. In cases where cell viability was reduced by more than 75% by the drug alone, the drug was re-screened at 10µM and 1µM. If the drug and the combination treatment did not affect viability in this screen (<25% reduction of non-treated controls), i.e. concentrations were too low, then the drug was tested in the third experiment at 50µM and 5µM). Potent viral sensitizers had to meet the criteria of 1) an enhancement factor (explained in the 'statistical analysis' section) of >2 in viability reduction in both of the tested GSCs, and an absolute enhancement of >25% in one the cultures, and 2) the viability of cells treated with the monotherapies had to be >25% compared to controls, as additional effects are difficult to distinguish below this threshold. After identification of the drugs that met these criteria, the drugs were further evaluated for available data on the blood-brain barrier penetration.

The validation of identified drugs was performed using the Chou-Talalay assays, to determine synergy between Delta24-RGD and the drugs by median effect equation calculation.16 For the Chou-Talalay assay, the IC50 values were determined via a concentration-range of 3-fold steps, ensuring no effect on the one end, and complete cell kill on the other end of the concentration-range. Similarly, combination effects were determined using a concentration range of the drug with a concentration range of the virus. Viability was measured by CellTiter-Glo. The assays were performed in triplicate using the glioblastoma culture GS79. The same cell culture as in the original drug screen was used for the Chou Talalay experiments. The combination index was calculated for every combination and considered synergistic if <1, additive if =1 and antagonistic if >1. The screen on a panel of GSCs was performed according to a same treatment regimen, by using two drug concentrations, namely the IC50 value as determined in GS79 and a 2-fold step lower doses. Two MOIs of Delta24-RGD were used (MOI 25 and MOI 75). The results are presented as percentage of non-treated controls with standard error.

Viral infection assays

The effects of the selected drugs on viral infection were assessed using the non-replicating vector Ad.luc.RGD as described previously.8 GS79 and GS102 cells were seeded at 5x103 cells/well in a 96-wells plate and kept overnight in an incubator. The cells were treated with one concentration of the four drugs and infected with Ad.Luc.RGD. Post-infection, the cells were incubated for 24 hours and permeabilized by a freeze/thaw cycle in Triton X-100 (0.9% v/v). Steady-Glo substrate (Promega) was added and luciferase was measured with an Infinite M200 plate reader (Tecan, Switzerland). The results are presented from three independent experiments as percentage of Ad.Luc-RGD only treated cells with standard error.

Viral protein expression and viral titration assays by hexon staining

The viral protein expression in Delta-24RGD infected cells was determined by direct staining for viral hexon protein at 48 hours post-infection of GS79 cells. The cells were seeded 1x103 cells/well in 96-wells plates and after 24 hours, the cells were treated with Delta24-RGD (Figure 1) or with Delta24-RGD and one of the viral sensitizers (Figure 3). After 48 hours cells were fixed with cold methanol and stained as described below. The results are displayed as mean counts/well of triplicates with standard deviation.

Viral titration assays were performed to determine progeny viral particle production. For this, GS79 cells were seeded at 5x104 cells per well and after 24h were treated with Delta24-RGD in combination with each of the four drugs. At both 48h and 96h the cells and supernatants were harvested. Three freeze-thaw cycles were performed, the cells were centrifuged at 1500 rpm for 3 minutes to remove cell debris, and the supernatants were collected. Supernatants were added in serial dilution to 1x103 cells per well of the A549 lung adenocarcinoma cell line. At 48h cells were fixed using ice-cold methanol and washed in PBS/0,05% Tween-20 (Sigma-Aldrich). Staining was done using the primary mouse anti-hexon antibody in PBS/1% BSA (Adeno-X™ Rapid Titer Kit, #632250, Clontech, CA, USA). The hexon plaques were quantified and viral titers were calculated in triplicate. The results are shown as mean of the three viral titers and were considered significant if $p<0.05$ (using the Students´ T-test)

Late viral transgene expression using Delta24-RGD-GFP

Late viral transgene expression was studied by evaluating GFP expression from a Delta24-RGD-GFP virus. GFP expression was monitored over time. GS79 cells were seeded at 2.5x103 cells/well in 96-well plates and were incubated with the identified drugs and/or Delta24-RGD-GFP at concentrations at which synergy had been detected by Chou Talalay analysis. The plates were placed in an IncuCyte real-time cell imaging incubator (Essen Bioscience) and GFP was measured for five consecutive days. The experiment was performed in duplicate and fluorescence was measured every two hours and graphically displayed as mean object counts/mm2.

Flow cytometry on integrin αvβ3 and CAR expression

GS79 cells were seeded at 5x104 cells per well in 6-well plates. After 24 hours the cells were treated with fluphenazine, indirubin, lofepramine and ranolazine at the concentrations shown in the results. At 4, 8 and 24 hours the cells were harvested, washed and incubated for 15 minutes in FACS buffer (PBS/0.25%, BSA/0.05%, NaN3/0.5mM, EDTA/2% human serum) using primary mouse anti-CD51/CD61 (1:50, Abcam (Cambridge, UK)) and primary rabbit anti-CAR (H-300, 1:50, Santa Cruz (Dallas, TX, USA)). After a washing step the cells were incubated with Alexa-488 anti-rabbit and PE-anti mouse secondary antibodies (Life Technologies). Next, the cells were fixed in BD FACS lysing buffer (BD Biosciences, CA, USA). In the flow cytometry analysis, a minimum of 3x104 events was obtained on a FACS Canto II (BD Bioscience). Flow cytometry data were analyzed by using the Infinicyt software (Cytognos, Salamanca, Spain), where debris and doublets were removed with FSC-H and FSC-A. The expression was plotted for the remaining events.

In silico analysis of pathways and target molecules

The Ingenuity Pathway Analysis (IPA) software was used for in silico analyses on the drugs of interest. We aimed to find mechanisms related to the efficacy of combination therapy, by analyzing downstream molecules influenced by the four drugs, fluphenazine, indirubin, lofepramine and ranolazine. We investigated overlapping functions of the four drugs to detect common pathways of interaction (IPA, Sept 2014). Firstly, molecules of common pathways were identified for fluphenazine, indirubin, lofepramine and ranolazine by in silico connection using the ‘build’ algorithm and addition of downstream direct and indirect molecules. The results were projected in a network for the four drugs (Figure S2). Furthermore, the ‘comparison analysis’ in the IPA software was used to analyze common pathways of the four drugs and discover potential novel drugs with the same mechanism of action. The top ten common pathways were considered significant if the p-value <0.05. The analysis was based on the first and second level of downstream affected molecules of the various drugs.

Caspase-3/7 activity

To evaluate Caspase-3/7 activity, cells were seeded 5x103 cells/well in a black-walled 96-well plate. The cells were treated with the four drugs as single treatment, virus alone, or in combination with Delta24-RGD, at a concentration at which synergy was observed in the Chou Talalay assays. Staurosporine (Sigma Aldrich, 20nM) was used as a positive control. The CellPlayer 96-Well Kinetic Caspase-3/7 Apoptosis Assay (Essen Bioscience) was added to the wells and, the caspase-3/7 activity was tracked by fluorescent images over a time period of 60 hours with the IncuCyte system using a 10X magnification at 37°C. Two fluorescent images/well of triplicates were collected every two hours up to sixty hours and displayed as object counts/mm2.

Lactate dehydrogenase assay

GS79 cells were seeded at 1.0x103 cells/well in a 96-well plate. After 24 hours, cells were incubated with two concentrations of the drugs fluphenazine, indirubin, lofepramine and ranolazine in the range at which synergy was detected and two concentrations of virus (MOI 100 and MOI 50). The cells were incubated for five days and placed at 37°C in a humidified 95% air/5% CO2 incubator. After this period, the amount of LDH in the supernatant was determined using the CytoTox-One assay (Promega). Fluorescence was measured in a Tecan Reader. Cell viability was measured by CellTiter-Glo assay to calculate the ratio of LDH per number of living cells. The results were presented as LDH per viable unit as percentage of non-treated controls with the standard errors. The experiments were performed in triplicate.

Statistical analysis

In the primary compound screens, the “Enhancement” was calculated according to the description of Chou63, namely the viability of the most effective monotherapy divided by the viability of the combination therapy. The criterion for designating a drug as potential viral sensitizer was as follows: an enhancement of >2 in both tested cultures, and an absolute reduction of the single drug treatment with >25% viability in at least one culture. The “Absolute Difference” is the viability of the most effective monotherapy minus the viability of the combination therapy, which determines the absolute reduction in viability of cells in the combination treatment compared to the single agent treatment.63 The drug alone had to reduce viability by no more than 75% as below 25% viability combination effects are difficult to detect.

The Chou-Talalay method was performed as described16 and means were plotted with standard deviations. To compare effects of different treatments, the Student’s T-test was used, and statistical significance was reached if p<0.05. The caspase-3/7 activity was calculated as objects counts/well. The caspase-3/7 activity and Delta24-RGD-GFP over time were analyzed by a two-way ANOVA with a Tukey’s Post-Test. The treatment effect was compared to the controls, and combination treatments to both single agent treatments.

Figure 1.

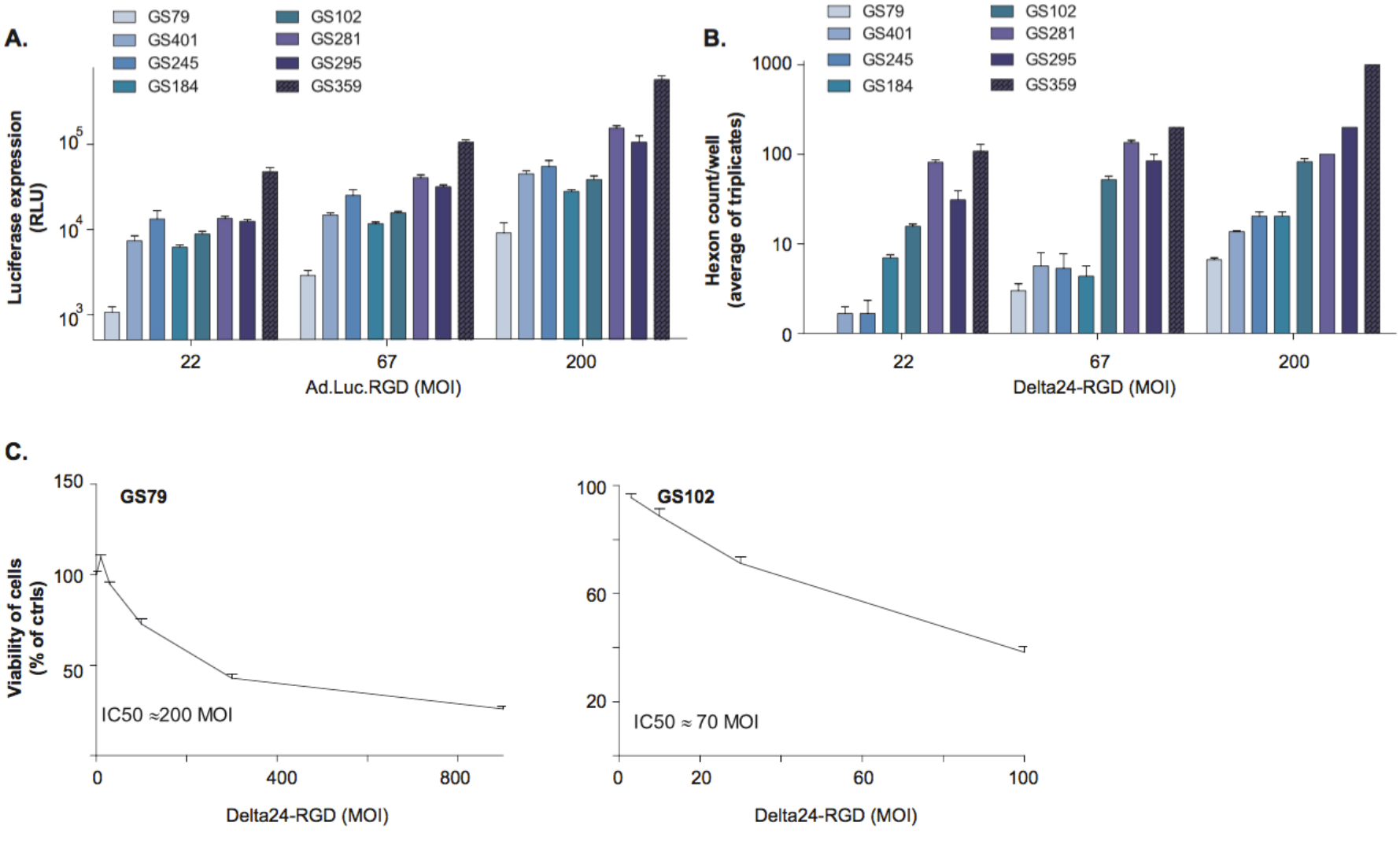

Figure 1. GSCs display heterogeneous susceptibility to adenovirus infection in vitro
(a) GSCs from eight individual patient samples were tested for susceptibility to adenovirus infection using the luciferase expressing non-replicating vector Ad.luc.RGD. The data are shown as RLU in a log10 scale with standard deviation for the three different MOIs of the virus. Read out was performed after 24 hours post-infection.
(b). Variability in adenoviral replication was assessed by staining for adenovirus hexon protein at 48 hours post-infection with three different MOIs Delta24-RGD. The data is presented as hexon counts/well (average of triplicate) in a log10 scale with standard deviation.
(c) Dose-response curves for Delta24-RGD on GS79 (relatively low infection and replication) and GS102 (relatively intermediate infection and replication). The data are presented as viability of cells (percentage of non-treated controls) with standard deviation and IC_{50} values are depicted as calculated by linear regression.

Results

GSCs demonstrate heterogeneous susceptibility to Delta24-RGD

The therapeutic efficacy of Delta24-RGD is heterogeneous between glioblastoma patients.3, 9 Therefore, investigations into potential viral sensitizers should be designed to yield insights both from responsive and resistant models. To achieve this, we screened eight GSCs for their responsiveness to Delta24-RGD. The non-replicating vector Ad.Luc.RGD was used to assess infectivity and the results show substantial variation between the eight GSCs (Figure 1a). GS79 was relatively resistant whereas GS359 was very sensitive to adenoviral infection. The remaining cultures GS401, GS245 GS184, GS102, GS281 and GS295 were intermediately sensitive.

Next, the viral protein production of Delta24-RGD during the first replication cycle was determined by staining for the adenoviral capsid protein hexon (Figure 1b) at 48 hours. The number of hexon counts at this time point revealed a similar pattern to the luciferase expression data of Figure 1a, with the most resistant GS79 having the lowest hexon counts and the most sensitive GS359 having the highest counts.

Two cultures were selected for the subsequent drug screen to investigate which drugs sensitize glioblastoma to OV therapy with Delta24-RGD. Based on the infection and viral protein production assays, GS79 was picked as the “resistant” sample and GS102 as the “intermediate resistant” sample. Accordingly, the IC50 values of Delta24-RGD in GS79 and GS102 were found to be high compared to the MOIs observed in conventional cell lines8; MOI200 for GS79 and MOI70 for GS102 (Figures 1c-d).

Clinical drug screening identifies potential sensitizers of OV therapy with Delta24-RGD

In order to identify viral sensitizers of OV therapy with Delta24-RGD in GSCs, the NIH clinical collection was explored (Figure S1a10). This col-

Table 1. Sensitizers to Delta24-RGD therapy identified by drug screening

Drug	100 µM	10 µM	5 µM	Mw kDa	Category	Application	Abs dif. % GS79	Abs dif. % GS102	Enh. GS79	Enh. GS102	IC_{50} (µM) in GS79	Chou Talalay	Cross BBB
Amlodipine base		NO	X	409	Ca+-channel-blocker	Hypertension	3.50%	41.20%	35.56	28.39	12	Antagonism	ND
Anagrelide HCl	X			254	Platelet aggregation inhibitor	Essential thrombocytemia, CML	60.70%	25.10%	607.5	252.4	142	Synergy	*Not reported*
Ebselen		NO	X	274	Anti-oxidant	Ulcer, inflammation	26.30%	13.30%	264.24	7.34	15	Synergy	*In vivo/ in vitro*
Fenoldopam mesylate	X			305	Dopamine-receptor1 agonist	Hypertension	73.30%	26.90%	12.42	1.87	62	Antagonism	ND
Fluphenazine		X	X	437	Dopamine-receptor-antagonist	Psychosis	29.00%	1.40%	3.5	15.17	4	Synergy	*In vivo*
Indirubin	X			262	Anti-neoplastic, anti-inflammatory	Cancer, inflammation	71.60%	61.20%	9.73	612.59	110	Synergy	*In vivo*
Lofepramine HCl		X	X	418	Tricyclic antidepressant	Depression	41.90%	32.10%	2.29	2.24	19	Additive	*In vivo*
Ranolazine diHcl	X			427	Na+-/Ca+-channel affector	Angina	36.50%	61.00%	2.56	23.09	431	Additive	*In vivo*
Stiripentol	X			234	GABA-agonist	Convulsions	78.70%	18.00%	75.87	1.39	263	Antagonism	ND
Sumatriptan succinate	X			295	5HT1-receptor-agonist	Migraine	77.60%	59.00%	36.23	13.2	622	Antagonism	ND

Table 1. Sensitizers to Delta24-RGD therapy identified by drug screening
The results are shown for all drug concentrations of the NIH clinical collection that were screened *in vitro*. This table shows the 'hits' that were selected for validation. The combinations of these drugs with Delta24-RGD were more effective than virus alone in both GS79 and GS102 cells at the indicated concentrations (column 2-4). The molecular weight of the agent is indicated (column 5), and the drug category and therapeutic indication are provided (columns 6 and 7). The results are shown of the absolute difference in viability between single and combination treatment as well as the enhancement factor of the combination therapy in the two GSC cultures (columns 8 – 11). The results of the validation experiments in GS79 are provided in columns 9-13. The IC_{50} values of the drugs are depicted in column 12. The outcome of the Chou Talalay analysis (synergy, additivity or antagonism) is provided in column 13. Results of a literature search for blood-brain barrier penetration of the drugs is listed in column 14. Legend: Mw kDa = molecular weight in kDa; absolute difference = mean difference between single agent and combination treatment; enhancement = fold increase of viability loss due to combination treatment; blanc = not tested; NO = no effect observed.

lection contains 446 drugs most of which have been approved by the FDA for use in humans for a wide spectrum of clinical indications.15 A third of these are central nervous system (CNS) drugs, including anti-epileptics, antidepressants, antipsychotics. The drug screening strategy is illustrated in a flow-chart (Figure S1b). The primary screen was performed on the two mentioned cultures GS79 and GS102 at a drug concentration of 100µM. Potential viral sensitizers were defined as described in the methods section, which resulted in two arms. The first arm consisted of 332 drugs for which monotherapy reduced viability between 25-75%. Of those drugs, six had viral sensitizing effects in both GS79 and GS120. The second arm consisted of drugs for which monotherapy at 100µM decreased GSC viability by more than 75% (n=114 drugs), since this is incompatible with a reliable evaluation of additive effects with Delta24-RGD. Therefore these drugs were titrated for combination therapy activity at 50, 10, 5 or 1µM, which resulted in the identification of four viral sensitizers with enhancement effect at a dosage of 10 or 5µM. In total ten drugs had a viral sensitizing effect in both GSCs. Table 1 provides an overview of these drugs which are; amlodipine, anagrelide, ebselen, fenoldopam, fluphenazine, indirubin, lofepramine, ranolazine, stiripentol and sumatriptan succinate.

Synergy was detected for six of the potential viral sensitizers

The ten identified viral sensitizers were validated and tested for synergistic activity in GS79 cells according to the Chou-Talalay methods.16 The IC50 values were determined by concentration-response assays (displayed in Table 1). The combination assays were performed and the combination indices (CIs) were calculated. Four of the ten identified drugs were synergistic (CI<1) and two were additive (CI=1) when combined with Delta24-RGD. These were anagralide, ebselen, fluphenazine, indirubin, lofepramine and ranolazine (Figures 2a-b, Table 1). The other drugs (amlodipine, fenoldopam, stiripentol and sumatriptan) failed to reproduce enhancement in the wider concentration range of in vitro testing and were therefore excluded from further validation. In addition, the literature was searched for the ability of the six drugs to cross the blood brain barrier in vivo.17-21 Anagrelide was excluded from further studies because it has not been reported to penetrate the blood-brain barrier in vivo (Table 1), whereas this has been reported for the other drugs.

Viral sensitizers increase adenoviral infection and replication efficacy

To determine whether the drugs improved the efficacy of viral infection, the luciferase expression of the Ad.Luc.RGD-infected GSCs was determined 24 hours after combination treatment with ebselen, fluphenazine, indirubin, lofepramine and ranolazine. The dosages at which synergy was observed were applied in these experiments. Fluphenazine, indirubin and lofepramine significantly increased Ad.Luc.RGD infection in both GS79 and GS102 (Figure 3a, $p<0.05$). Ranolazine increased viral infection only in GS102. Ebselen decreased luciferase expression in both GSCs ($p<0.05$ in GS79 and GS102)

Triggered by the effect of these viral sensitizers on infection efficacy it was hypothesized that these drugs may alter the expression of viral entry receptors CAR and integrin αvβ3. Flow cytometry was performed to investigate the expression of CAR and integrin αvβ3 before and after treatment with the viral sensitizers (Figure 3b). Both indirubin and lofepramine were demonstrated to influence the adenoviral receptor expression at 4 and 8 hours post-treatment. We did not find up-regulation of entry receptors by fluphenazine although the viral infectivity was increased as shown in Figure 3a. For ranolazine, no effects on the surface receptors were observed. In summary, fluphenazine, indirubin, and lofepramine increased viral infection. For lofepramine and indirubin this was associated

Figure 2.

A.

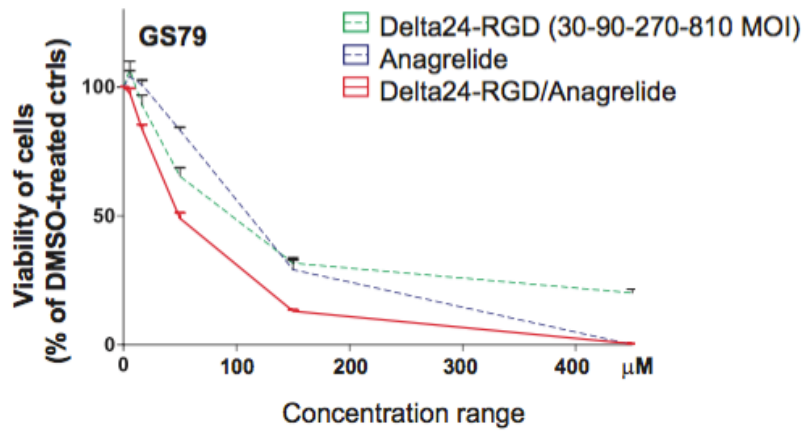

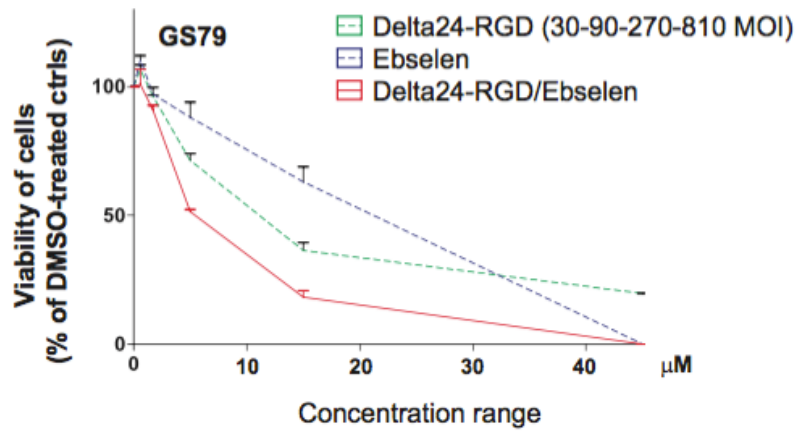

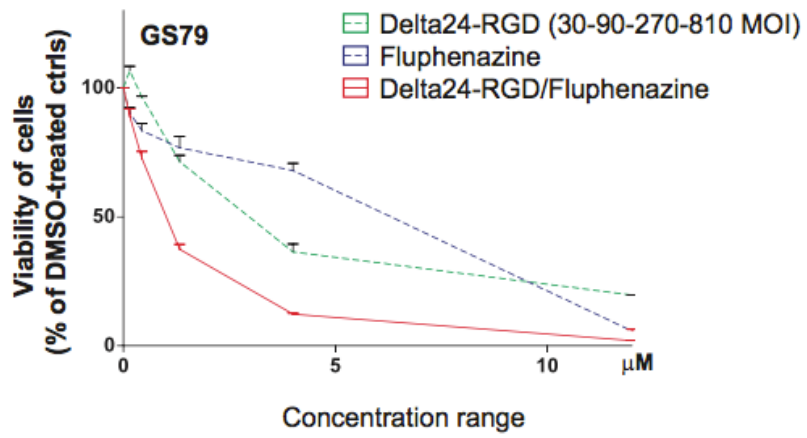

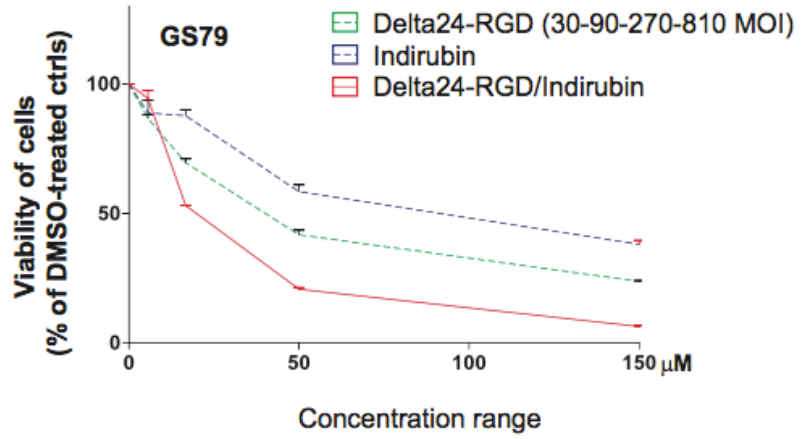

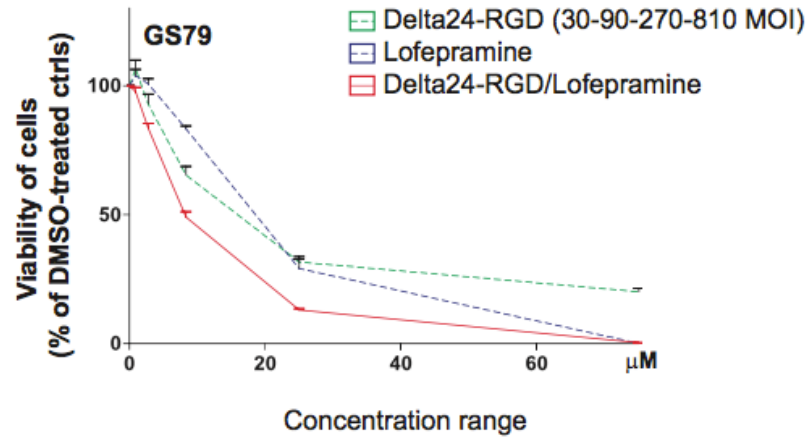

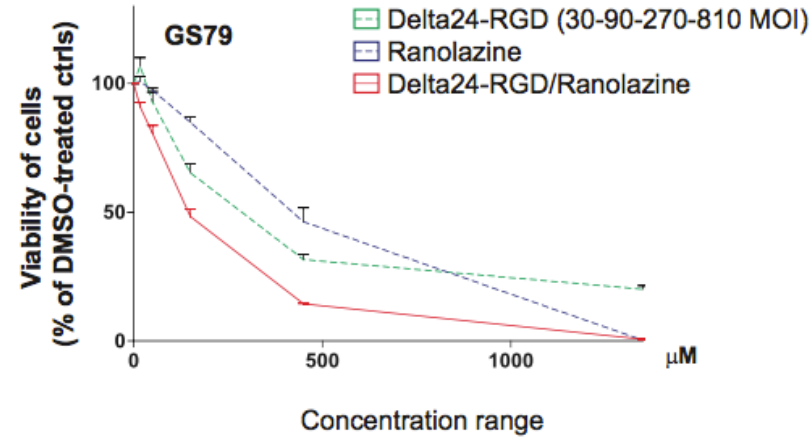

B.

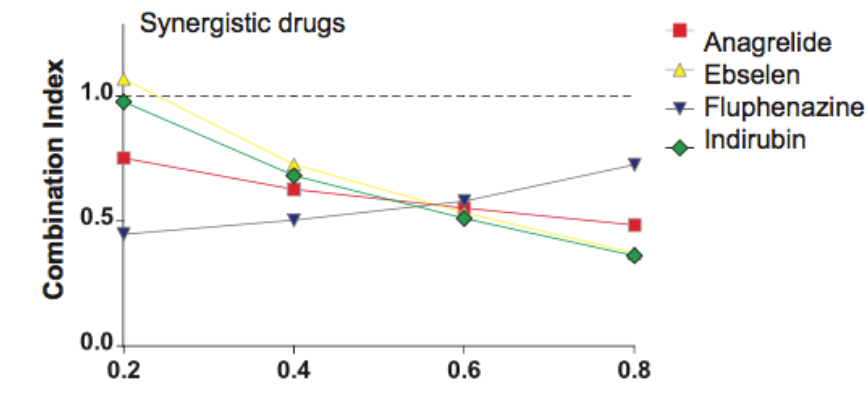

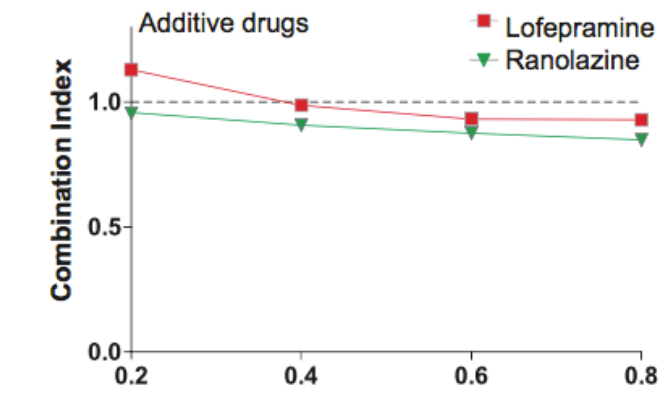

Figure 2. Chou-Talalay synergy analysis on the potential viral sensitizers

(a) Dose-response assays were performed on GS79 cells using the Chou-Talalay method to determine synergy between Delta24-RGD and ten different drugs that were identified by the initial screen. The results are shown for the six drugs that were classified by this method as synergistic or additive. Results are presented as percentage of controls with standard deviation. Read out was performed at five days post-infection.

(b) The combination index (CI) for each drug in combination with Delta24-RGD was calculated by the Chou-Talalay method. A CI of <1 is classified as synergy, a CI of = 1 as additive and a CI >1 as antagonism. The synergistically acting drugs (anagrelide, fluphenazine, indirubin and ranolazine) are shown in the left CI/Fa-plot, whereas additively acting drugs (lofepramine and rabeprazole) are plotted in the right CI/Fa-plot.

Figure 3.

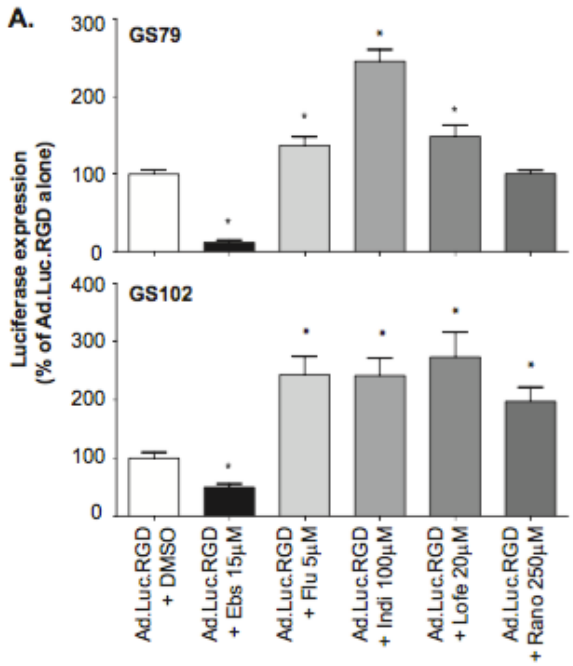

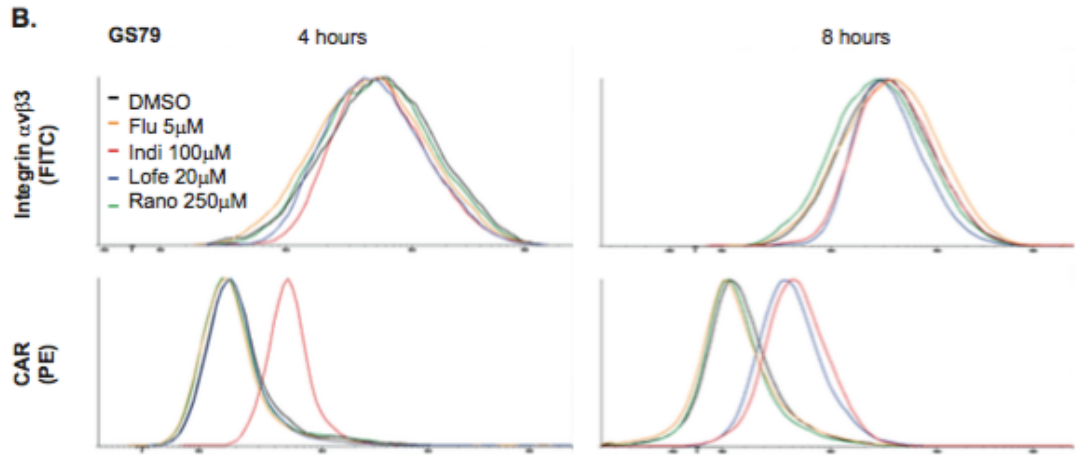

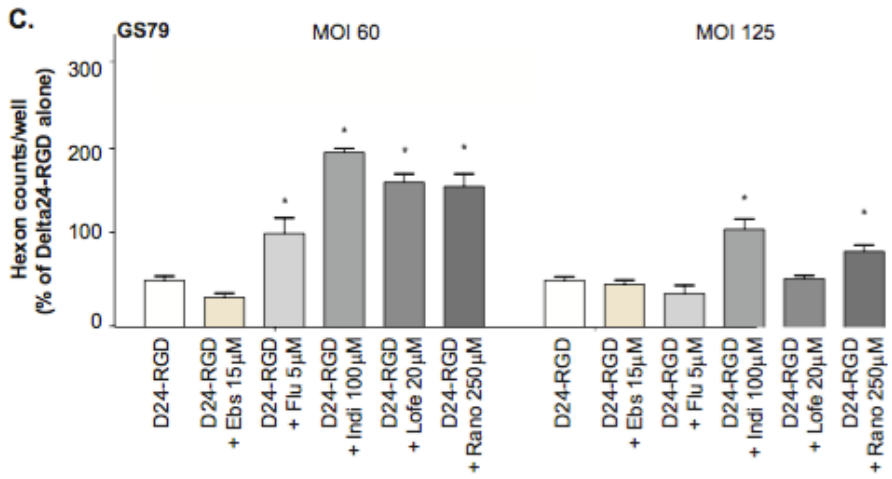

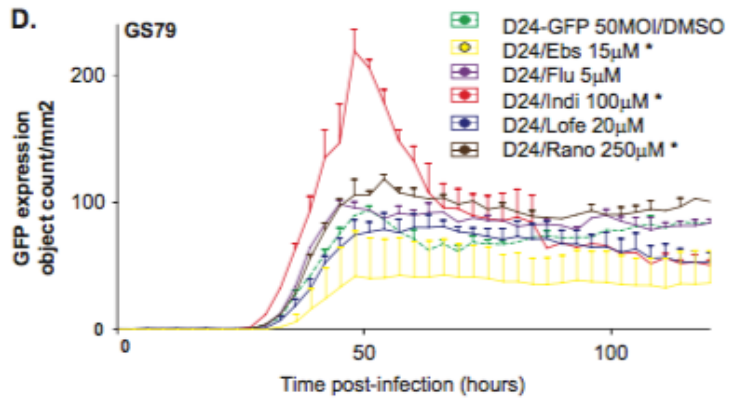

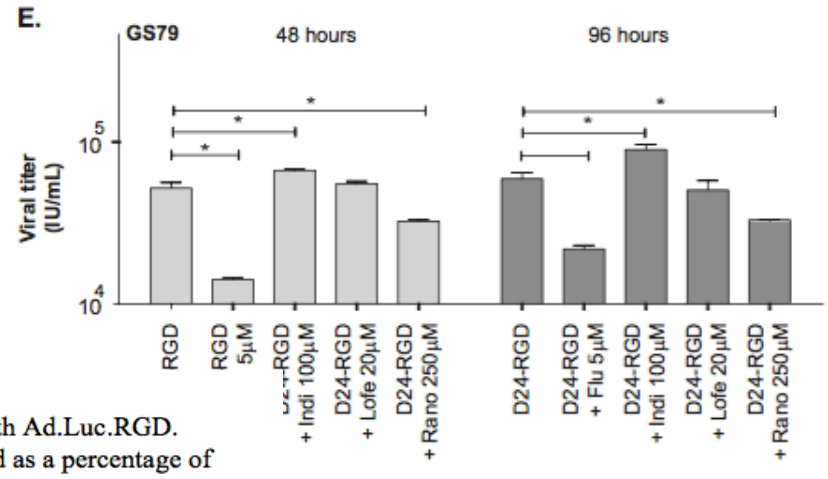

Figure 3. Viral sensitizers increase adenoviral infectivity and replication.
(a) GS79, GS102 and GS245 cells were treated with the indicated drugs and infected with Ad.Luc.RGD. Luciferase expression was measured at 24 hours post-infection. The results are presented as a percentage of DMSO/Ad.Luc-RGD-infected samples with the standard deviation. *Indicates significance difference between Ad.Luc.RGD alone and Ad.Luc.RGD/drug at the $p<0.05$ level.
(b) GS79 cells were treated with indicated drugs. After 4 hours, 8 hours and 24 hours (not shown), the cells were harvested and both CAR and integrin levels were analyzed for differences between the Delta24-RGD alone and Delta24-RGD/drug treated samples. Flow cytometry histograms are presented.
c) GS79 cells were treated with three different MOIs of Delta24-RGD and the four viral sensitizers. The adenoviral replication in the first viral cycle was measured as indicated by hexon counts which are plotted as a percentage of DMSO/Delta24-RGD treated controls with standard deviations. *Indicates significance at $p<0.05$ level of combination treatment compared to Delta24-RGD alone.
(d) GS79 cells were treated with the four drugs and infected with Delta24-RGD-GFP. The fluorescence intensity was measured and analyzed with the IncuCyte software. GFP expression was counted as object count/mm^2 per time point. The results are shown as means with the standard deviation. *Indicates significance at $p<0.01$ level of the combination treatments compared to Delta24-RGD alone.
(e) GS79 cells were concomitantly treated with Delta24-RGD and each of the four drugs, as indicated. The infectious viral particle titers in the cell extracts and supernatants at 48 and 96 hours post-infection were determined by viral titration assay and are displayed graphically. *Indicates significant difference in the viral titers of Delta24-RGD alone compared to the combination treatments with drugs and Delta24-RGD ($p<0.05$).

Figure 4.

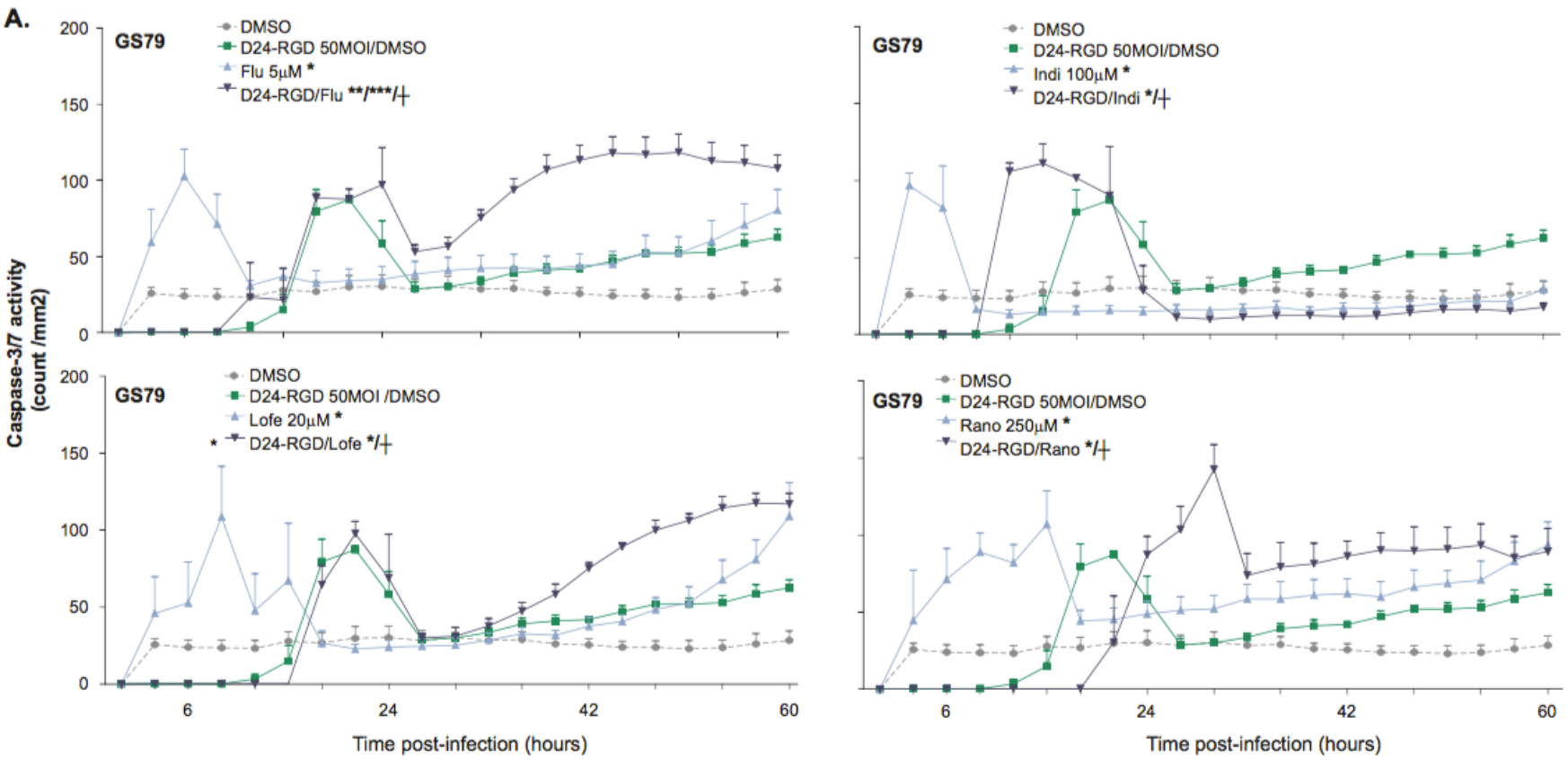

Figure 4. The selected viral sensitizers increase Delta24-RGD oncolytic efficacy by enhancing apoptosis and/or necrosis

(a) GS79 cells were treated with the four drugs and Delta24-RGD. The caspase-3/7 activity levels were measured during a time lapse of 60 hours. The fluorescent spots were counted and are shown as count/mm^2. *Significance at $p<0.05$ combination vs. DMSO-controls;**Significance at $p<0.05$ combination vs. Delta24-RGD; ***Significance at $p<0.05$ combination vs. drug. (two-way ANOVA over whole episode). ┼In the graph indicates significance at $p<0.05$ using the Students' T-test of combination vs. both single agent treatments at single time points.

(b) GS79 cells were treated with the four drugs and two MOIs of Delta24-RGD. LDH activity was measured at five days post-incubation. Fluorescence and viability were measured, to correct for the amount of viable cells. The LDH levels are presented as percentage of DMSO-controls with standard deviation, and corrected for viability. *Significance at $p<0.05$ level of combination vs. Delta24-RGD or agent alone.

Figure 5.

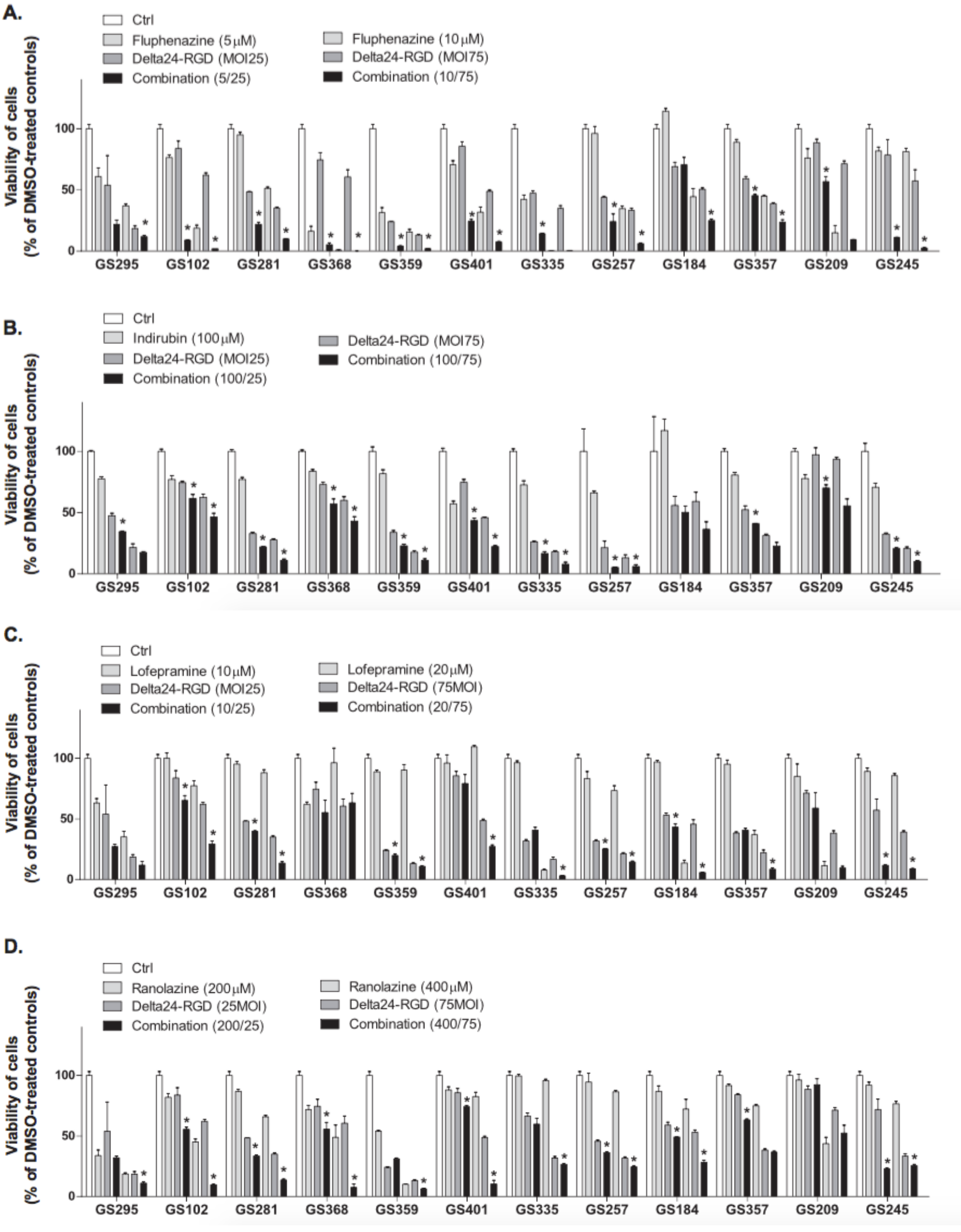
A.
Ctrl
Fluphenazine (5μM)
Delta24-RGD (MOI25)
Combination (5/25)
Fluphenazine (10μM)
Delta24-RGD (MOI75)
Combination (10/75)
Viability of cells
(% of DMSO-treated controls)
100
50
0
GS295
GS102
GS281
GS368
GS359
GS401
GS335
GS257
GS184
GS357
GS209
GS245
B.
Ctrl
Indirubin (100μM)
Delta24-RGD (MOI25)
Combination (100/25)
Delta24-RGD (MOI75)
Combination (100/75)
Viability of cells
(% of DMSO-treated controls)
100
50
0
GS295
GS102
GS281
GS368
GS359
GS401
GS335
GS257
GS184
GS357
GS209
GS245
C.
Ctrl
Lofepramine (10μM)
Delta24-RGD (MOI25)
Combination (10/25)
Lofepramine (20μM)
Delta24-RGD (75MOI)
Combination (20/75)
Viability of cells
(% of DMSO-treated controls)
100
50
0
GS295
GS102
GS281
GS368
GS359
GS401
GS335
GS257
GS184
GS357
GS209
GS245
D.
Ctrl
Ranolazine (200μM)
Delta24-RGD (25MOI)
Combination (200/25)
Ranolazine (400μM)
Delta24-RGD (75MOI)
Combination (400/75)
Viability of cells
(% of DMSO-treated controls)
100
50
0
GS295
GS102
GS281
GS368
GS359
GS401
GS335
GS257
GS184
GS357
GS209
GS245

Table 2. Molecular subtypes of the panel of GSC cultures.

Primary GSC culture	Molecular subtype	MGMT methylation status
GS79	CLA	UM
GS102	NEU	M
GS184	CLA	M
GS209	PRO	UM
GS245	NEU	UM
GS257	CLA	UM
GS281	MES	UM
GS295	MES	UM
GS335	CLA	M
GS357	CLA	M
GS359	MES	M
GS368	CLA	UM
GS401	PRO	M

Table 2. Molecular subtypes of the panel of GSC cultures
Twelve patient-derived GSC cultures were used for screening of the identified viral sensitizers in a larger panel. The culture used for the initial experiments (GS79) is also included in the table. The molecular characteristics are shown, including the molecular subtype according to The Cancer Genome Atlas (TCGA) and the MGMT promotor methylation status.

with increased levels of CAR and slightly increased levels of αvβ3 integrins.

Effects of the drugs on Delta24-RGD early viral replication, late viral gene expression and progeny production

We investigated the Delta24-RGD viral hexon production during the first viral cycle as a measure of replication efficacy after combination therapy with the viral sensitizers. At MOI 60, the four drugs increased the number of hexon spots at 48 hours ($p<0.05$). Ebselen slightly decreased the number of hexon counts/well ($p<0.01$). Fluphenazine, lofepramine, and ranolazine all increased viral protein production by 2 to 3-fold and indirubin was most effective, increasing the hexon counts by 3.7-fold ($p<0.01$) At the higher virus concentration of MOI 125, only indirubin and ranolazine were still significantly increased compared to control (Figure 3c).

To measure the effects of the four drugs on the viral cycle in a longitudinal manner, we performed time-lapse fluorescence imaging of Delta24-RGD-GFP infected cells. GFP is expressed late in the replication cycle (Figure 3d). Indirubin, ranolazine and fluphenazine peaked earlier than controls suggesting more efficient replication and lysis. The GFP data was in line with the results of the hexon staining. Both indirubin and ranolazine enhanced Delta24-RGD-GFP expression ($p<0.01$ and $p<0.001$ respectively). Differences in the kinetics were observed, namely indirubin

increased peak levels of GFP expression whereas ranolazine increased the fluorescence levels consistently over time without evidently enhancing peak levels. In accordance with the previous findings, ebselen reduced viral replication of Delta24-RGD-GFP ($p<0.05$). Due to the pronounced inhibitory effects of ebselen in both the viral infection and replication assays this drug was not further evaluated.

To assess whether the enhancement of early and late viral protein production translates to increased viral progeny production, viral titration assays were performed (Figure 3e). Only indirubin increased the viral progeny production in GS79 cells at both 48 and 96 hours post-infection from 5.2x104 to 6.7x104 ($p<0.05$) and from 5.9x104 to 9.0x104 ($p<0.05$), respectively, compared to Delta24-RGD alone. Interestingly, fluphenazine and ranolozine achieved the opposite effect from indirubin: a decrease in viral progeny production at both time points ($p<0.05$). Lofepramine did not significantly alter the viral progeny production. In summary, the viral progeny production was increased by indirubin and was decreased by both fluphenazine and ranolazine.

Viral sensitizers increase Delta24-RGD-induced oncolysis by enhancing apoptosis and necrosis

We performed an in silico analysis using the Ingenuity Pathway Analysis (IPA) software (Figure S2, IPA, September 2014) to identify which pathways are activated or inhibited by the four viral sensitizers. Next, we evaluated whether identified cell death pathways are relevant for viral oncolysis. Fluphenazine targets the dopamine receptor, indirubin targets the aryl hydrocarbon receptor and the apoptotic signaling molecules Bcl-2, BIRC5 and NFκB, lofepramine affects pro-apoptosis associated SMPD1 and ranolazine affects the adrenergic receptor. The top ten of overlapping functions of the downstream molecules of these drugs included relevant mechanisms for viral oncolysis such as cell death, apoptosis and necrosis.

Others have found cell death pathways to be affected by OV therapy.22, 23 Since oncolysis induced by the adenovirus is reported to be associ-

Previous page: Figure 5. Viral sensitizers enhance Delta24-RGD efficacy in a broad panel of distinct GSCs
Twelve patient-derived GSCs were tested with two different concentrations of the drugs in combination with two different MOIs of the virus. The viability is shown as percentage of DMSO-controls with the standard deviation. Fluphenazine/Delta24-RGD combination therapy demonstrated enhancement in all GSCs tested (a), indirubin/Delta24-RGD in 11/12 GSCs (b), lofepramine/Delta24-RGD in 9/12 GSCs and (c) ranolazine/Delta24-RGD in 11/12 GSCs (d). *Indicates significance at the $p<0.05$ level for the combination treatment compared to both single agent treatments.

Figure 6.

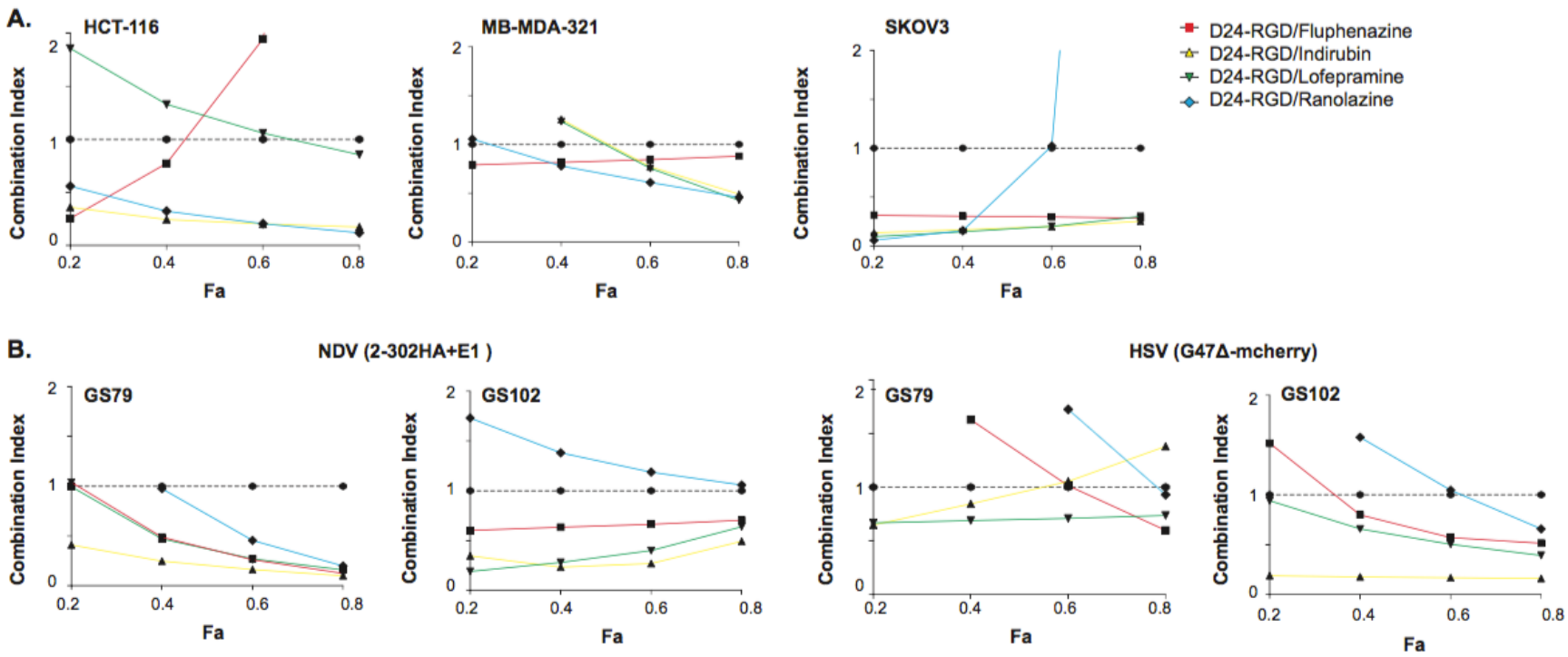

Figure 6. Viral sensitization is reproduced in vitro in 3 additional solid tumor models and 2 additional OV's suggesting broad applicability

(a) Dose-response combination assays were performed using Chou-Talalay analysis to study interaction between Delta24-RGD and the four viral sensitizers in three tumor cell lines, being triple negative breast, ovarian and colon carcinoma cells. Viability was measured at day five post-treatment. The combination indices (CI) were calculated and are shown for the various treatment combinations in these cell lines.

(b) Dose-response combination assays were performed using Chou-Talalay assays to study interaction between the four viral sensitizers and oncolytic HSV and NDV in the GSCs GS79 and GS102. Viability was measured at day five post-treatment. The combination indices (CI) are shown for the various treatment combinations in these cell lines.

ated with both apoptosis and necrosis, we investigated the role of the viral sensitizers in both cellular responses. A longitudinal assessment of caspase-3/7 activity was performed to study the role of the viral sensitizers on apoptosis. All four viral sensitizers induced caspase 3/7 activity at early time points post-treatment (Figure 4a). Infection with Delta24-RGD led to a delayed onset of caspase 3/7 activity. Combination treatments of Delta24-RGD with each of the four viral sensitizers also led to a delayed onset of caspase 3/7 expression but with a higher peak activity level for indirubin at 9 – 15 hours and prolonged higher caspase 3/7 activity for fluphenazine, lofepramine and ranolazine at 30-60 hours ($p<0.05$).

To determine necrotic cell death, a lactate dehydrogenase (LDH) assay was used. This assay measures the release of LDH in the culture medium, which serves as a dynamic marker for loss of cellular membrane integrity, an early event in necrotic cell death. (Figure 4b). Delta24-RGD (MOI 75) monotherapy increased LDH levels five days post-infection ($p<0.05$ compared to controls). Fluphenazine was the only viral sensitizer that increased LDH levels in combination with the virus compared to both single agents ($p<0.05$). Indirubin and lofepramine combined with the virus increased LDH levels compared to the drugs alone, whereas ranolazine increased LDH compared to the virus alone ($p<0.05$). In conclusion, viral sensitizers combined with Delta24-RGD effectively induced both apoptotic and necrotic cell death in vitro. The four drugs interacted with apoptotic cell death as derived from caspase-3/7 activity. Enhanced necrosis was demonstrated using ranolazine and fluphenazine.

Viral sensitizers are effective in a broad panel of heterogeneously responding patient-derived GSCs

Glioblastoma is a heterogeneous tumor, which has profound consequences for efficacy of therapeutics. To place the viral sensitizing ability of the four drugs in the context of this molecular heterogeneity, a broader panel of GSCs was employed to investigate their general applicability. Table 2 shows the molecular characteristics of the panel of GSC cultures indicating that all TCGA-defined subtypes are represented as well as both methylated and unmethylated MGMT promoter subtypes. The viral sensitizers were combined with Delta24-RGD in the GSCs that were used in the initial infectivity studies (Figures 1a-b) and expanded with an additional set amounting to a total of twelve GSC cultures. The four viral sensitizers were applied in two different concentrations in combination with two MOIs of Delta24-RGD (Figures 5a-d). Significant enhancement was considered if the combination therapy decreased the viability com-

pared to both single agents therapies ($p<0.05$). Fluphenazine was effective in enhancing Delta24-RGD oncolysis in all twelve patient-derived GSCs. Indirubin was effective in 11/12 GSCs. Lofepramine was effective in 9/12 cultures mainly at the higher concentration of 20μM and ranolazine was effective in 11/12 cultures. Overall, these data confirm that the four drugs that were identified as potential viral enhancers by a screen on GS79 are effective in a broader panel of patient-derived GSCs, which bears distinct molecular characteristics and shows differential sensitivity to Delta24-RGD. These findings suggest that the identified sensitizers could be effective in enhancing Delta24-RGD oncolytic therapy in a broader context of heterogeneous glioblastomas.

General applicability of the drugs: enhancement in other tumor cell lines and enhancement of other viruses

The applicability of the four drugs as viral sensitizers was subsequently investigated in a broader perspective. We tested the combination of Delta24-RGD and the viral sensitizers in other tumor cell lines, namely the breast carcinoma cell line MB-MDA-231, the ovarian cancer cell line SKOV3 and the colon carcinoma cell line HCT-116 (Figure 6a; Supplemental Figure 3-4). Chou-Talalay assays were performed to determine synergy, additivity or antagonism. The results reveal that fluhpenazine, indirubina and ranolazine show synergy in all three cell lines, however there are large differences in the actual enhancement. Lofepramine showed additive enhancement in HCT-116 and synergy in SKOV3 and MB-MDA-231 cell lines. Ranolazine showed synergy at low concentrations in SKOV3 cells, at high concentrations in MB-MDA-231 cells and at all concentrations in HCT-116 cells. In summary, the four drugs, and in specific, ranolazine and indirubin are effective sensitizers of Delta24-RGD in other tumor cell lines including those originating from triple negative breast carcinoma, colon carcinoma and ovarian carcinoma. The extent of the enhancement could be tumor type dependent. In addition, we assessed the sensitizing effects of the four compounds on two other OVs, the Newcastle disease virus (NDV) and the Herpes Simplex Virus-based G47Δ-mcherry in GS79 and GS102 (Figure 6b; Figure S4). The results show that fluphenazine, indirubin and lofepramine effectively synergized with G47Δ-mcherry in both GSCs. All four drugs were effective in combination with NDV, where ranolazine was the least effective drug. Also, the extent of the enhancement depended on both the virus and the cell culture . In summary, fluphenazine, indirubin and lofepramine are effective viral sensitizers for the OVs based on NDV and HSV vectors.

Discussion

The present study has identified four clinical approved viral sensitizers for the oncolytic adenovirus Delta24-RGD in patient-derived GSCs, namely fluphenazine, indirubin, lofepramine and ranolazine. Mechanistic studies attributed the synergistic activity with the virus partly to enhanced infection, replication or both. Not in the least, the induction of programmed cell death through apoptosis and or necrosis, was found to be increased and accelerated. As such, we conclude that these four viral sensitizers are potentially promising adjuvants to virotherapy for glioblastoma.

Previously, we have reported the strength of implementing a panel of GSCs for the assessment of combination therapy for glioblastoma in vitro.9, 24-26 The NIH clinical compound library has been applied to GSCs before27, 28 which resulted in the identification of numerous GSC specific compounds, and established the use of GSCs as a useful tool for drug screening experiments. Interestingly, Pollard et al., identified fluphenazine as a monotherapeutic agent in three GSC cultures as well. We here performed the first systematic drug screen to identify clinically approved drugs that enhance oncolytic adenovirus potency. Others have identified synergizing compounds in a mechanism driven strategy, 29, 30 or by combining the current clinical standard therapeutics31-33 and radiation therapy.4, 34, 35 Compound screenings for oncolytic HSV, myxoma and VSV have been reported using other chemical libraries.36-38 The strategy to detect viral sensitizers through high throughput screening, as implemented in this study, results in the unbiased detection of very potent FDA approved compounds.

One of the advantages of screening panels of GSCs is the identification of responders and non-responders, which grants the opportunity to investigate underlying mechanisms.25 Accordingly we have observed that the response to Delta24-RGD therapy is heterogeneous8, and may be driven by cell-entry receptors, autophagy mediated lysis and cellular anti-viral response.22, 39, 40 Viral sensitization by these four compounds was reproduced in a panel of twelve GSCs, which suggests applicability of combination therapy in both intrinsically resistant and susceptible glioblastoma patients. Furthermore, viral sensitizing by the four drugs was not restricted to Delta24-RGD; both NDV and HSV virotherapy synergized with these compounds, nor was is restricted to glioblastoma, as viral sensitizing was observed in cell lines derived from other tumors. These results suggest that a more general mechanism of action underlies these combination therapies.

The combination of the in vitro drug screen and the in silico pathway analysis on the identified compounds was shown to be a powerful tool to predict mechanisms of action. As indicated by the in silico analysis, the four compounds converge on cell death pathway enhancement, which we could substantiate in the validation experiments. The pathways identified were of specific interest for combination treatment with Delta24-RGD, as apoptosis and necrosis have been shown to be involved in oncolytic cell death.41-43

The identified viral sensitizers have been sparsely investigated in the context of OV therapy. Below, we discuss the four viral sensitizers individually with regard to the mechanism of action, the reported effects in combination with viruses and their known effects on the immune response. The immune response is crucial for Delta24-RGD efficacy in vivo.44

Fluphenazine is a neuroleptic drug used for the treatment of psychosis and has not been previously identified as a viral enhancer. The drug enhanced infection, viral protein synthesis as well as oncolysis in the whole panel of patient-derived GSC cultures. Interestingly the viral progeny yield was decreased which may be related to the enhanced apoptotic and necrotic cell death possibly interfering with efficient viral particle production. Earlier fluphenazine was reported to inhibit leukemia and brain

tumor cells27, 45, 46, which may be related to the inhibition of calmodulin that contributes to apoptosis through caspase-8 and Akt-pathway inhibition.47

Indirubin is used in Chinese medicine as an antipsoriatic48 and anti-leukemia drug.49 In OV therapy using Delta24-RGD, we showed that indirubin increases infection, CAR and integrin expression, viral protein production during the first cycle, viral gene expression over time and viral progeny production. Increased viral activity by indirubin has thus far not been reported. Indeed, indirubin derivatives have been shown to affect viral activities. Indirubin-3'-monoxime was effective in increasing viral transduction of an adeno-associated viral vector.50 Another derivative was shown to inhibit viral replication of H5N151, cytomegalovirus52, and the pseudorabies virus.53 These reports and the results within this study, suggest that the effects of indirubin on viral replication may depend on the indirubin-derivative used, and/or on type of virus investigated. In our study, indirubin consistently augmented adenoviral oncolysis in multiple GSC cultures and other cancer cell lines, as well as the oncolytic activity of two other viruses, NDV and HSV. The downstream molecules of indirubin are associated with apoptosis54, which was confirmed by our in vitro studies. Indirubins may also have specific effects on the immune system as indirubin-3'-monoxime has been reported to induce immunosuppressive and anti-inflammatory effects on dendritic cells.55 Moreover, inhibition of the indirubin target GSK-3 reduces microglial inflammatory responses.56 Additional studies are warranted to investigate the effects on the immune response by indirubin in combination with Delta24-RGD.

The anti-depressant lofepramine has not previously been identified as an enhancer of viral efficacy. We show that this drug increases viral infection, which was associated with up-regulation of viral entry receptors, and enhances viral replication. The in silico pathway analysis revealed that lofepramine as a monotherapy affects downstream molecules related to apoptosis. This was translated to the combination therapy as well, as we confirmed in vitro. As a single drug treatment, lofepramine has been reported to block leukemia cell proliferation and to sensitize cells to apoptosis.57

The anti-anginal drug ranolazine is a sodium-channel blocker that has not been studied in combination with oncolytic viruses. Ranolazine enhanced the viral infection (culture specific) and viral protein production during the first viral cycle. However, viral progeny production was decreased, which is possibly related to enhanced induction of apoptosis and necrosis. Ranolazine has not been reported to possess direct tumor killing activity, however, a role for this drug in sodium channel–mediated breast cancer invasiveness has been reported.58 The current study reveals novel mechanisms associated with this drug, which were not previously identified. Neither ranolazine nor lofepramine have been studied in the context of the immune system.

In conclusion, our study identified four effective viral sensitizers for Delta24-RGD oncolytic therapy in glioblastoma. These drugs include fluphenazine, indirubin, lofepramine and ranolazine. This study reveals the interaction of the drugs with important viral oncolytic cell death mechanisms, as shown in silico and in vitro. The identified drugs are not only applicable in glioblastoma but show synergy with Delta24-RGD in multiple cancer types. Moreover, all drugs except ranolazine act synergistically with other oncolytic viruses as well. Although the identified viral sensitizers are clinically applicable, future studies should focus on finding the optimal administration to achieve maximal effects in vivo. Moreover, in vivo studies with these agents are required to interrogate their effects on the immune response to OV therapy, a factor known to play a pivotal role in therapeutic outcome of these therapies.

Acknowledgements

This research was partially supported by a Travel Fund of the Royal Dutch Wilhelmina Fund (KWF) and a travel fund of the EUR Trustfonds, Rotterdam, The Netherlands.

A.

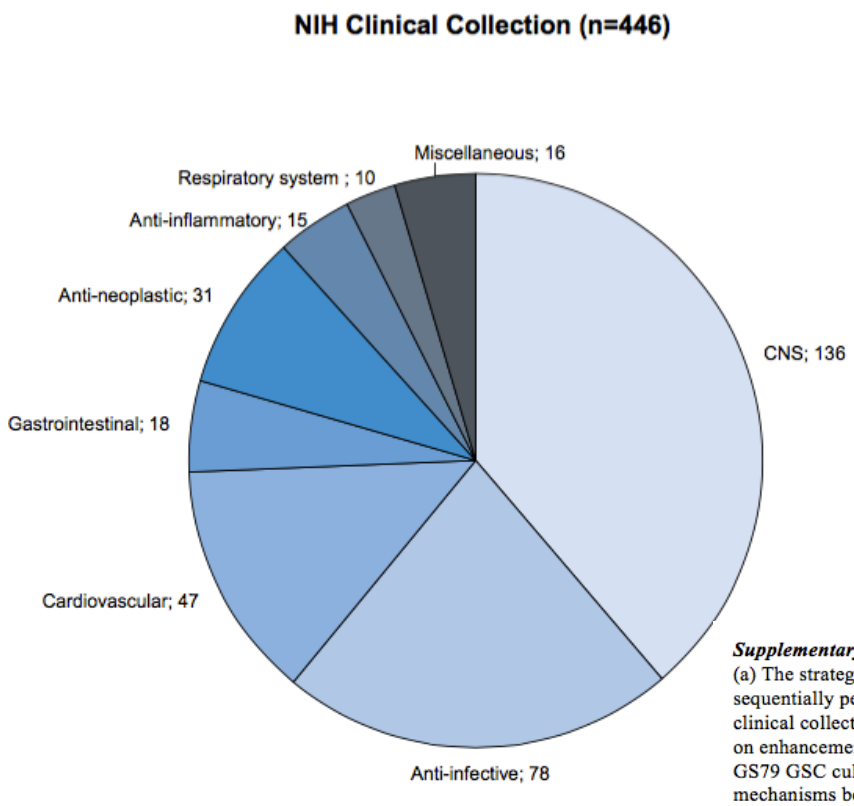

B.

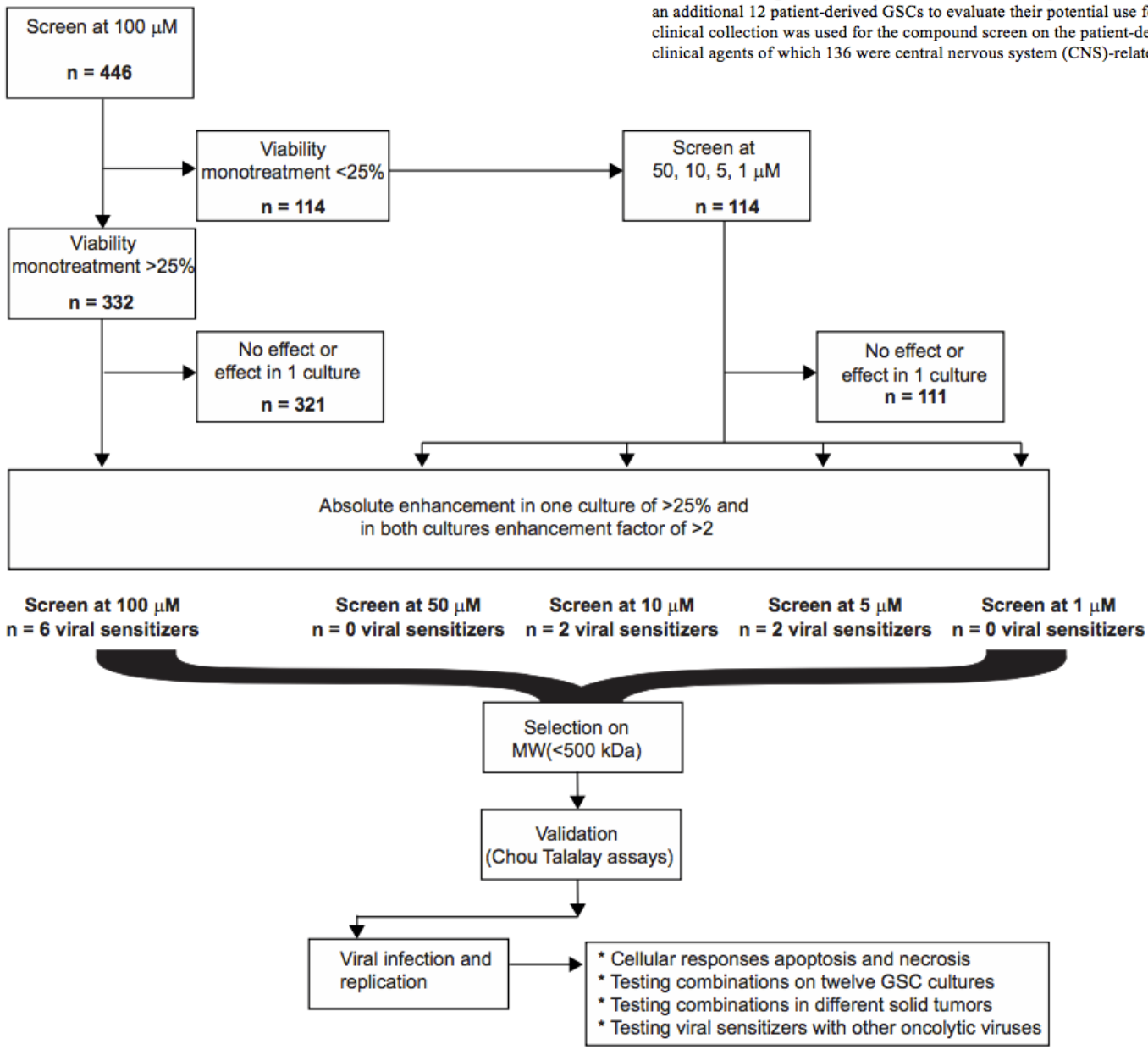

Supplementary Figure 1. The contents of the NIH clinical collection and the drug screening strategy.
(a) The strategy of the compound screening approach is shown schematically. A total of three screens were sequentially performed (first at 100μM, followed by 10 and 1μM, and lastly at 50 and 5μM) using the NIH clinical collection which contains 446 drugs.[12] After these screens, potential viral sensitizers were selected based on enhancement, and ten of the agents were validated using the Chou-Talalay method in the patient-derived GS79 GSC culture. After that, the validated potential viral sensitizers were evaluated for their effects on viral mechanisms being infection, replication and cellular responses. Finally, four selected compounds were tested on an additional 12 patient-derived GSCs to evaluate their potential use for further *in vivo* studies. (b) The NIH clinical collection was used for the compound screen on the patient-derived GSCs.[12] It contains 446 different clinical agents of which 136 were central nervous system (CNS)-related compounds.

Suppemental Figure 2.

A. **Fluphenazine**

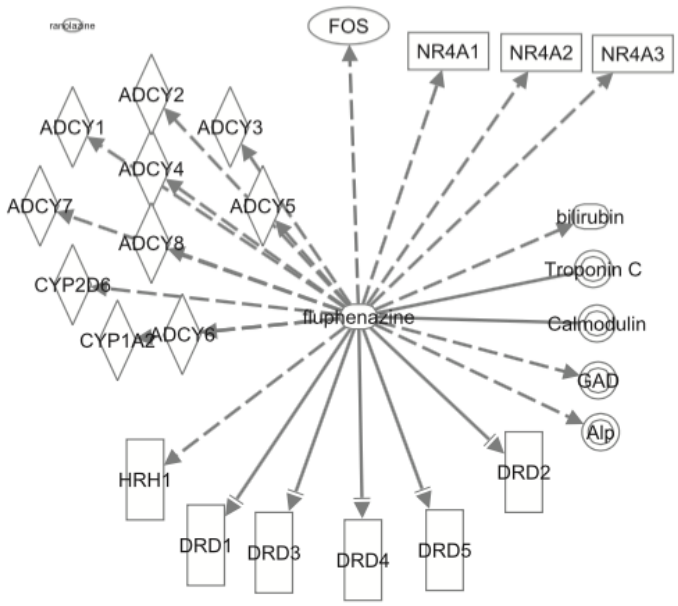

D. **Ranolazine**

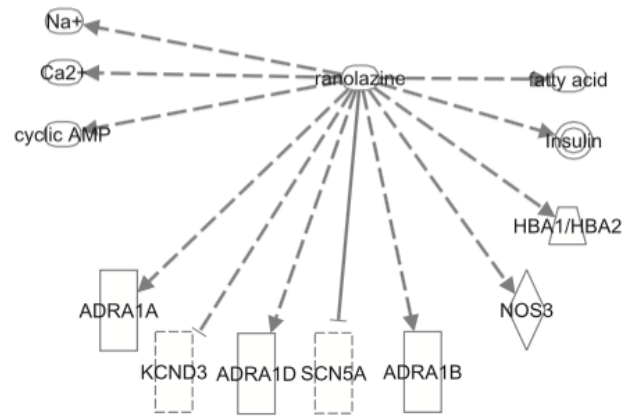

B. **Indirubin**

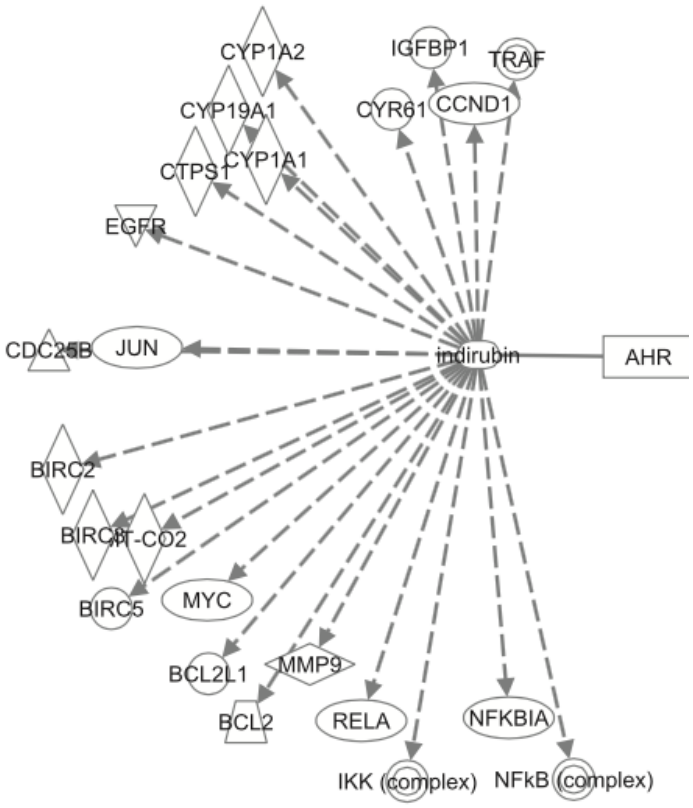

E. **Functions and diseases hierarchical clustering**

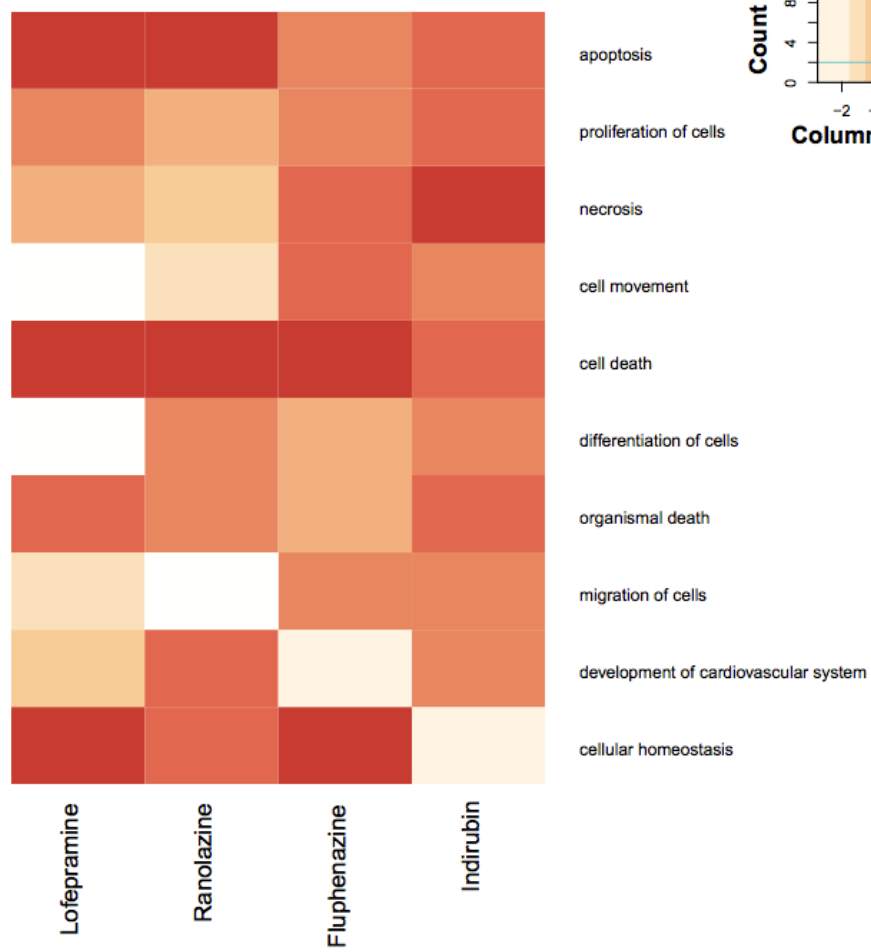

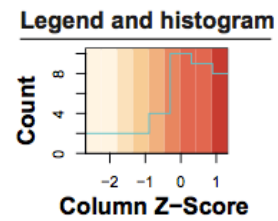

C. **Lofepramine**

Supplementary Figure 2. In silico analysis confirms viral sensitizers interact with pathways canonical for Delta24-RGD therapeutic outcome

(a-d) The direct and indirect downstream molecules and proteins (only first order) of the four viral sensitizers (a-d). The dashed arrows indicate indirect relationships whereas the closed arrows show direct relationships with the molecules.

(e) The common functions and diseases for the four compounds in hierarchical clustered based on p-value of the overlap. All were significant (<0.001), and the data was derived using the IPA September 2014. The top ten of functions and diseases are shown in the heat map. The z-value represents the normalized p-value for each agent.

Supplemental Figure 3.

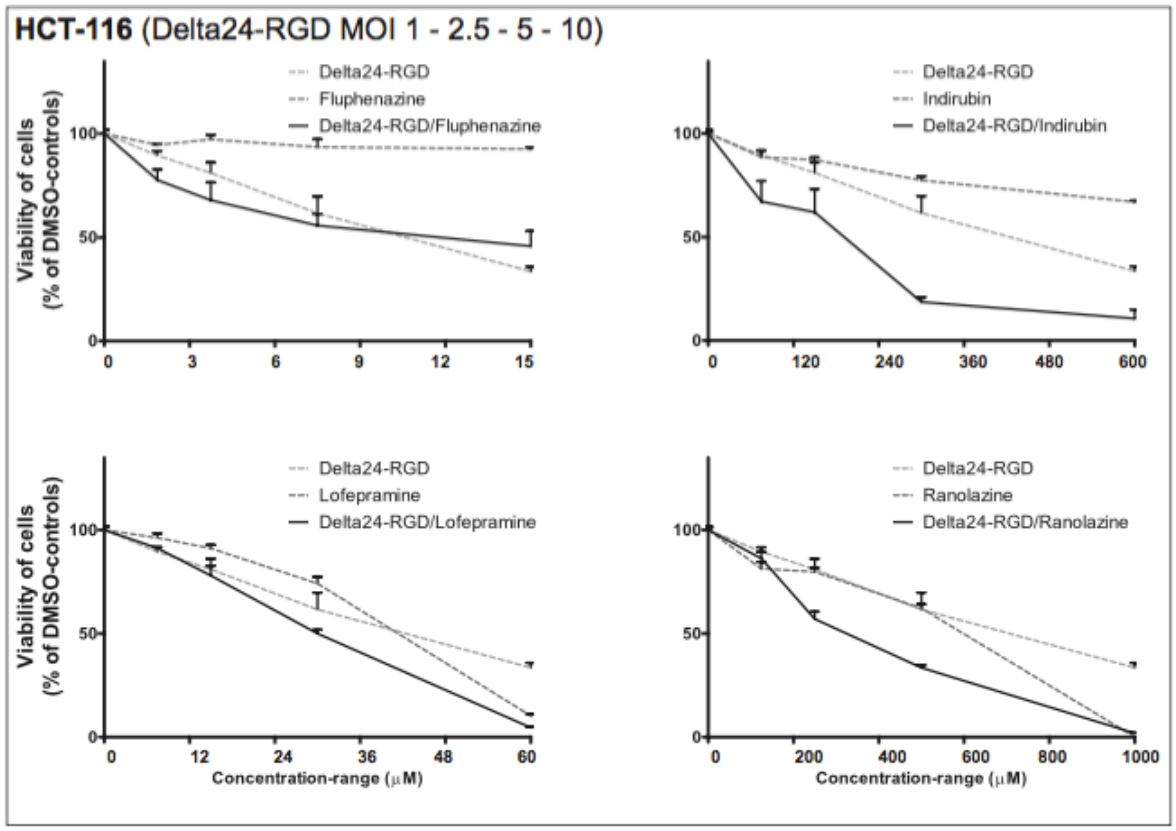

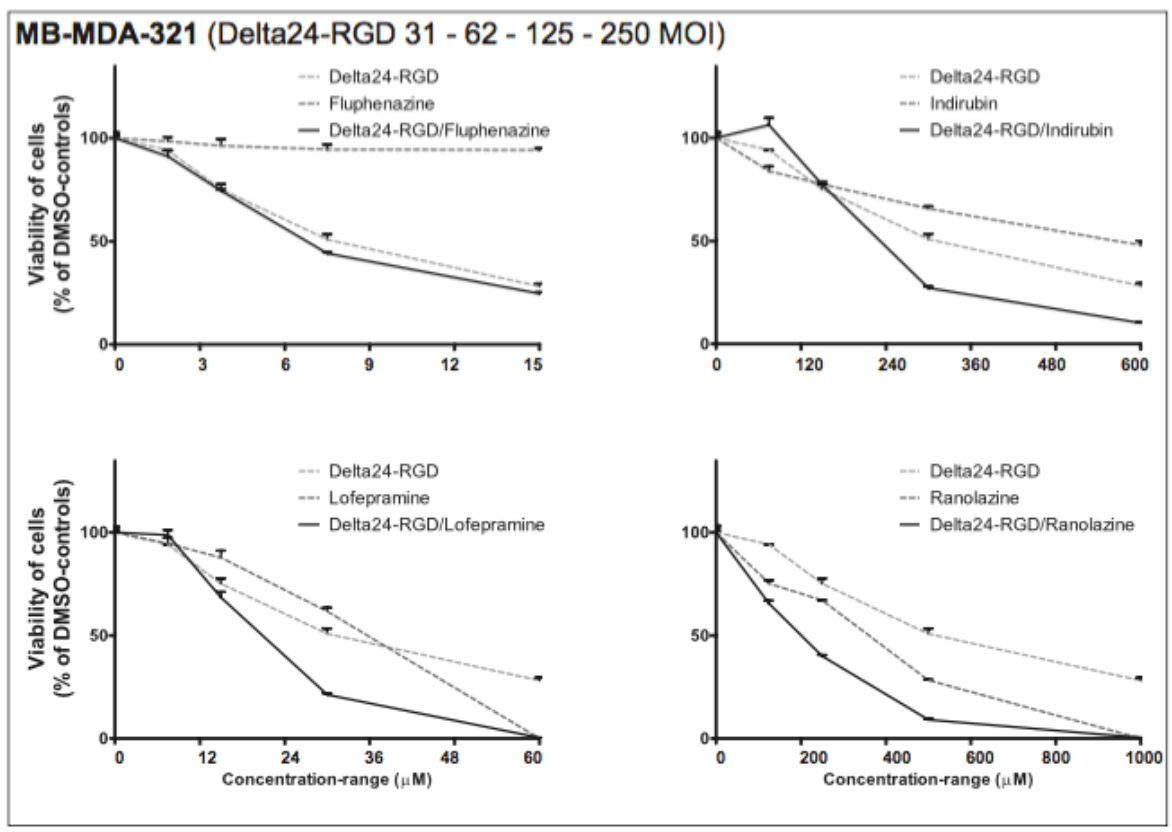

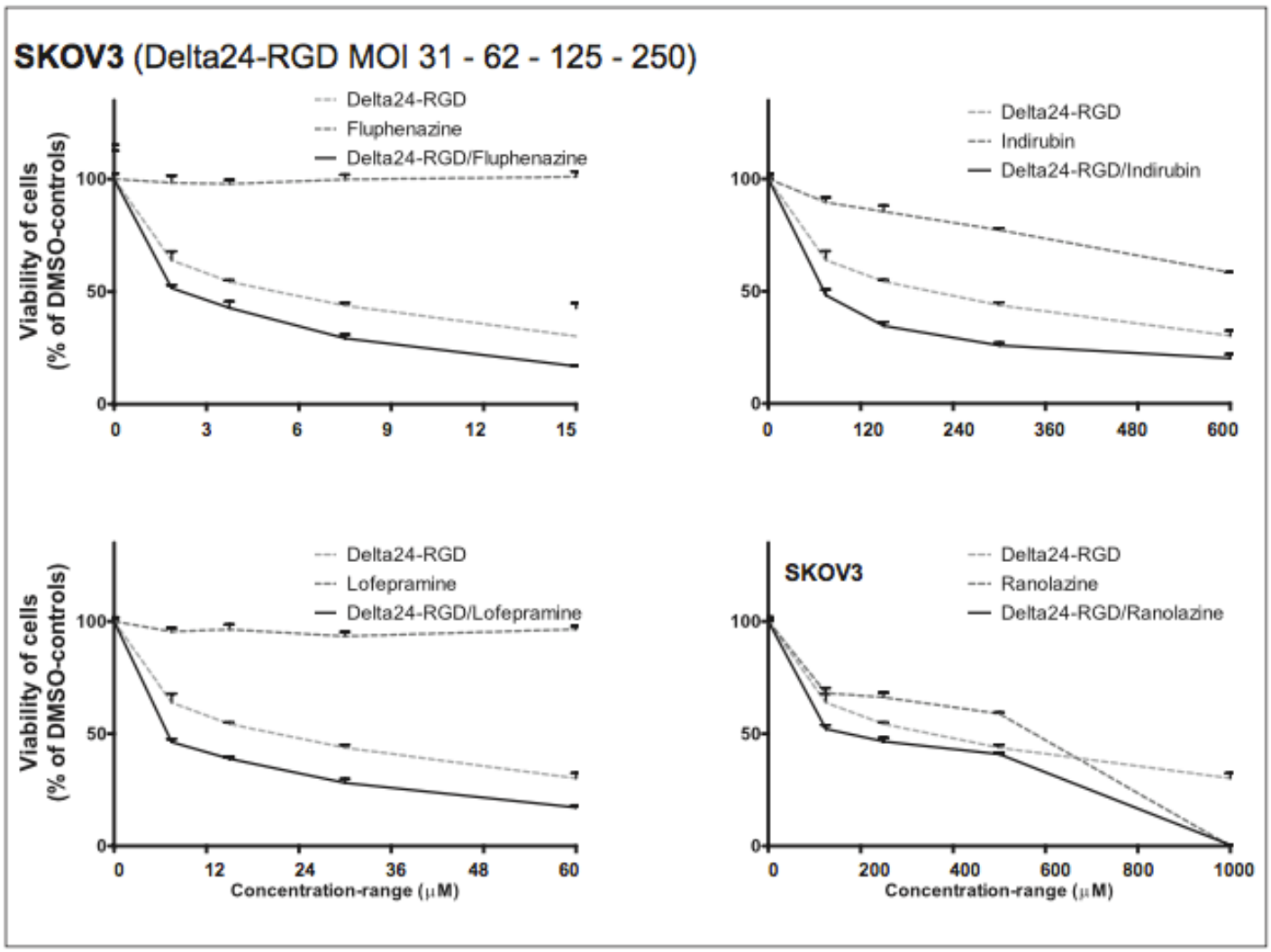

Supplementary Figure 3. Drug/virus combination effects in different solid tumor cell lines.
Dose-response combination assays were performed using Chou-Talalay analysis to study synergy between Delta24-RGD and the four viral sensitizers in three tumor cell lines, being triple negative breast, ovarian and colon carcinoma cells. Viability was measured at day five post-treatment. The dose-response graphs are shown as mean percentage viability compared to DMSO treated controls with the standard deviation.

Supplemental Figure 4.

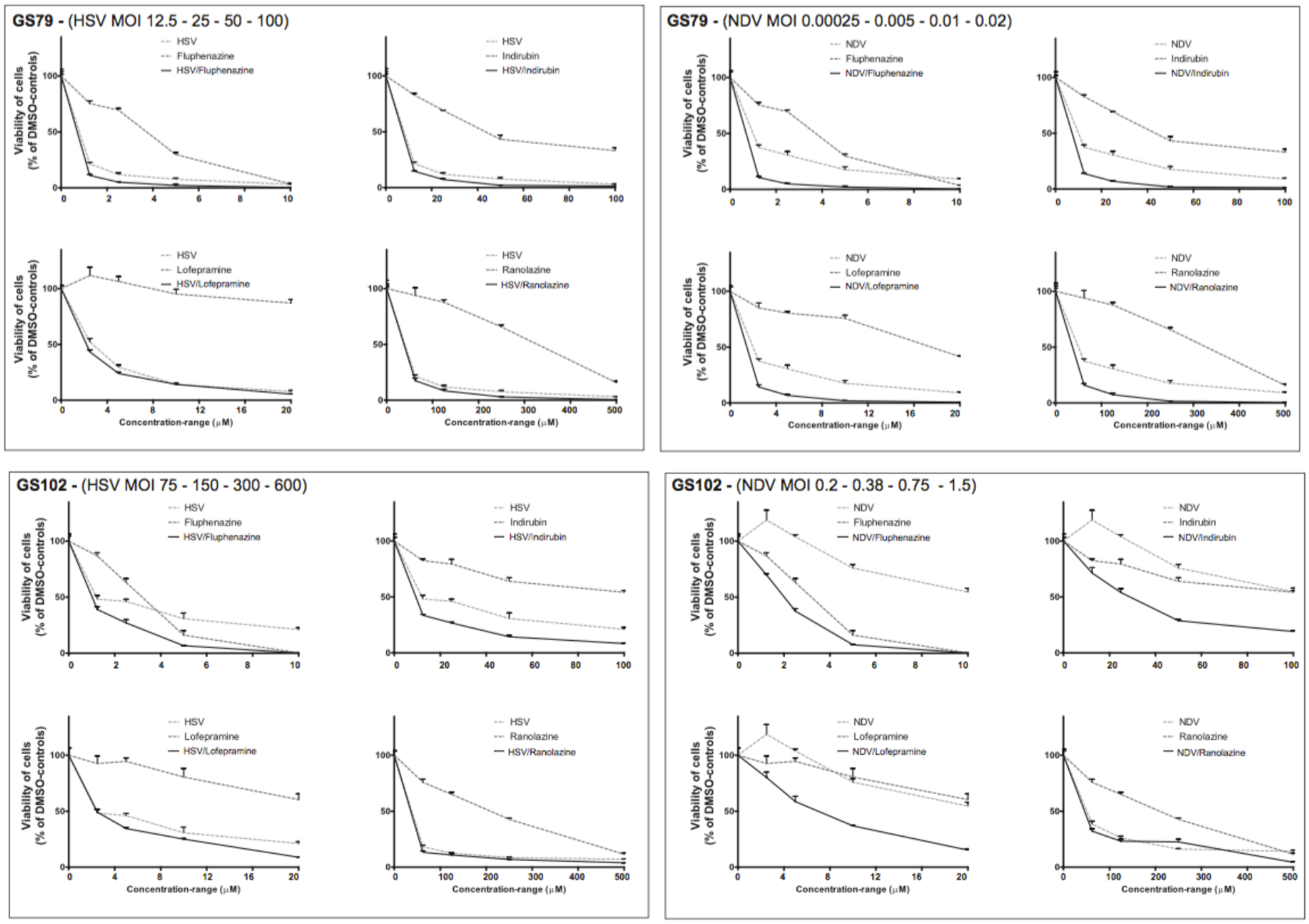

Supplementary Figure 4. Drug/virus combination effects with different OVs.
Dose-response combination assays were performed using Chou-Talalay assays to study synergy between the four viral sensitizers and the HSV-based and NDV oncolytic viruses in the GSCs GS79 and GS102. Viability was measured at day five post-treatment. The dose-response graphs are shown as mean percentage viability compared to DMSO treated controls with the standard deviation.

References

1. Stupp R, Hegi ME, Mason WP, van den Bent MJ, Taphoorn MJ, Janzer RC et al. Effects of radiotherapy with concomitant and adjuvant temozolomide versus radiotherapy alone on survival in glioblastoma in a randomised phase III study: 5-year analysis of the EORTC-NCIC trial. Lancet Oncol 2009; 10(5): 459-66.

2. Stupp R, Mason WP, van den Bent MJ, Weller M, Fisher B, Taphoorn MJ et al. Radiotherapy plus concomitant and adjuvant temozolomide for glioblastoma. The New England journal of medicine 2005; 352(10): 987-96.

3. Lang FF, Conrad C, Gomez-Manzano C, Tufaro F, Yung W, Sawaya R et al. First-in-human phase I clinical trial of oncolytic delta-24-rgd (dnx-2401) with biological endpoints: implications for viro- immunotherapy. Neuro Oncol 2014; 16 Suppl 3: iii39.

4. Lamfers ML, Grill J, Dirven CM, Van Beusechem VW, Geoerger B, Van Den Berg J et al. Potential of the conditionally replicative adenovirus Ad5-Delta24RGD in the treatment of malignant gliomas and its enhanced effect with radiotherapy. Cancer Res 2002; 62(20): 5736-42.

5. Kaufmann JK, Chiocca EA. Oncolytic virotherapy for gliomas: steps toward the future. CNS oncology 2013; 2(5): 389-92.

6. Suzuki K, Fueyo J, Krasnykh V, Reynolds PN, Curiel DT, Alemany R. A conditionally replicative adenovirus with enhanced infectivity shows improved oncolytic potency. Clin Cancer Res 2001; 7(1): 120-6.

7. Fuxe J, Liu L, Malin S, Philipson L, Collins VP, Pettersson RF. Expression of the coxsackie and adenovirus receptor in human astrocytic tumors and xenografts. Int J Cancer 2003; 103(6): 723-9.

8. de Jonge J, Berghauser Pont LM, Idema S, Kloezeman JJ, Noske D, Dirven CM et al. Therapeutic concentrations of anti-epileptic drugs do not inhibit the activity of the oncolytic adenovirus Delta24-RGD in malignant glioma. J Gene Med 2013; 15(3-4): 134-41.

9. Berghauser Pont LM, Kleijn A, Kloezeman JJ, van den Bossche W, Kaufmann JK, de Vrij J et al. The HDAC Inhibitors Scriptaid and LBH589 Combined with the Oncolytic Virus Delta24-RGD Exert Enhanced Anti-Tumor Efficacy in Patient-Derived Glioblastoma Cells. PLoS One 2015; 10(5): e0127058.

10. US National Institutes of Health. http://dtp.cancer.gov. 2014; (14.10.15).

11. Balvers RK, Kleijn A, Kloezeman JJ, French PJ, Kremer A, van den Bent MJ et al. Serum-free culture success of glial tumors is related to specific molecular profiles and expression of extracellular matrix-associated gene modules. Neuro Oncol 2013; 15(12): 1684-95.

12. Lee J, Kotliarova S, Kotliarov Y, Li A, Su Q, Donin NM et al. Tumor stem cells derived from glioblastomas cultured in bFGF and EGF more closely mirror the phenotype and genotype of primary tumors than do serum-cultured cell lines. Cancer Cell 2006; 9(5): 391-403.

13. Cheema TA, Wakimoto H, Fecci PE, Ning J, Kuroda T, Jeyaretna DS et al. Multifaceted oncolytic virus therapy for glioblastoma in an immunocompetent cancer stem cell model. Proc Natl Acad Sci U S A 2013; 110(29): 12006-11.

14. Buijs PR, van Eijck CH, Hofland LJ, Fouchier RA, van den Hoogen BG. Different responses of human pancreatic adenocarcinoma cell lines to oncolytic Newcastle disease virus infection. Cancer Gene Ther 2014; 21(1): 24-30.

15. http://nihclinicalcollection.com/. In, last visited september 2014.

16. Chou TC, Talalay P. Quantitative analysis of dose-effect relationships: the combined effects of multiple drugs or enzyme inhibitors. Advances in enzyme regulation 1984; 22: 27-55.

17. Luo Z, Sheng J, Sun Y, Lu C, Yan J, Liu A et al. Synthesis and evaluation of multi-target-directed ligands against Alzheimer's disease based on the fusion of donepezil and ebselen. J Med Chem 2013; 56(22): 9089-99.

18. Singh N, Halliday AC, Thomas JM, Kuznetsova OV, Baldwin R, Woon EC et al. A safe lithium mimetic for bipolar disorder. Nature communications 2013; 4: 1332.

19. Tsuneizumi T, Babb SM, Cohen BM. Drug distribution between blood and brain as a determinant of antipsychotic drug effects. Biological psychiatry 1992; 32(9): 817-24.

20. Wang W, Yang Y, Ying C, Li W, Ruan H, Zhu X et al. Inhibition of glycogen synthase kinase-3beta protects dopaminergic neurons from MPTP toxicity. Neuropharmacology 2007; 52(8): 1678-84.

21. Leonard BE. A comparison of the pharmacological properties of the novel tricyclic antidepressant lofepramine with its major metabolite, desipramine: a review. International clinical psychopharmacology 1987; 2(4): 281-97.

22. Jiang H, White EJ, Rios-Vicil CI, Xu J, Gomez-Manzano C, Fueyo J. Human adenovirus type 5 induces cell lysis through autophagy and autophagy-triggered caspase activity. J Virol 2011; 85(10): 4720-9.

23. Bartlett DL, Liu Z, Sathaiah M, Ravindranathan R, Guo Z, He Y et al. Oncolytic viruses as therapeutic cancer vaccines. Mol Cancer 2013; 12(1): 103.

24. Berghauser Pont LM, Spoor JK, Venkatesan S, Swagemakers S, Kloezeman JJ, Dirven CM et al. The Bcl-2 inhibitor Obatoclax overcomes resistance to histone deacetylase inhibitors SAHA and LBH589 as radiosensitizers in patient-derived glioblastoma stem-like cells. Genes Cancer 2014; 5(11-12): 445-59.

25. Berghauser Pont LM, Naipal K, Kloezeman JJ, Venkatesan S, van den Bent M, van Gent DC et al. DNA damage response and anti-apoptotic proteins predict radiosensitization efficacy of HDAC inhibitors SAHA and LBH589 in patient-derived glioblastoma cells. Cancer Lett 2014.

26. Balvers RK, Lamfers ML, Kloezeman JJ, Kleijn A, Berghauser Pont LM, Dirven CM et al. ABT-888 enhances cytotoxic effects of temozolomide independent of MGMT status in serum free cultured glioma cells. J Transl Med 2015; 13(1): 74.

27. Pollard SM, Yoshikawa K, Clarke ID, Danovi D, Stricker S, Russell R et al. Glioma stem cell lines expanded in adherent culture have tumor-specific phenotypes and are suitable for chemical and genetic screens. Cell Stem Cell 2009; 4(6): 568-80.

28. Jiang P, Mukthavaram R, Chao Y, Bharati IS, Fogal V, Pastorino S et al. Novel anti-glioblastoma agents and therapeutic combinations identified from a collection of FDA approved drugs. J Transl Med 2014; 12: 13.

29. Alonso MM, Jiang H, Yokoyama T, Xu J, Bekele NB, Lang FF et al. Delta-24-RGD in combination with RAD001 induces enhanced anti-glioma effect via autophagic cell death. Mol Ther 2008; 16(3): 487-93.

30. Lamfers ML, Fulci G, Gianni D, Tang Y, Kurozumi K, Kaur B et al. Cyclophosphamide increases transgene expression mediated by an oncolytic adenovirus in glioma-bearing mice monitored by bioluminescence imaging. Mol Ther 2006; 14(6): 779-88.

31. Alonso MM, Gomez-Manzano C, Jiang H, Bekele NB, Piao Y, Yung WK et al. Combination of the oncolytic adenovirus ICOVIR-5 with chemotherapy provides enhanced anti-glioma effect in vivo. Cancer Gene Ther 2007; 14(8): 756-61.

32. Ulasov IV, Sonabend AM, Nandi S, Khramtsov A, Han Y, Lesniak MS. Combination of adenoviral virotherapy and temozolomide chemotherapy eradicates malignant glioma through autophagic and apoptotic cell death in vivo. Br J Cancer 2009; 100(7): 1154-64.

33. Holzmuller R, Mantwill K, Haczek C, Rognoni E, Anton M, Kasajima A et al. YB-1 dependent virotherapy in combination with temozolomide as a multimodal therapy approach to eradicate malignant glioma. Int J Cancer 2011; 129(5): 1265-76.

34. Idema S, Lamfers ML, van Beusechem VW, Noske DP, Heukelom S, Moeniralm S et al. AdDelta24 and the p53-expressing variant AdDelta24-p53 achieve potent anti-tumor activity in glioma when combined with radiotherapy. J Gene Med 2007; 9(12): 1046-56.

35. Geoerger B, Grill J, Opolon P, Morizet J, Aubert G, Lecluse Y et al. Potentiation of radiation therapy by the oncolytic adenovirus dl1520 (ONYX-015) in human malignant glioma xenografts. Br J Cancer 2003; 89(3): 577-84.

36. McKenzie BA, Zemp FJ, Pisklakova A, Narendran A, McFadden G, Lun X et al. In vitro screen of a small molecule inhibitor drug library identifies multiple compounds that synergize with oncolytic myxoma virus against human brain tumor-initiating cells. Neuro Oncol 2015.

37. Diallo JS, Le Boeuf F, Lai F, Cox J, Vaha-Koskela M, Abdelbary H et al. A high-throughput pharmacoviral approach identifies novel oncolytic virus sensitizers. Mol Ther 2010; 18(6): 1123-9.

38. Passer BJ, Cheema T, Zhou B, Wakimoto H, Zaupa C, Razmjoo M et al. Identification of the ENT1 antagonists dipyridamole and dilazep as amplifiers of oncolytic herpes simplex virus-1 replication. Cancer Res 2010; 70(10): 3890-5.

39. Bieler A, Mantwill K, Dravits T, Bernshausen A, Glockzin G, Kohler-Vargas N et al. Novel three-pronged strategy to enhance cancer cell killing in glioblastoma cell lines: histone deacetylase inhibitor, chemotherapy, and oncolytic adenovirus dl520. Hum Gene Ther 2006; 17(1): 55-70.

40. Liikanen I, Monsurro V, Ahtiainen L, Raki M, Hakkarainen T, Diaconu I et al. Induction of interferon pathways mediates in vivo resistance to oncolytic adenovirus. Mol Ther 2011; 19(10): 1858-66.

41. Jiang H, Gomez-Manzano C, Aoki H, Alonso MM, Kondo S, McCormick F et al. Examination of the therapeutic potential of Delta-24-RGD in brain tumor stem cells: role of autophagic cell death. J Natl Cancer Inst 2007; 99(18): 1410-4.

42. Abou El Hassan MA, van der Meulen-Muileman I, Abbas S, Kruyt FA. Conditionally replicating adenoviruses kill tumor cells via a basic apoptotic machinery-independent mechanism that resembles necrosis-like programmed cell death. J Virol 2004; 78(22): 12243-51.

43. Baird SK, Aerts JL, Eddaoudi A, Lockley M, Lemoine NR, McNeish IA. Oncolytic adenoviral mutants induce a novel mode of programmed cell death in ovarian cancer. Oncogene 2008; 27(22): 3081-90.

44. Kleijn A, Kloezeman J, Treffers-Westerlaken E, Fulci G, Leenstra S, Dirven C et al. The In Vivo Therapeutic Efficacy of the Oncolytic Adenovirus Delta24-RGD Is Mediated by Tumor-Specific Immunity. PLoS One 2014; 9(5): e97495.

45. Schleuning M, Brumme V, Wilmanns W. Growth inhibition of human leukemic cell lines by the phenothiazine derivative fluphenazine. Anticancer Res 1993; 13(3): 599-602.

46. Gil-Ad I, Shtaif B, Levkovitz Y, Dayag M, Zeldich E, Weizman A. Characterization of phenothiazine-induced apoptosis in neuroblastoma and glioma cell lines: clinical relevance and possible application for brain-derived tumors. Journal of molecular neuroscience : MN 2004; 22(3): 189-98.

47. Hwang MK, Min YK, Kim SH. Calmodulin inhibition contributes to sensitize TRAIL-induced apoptosis in human lung cancer H1299 cells. Biochemistry and cell biology = Biochimie et biologie cellulaire 2009; 87(6): 919-26.

48. Lin YK, Leu YL, Yang SH, Chen HW, Wang CT, Pang JH. Anti-psoriatic effects of indigo naturalis on the proliferation and differentiation of keratinocytes with indirubin as the active component. Journal of dermatological science 2009; 54(3): 168-74.

49. Hoessel R, Leclerc S, Endicott JA, Nobel ME, Lawrie A, Tunnah P et al. Indirubin, the active constituent of a Chinese antileukaemia medicine, inhibits cyclin-dependent kinases. Nat Cell Biol 1999; 1(1): 60-7.

50. Rahman SH, Bobis-Wozowicz S, Chatterjee D, Gellhaus K, Pars K, Heilbronn R et al. The nontoxic cell cycle modulator indirubin augments transduction of adeno-associated viral vectors and zinc-finger nuclease-mediated gene targeting. Hum Gene Ther 2013; 24(1): 67-77.

51. Mok CK, Kang SS, Chan RW, Yue PY, Mak NK, Poon LL et al. Anti-inflammatory and antiviral effects of indirubin derivatives in influenza A (H5N1) virus infected primary human peripheral blood-derived macrophages and alveolar epithelial cells. Antiviral research 2014; 106: 95-104.

52. Hertel L, Chou S, Mocarski ES. Viral and cell cycle-regulated kinases in cytomegalovirus-induced pseudomitosis and replication. PLoS Pathog 2007; 3(1): e6.

53. Hsuan SL, Chang SC, Wang SY, Liao TL, Jong TT, Chien MS et al. The cytotoxicity to leukemia cells and antiviral effects of Isatis indigotica extracts on pseudorabies virus. Journal of ethnopharmacology 2009; 123(1): 61-7.

54. Leclerc S, Garnier M, Hoessel R, Marko D, Bibb JA, Snyder GL et al. Indirubins inhibit glycogen synthase kinase-3 beta and CDK5/p25, two protein kinases involved in abnormal tau phosphorylation in Alzheimer's disease. A property common to most cyclin-dependent kinase inhibitors? J Biol Chem 2001; 276(1): 251-60.

55. Benson JM, Shepherd DM. Dietary ligands of the aryl hydrocarbon receptor induce anti-inflammatory and immunoregulatory effects on murine dendritic cells. Toxicol Sci 2011; 124(2): 327-38.

56. Yuskaitis CJ, Jope RS. Glycogen synthase kinase-3 regulates microglial migration, inflammation, and inflammation-induced neurotoxicity. Cellular signalling 2009; 21(2): 264-73.

57. Samudio I, Harmancey R, Fiegl M, Kantarjian H, Konopleva M, Korchin B et al. Pharmacologic inhibition of fatty acid oxidation sensitizes human leukemia cells to apoptosis induction. J Clin Invest 2010; 120(1): 142-56.

58. Driffort V, Gillet L, Bon E, Marionneau-Lambot S, Oullier T, Joulin V et al. Ranolazine inhibits NaV1.5-mediated breast cancer cell invasiveness and lung colonization. Mol Cancer 2014; 13: 264.

59. Pasqualini R, Koivunen E, Ruoslahti E. Alpha v integrins as receptors for tumor targeting by circulating ligands. Nature biotechnology 1997; 15(6): 542-6.

60. Balvers RK, Belcaid Z, van den Hengel SK, Kloezeman J, de Vrij J, Wakimoto H et al. Locally-delivered T-cell-derived cellular vehicles efficiently track and deliver adenovirus delta24-RGD to infiltrating glioma. Viruses 2014; 6(8): 3080-96.

61. Galli R, Binda E, Orfanelli U, Cipelletti B, Gritti A, De Vitis S et al. Isolation and characterization of tumorigenic, stem-like neural precursors from human glioblastoma. Cancer Res 2004; 64(19): 7011-21.

62. Gursel DB, Shin BJ, Burkhardt JK, Kesavabhotla K, Schlaff CD, Boockvar JA. Glioblastoma stem-like cells-biology and therapeutic implications. Cancers 2011; 3(2): 2655-66.

63. Chou TC. Preclinical versus clinical drug combination studies. Leuk Lymphoma 2008; 49(11): 2059-80.

7

Locally-Delivered T-Cell-Derived Cellular Vehicles Efficiently Track

Chapter was published as;

Locally-Delivered T-Cell-Derived Cellular Vehicles Efficiently Track and Deliver Adenovirus Delta24-RGD to Infiltrating Glioma. *Rutger K. Balvers, Zineb Belcaid, Sanne K. van den Hengel, Jenneke Kloezeman, Jeroen de Vrij, Hiroaki Wakimoto, Rob C. Hoeben, Reno Debets, Sieger Leenstra, Clemens Dirven and Martine L.M. Lamfers*

Viruses 2014, 6, 3080-3096; doi:10.3390/v6083080

Published online 12th August 2014

Abstract: Oncolytic adenoviral vectors are a promising alternative for the treatment of glioblastoma. Recent publications have demonstrated the advantages of shielding viral particles within cellular vehicles (CVs), which can be targeted towards the tumor microenvironment. Here, we studied T-cells, often having a natural capacity to target tumors, for their feasibility as a CV to deliver the oncolytic adenovirus, Delta24-RGD, to glioblastoma. The Jurkat T-cell line was assessed in co-culture with the glioblastoma stem cell (GSC) line, MGG8, for the optimal transfer conditions of Delta24-RGD in vitro. The effect of intraparenchymal and tail vein injections on intratumoral virus distribution and overall survival was addressed in an orthotopic glioma stem cell (GSC)-based xenograft model. Jurkat T-cells were demonstrated to facilitate the amplification and transfer of Delta24-RGD onto GSCs. Delta24-RGD dosing and incubation time were found to influence the migratory ability of T-cells towards GSCs. Injection of Delta24-RGD-loaded T-cells into the brains of GSC-bearing mice led to migration towards the tumor and dispersion of the virus within the tumor core and infiltrative zones. This occurred after injection into the ipsilateral hemisphere, as well as into the non-tumor-bearing hemisphere. We found that T-cell-mediated delivery of Delta24-RGD led to the inhibition of tumor growth compared to non-treated controls, resulting in prolonged survival ($p = 0.007$). Systemic administration of virus-loaded T-cells resulted in intratumoral viral delivery, albeit at low levels. Based on these findings, we conclude that T-cell-based CVs are a feasible approach to local Delta24-RGD delivery in glioblastoma, although efficient systemic targeting requires further improvement.

1. Introduction

Glioblastoma is the most frequently diagnosed primary brain tumor in adults, with a median survival of only 15 months after the initial diagnosis [1]. Despite the extensive scientific progress that has been made into the molecular characteristics of glioblastoma, patient prognosis has remained virtually unaltered. As a result, translational research is warranted for the development of new therapeutic agents. Oncolytic virotherapy has been extensively studied for the treatment of glioblastoma and has proven to be a safe and feasible strategy from preclinical [2,3] and clinical safety studies [4,5]. Delta24-RGD is a conditionally replicating oncolytic adenovirus that has demonstrated therapeutic efficacy in preclinical models of glioblastoma [6–8]. The Delta24 mutation consists of a 24-base pair deletion in the E1A gene of the serotype 5 adenovirus [9]. This alteration facilitates selective viral replication in cells that harbor altered Rb pathway signaling, which is a common (75%) phenomenon in glioblastoma [10]. The addition of the RGD motif enhances the potency of Delta24 by targeting the virus to alpha (V)-beta(3) integrins that are frequently expressed on tumor cells and vasculature [11]. This omits the dependency on the expression of the Coxsackievirus and Adenovirus receptor (CAR).

One of the major hurdles for virotherapy to target glioblastoma is efficient vector delivery, preferably over a prolonged period of administration [12]. Several strategies have been proposed to overcome this problem [5], of which cellular vehicles (CV) are a particularly interesting option [13]. CV-systems are comprised of cells that are incubated with oncolytic virus ex vivo. Subsequently, these cells are administered systemically to employ their intrinsic tropism towards the tumor microenvironment, where efficient delivery takes place in the form of viral transfer or lysis of the CV [14]. Some of the proposed potential advantages of CV are the shielding of viral particles from systemic neutralizing barriers, the ability of dosage amplification by replication of virus within infected vehicle cells and the ability to target tumor cells in multiple administrations.

A myriad of vehicle cells from different tissue lineages have been investigated for their capacity to deliver oncolytic adenovirus into glioblastoma, such as mesenchymal [15–17], neural [18–20] and adipose-derived stem cells [21]. While other oncolytic viruses have been used in combination with hematological lineage-derived cellular vehicles [22], oncolytic adenovirus has to date not been utilized in such a CV-system. The use of myeloid derived cells as CV for oncolytic adenovirus has been proven effective in prostate cancer xenografts [23]. We have investigated the feasibility of the Jurkat T-cell line as a model for T-cell-based cellular delivery of Delta24-RGD in a glioblastoma stem cell (GSC)-based preclinical xenograft model. The presented study addresses the feasibility of this approach as a step towards targeted delivery of oncolytic adenovirus in combination with an adoptive immunotherapy treatment.

2. Methods

2.1. Cell Culture

The glioblastoma stem cell line MGG8-Fluc-Mcherry was established and characterized as previously described [24,25]. Tumor spheres were grown in DMEM-F12 supplemented with penicillin-streptomycin, B27, EGF (5µg/mL), FGF(5µg/mL) and heparin(5mg/mL). Tumor spheres were passed by mechanical and chemical dissociation (Life Technologies, Bleiswijk, The Netherlands). For viability assays, cells were grown as monolayers by coating 96-well plates with growth factor-reduced matrigel coating (BD Bioscience, Breda, The Netherlands). The A549 lung adenocarcinoma cell line (ATCC, Manassas, VA, USA) was cultured in DMEM supplemented with 10% FCS and 1% penicillin-streptomycin. Jurkat T-cell E6.1 and Jurkat T-cell-GFP cells were grown in suspension in RPMI supplemented with 10% FCS and 1% penicillin-streptomycin. For systemic delivery, retroviral vectors encoding human CD8α, as well as TCR genes (see below) were used to transduce Jurkat T-cells. The CD8α gene was described previously [26] and the TCRα and β genes originated from the gp100/HLA-A2-specific CTL clone 296 [27]. Following gene transduction, Jurkat T-cells were sorted for TCR expression (as described previously [28]). Our in vivo studies, using T-cells expressing a defined TCR, allowed us to use gp100 as a test target antigen for viral treatment of glioma.

2.2. Virus Construction and Propagation

Delta24-RGD was constructed as previously described [9]. For the construction of Delta24-RGD-GFP, a set of previously developed plasmids was used to create the virus HAdV-5.Δ24.Fib.RGD.eGFP. This virus combines the unique properties of Delta24-RGD with a replication-dependent expression of the eGFP imaging marker, as a result of incorporating

eGFP in the viral promoter-driven E3 region [29]. To this end, the RGD motif was excised from the plasmid, pVK526 [30], by NdeI + PacI digestion and re-ligated into the plasmid, pShuttle-ΔE3-ADP-EGFP-F2 [29], resulting in pShuttle-ΔE3-Fib.RGD.ADP-EGFP. After removal of the kanamycin resistance gene (by ClaI digestion and re-ligation), PacI + AatII digestion was used to isolate the fragment containing the ΔE3-Fib.RGD.ADP-EGFP sequence, which was recombined with SpeI-linearized pAdEasy-1 [30], resulting in pAdEasy-ΔE3-Fib.RGD.ADP-EGFP. The 24-bp deletion was introduced in the plasmid, pSh + pIX [31], by replacement of the SspI-to-XbaI fragment with the corresponding fragment from the plasmid pXE.Δ24 [32], resulting in the plasmid, pSh + pIX.Δ24. The full-genomic sequence of HAdV-5.Δ24.Fib.RGD.eGFP was constructed by recombination in E. coli of pAdEasy-ΔE3-Fib.RGD.ADP-EGFP with pSh + pIX.Δ24. The virus was rescued in 911 cells [33], using a previously described protocol. [30] To prevent heterologous recombination with the viral E1 sequence present in the 911 genome, upscaling of the virus was performed in A549 cells. After preparation of the virus stock, the presence of Δ24 and Fib.RGD was confirmed by PCR and restriction analysis.

2.3. Delta24-RGD Infection and Replication Assay

Jurkat T-cells were infected with Delta24-RGD at multiplicities of infection (MOI) 1, 10, 50, 100, 500 and 1,000 by plating cells for 2 h in serum free RPMI at room temperature. After 2 h, cells were washed and spun down twice in serum supplemented RPMI. Subsequently, cells were plated in triplicates of 1 ×103 cells per well in flat-bottomed 96-well plates. Cells were allowed to proliferate for 4 and 6 days, after which we performed the Cell Titer GLO viability assay (Promega, Leiden, The Netherlands), as described by the manufacturer. For the treatment of MGG8-spheres, the MOI was calculated based on the seeded cells counted from dissociated spheres. Cells were incubated for one day in which spheres form through adherence, and incubation followed 24 h post-seeding, making the MOI in our hands reproducible and accurate.

Transfer of Delta24-RGD-GFP from Jurkat T-cells towards MGG8-Mcherry-FLuc was assessed by infecting Jurkat T-cells at MOI 0, 1, 10 for 24 h, washed twice and co-cultured at a 1:1 ratio with MGG8 cells for 5 days. Microscopic examination and image capture were performed on a conventional wide-field fluorescence microscope. For these experiments, MGG8 cells were cultured on growth factor-reduced matrigel coating.

The replication assay was performed with the above-described infection protocol at MOI 10, 50 and 100. Jurkat T-cells were harvested 1.5 h and 4 days post-infection. Pellets and supernatants were collected and separately freeze-thawed three times, and subsequently, pellets were reconstituted in medium to equal volumes, as present in the supernatants. After 48 h, A549 cells were fixed with ice-cold methanol, and the Ad Rapid Titer plaque-forming assay (Clontech, Saint-Germain-en-Laye, France) was performed according to manufacturer's protocol. Experiments were performed twice, in triplicates.

2.4. T-Cell Migration Assays

Suspensions of 1 × 106 cells/ml Jurkat T-cells in RMPI were prepared. Cells were infected with Delta24-RGD dilutions at an MOI of 10, 50 and 100 in 1 mL of serum free RPMI. Cells were incubated for 2 h and subsequently washed twice with serum supplemented RPMI and incubated for another 2, 24 or 48 h. Hereafter, 5 ×105 cells were inserted onto matrigel-coated transwell chamber inserts with 5-μm pores (Corning Inc., Amsterdam, The Netherlands). Cells were allowed to migrate into the bottom compartment for 12 h, after which cell numbers were quantified by performing a Cell Titer GLO viability assay (Promega, Leiden, The Netherlands) according to the manufacturer's instructions. Experiments were performed twice, in duplicates.

2.5. In Vivo Experiments

All animal experiments were performed in accordance with the local Animal Ethical Committee, Erasmus MC Rotterdam. Experiments were performed on 10–12-week-old NOD-SCID (Non-obese diabetic severe combined immunodeficient) female mice (strain C.B-17/IcrHantmhsd-Prkdcs), Harlan, (Horst, The Netherlands). On Day 0, intra-striatal injections of 5 × 104 MGG8-Fluc-Mcherry cells were performed as described previously [34]. In short, a burr hole was drilled 2.5 mm lateral and 0.5 mm anterior to the bregma, through which 5×10*4 MGG8-Fluc-Mcherry cells in 5μL PBS were injected at a depth of 3 mm. After 14 days, mice were treated with intratumoral injections through the previously established burr hole. Treatment consisted of 5 μL PBS, Delta24-RGD 5 ×106 IUs in 5 μL PBS or 5 ×104 Jurkat T-cells infected with MOI 100 Delta24-RGD in 5 μL PBS. Jurkat T-cells were incubated in Delta24-RGD (MOI-100) 2 h prior to intratumoral injections. Mice were sacrificed upon symptoms of tumor burden or when more than 20% weight loss occurred.

For systemic delivery of Jurkat T-cells infected with Delta24-RGD, mice were grafted with MGG8-Fluc-Mcherry, as described above. After 14 days, treatment consisted of tail vein injections with 5 ×105 Jurkat T-cell-gp100TCR cells pretreated with Delta24-RGD MOI 100 for 2 h, as described above. Animals were treated with one (n = 3), two (n = 3) or three (n = 3) subsequent injections with a two-day interval. Animals were sacrificed after 48 h, 96 h and 144 h after the first injection, allowing a cumulative dosing effect in the latter two time points. Control animals were treated with equivalent dosages of Delta24-RGD through tail vein injections. Brains were snap frozen and assessed for viral delivery by hexon staining.

2.6. Immunohistochemistry

Snap frozen tumor tissue sections (8–10 μm) were cut on a cryotome. Sections were fixed with acetone. After permeabilization (Triton-X 0.01%) and blocking, slices were incubated with goat anti-hexon (Millipore, Billerica MA, USA) and mouse anti-vimentin (from DAKO, Heverlee, Belgium). Negative controls were performed by omitting the primary antibodies. Counterstaining was applied using Vectastain mounting medium, including DAPI, according to the manufacturer's instruction (Vector Labs, Peterborough, U.K.).

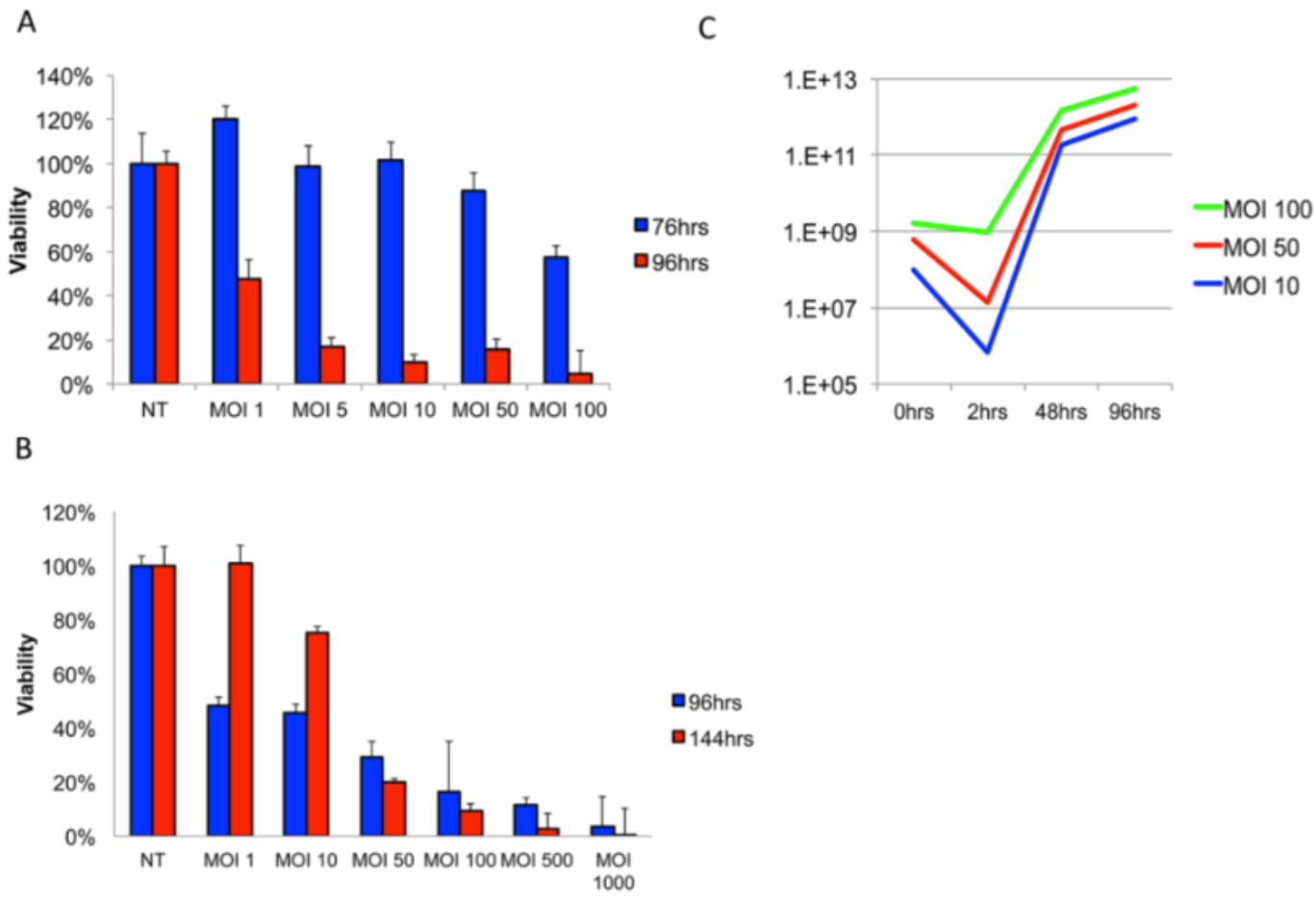

Figure 1. Delta24-RGD effectively infects, replicates and amplifies in Jurkat T-cells. (**A**) Viability assay on MGG8-GSC neurospheres infected with a dose range of Delta24-RGD; (**B**) viability assay on Jurkat T-cells infected with a dose range of Delta24-RGD. Note the increased viability at MOI 1–10 after 144 h (**C**). The viral titer assay for Delta24-RGD-treated Jurkat T-cells after two wash steps at indicated time points. Lines are representative of viral yield at indicated time points post-infection. (IUs = viral infectious units).

2.7. Statistics

Statistical analyses were conducted and illustrated in SPSS Statistics Software 19 (IBM, Amsterdam, The Netherlands).

3. Results

3.1. Delta24-RGD Efficiently Infects and Replicates in GSC and Jurkat T-Cells

Delivery of Delta24-RGD by Jurkat T-cell-CV was assessed in a series of in vitro assays. First, the optimal dosage for Delta24-RGD-mediated lysis of MGG8 GSCs was assessed by viability assay (Figure 1A). MGG8 tumor neurospheres were found to be susceptible to Delta24-RGD-induced oncolysis with an IC50 value of MOI 0.89 at 96 h post-infection (R2 = 0.92–0.99).

Efficient adenoviral infection of leukocytes has been described as problematic in several reports [35,36], while others have demonstrated efficient use of conditionally replicating adenoviruses in a subset of T-cell derived neoplastic cell lines, including Jurkat T-cells [37,38]. To investigate the infectivity and replication capacity of Delta24-RGD in Jurkat T-cells, we performed viability and viral titer assays on cells and supernatants. A dose-response effect of Delta24-RGD on Jurkat T-cell viability at 96 h post-infection was found (Figure 1B). However, after 144 h, cells exposed to MOI 10 or lower had repopulated the well. This is reflected in the IC50 values of MOI 9.2 at 96 h and MOI 20.4, at 144 h (R2 0.92–0.97). At MOI 50 and higher, the in vitro administration of Delta24-RGD was sufficient to warrant efficient lysis and prevent population renewal.

The ability of Delta24-RGD to replicate and produce progeny in Jurkat T-cells is demonstrated in Figure 1C. The infection of Delta24-RGD in Jurkat T-cells was dose-dependent and reached a saturation level at MOI 100. This was observed by a decrease in viral concentration in supernatants at 2 h post-infection at MOI 10 and 50 of 99.99% and 98% of input virus, respectively, whereas only a 7% decrease in input virus was found at MOI 100 (Figure 1C, blue bars). In retrospect, we also derived an explanation from this data for the ability of Jurkat cells to repopulate after infection with an MOI below 10, since the infectivity will not suffice to cause timely replication in Jurkat cells. A significant amplification of input viral load was demonstrated at all three dosages by 48 h (5.28 ×102–1.82 ×103-fold), which further increased at 96 h (2.12 ×103–9.16 ×103-fold). Interestingly, the relative amplification was highest in MOI 10-treated cells, suggesting a plateau for the replication-to-infection ratio.

3.2. T-Cells Efficiently Deliver Delta24-RGD to GSCs In Vitro

Since both Jurkat T-cells and MGG8 cells were found to be susceptible to Delta24-RGD-mediated oncolysis, the ability of Jurkat T-cells to function as a carrier cell to deliver virus was tested. To this end, we utilized a GFP-expressing variant of Delta24-RGD with a GFP-imaging cassette inserted into the E3 region of the viral genome. First, we tested the ability of (twice washed) Jurkat T-cell-CV to deliver virus onto MGG8 cells in a co-culture experiment. Delta24-RGD-incubated Jurkat T-cells were able to efficiently transfer virus onto MGG8 cells, as demonstrated by the accumulation of hexon-positive Jurkat T-cells and MGG8 cells over a timespan of 96 h post-infection in co-cultures (Figure 2). Similar to viability

assays with Delta24-RGD monotherapy, survival of both Jurkat T-cells and MGG8 was dose dependent in this co-culture experiment, as demonstrated by a greater loss of both cell types at MOI 10, as compared to MOI 1.

3.3. The Migratory Capacity of T-Cells Is Preserved Following Short Incubation Times with Delta24-RGD

The brain tumor tropism of stem cells and leukocytes is influenced by secreted cytokines and chemokines by tumor and stromal cells [39–41]. Furthermore, the components of the extracellular matrix proteins can both attenuate and enhance T-cell infiltration into brain parenchyma [42]. Little is known about the role of adenoviral infection on leukocyte migration towards tumors. However, a positive influence on migration with low-dosages of oncolytic VSV (vesicular stomatitis virus) has been reported by others [43,44]. To address the influence of both Delta24-RGD and the aforementioned factors on Jurkat T-cell migration was assessed in a transwell migration assay (schematic representation in Figure 3A). To be able to fine-tune future administration of cells in vivo, separate time-points were chosen to correct for the latency between infection and administration. Both commercial extracellular matrix protein, as well as MGG8-derived matrix coating slightly reduced (non-infected) Jurkat T-cell migration towards the lower compartment (data not shown). The effect of Delta24-RGD infection on Jurkat T-cell tropism toward serum-supplemented medium was assessed in ECM-coated transwell filters at 2, 24 and 48 h post-infection (MOI 10, 50 and 100). A short virus incubation time of 2 h best conserved the migratory capacity of the Jurkat T-cells when compared to non-infected controls. Interestingly, dosing at MOI 10 led to increased migration, which may be a result of virus-mediated activation of the Jurkat T-cells [42]. Prolonged incubation (24–48 h) had a significant inhibitory effect on Jurkat T-cell migration (Figure 3B).

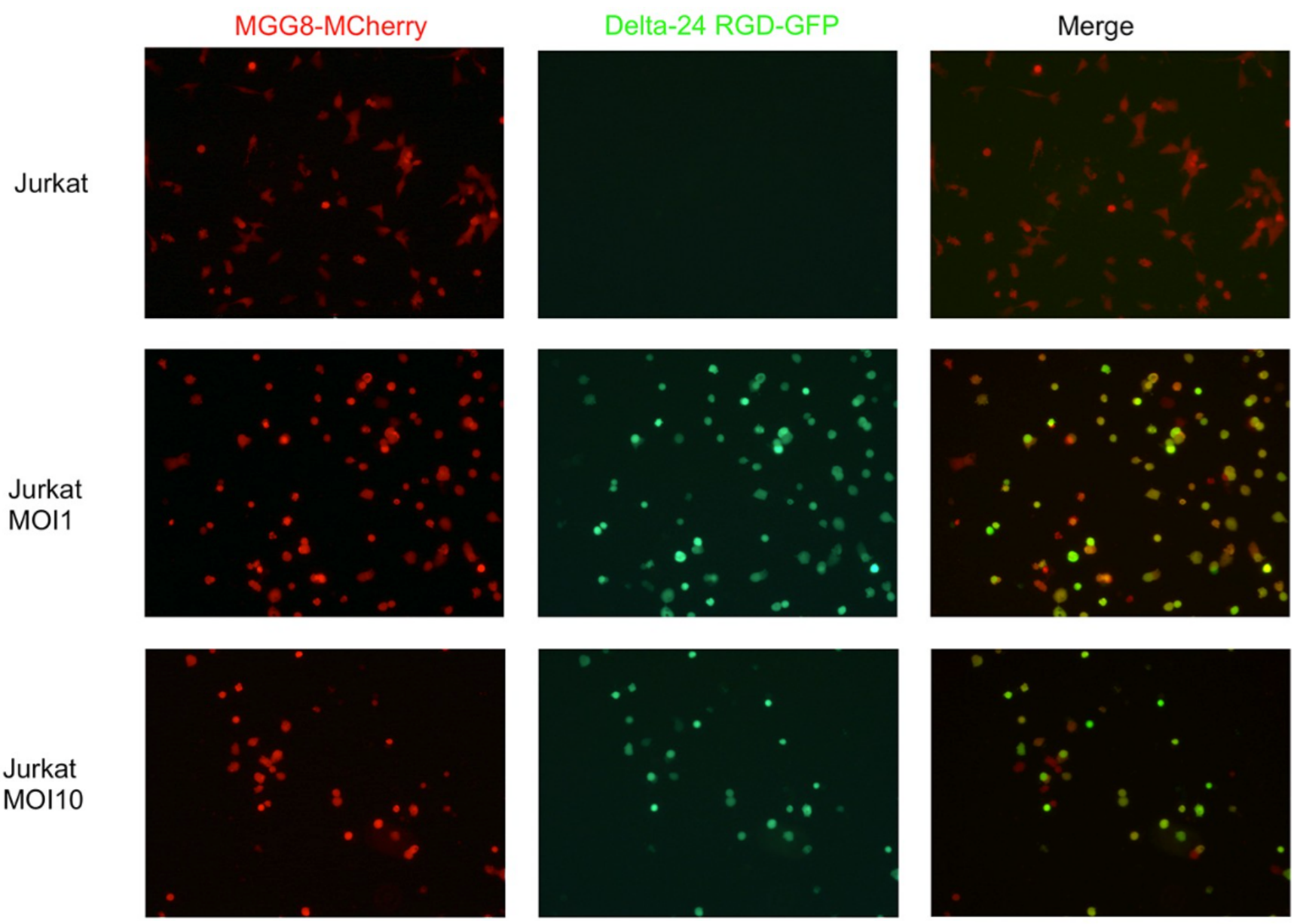

Figure 2. Jurkat T-cells efficiently deliver Delta24-RGD onto MGG8-GSCs *in vitro*. Cells were co-cultured for 96 h after prior incubation (24 h) of Jurkat T-cells with Delta24-RGD at the indicated dosages. (**Left**) mCherry fluorescence as assessed by conventional fluorescence microscopy with 25× optic zoom. (**Middle**) GFP fluorescence, indicating the presence of Delta24-RGD-GFP within cells. (**Right**) A merge of both mCherry and GFP results, demonstrating colocalization (yellow cells) indicative of Delta24-RGD-GFP transfer onto MGG8-mCherry cells.

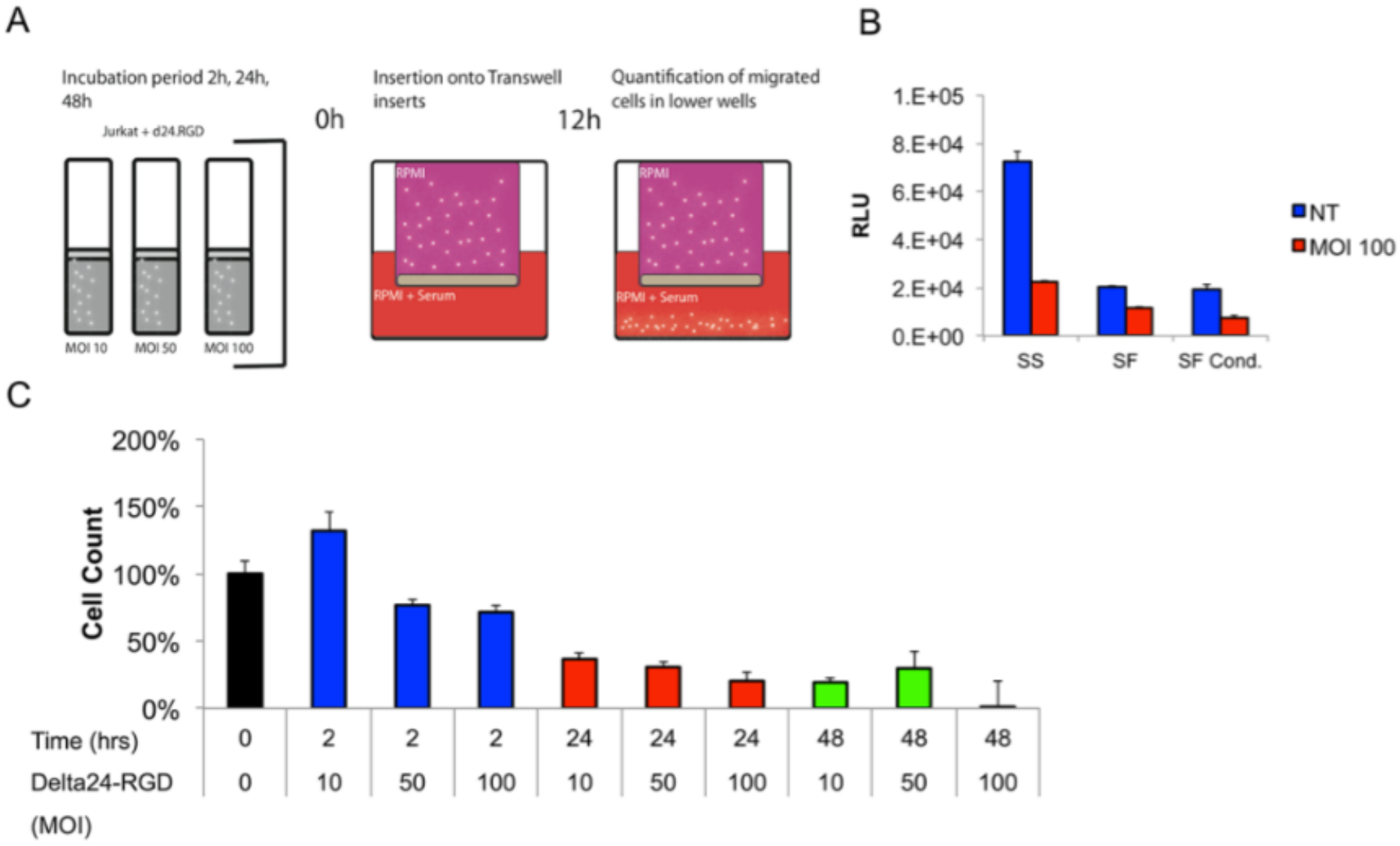

Figure 3. The Jurkat T-cell cell migration ability is influenced by Delta24-RGD dosage and incubation time. **(A)** Schematic illustration of the transwell experiments; **(B)** titration of Delta24-RGD dosage and incubation window. All time points and dosages are significantly different ($p < 0.05$) when compared to the non-treated (NT) control. Note the increased cell count in MOI 10 after 2 h, which could be indicative of T-cell activation. **(C)** Quantification of Jurkat T-cell tropism towards serum-supplemented (SS), serum-free (SF) and MGG8-conditioned serum-free medium (SF cond.). All comparisons between NT and Delta24-RGD resulted in $p < 0.05$. SS NT *vs*. SF/SF cond. NT were both $p < 0.05$.

Furthermore, Jurkat T-cells migrated most efficiently to serum-rich medium. Both serum-free (EGF and bFGF supplemented) as well as MGG8-conditioned medium led to similar levels of reduction of Jurkat T-cell migration over matrix-coated inlays (Figure 3C).

3.4. Delta24-RGD-Loaded T-Cells Demonstrate Intraparenchymal Tumor Tropism and In Vivo Viral Transfer

Based on the optimal dosing and incubation time in vitro, we proceeded to assess the in vivo potential of CV-based delivery of Delta24-RGD. For this, virus-loaded Jurkat T-cell CVs were injected intratumorally in MGG8-bearing mice (schematic representation of the experiment is provided in Figure 4A). Jurkat T-cells were incubated for 2 h at MOI 100 to achieve maximal infection and minimal loss of migratory capacity. First, the distribution of viral hexon-positive cells was assessed at early time points (24–144 h) post-intratumoral Jurkat T-cell delivery. Hexon staining revealed the presence of adenovirus, both in the core of the tumor, as well as at the peripheral margins (such as the contralateral hemisphere) of the tumor, where infiltrating single tumor cells reside (Figure 4B). Jurkat T-cell-GFP cells were especially present in (and around) the tumor core, suggesting preferential targeting for the xenografted tumor cells (Figure 4C). Encouraged by these results, the distribution of virus after contralateral injections (in the non-tumor-bearing hemisphere) at early time-points was assessed (schematic representation in Figure 4D). As expected, hexon staining was demonstrated within the Jurkat T-cell injection site, suggestive of the T-cell-based Delta24-RGD distribution, which left a necrotic cavity (Figure 4E). Strikingly, additional hexon staining was detected in the tumor-bearing hemisphere in small tumor colonies at the invading margins of the tumor. These results demonstrate the intraparenchymal tropism of CV to the tumor, subsequently resulting in the in vivo transfer of oncolytic adenovirus to distant tumor cells (Figure 4E).

3.5. Intratumoral Delivery of Delta24-RGD by T-Cells Leads to Prolonged Survival

Therapeutic effect of Jurkat T-cell-mediated Delta24-RGD delivery was compared to both PBS and Delta24-RGD intratumoral injections. Delta24-RGD-loaded T-cells (CV) prolonged the overall survival of mice bearing MGG8 orthotopic xenografts to a similar extent as direct intratumoral injection of Delta24-RGD. When compared to PBS-treated controls (mean: 38.6 days), both treatment conditions prolonged survival significantly (CV mean survival: 46.2 days, Log Rank $p = 0.007$; and Delta24-RGD mean: 49.6 days, Log Rank $p < 0.001$) (Figure 5A). There was no difference in survival between the CV and Delta24-RGD treatment groups ($p = 0.251$).

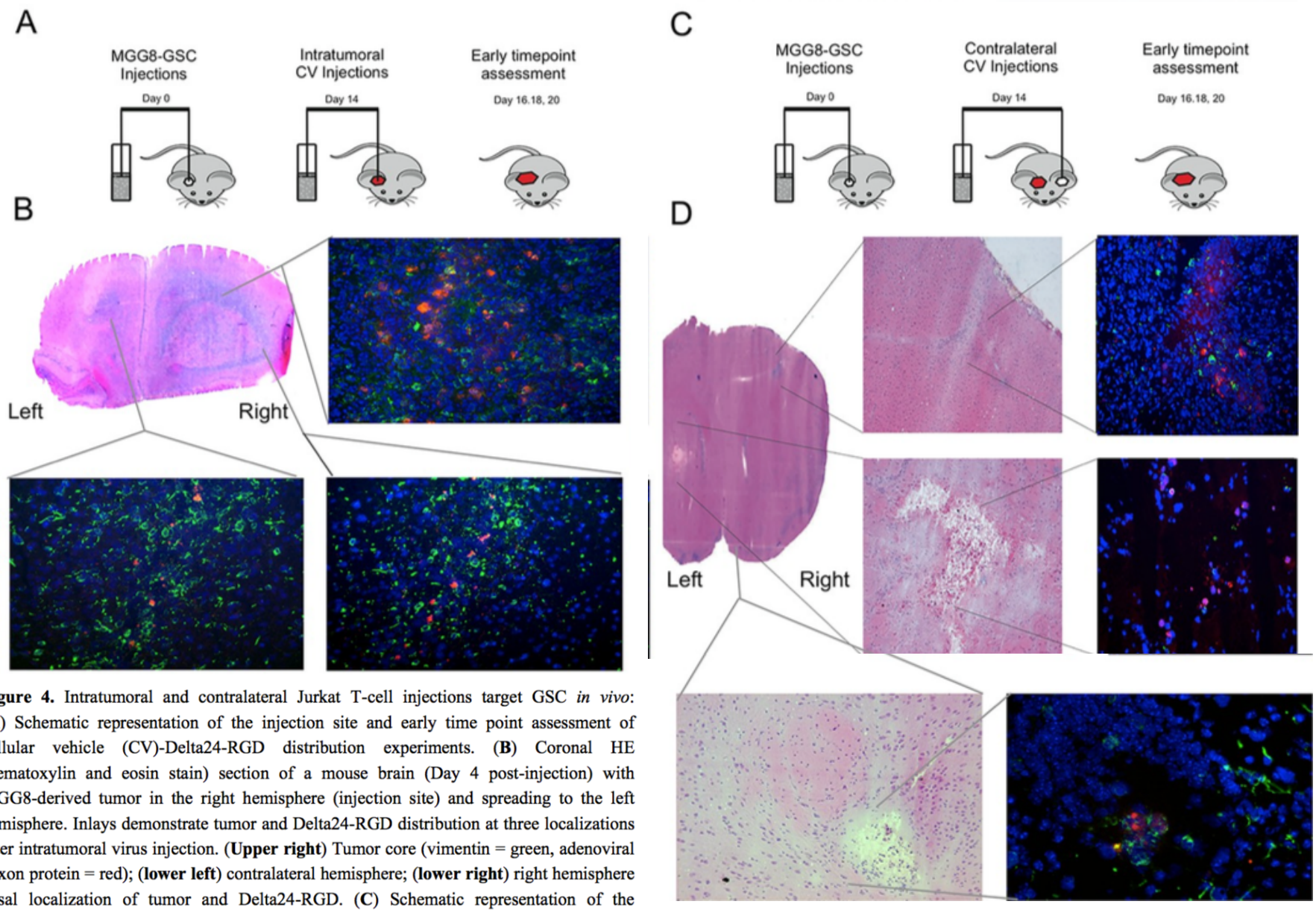

Figure 4. Intratumoral and contralateral Jurkat T-cell injections target GSC *in vivo*: (**A**) Schematic representation of the injection site and early time point assessment of cellular vehicle (CV)-Delta24-RGD distribution experiments. (**B**) Coronal HE (hematoxylin and eosin stain) section of a mouse brain (Day 4 post-injection) with MGG8-derived tumor in the right hemisphere (injection site) and spreading to the left hemisphere. Inlays demonstrate tumor and Delta24-RGD distribution at three localizations after intratumoral virus injection. (**Upper right**) Tumor core (vimentin = green, adenoviral hexon protein = red); (**lower left**) contralateral hemisphere; (**lower right**) right hemisphere basal localization of tumor and Delta24-RGD. (**C**) Schematic representation of the injection sites and early time point assessment after CV-Delta24-RGD injections into the contralateral hemisphere. (**D**) Coronal HE section with inlays demonstrating in the **upper left** and **right panel** the cortical invasion of localized tumor cells in both HE and immunofluorescence images. The **upper right** inlay demonstrates hexon distribution in the upper right hemisphere (contralateral from Jurkat T-cell-CV injection) adjacent to dispersed invasive MGG8 cells. The **lower left** and **lower right** panel illustrate the necrotic cavity resulting from the contralateral injections of Jurkat T-cell-CV, together with fluorescence images demonstrating hexon-positive cells locally. In the **bottom** two inlays, a second localization of Delta24-RGD localized in the proximity of tumor cells is demonstrated from the basolateral margins of the right hemisphere.

3.6. Delta24-RGD-Loaded T-Cells Demonstrate Tropism for Intracranial Tumors

Based on these results, a study was undertaken to assess the ability of CV to deliver Delta24-RGD after systemic tail-vein injections. To this end, MGG8-bearing mice received i.v. injections of Delta24-RGD-loaded Jurkat T-cells. The control group received i.v. injections of similar doses Delta24-RGD virus. To enhance CV tropism towards MGG8, Jurkat T-cells were transduced with a T-cell receptor that specifically recognizes gp100 antigen presented bij HLA-A2. Gp100 is a tumor-antigen commonly expressed in Glioblastoma and MGG8 in vitro and in vivo (data not shown) [45,46]. Intratumoral dispersion of CV and/or infection of the tumor cells was assessed by hexon staining after sacrificing the animals after 48–144 h post-treatment. Analyses of the brains revealed that direct intravenous injection of Delta24-RGD did not lead to infection of MGG8 tumors in any of the analyzed animals, with the exception of a small vascular structure in one animal at 144 h post-injection (Figure 5B, upper left). Contrary to virus-only injections, in mice that received Delta24-RGD-loaded Jurkat T-cells, we observed multiple small hexon-positive cells at 48 and 96 h post-injection (Figure 5B, upper right and lower left). At 144 h after systemic administration, however, no hexon-positive cells were detected, nor where there any indications of intratumoral viral spreading observed (Figure 5B, lower right).

4. Discussion

In the current study we investigated the feasibility of T-cell-mediated delivery of Delta24-RGD to glioblastoma. The application of cellular vehicles to deliver oncolytic viruses potentially overcomes several limitations of oncolytic virotherapy as a therapeutic alternative for glioblastoma (e.g., limited window of drug administration). For this reason, the use of leukocytes as cellular vehicles would be a step up in studies investigating targeted autologous T-cells, as a means to combine oncolytic virotherapy with immunotherapy. The data presented here demonstrate the ability of Delta24-RGD to efficiently infect and amplify viral progeny in a T-cell-derived cellular vehicle system. Indeed, T-cell cells were found to succumb to Delta24-RGD infection, albeit at higher MOIs compared to

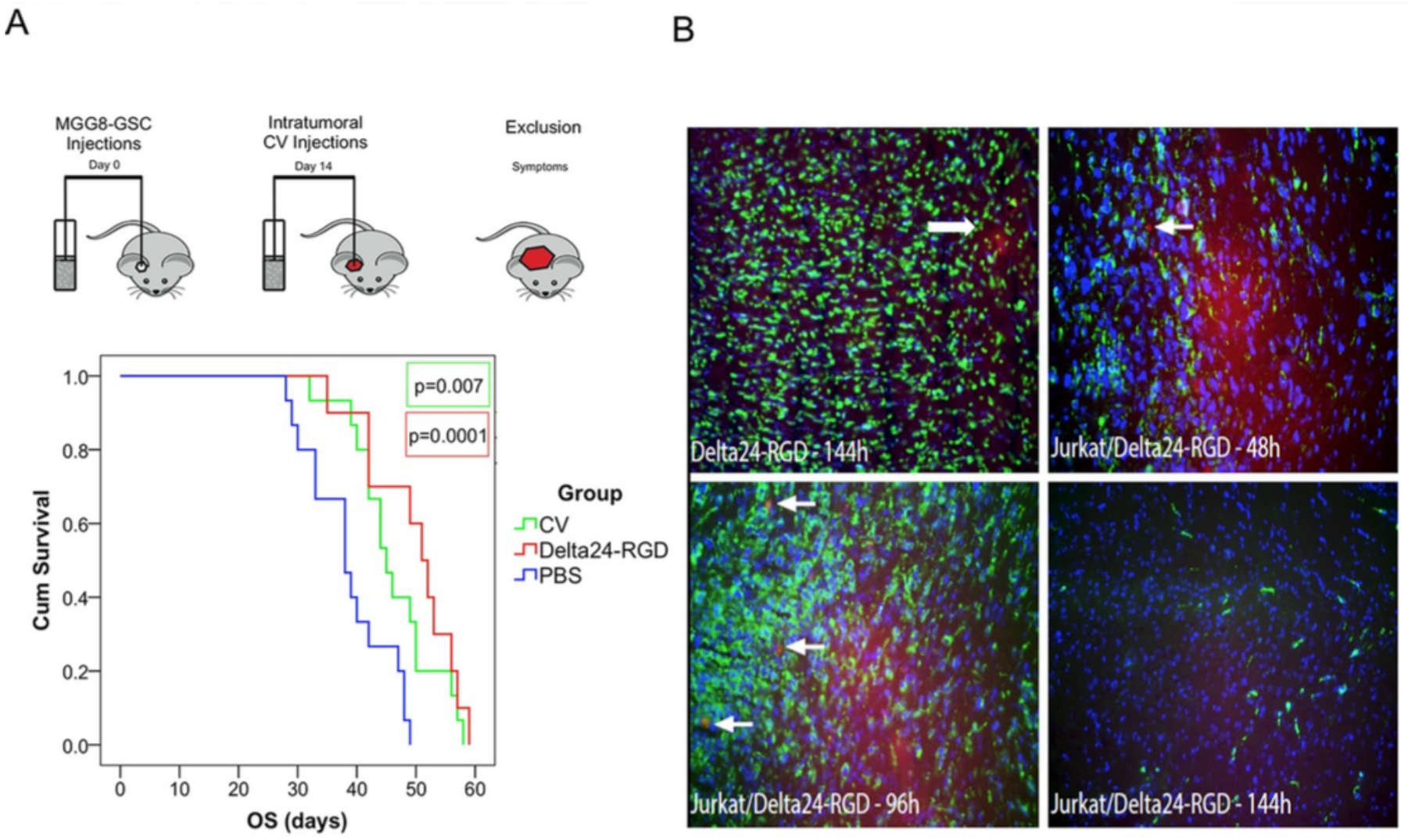

Figure 5. Intratumoral injection of Jurkat T-cell-CV leads to prolonged survival, and systemic therapy is a feasible mode of administration for intracranial targeting of MGG8 xenografts. (**A**) Schematic representation of the survival experiment with PBS and Delta24-RGD monotherapy as control groups for the Jurkat T-cell-CV treatment of MGG8 xenografts. Kaplan Meier graphs demonstrating a significant treatment effect of both intratumoral Delta24-RGD, as well as Jurkat T-cell-CV treatment. *p*-values are derived from a Wilcoxon log rank pairwise comparison to PBS-treated controls. There was no significant difference between CV and Delta24-RGD monotherapy. (**B**) MGG8 xenografts attract systemically-administered Delta24-RGD-loaded Jurkat T-cell-gp100^{TCR}. (**Upper left**) Intratumoral controls after systemic Delta24-RGD monotherapy with localized hexon staining (arrow). (**Upper right**) Intratumoral hexon-positive cells (arrow) 48 h after Jurkat T-cell delivery, indicative of the homing of Jurkat T-cells to the tumor. (**Bottom left**) Similar hexon-positive cells (arrows) at 96 h post-treatment. (**bottom right**) No hexon-positive cells were noted at 144 h post-treatment. (vimentin = green, adenoviral hexon = red).

the dose ranges used in glioma cell cultures [6]. This is congruent with a previous study by Yotnda et al. [38], demonstrating that higher dosages are needed to efficiently start replication and lysis in leukocytes. This can be accomplished by inserting the RGD-motif into the surface exposed loop of the fiber-knob, which results in increased infectivity.

Based on these in vitro findings, we set-up a proof of concept study, which demonstrated that intratumoral CV-based delivery of Delta24-RGD yields comparable results to direct Delta24-RGD injections with regard to therapeutic efficacy. Importantly, delivery of Delta24-RGD into peripheral tumor regions was demonstrated after injections of cellular vehicles into the contralateral hemisphere in GSC xenografts. This indicates the strong tropism and migratory capacity of virus-loaded T-cells in the tracking of tumor cells in the brain environment. Moreover, systemically delivered Delta24-RGD-loaded CVs were detected in small numbers within the orthotopic xenografts within 48–96 h, although efficient virus handover to the tumor was not observed in this setting. We conclude that T-cells have the ability to serve as cellular vehicles to deliver Delta24-RGD to glioblastoma at a distance, in particular to infiltrating tumor cells in the brain parenchyma. This may suggest a potential for CV approaches as a post-surgical adjuvant therapy, where CVs may be deposited in the resection cavity to track residual and surgically-inaccessible tumor cells.

Several hurdles for successful implementation of this T-cell-mediated CV delivery strategy have been addressed. Our in vitro studies demonstrate an inhibitory effect of Delta24-RGD infection on Jurkat T-cell migration in tropism assays, which is dependent on both incubation time, as well as viral dosage. Intriguingly, lower MOIs seemed to increase tropism in our transwell assay. Similar enhancement of the T-cell migratory phenotype was reported in a VSV-based cellular vehicle system [44]. It remains to be determined whether infection with lower MOIs would further improve efficient delivery of Delta24-RGD in vivo. At present, lower dosages could not be applied in our xenograft model for the risk of developing hematological malignancy from remaining Jurkat T-cells that escape from viral infection; however, the use of an autologous T-cell population may possibly circumvent this problem. As shown, tail vein injections in orthotopic xenograft-bearing mice did not lead to widespread intratumoral delivery of Delta24-RGD. The administration of L1210 leukemic cells in a syngeneic CV model did yield appreciable intracerebral carrier cell infiltration in a VSV delivery model for lung cancer [22], indicating that the choice of oncolytic virus or tumor type may influence intracranial tropism. With regard to this route of administration, it is important to con-

sider that administration through injections into the common carotid artery may increase intratumoral delivery of CVs to the brain, as demonstrated by others for Delta24-RGD delivery by mesenchymal stem cells [15].

The in vitro transwell migration assays demonstrated that MGG8-conditioned medium was less effective for the attraction of T-cells compared to serum-supplemented medium. This could either be due to immunologically repressive factors secreted by the tumor or the relative abundance of chemo-attractants available in serum-supplemented medium for T-cells. Recent studies have shown that the secretion of several chemokines plays a crucial role in the influx of both mesenchymal stem cells, as well as lymphocytes in the glioblastoma microenvironment [39,47,48]. Further investigation is warranted to appreciate which factors contribute to CV tropism, and the development of patient-tailored vectors (i.e., specific TCRs, chemokines, suicide genes) may need to be included into the CV system to enhance therapeutic efficacy.

We conclude that CV-mediated delivery of Delta24-RGD holds promise for future therapeutic application. The current results warrant further investigations into the delivery of Delta24-RGD by T-cells, possibly in combination with adoptive immunotherapy strategies.

References

1. Huse, J.T.; Holland, E.C. Targeting brain cancer: Advances in the molecular pathology of malignant glioma and medulloblastoma. Nat. Rev. Cancer 2010, 10, 319–331.

2. Kroeger, K.M.; Muhammad, A.K.; Baker, G.J.; Assi, H.; Wibowo, M.K.; Xiong, W.; Yagiz, K.; Candolfi, M.; Lowenstein, P.R.; Castro, M.G. Gene therapy and virotherapy: Novel therapeutic approaches for brain tumors. Discov. Med. 2010, 10, 293–304.

3. Murphy, A.M.; Rabkin, S.D. Current status of gene therapy for brain tumors. Transl. Res. 2013, 161, 339–354.

4. Lang, F.F.; Bruner, J.M.; Fuller, G.N.; Aldape, K.; Prados, M.D.; Chang, S.; Berger, M.S.; McDermott, M.W.; Kunwar, S.M.; Junck, L.R.; et al. Phase I trial of adenovirus-mediated p53 gene therapy for recurrent glioma: Biological and clinical results. J. Clin. Oncol. 2003, 21, 2508–2518.

5. Chiocca, E.A.; Broaddus, W.C.; Gillies, G.T.; Visted, T.; Lamfers, M.L.M. Neurosurgical delivery of chemotherapeutics, targeted toxins, genetic and viral therapies in neuro-oncology. J. Neurooncol. 2004, 69, 101–117.

6. Lamfers, M.L.; Grill, J.; Dirven, C.M.; van Beusechem, V.W.; Geoerger, B.; van Den Berg, J.; Alemany, R.; Fueyo, J.; Curiel, D.T.; et al. Potential of the conditionally replicative adenovirus Ad5-Delta24RGD in the treatment of malignant gliomas and its enhanced effect with radiotherapy. Cancer Res. 2002, 62, 5736–5742.

7. Jiang, H.; Gomez-Manzano, C.; Aoki, H.; Alonso, M.M.; Kondo, S.; McCormick, F.; Xu, J.; Kondo, Y.; Bekele, B.N.; Colman, H.; et al. Examination of the therapeutic potential of Delta-24-RGD in brain tumor stem cells: Role of autophagic cell death. J. Natl. Cancer Inst. 2007, 99, 1410–1414.

8. Fueyo, J.; Alemany, R.; Gomez-Manzano, C.; Fuller, G.N.; Khan, A.; Conrad, C.A.; Liu, T.J.; Jiang, H.; Lemoine, M.G.; Suzuki, K.; et al. Preclinical characterization of the antiglioma activity of a tropism-enhanced adenovirus targeted to the retinoblastoma pathway. J. Natl. Cancer Inst. 2003, 95, 652–660.

9. Suzuki, K.; Fueyo, J.; Krasnykh, V.; Reynolds, P.N.; Curiel, D.T.; Alemany, R. A conditionally replicative adenovirus with enhanced infectivity shows improved oncolytic potency. Clin. Cancer Res. 2001, 7, 120–126.

10. Cancer Genome Atlas Research Network. Comprehensive genomic characterization defines human glioblastoma genes and core pathways. Nature 2008, 455, 1061–1068.

11. Grill, J.; van Beusechem, V.W.; van Der Valk, P.; Dirven, C.M.; Leonhart, A.; Pherai, D.S.; Haisma, H.J.; Pinedo, H.M.; Curiel, D.T.; Gerritsen, W.R. Combined targeting of adenoviruses to integrins and epidermal growth factor receptors increases gene transfer into primary glioma cells and spheroids. Clin. Cancer Res. 2001, 7, 641–650.

12. Jiang, H.; Gomez-Manzano, C.; Lang, F.F.; Alemany, R.; Fueyo, J. Oncolytic adenoviruses for malignant glioma therapy. Front. Biosci. 2003, 8, 577–588.

13. Tabatabai,G.;Wick,W.;Weller,M.Stemcell-mediatedgenetherapiesformalignantgliomas:A promising targeted therapeutic approach? Discov. Med. 2011, 11, 529–536.

14. Willmon, C.; Harrington, K.; Kottke, T.; Prestwich, R.; Melcher, A.; Vile, R. Cell carriers for oncolytic viruses: Fed Ex for cancer therapy. Mol. Ther. 2009, 17, 1667–1676.

15. Yong,R.L.;Shinojima,N.;Fueyo,J.;Gumin,J.;Vecil,G.G.;Marini,F.C.;Bogler,O.;Andreeff,M.; Lang, F.F. Human bone marrow-derived mesenchymal stem cells for intravascular delivery of oncolytic adenovirus Delta24-RGD to human gliomas. Cancer Res. 2009, 69, 8932–8940.

16. Ahmed, A.U.; Tyler, M.A.; Thaci, B.; Alexiades, N.G.; Han, Y.; Ulasov, I.V.; Lesniak, M.S. A comparative study of neural and mesenchymal stem cell-based carriers for oncolytic adenovirus in a model of malignant glioma. Mol. Pharm. 2011, 8, 1559–1572.

17. Xia, X.; Ji, T.; Chen, P.; Li, X.; Fang, Y.; Gao, Q.; Liao, S.; You, L.; Xu, H.; Ma, Q.; et al. Mesenchymal stem cells as carriers and amplifiers in CRAd delivery to tumors. Mol. Cancer 2011, 10, 134.

18. Ahmed, A.U.; Thaci, B.; Tobias, A.L.; Auffinger, B.; Zhang, L.; Cheng, Y.; Kim, C.K.; Yunis, C.; Han, Y.; Alexiades, N.G.; et al. A preclinical evaluation of neural stem cell-based cell carrier for targeted antiglioma oncolytic virotherapy. J. Natl. Cancer Inst. 2013, 105, 968–977.

19. Tyler, M.A.; Ulasov, I.V.; Sonabend, A.M.; Nandi, S.; Han, Y.; Marler, S.; Roth, J.; Lesniak, M.S. Neural stem cells target intracranial glioma to deliver an oncolytic adenovirus in vivo. Gene Ther. 2009, 16, 262–278.

20. Kim, C.K.; Ahmed, A.U.; Auffinger, B.; Ulasov, I.V.; Tobias, A.L.; Moon, K.S.; Lesniak, M.S. N-acetylcysteine amide (NACA) Augments the Therapeutic Effect of Neural Stem Cell.-Based Anti-Glioma Oncolytic Virotherapy. Mol. Ther. 2013, 21, 2063–2073.

21. Lamfers, M.; Idema, S.; van Milligen, F.; Schouten, T.; van der Valk, P.; Vandertop, P.; Dirven, C.; Noske, D. Homing properties of adipose-derived stem cells to intracerebral glioma and the effects of adenovirus infection. Cancer Lett. 2009, 274, 78–87.

22. Power, A.T.; Wang, J.; Falls, T.J.; Paterson, J.M.; Parato, K.A.; Lichty, B.D.; Stojdl, D.F.; Forsyth, P.A.; Atkins, H.; Bell, J.C. Carrier cell-based delivery of an oncolytic virus circumvents antiviral immunity. Mol. Ther. 2007, 15, 123–130.

23. Muthana,M.;Giannoudis,A.;Scott,S.D.;Fang,H.Y.;Coffelt,S.B.;Morrow,F.J.; Murdoch,C.; Burton, J.; Cross, N.; Burke, B.; et al. Use of macrophages to target therapeutic adenovirus to human prostate tumors. Cancer Res. 2011, 71, 1805–1815.

24. Wakimoto, H.; Kesari, S.; Farrell, C.J.; Curry, W.T., Jr.; Zaupa, C.; Aghi, M.; Kuroda, T.; Stemmer-Rachamimov, A.; Shah, K.; Liu, T.C.; et al. Human glioblastoma-derived cancer stem cells: establishment of invasive glioma models and treatment with oncolytic herpes simplex virus vectors. Cancer Res. 2009, 69, 3472–3481.

25. Wakimoto, H.; Mohapatra, G.; Kanai, R.; Curry, W.T., Jr.; Yip, S.; Nitta, M.; Patel, A.P.; Barnard, Z.R.; Stemmer-Rachamimov, A.O.; Louis, D.N.; et al. Maintenance of primary tumor phenotype and genotype in glioblastoma stem cells. Neuro Oncol. 2012, 14, 132–144.

26. Schaft, N.; Willemsen, R.A.; de Vries, J.; Lankiewicz, B.; Essers, B.W.; Gratama, J.W.; Figdor, C.G.; Bolhuis, R.L.; Debets, R.; Adema, G.J. Peptide fine specificity of anti-glycoprotein 100 CTL is preserved following transfer of engineered TCR alpha beta genes into primary human T lymphocytes. J. Immunol. 2003, 170, 2186–2194.

27. Willemsen, R.A.; Sebestyén, Z.; Ronteltap, C.; Berrevoets, C.; Drexhage, J.; Debets, R. CD8 alpha coreceptor to improve TCR gene transfer to treat melanoma: Down-regulation of tumor-specific production of IL-4, IL-5, and IL-10. J. Immunol. 2006, 177, 991–998.

28. Schaft,N.;Lankiewicz,B.;Gratama,J.W.;Bolhuis,R.L.;Debets,R.Flexibleandsensitivemethodto functionally validate tumor-specific receptors via activation of NFAT. J. Immunol. Methods 2003, 280, 13–24.

29. Ono, H.A.; Le, L.P.; Davydova, J.G.; Gavrikova, T.; Yamamoto, M. Noninvasive visualization of adenovirus replication with a fluorescent reporter in the E3 region. Cancer Res. 2005, 65, 10154–10158.

30. He,T.C.;Zhou,S.;daCosta,L.T.;Yu,J.;Kinzler,K.W.;Vogelstein,B.Asimplifiedsystemfor generating recombinant adenoviruses. Proc. Natl. Acad. Sci. USA 1998, 95, 2509–2514.

31. De Vrij, J.; van den Hengel, S.K.; Uil, T.G.; Koppers-Lalic, D.; Dautzenberg, I.J.; Stassen, O.M.; Bárcena, M.; Yamamoto, M.; de

Ridder, C.M.; Kraaij, R. Enhanced transduction of CAR-negative cells by protein IX-gene deleted adenovirus 5 vectors. Virology 2011, 410, 192–200.

32. Fueyo, J.; Gomez-Manzano, C.; Alemany, R.; Lee, P.S.; McDonnell, T.J.; Mitlianga, P.; Shi, Y.X.; Levin, V.A.; Yung, W.K.; Kyritsis, A.P. A mutant oncolytic adenovirus targeting the Rb pathway produces anti-glioma effect in vivo. Oncogene 2000, 19, 2–12.

33. Fallaux, F.J.; Kranenburg, O.; Cramer, S.J.; Houweling, A.; van Ormondt, H.; Hoeben, R.C.; Van Der Eb, A.J. Characterization of 911: A new helper cell line for the titration and propagation of early region 1-deleted adenoviral vectors. Hum. Gene Ther. 1996, 7, 215–222.

34. Lamfers, M.L.; Fulci, L.G.; Chiocca, E.A. Cyclophosphamide increases transgene expression mediated by an oncolytic adenovirus in glioma-bearing mice monitored by bioluminescence imaging. Mol. Ther. 2006, 14, 779–788.

35. Mentel,R.;Döpping,G.;Wegner,U.;Seidel,W.;Liebermann,H.;Döhner,L.Adenovirus-receptor interaction with human lymphocytes. J. Med. Virol. 1997, 51, 252–257.

36. Leon, R.P.; Hedlund, T.; Meech, S.J.; Li, S.; Schaack, J.; Hunger, S.P.; Duke, R.C.; Degregori, A.J. Adenoviral-mediated gene transfer in lymphocytes. Proc. Natl. Acad. Sci. USA 1998, 95, 13159–13164.

37. Yotnda, P.; Onishi, H.; Heslop, H.E.; Shayakhmetov, D.; Lieber, A.; Brenner, M.; Davis, A. Efficient infection of primitive hematopoietic stem cells by modified adenovirus. Gene Ther. 2001, 8, 930–937.

38. Yotnda, P.; Zompeta, C.; Heslop, H.E.; Andreeff, M.; Brenner, M.K.; Marini, F. Comparison of the efficiency of transduction of leukemic cells by fiber-modified adenoviruses. Hum. Gene Ther. 2004, 15, 1229–1242.

39. Shinojima,N.;Hossain,A.;Takezaki,T.;Fueyo,J.;Gumin,J.;Gao,F.;Nwajei,F.;Marini,F.C.; Andreeff, M.; Kuratsu, J.; et al. TGF-beta mediates homing of bone marrow-derived human mesenchymal stem cells to glioma stem cells. Cancer Res. 2013, 73, 2333–2344.

40. Gondi, C.S.; Veeravalli, K.K.; Gorantla, B.; Dinh, D.H.; Fassett, D.; Klopfenstein, J.D.; Gujrati, M.; Rao, J.S. Human umbilical cord blood stem cells show PDGF-D-dependent glioma cell tropism in vitro and in vivo. Neuro Oncol. 2010, 12, 453–465.

41. Lohr,J.;Ratliff,T.;Huppertz,A.;Ge,Y.;Dictus,C.;Ahmadi,R.;Grau,S.;Hiraoka,N.;Eckstein,V.; Ecker, R.C.; et al. Effector T-cell infiltration positively impacts survival of glioblastoma patients and is impaired by tumor-derived TGF-beta. Clin. Cancer Res. 2011, 17, 4296–308.

42. Huang, J.Y.; Cheng, Y.J.; Lin, Y.P.; Lin, H.C.; Su, C.C.; Juliano, R.; Yang, B.C. Extracellular matrix of glioblastoma inhibits polarization and transmigration of T cells: The role of tenascin-C in immune suppression. J. Immunol. 2010, 185, 1450–1459.

43. Qiao,J.;Wang,H.;Kottke,T.;Diaz,R.M.;Willmon,C.;Hudacek,A.;Thompson,J.;Parato,K.; Bell, J.; Naik, J.; et al. Loading of oncolytic vesicular stomatitis virus onto antigen-specific T cells enhances the efficacy of adoptive T-cell therapy of tumors. Gene Ther. 2008, 15, 604–616.

44. Kottke, T.; Diaz, R.M.; Kaluza, M.; Pulido, J.; Galivo, F.; Wongthida, P.; Thompson, J.; Willmon, C.; Barber, G.N.; Cheste, J.; et al. Use of biological therapy to enhance both virotherapy and adoptive T-cell therapy for cancer. Mol. Ther. 2008, 16, 1910–1918.

45. Zhang,J.G.;Kruse,C.A.;Driggers,L.;Hoa,N.;Wisoff,J.;Allen,J.C.;Zagzag,D.;Newcomb,E.W.; Jadus, M.R. Tumor antigen precursor protein profiles of adult and pediatric brain tumors identify potential targets for immunotherapy. J. Neurooncol. 2008, 88, 65–76.

46. Zhang, J.G.; Eguchi, J.; Kruse, C.A.; Gomez, G.G.; Fakhrai, H.; Schroter, S.; Ma, W.; Hoa, N.; Minev, B.; Delgado, C.; et al. Antigenic profiling of glioma cells to generate allogeneic vaccines or dendritic cell-based therapeutics. Clin. Cancer Res. 2007, 13, 566–575.

47. Beier,C.P.;Kumar,P.;Meyer,K.;Leukel,P.;Bruttel,V.;Aschenbrenner,I.;Riemenschneider,M.J.; Fragoulis, A.; Rümmele, P.; Lamszus, K.; et al. The cancer stem cell subtype determines immune infiltration of glioblastoma. Stem Cells Dev. 2012, 21, 2753–2761.

48. Rutledge, W.C.; Kong, J.; Gao, J.; Gutman, D.A.; Cooper, L.A.; Appin, C.; Park, Y.; Scarpace, L.; Mikkelsen, T.; Cohen, M.L.; Aldape, K.D.; et al. Tumor-infiltrating lymphocytes in glioblastoma are associated with specific genomic alterations and related to transcriptional class. Clin. Cancer Res. 2013, 19, 4951–4960.

8

Heterogeneous reovirus susceptibility in human

Chapter was published as:

Heterogeneous reovirus susceptibility in human glioblastoma stem-like cell cultures. *SK van den Hengel, RK Balvers, IJC Dautzenberg, DJM van den Wollenberg, JJ Kloezeman, ML Lamfers, PAE Sillivis-Smit and RC Hoeben*

Cancer Gene Therapy, doi:10.1038/cgt.2013.47

Published: 2nd of August 2013

ABSTRACT

Glioblastoma (GB) is a devastating disease for which new treatment modalities are needed. Efficacious therapy requires the removal of stem-cell like cells, these cells drive tumor progression because of their ability to self-renew and differentiate. In glioblastoma, the GB stem-like cells (GSC) form a small population of tumor cells and possess high resistance to chemo and radiation therapies. To assess the sensitivity of GSC to reovirus-mediated cytolysis, a panel of GSC cultures was exposed to wild-type reovirus Type 3 Dearing (T3D) and its junction adhesion molecule-A (JAM-A)-independent mutant, jin-1. Several parameters were evaluated, including the fraction of cells expressing the JAM-A reovirus receptor, the fraction of cells synthesizing reovirus proteins, the number of infectious reovirus particles required to reduce cell viability, the amount of infectious progeny reovirus produced and the capacity of the reoviruses to infect the GSC in 3-dimensional (3D) tumor cell spheroids. Our data demonstrate a marked heterogeneity in the susceptibility of the cultures to reovirus-induced cytolysis. While in monolayer cultures the jin-1 reovirus was generally more cytolytic than the wild-type reovirus T3D, in the 3D GSC spheroids, these viruses were equally effective. Despite the variation in reovirus sensitivity between the different GSC cultures, our data support the use of reovirus as an oncolytic agent. It remains to be established whether the variation in the reovirus sensitivity correlates with a patient's response to reovirus therapy. Moreover, our data show that the expression of the JAM-A receptor is not a major determinant of reovirus sensitivity in 3D GSC cultures.

INTRODUCTION

Treatment of glioblastoma (GB) remains a significant clinical challenge. Despite intensive treatment, which includes surgical resection, followed by chemo-irradiation therapy, the prognosis remains dismal. This is largely due to the high tumor recurrence rate caused by the highly infiltrative and aggressive nature of these tumors. Despite the extensive research in the past decades, the patient survival rates have only incrementally improved.1 An important role in the recurrence of GBs has been assigned to a small population of cells, the GB stem-like cells (GSC).1–3 These cells possess high resistance to radio- and chemotherapy4–6 and can self-renew and differentiate into the heterogeneous cell types that drive tumorigenesis.2,7,8 Additionally, genotypic and phenotypic analyses of cultured GSC revealed that they retain the molecular characteristics of the parental tumors better than cells cultured in conventional serum-containing media.7,8

The notion that GSCs are relatively resistant to the conventional radiation and chemotherapies stresses the importance of exploring other means of eliminating these cells. An approach that has gained much interest for cancer treatment over the past decades is virotherapy. So far, at least fifteen different viruses have been evaluated in preclinical studies. Of these, at least four, that is, herpes simplex virus, human adenovirus, Newcastle disease virus and mammalian reovirus, have been evaluated in clinical studies for the treatment of GB. The results demonstrated that the approach is safe and well tolerated, and provided anecdotal evidence of anti-tumor efficacy (as reviewed in Wollman et al.9 and Zemp et al.10) Nevertheless, these studies revealed that the therapeutic efficacy needs further improvement. One way to accomplish this is to focus the treatment modalities by identifying those tumors and patients who are more likely than others to respond to a specific therapy.

Here we evaluated the susceptibility of a panel of cultured GSCs, isolated from tumor resections of GB patients, to mammalian reovirus Type 3. Reovirus Type 3 Dearing (T3D) has been evaluated extensively as oncolytic agent. It has a segmented double-stranded RNA genome. Reovirus attachment and entry are mediated by the junction adhesion molecule-A (JAM-A), which is an integral tight junction protein.11,12 Research indicates that the absence or incorrect expression of JAM-A on colorectal tumor cells inhibits reovirus infection.13 In addition, upon infection, reoviruses preferentially lyse cells with an activated RAS/RalGEF/p38 pathway.14–16 This tumor cell preference leads to the initiation of at least 30 clinical studies involving the use of wild-type (wt) T3D as oncolytic agent.17 So far, one phase-I clinical trial involving intratumoral administration of reovirus to patients with recurrent malignant glioma was completed. This study showed that this approach is safe and well tolerated, but anti-tumor efficacy has been limited.18

To evaluate the capacity of reovirus to establish a lytic infection in brain tumor stem cells, we assessed the cytolytic capacity of reoviruses in GSC cultures. First, the expression of the canonical mammalian reovirus receptor, JAM-A,11 was analyzed by flow cytometry. A wide heterogeneity in JAM-A expression between the GSC cultures was observed. Therefore, the susceptibility to wt T3D was compared with the susceptibility to the T3D mutant jin-1. This mutant, in contrast to wt T3D, can infect cells independent of JAM-A expression.19 To evaluate the susceptibility of the GSCs, early viral protein synthesis, the virus-induced cytopathic effect and progeny virus yields were determined. Progeny virus yields are relevant, as virus spread and amplification are dependent on progeny production. Moreover, virus penetration and spread in 3-dimensional (3D) GSC spheroid cultures were determined. The 3D cultures serve as an intermediate between monolayer cultures and animal model systems, and these 3D cultures may mimic the intratumor environment more than monolayer cultures.20,21 Moreover, distribution, spread and oncolysis can be studied in 3D spheroid models.22 Our data reveal a wide heterogeneity in reovirus susceptibility among the different GSC cultures and that the reovirus replication can be hampered at various stages of infection. In addition, we demonstrate that the jin-1 mutant infects cells more efficient in GSCs in monolayer cultures, is more cytolytic and produces more progeny virus upon GSC infection. However, in 3D GSC spheroid cultures, the pattern of viral spread and infection of jin-1 was similar to wt T3D.

MATERIALS AND METHODS

Cell lines

The established cell lines 911 and U118MG were cultured in high glucose Dulbecco's modified Eagle medium (DMEM) (Invitrogen, Breda, The Netherlands), supplemented with penicillin, streptomycin (pen-strep) and 8% fetal bovine serum (Invitrogen, Bleiswijk, The Netherlands). A detailed

protocol for establishment of GSC cultures from glioma resection specimens is described elsewhere.23 In brief, GSCs were grown on growth factor-reduced extracellular matrix-(Cultrex BME Reduced Growth Factor, R&D systems, Abingdon, UK) coated dishes and cultured in DMEM-F12 supplemented with 1% pen-strep, B27 (Invitrogen), human EGF (5 mg ml 1), human basic FGF (5 mg ml 1) (both Tebu-Bio, Heerhugowaard, The Netherlands) and heparin (5 mg ml 1) (Sigma-Aldrich, Zwijndrecht, The Netherlands). The tumor material was acquired with informed consent from patients as approved by the Institutional Review Board of the Erasmus Medical Center, Rotterdam. All cell cultures were cultured in humidified atmosphere of 5% CO2 at 37 1C.

Reovirus

The wt mammalian reovirus Type 3 Dearing strain R124 (referred in the text as wt T3D), and the jin-1 mutant were propagated as described before.19 Cultures of 911 cells were exposed to wt T3D in DMEM 2% fetal bovine serum. At 4h post infection, the medium was replaced with DMEM 8% fetal bovine serum. The wt T3D virus was harvested 48 h after infection by collecting the cells in 2% fetal bovine serum/phosphate-buffered saline and the virus was released by three cycles of freeze-thawing. The jin-1 virus was propagated on the JAM-A-deficient cell line, U118MG, and was harvested at 72h post infection. Infectious titers of both viruses were determined by plaque assay on 911 cell cultures.

Cell viability assay

Cells were infected in suspension with wt T3D or jin-1 at a multiplicity of infection (MOI) range 0–100 pfu911 per cell. Subsequently cells were transferred to an EMC growth factor-reduced pre-coated 96-well plate in which 10 000 cells per well were seeded. The viability of the cultures was measured 72h post infection by CellTiter-Glo Luminescent Cell Viability assay, according to manufacturer's instructions (Promega, Leiden, The Netherlands). Briefly, the reagent was added to the cell cultures and incubated at room temperature in the dark for 10min. Next, samples were transferred to black 96-well plates and luminescence was measured by a plate reader (Tecan Infinite M200, Tecan Group Ltd, Ma¨nnedorf, Switzerland). Luminescence count data of the plate reader were transferred to Microsoft office Excel and half maximal effective concentration (EC50) values were calculated from the mean residual luminescence from three independent samples.

Flow cytometry analysis

Anti-JAM-A immunostaining. GSC cultures, 911 cells and U118MG cells, in suspension as single cells, were incubated with mouse monoclonal anti- JAM-A antibody (clone M.Ab.F11, Cat. No. ab17261, Abcam, Cambridge, UK) for 1 h on ice. Subsequently, the cells were incubated in the dark with PE fluorochrome-conjugated rat anti-mouse serum (Cat. No. 340270, BD Bioscience, Erembodegem, Belgium) for 30 min on ice. After washing, the samples were taken up in FACS buffer (phosphate-buffered saline, 0.5% BSA, 2 mM EDTA) and assayed on a BD LSRII flow cytometer. Data were analyzed with FACSdiva software (BD Bioscience). Anti-Sigma 3 immunostaining. Cells were infected in suspension with wt T3D or jin-1 at an MOI 1⁄4 3 pfu per cell and transferred to a 6-well plate at 20000 cells per well. After 30h, the cells were harvested and fixed in 4% formaldehyde for 10min. Subsequently, cells were washed and permeabilized with Perm/Wash buffer (Cat. No. 554714, BD Cytofix/ Cytoperm Fixation Permeabilization kit, BD Bioscience) followed by incubation with the anti-Sigma 3 mouse antibody (4F2, monoclonal antibody, Developmental Studies Hybridoma Bank (DSHB), University of Iowa, Iowa, IA, US) for 1h at 41C. After washing twice with Perm/Wash buffer, the samples were incubated in the dark with the PE fluorochrome- conjugated rat anti-mouse serum (Cat. No. 340269, BD Bioscience) for 30 min. Subsequently, the samples were washed extensively, resuspended in FACS buffer and assayed on a BD LSRII flow cytometer and data of a gated population of 10000 cells were analyzed with FACSDiva software (BD Bioscience).

Viral progeny

Cells were exposed in suspension at 371C for 1h with wt T3D or jin-1, MOI 1⁄4 3 pfu911 per cell. Next, unbound virus was removed by centrifugation, removal of the medium and plating the cells in fresh medium in 24- well plates. After 72 h, cells and media were collected and freeze-thawed three times to release virus from the cells. Viral titers were determined by plaque assays on 911 cells as described.24 The plaque titration conditions used have an inter-experimental variation of o15%. The virus production by the cell cultures was expressed as the fold-increase and calculated by dividing the total yield by the amount of virus used to infect the culture.

Spheroid 3D cultures

Multicellular spheroids were generated by seeding 10 000 cells per well in a non-adherent 96-well round-bottom plate in culture media supplemen- ted with 2.4% methylcellulose (Sigma-Aldrich). After 1 day, the multi- cellular spheroids were washed three times and placed in fresh media. Two days later, the spheroids were mock infected or exposed to wt T3D or jin-1 at a MOI 1⁄4 10 pfu per cell. Three days after infection, the spheroids were fixed overnight with 4% formaldehyde and embedded in paraffin. Analyses of 6mm paraffin sections were performed by 3,30-Diaminobenzidine immunocytochemistry. First, sections were incubated overnight with the primary antibody against Sigma 3 (4F2, DSHB) followed by a wash and subsequent incubation with the secondary horse radish peroxidase- conjugated antibody (Cat. no. P0447, Dako, Glostrup, Denmark).

RESULTS

The aim of our research is to develop an oncolytic virus-based therapy for glioblastoma. To assess the susceptibility, we defined the sensitivity of GSCs to reovirus by measuring five parameters. A panel of seven independent serum-free GSC cultures23 was evaluated in parallel to the highly reovirus-susceptible human embryonic retinoblast cell line 91119,24 and the JAM-A negative U118MG cell line.19 All of the serum-free GSC cultures are derived from GB resections, five from primary tumor specimens, and two from recurrent disease cases. The characteristics of the patients from whom the GSC cultures were derived are summarized in Table 1. The expression of the JAM-A reovirus receptor was assessed in each of these cultures by flow cytometry. The expression is heterogeneous and could be categorized in four groups. The GS187 and

Table 1. Patient characteristics of glial stem-like cells cultures

GSC culture	*Male/female*	*Age*	*Type*
GS79	F	74	GB
GS184	M	50	GB
GS186	F	48	GB
GS187	F	63	GB recurrent
GS224	M	49	GB recurrent
GS245	M	70	GB
GS249	M	43	GB

Abbreviations: F, female; GB, glioblastoma; M, male.

GS249 cultures were JAM-A negative whereas the GS184 and GS186 have only a low-level of JAM-A expression. Moderate JAM-A expression was measured in GS79 and GS245 cultures, respectively, with between 30 and 50% of the cell population expressing JAM-A. The highest expression was observed in GS224, in which almost the entire population expressed JAM-A (Figure 1 and Table 2). The latter closely resembled the JAM-A expression of the control cell line 911. The high variation in JAM-A expression prompted us to include in our studies the T3D reovirus jin-1. In contrast to the wt T3D, the jin-1 mutants can infect cells independent of JAM-A expression.19

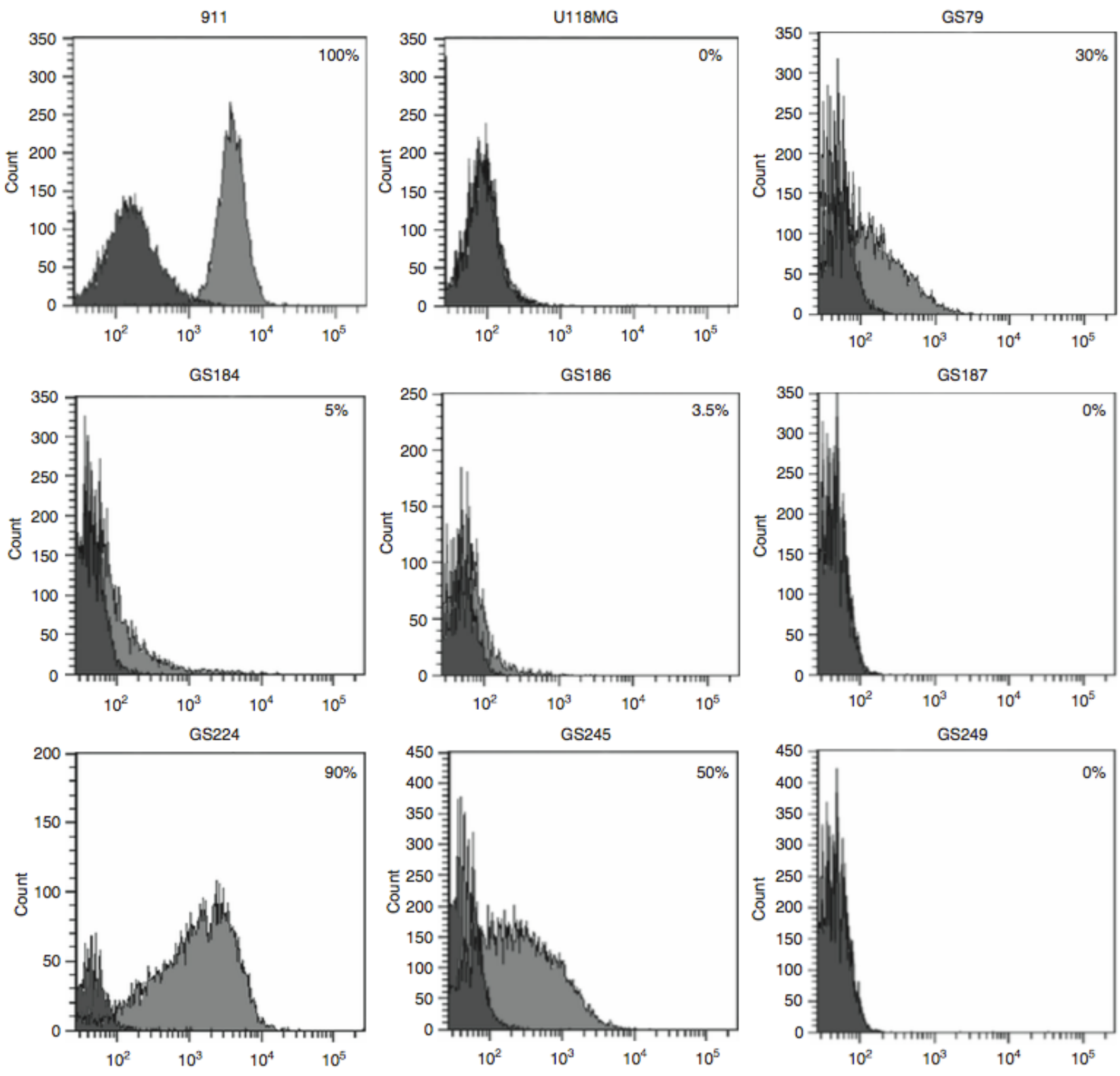

Figure 1. Flow cytometry analyses of junction adhesion molecule-A (JAM-A) expression on glioblastoma stem-like cell (GSC) cultures and 911 and U118MG cells. Staining was performed with an anti-JAM-A mouse monoclonal antibody followed by a secondary rat anti-mouse PE-conjugated antibody (light gray histograms). The dark gray histograms represent the incubation with secondary antibody only. The analysis was performed on a gated population of 10 000 cells. The percentages represent the JAM-A-positive population with respect to only secondary antibody-treated cells.

Within the GSC cultures, a highly variable sensitivity to wt T3D reovirus infection was observed (Table 2). In five out of seven GSC cultures, the fraction of reovirus-positive cells did not exceed 1%. This indicates that virus entry in these cultures is inhibited or that the infection is blocked prior to the initiation of reovirus protein synthesis. In contrast, upon wt T3D reovirus exposure, approximately 20% of the GS79 cells were positive for s3, whereas in GS224, more than 50% of the cells synthesized s3 (Table 2).

To establish the EC50, each culture was exposed to serial dilutions of the wt T3D reovirus stocks and the viability was determined. No clear cytopathic effects were observed in four GSC cultures. The viability assay demonstrated that GS187 and GS249 are fully resistant to wt T3D. The GS184 and the GS245 cultures exhibited a minimal reduction in viability at the highest MOI used and therefore their EC50 values were scored as 4100 pfu per cell. Infection of wt T3D was clearly discernible in GS79, GS186 and GS224 cultures (Table 2). In GS186 cultures, the reovirus cytolysis was not accompanied by reovirus protein synthesis.

To study whether GSC infection results in the production of infectious progeny reovirus, the viral yields were determined at 72 h post infection. From these data, the fold-increase in progeny was calculated (Table 2). Significant amounts of progeny virus particles were obtained in six out of the seven GSC cultures. Only from the GS184 culture the amount of reovirus recovered was below the amount used to infect the cultures. The highest yields were collected from GS79 and GS186, with a 20-fold-increase in infectious titer. A 10-fold-increase was produced by GS224. The cultures of GS245 and GS249 both yielded almost four times more virus particles. A doubling of the infectious virus particle number was achieved by GS187. From these data we conclude that several of the GSC cultures are productively infected with wt T3D, albeit with highly variable yields.

In order to determine the virus production per cell, the data of the s3-positive population was combined with the virus yields (Table 2). The viral yield per cell obtained from GS79, GS184 and GS224 was low, and does not exceed the 300 pfu per cell. The production per cell from GS187, GS245 and GS249 cultures ranged from 1.5 x10*3 to 3 x10*3 pfu per cell. The highest yields were produced by GS186 with approximately 10*4 pfu per cell. These data show that, whereas some cultures are susceptible to reovirus infection, they do not replicate reoviruses to high titers.

The GSC cultures were grown as spheroids to study the reovirus spread in 3D cultures that mimic the tumor structure more faithfully than monolayer cultures.21,25 Immunocytochemistry revealed the presence of reovirus-infected cells in all GSC spheroid cultures. The distribution and the abundance of the reovirus-infected cells differed within the GSC spheroids (Figure 2). In GS184, only a few reovirus-positive cells were detected throughout the spheroid. In GS79 and GS245, the entire outer rim of the spheroids was infected. Already at visual inspection of the spheroid cultures cellular debris was observed surrounding the spheroids. These detached cells were lost during sample processing prior to analysis. In GS187 and GS249, the wt T3D infected cells were concentrated at a single side of the spheroids, suggesting that the virus infection was initiated at a single point near the outer rim, and then spread inward from there. Additionally, visual inspection of GS187 spheroids revealed abnormal blown-up cell structures on the edge of the spheroid, indicative of reovirus infection. The GS224 spheroids showed a mixed pattern of infection with the entire outer layer being reovirus infected in combination with inward spread on one side of the spheroids. On GS186 spheroids, the s3 staining revealed that all cells of the spheroids were infected with the exception of the core cells in a few spheroids. Taken together, these data show that there is a high variation in the extent of reovirus infection and pattern of spreading in the different GSC spheroid cultures.

To study whether the jin-1 mutant is more effective in the GSC cultures, we repeated the experiments described above with this mutant virus. Overall, the fraction of positive cells exceeded the fraction of reovirus positive cells after infection with wt T3D. The cultures with the lowest number of reovirus s3-positive cells included GS184 and GS245. In the GS186, GS187 and GS249 cultures, more than 60% of the cell popula-

Table 2. Reovirus infection in GSC cultures exposed to *wt* T3D or *jin-1*

GSC culture	*JAM-A expression*	*Fraction of reovirus σ3-positive cells (%)*		*EC_{50} (p.f.u./cell)*		*Reovirus yield fold-increase over input*		*Reovirus yield per σ3-positive cell (p.f.u. per cell)*	
		wt T3D	*jin-1*	*wt T3D*	*jin-1*	*wt T3D*	*jin-1*	*wt T3D*	*jin-1*
911	High	88	59	0.2	0.1	430	700	15 000	36 000
U118MG	Negative	0.2	1.3	Insensitive	>100	0.33	14.1	5000	33 000
GS79	Moderate	22	99	64	4.1	20	30	300	90
GS184	Low	0.8	19	>100	26	0.5	15	200	9100
GS186	Low	0.6	66	9.3	<1	21	570	10 500	2600
GS187	Negative	0.4	62	Insensitive	8.2	2	250	1500	1200
GS224	High	54	89	7.6	1.2	11	14	60	50
GS245	Moderate	0.5	16	>100	40	3.7	108	2200	2000
GS249	Negative	0.4	67	Insensitive	>100	3.7	670	2800	3000

Abbreviations: GSC, glioblastoma stem-like cells; JAMA-A, junction adhesion molecule-A; T3D, Type 3 Dearing; WT, wild type.

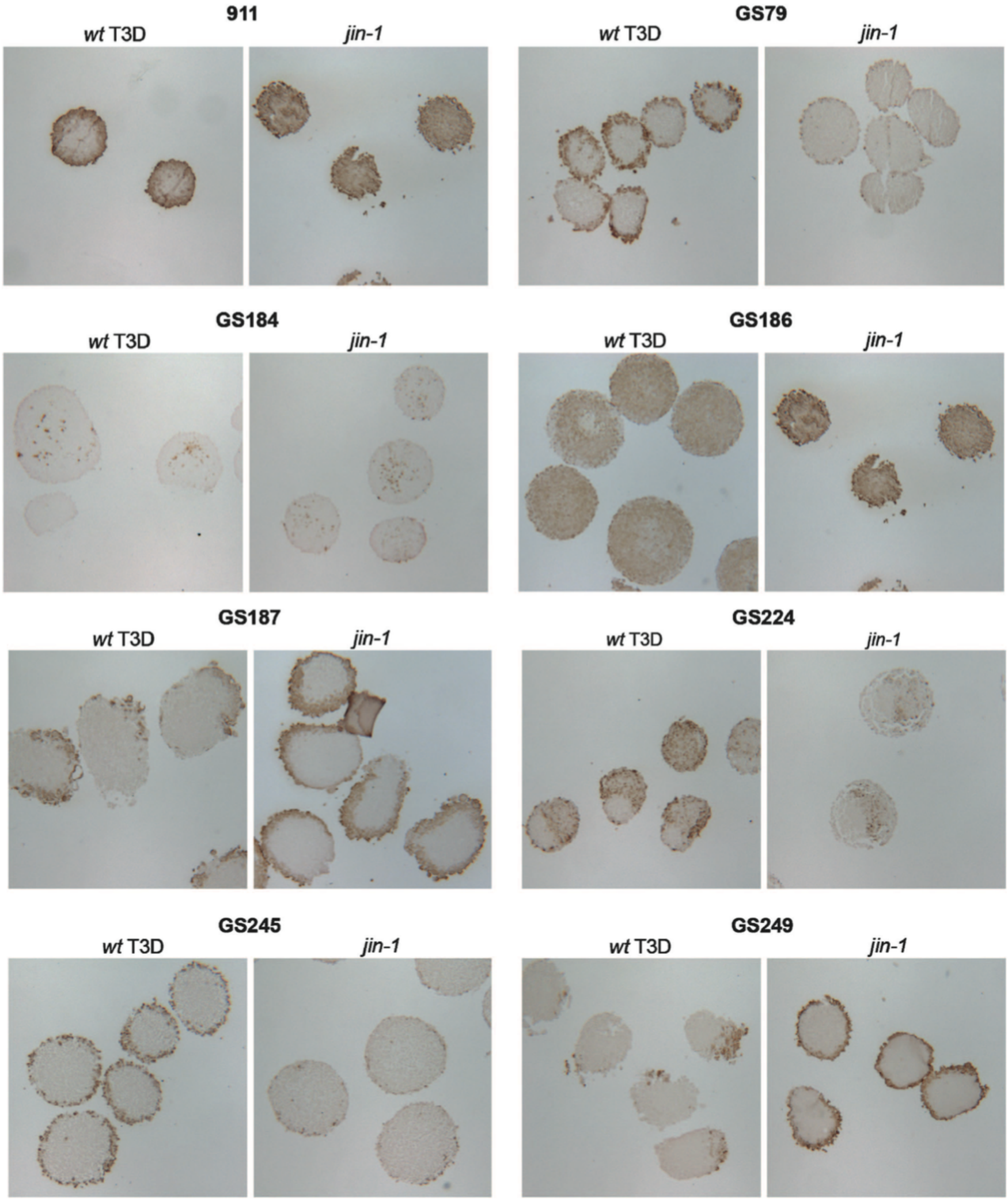

Figure 2. Wild type (*wt*) Type 3 Dearing (T3D) and *jin-1* reovirus infection pattern in GSC spheroids. Glioblastoma stem-like cell (GSC) spheroids generated of 10 000 cells were incubated with *wt* T3D or *jin-1* at multiplicity of infection = 10. After 72 h, the spheroids were fixed and processed into paraffin sections. To analyze the σ3 pattern, sections were incubated with the monoclonal antibody 4F2 against σ3 followed by secondary antibody horse radish peroxidase (HRP)-conjugated polyclonal Goat anti-Mouse immunoglobulins. HRP activity was visualized by 3,3′-Diaminobenzidine staining. The brown color indicates the presence of σ3 protein indicative of reovirus infection.

tion stained positive for s3 reovirus protein. Most susceptible to jin-1 were GS79 and GS224 with, respectively, 99 and 89% of the cells being reovirus positive (Table 2).

Similar to the experiments with wt T3D reovirus, the EC50 values were determined (Table 2). All values of jin-1 infection were found to be lower than after infection with wt T3D. On GS249, a moderate cytopathic effect of jin-1 was seen at MOI 1⁄4 100. In all the other six cultures, cytopathic effects were clearly seen in higher dilution ranges. The EC50 determined on GS245 and GS184 was 40 and 26 pfu per cell, respectively. The remaining four cultures scored an EC50 below 10 pfu per cell. The culture most sensitive to jin-1 was GS186, in which an effect was already observed at MOI 1⁄4 0.1.

The lowest effective viral progeny yield was obtained from GS79, GS184 and GS224 with less than a hundred-fold-increase in virus titer. Higher yields were obtained in GS245 and GS187 with a 200 and 500-fold amplification, whereas in the GS186 and GS249 cultures the yields exceeded the input dose by three orders of magnitude (Table 2). Moreover, the calculated yield per infected cell in four of the seven cultures was similar for the jin-1 and wt T3D viruses. In three cultures, the yields per cell were different from those of wt T3D and jin-1. In GS79 and GS186, the yield of progeny virus is higher for wt T3D than for jin-1, whereas in GS184 the yield of the jin-1 was 45-fold higher than in wt T3D-exposed cultures.

To study the distribution and abundance of reovirus-infected cells in 3D cultures, GSC spheroids were exposed to jin-1 (Figure 2). Similar to wt T3D, variable results were obtained upon exposure to jin-1. In four GSC spheroids, the cells at the outer rim stained positive for s3, although at varying levels. GS187 and GS249 were more effectively infected than GS79 and GS245. Viral spread into the core of the spheroids was seen in GS184, GS186 and GS224. In GS184 and GS224, only some isolated reovirus-infected cells were seen, whereas in GS186 spheroids, s3-stained cells were found throughout the spheroid.

DISCUSSION

The identification of GSCs, their role in tumor recurrence, metastases and therapy resistance, stresses their importance in brain cancer research. Treatment procedures aiming at eliminating these cells may improve brain cancer outcomes.1,26 The aim of this study was to test the susceptibility of GSC cultures to the wt mammalian reovirus T3D and the JAM-A-independent jin-1 mutant. In previous studies, the susceptibility to reovirus was tested in tumor cells in serum-supplemented cultures,27,28 which lose their parental tumor characteristics during culturing7,8 and therefore may be less representative for the clinical situation.

In this study, we measured the GSC cultures on four parameters; reoviral protein synthesis, the induction of cytopathic effects, the production of progeny virus and the spread and penetration of the virus in a 3D spheroid culture of the GSC. These parameters are all independently evaluated in addition to cell lysis, production and spread. Moreover, because the expression of the high-affinity reovirus receptor JAM-A varied on the GSC cells, we evaluated if jin-1 was more potent in this regard than wt T3D.

From this study we conclude that there is marked heterogeneity between the GSC cultures in their sensitivity to reovirus-mediated cytolysis. The differences in reoviral s3 protein synthesis may reflect variation differences in reovirus binding to the cells, reovirus egress from endosomes or differences in positive-strand messenger RNA generation.29,30 The efficiency of reovirus s3 protein synthesis does not correlate with the sensitivity to reovirus-mediated cytolysis. While GS186 is poorly susceptible to wt T3D reovirus synthesis, as evidenced by the fraction of cells that produces s3 proteins, it is relatively sensitive to reovirus- induced cytolysis. In contrast, GS79 synthesizes s3-proteins in a relatively high percentage of the cells, while it is relatively insensitive and requires a high MOI for induction of cytopathic effects by wt T3D. Similarly, we see a highly variable capacity to support reovirus propagation. The amount of progeny reovirus produced per productively infected cells varies over 2 orders of magnitude with the GS186 culture being the most effective wt T3D producer, and the GS224 being least effective. With the use of the jin-1 reovirus, we see a similar heterogeneity. Whereas minor variation is seen in fraction of reovirus-infected cells in the different GSC cultures, the sensitivity to reovirus-induced cytolysis, as well as the capacity to produce progeny reovirus is much more heterogeneous.

The infection efficiency, the reovirus-induced cytolysis and the virus production in the monolayer cultures are more efficient with jin-1 than with wt T3D. In contrast, the distribution and abundance of s3-positive cells in spheroid cultures is similar with these viruses. This suggests that the JAM-A receptor expression is not a prime determinant of the reoviruses' capacity to spread in spheroid cultures. Although this was unexpected, it is not unprecedented. Recently it was established that wt T3D infects and spreads efficiently in 3D tumor spheroids established from JAM-A-deficient U118MG cells. In contrast, wt T3D infection of U118MG cells in monolayer cultures is dependent on JAM-A expression (Dautzenberg et al., Factors affecting reovirus spread in 3D cultures; manuscript in preparation). This demonstrates that the canonical T3D entry route, which starts by the reovirus s1 protein's engagement of JAM-A, is not essential in 3D cultures, and that under these growth conditions alternative entry routes can be used by the reovirus.

Spread of the oncolytic viruses within the tumor is essential for antitumor efficacy. The compartmentalization brought about by depositions of extracellular matrix presents itself as a physical barrier.31 Also, the vasculature and the tumor-stroma may impose limitations to viral spread.32 An appealing option for enhancing the spread of the oncolytic viruses is the use of carrier cells loaded with oncolytic viruses.33–35 The carrier cells need to possess the capacity to home to tumors. Several cell types have been identified that can home to tumors, such as dendritic cells, T cells, macrophages and several types of stem cells. After loading, the virus should hitchhike on these cells and be released in the tumor.34,35 If the viruses are associating with the cells in a manner that shields them from neutralizing antibodies, the approach may also be effective in those patients with pre-existing neutralizing immunity against reovirus. That this strategy can be applied for reovirus delivery was

shown by Ilett et al.,36,37 who showed that reovirus can hitchhike onto dendritic cells and T cells. Additionally, internalization of reovirus by dendritic cells protected the virus from neutralizing antibodies.36

So far, only single GSC cultures were established and studied from the individual patients. It therefore remains to be established whether the heterogeneity observed between different cultures faithfully reflects phenotypic inter-patient or inter-tumor variations, or whether the heterogeneity is the result of intratumor heterogeneity38 or even phenotypic drift in the cultures. The latter could result from the preferential outgrowth of specific populations of cells in the tumor cell cultures. Such culture bias could limit the predictive value as model for the clinical tumors in situ. It would therefore be extremely useful if clinical studies on the efficacy of oncolytic reovirus therapy were paralleled with in vitro studies on reovirus sensitivity in cultures of tumor cells derived from the same patients. Such studies may eventually reveal which of the in vitro parameters would best predict the efficiency of therapeutic reovirus replication in vivo.

REFERENCES

1 Ricard D, Idbaih A, Ducray F, Lahutte M, Hoang-Xuan K, Delattre JY. Primary brain tumours in adults. Lancet 2012; 379: 1984–1996.

2 Galli R, Binda E, Orfanelli U, Cipelletti B, Gritti A, De Vitis S et al. Isolation and characterization of tumorigenic, stem-like neural precursors from human glioblastoma. Cancer Res 2004; 64: 7011–7021.

3 Vescovi A L, Galli R, Reynolds BA. Brain tumour stem cells. Nat Rev Cancer 2006; 6: 425–436.

4 Bao S, Wu Q, McLendon R E, Hao Y, Shi Q, Hjelmeland A. B et al. Glioma stem cells promote radioresistance by preferential activation of the DNA damage response. Nature 2006; 444: 756–760.

5 Eramo A, Ricci-Vitiani L, Zeuner A, Pallini R, Lotti F, Sette G et al. Chemotherapy resistance of glioblastoma stem cells. Cell Death Differ 2006; 13: 1238–1241.

6 Liu G, Yuan X, Zeng Z, Tunici P, Ng H, Abdulkadir IR et al. Analysis of gene expression and chemoresistance of CD133 þ cancer stem cells in glioblastoma. Mol Cancer 2006; 5: 67.

7 Lee J, Kotliarova S, Kotliarov Y, Li A, Su Q, Donin NM et al. Tumor stem cells derived from glioblastomas cultured in bFGF and EGF more closely mirror the phenotype and genotype of primary tumors than do serum-cultured cell lines. Cancer Cell 2006; 9: 391–403.

8 Vik-Mo EO, Sandberg C, Olstorn H, Varghese M, Brandal P, Ramm-Pettersen J et al. Brain tumor stem cells maintain overall phenotype and tumorigenicity after in vitro culturing in serum-free conditions. Neuro Oncol 2010; 12: 1220–1230.

9 Wollmann G, Ozduman K, van den Pol AN. Oncolytic virus therapy for glio- blastoma multiforme: concepts and candidates. Cancer J 2012; 18: 69–81.

10 Zemp FJ, Corredor JC, Lun X, Muruve DA, Forsyth PA. Oncolytic viruses as experimental treatments for malignant gliomas: using a scourge to treat a devil. Cytokine Growth Factor Rev 2010; 21: 103–117.

11 Barton ES, Forrest JC, Connolly JL, Chappell JD, Liu Y, Schnell FJ et al. Junction adhesion molecule is a receptor for reovirus. Cell 2001; 104: 441–451.

12 Campbell JA, Schelling P, Wetzel JD, Johnson EM, Forrest JC, Wilson GA et al. Junctional adhesion molecule a serves as a receptor for prototype and field- isolate strains of mammalian reovirus. J Virol 2005; 79: 7967–7978.

13 van Houdt WJ, Smakman N, Van Den Wollenberg DJ, Emmink BL, Veenendaal LM, van Diest PJ et al. Transient infection of freshly isolated human colorectal tumor cells by reovirus T3D intermediate subviral particles. Cancer Gene Ther 2008; 15: 284–292.

14 Norman KL, Hirasawa K, Yang AD, Shields MA, Lee PW. Reovirus oncolysis: the Ras/ RalGEF/p38 pathway dictates host cell permissiveness to reovirus infection. Proc Natl Acad Sci USA 2004; 101: 11099–11104.

15 Smakman N, Van Den Wollenberg DJ, Elias SG, Sasazuki T, Shirasawa S, Hoeben RC et al. KRAS(D13) Promotes apoptosis of human colorectal tumor cells by Reovir- usT3D and oxaliplatin but not by tumor necrosis factor-related apoptosis-indu- cing ligand. Cancer Res 2006; 66: 5403–5408.

16 Strong JE, Coffey MC, Tang D, Sabinin P, Lee PW. The molecular basis of viral oncolysis: usurpation of the Ras signaling pathway by reovirus. EMBO J 1998; 17: 3351–3362.

17 Russell SJ, Peng KW, Bell JC. Oncolytic virotherapy. Nat Biotechnol 2012; 30: 658–670.

18 Forsyth P, Roldan G, George D, Wallace C, Palmer CA, Morris D et al. A phase I trial of intratumoral administration of reovirus in patients with histologically con- firmed recurrent malignant gliomas. Mol Ther 2008; 16: 627–632.

19 Van Den Wollenberg DJ, Dautzenberg IJ, van den Hengel SK, Cramer SJ, de Groot RJ, Hoeben RC. Isolation of reovirus T3D mutants capable of infecting human tumor cells independent of junction adhesion molecule-A. PLoS One 2012; 7: e48064.

20 Elliott N.T, Yuan F. A review of three-dimensional in vitro tissue models for drug discovery and transport studies. J Pharm Sci. 2011; 100: 59–74.

21 Hirschhaeuser F, Menne H, Dittfeld C, West J, Mueller-Klieser W, Kunz-Schughart LA. Multicellular tumor spheroids: an underestimated tool is catching up again. J Biotechnol 2010; 148: 3–15.

22 Grill J, Lamfers ML, van Beusechem VW, Dirven CM, Pherai DS, Kater M et al. The organotypic multicellular spheroid is a relevant three-dimensional model to study adenovirus replication and penetration in human tumors in vitro. Mol Ther 2002; 6: 609–614.

23 Balvers RK, Kleijn A, Kloezeman JJ, French PJ, Kremer A, van den Bent MJ et al. Serum-free culture success of glial tumors is related to specific molecular profiles and expression of extracellular matrix-associated gene modules. Neuro-Oncology 2013 (in press).

24 Fallaux FJ, Kranenburg O, Cramer SJ, Houweling A, Van Ormondt H, Hoeben RC et al. Characterization of 911: a new helper cell line for the titration and propagation of early region 1-deleted adenoviral vectors. Hum Gene Ther 1996; 7: 215–222.

25 Herrmann R, Fayad W, Schwarz S, Berndtsson M, Linder S. Screening for com- pounds that induce apoptosis of cancer cells grown as multicellular spheroids. J Biomol Screen 2008; 13: 1–8.

. 26 Nduom E K, Hadjipanayis CG, Van Meir EG. Glioblastoma cancer stem-like cells: implications for pathogenesis and treatment. Cancer J 2012; 18: 100–106.

. 27 Alloussi SH, Alkassar M, Urbschat S, Graf N, Gartner B. All reovirus subtypes show oncolytic potential in primary cells of human high-grade glioma. Oncol Rep. 2011; 26: 645–649.

. 28 Wilcox ME, Yang W, Senger D, Rewcastle NB, Morris DG, Brasher PM et al. Reovirus as an oncolytic agent against experimental human malignant gliomas. J Natl Cancer Inst 2001; 93: 903–912.

. 29 Coombs KM. Reovirus structure and morphogenesis. Curr Top Microbiol Immunol 2006; 309: 117–167.

. 30 Schiff LA. Reovirus capsid proteins sigma 3 and mu 1: interactions that influence viral entry, assembly, and translational control. Curr Top Microbiol Immunol 1998; 233: 167–183.

. 31 Kuriyama N, Kuriyama H, Julin C M, Lamborn K, Israel MA. Pretreatment with protease is a useful experimental strategy for enhancing adenovirus-mediated cancer gene therapy. Hum Gene Ther 2000; 11: 2219–2230.

32 Kuppen PJ, van der Eb MM, Jonges LE, Hagenaars M, Hokland ME, Nannmark U et al. Tumor structure and extracellular matrix as a possible barrier for therapeutic approaches using immune cells or adenoviruses in colorectal cancer. Histochem Cell Biol 2001; 115: 67–72.

33 Lamfers M, Idema S, van Milligen F, Schouten T, van der Valk P, Vandertop P et al. Homing properties of adipose-derived stem cells to intracerebral glioma and the effects of adenovirus infection. Cancer Lett 2009; 274: 78–87.

34 Power AT, Bell JC. Taming the Trojan horse: optimizing dynamic carrier cell/ oncolytic virus systems for cancer biotherapy. Gene Ther 2008; 15: 772–779.

35 Willmon C, Harrington K, Kottke T, Prestwich R, Melcher A, Vile R. Cell carriers for oncolytic viruses: Fed Ex for cancer therapy. Mol Ther 2009; 17: 1667–1676.

36 Ilett EJ, Barcena M, Errington-Mais F, Griffin S, Harrington KJ, Pandha HS et al. Internalization of oncolytic reovirus by human dendritic cell carriers protects the virus from neutralization. Clin Cancer Res 2011; 17: 2767–2776.

37 Ilett EJ, Prestwich RJ, Kottke T, Errington F, Thompson JM, Harrington KJ et al. Dendritic cells and T cells deliver oncolytic reovirus for tumour killing despite pre- existing anti-viral immunity. Gene Ther 2009; 16: 689–699.

38 Sottoriva A, Spiteri I, Piccirillo S G, Touloumis A, Collins VP, Marioni JC et al. Intratumor heterogeneity in human glioblastoma reflects cancer evolutionary dynamics. Proc Natl Acad Sci USA 2013; 110: 4009–4014.

.

9

Summary and conclusions

Summary and conclusions of the thesis

Malignant glioma will remain a catastrophic diagnosis to patients and huge challenge for the daily practice of clinicians the coming decades. While the perspectives for patients with other solid tumors, such as breast or prostate cancer, have improved significantly over the last decade with a substantial group of patients being cured or chronically in remission, the prognosis of primary GBM remains dismal. This thesis investigated potential therapeutic strategies for malignant glioma in the context of a novel in vitro model of this disease. Multiple strategies were investigated for therapeutic enhancement of clinical standard of care (TMZ) and alternative (Delta24-RGD) agents that have shown efficacy for GBM. The following text summarizes the findings that were presented in this thesis.

In chapter 2, the GSC model was prospectively analyzed for its recapitulation of the human condition in vitro by interrogating hallmark molecular alterations and their distribution amongst prospectively analyzed patient cases and derived GSCs. Subsequently, we concluded that this model recapitulates canonical genomic alterations and gene expression based subtypes of malignant glioma. However, not all patient samples are propagatable under these culture conditions, and a selection seems to be made for IDH-WT samples, tumors with a copy number trait (Chr7p gain, Chr10q del) and enrichment for the Classical subtype is observed. In addition, there is substantial doubt raised both by this thesis, as well by other groups, that GCIMP tumors are not covered in GSC culture assays. This is important, since the GCIMP/IDH mutant tumors may be derived from a separate entity of malignant glioma, which is predominantly represented in low-grade glioma.

Chapter 3 demonstrates GSCs to serve as a valuable platform for the identification of response profiles of combination therapy for malignant glioma. We demonstrate that GSCs mimic the response-profile of the current clinical chemotherapeutic of choice (temozolomide), and that susceptibility to TMZ corresponds to MGMT protein expression, similar to the clinical situation. PARP inhibition, through the compound ABT-888 (Veliparib), was demonstrated to enhance temozolomide based chemotherapy irrespective of MGMT expression. These findings are important since this molecular substrate of therapeutic response is one of the few straightforward clinical parameters that predict outcome in a subset of malignant glioma. Since temozolomide is likely to remain the golden standard first line treatment for the majority of malignant glioma patient in the near future, enhancement/synergism of new drugs in combination with temozolomide increases the likelihood of clinical translation. Future studies will be needed to identify biomarkers that can be used to predict therapeutic response and longitudinally measure the response (or lack thereof) to therapy in patients.

In chapter 4 a contemporary overview is presented of the literature on molecular characterization of GSCs. Similar to the conclusions of chapter 2, it is demonstrated that GSCs retain most of the hallmark characteristics as found in the human disease. In addition, this chapter highlights some of the current caveats to GSC based research, such as the selection of subtypes (CLA/MES/PRO contra GCIMP) of malignant glioma, the implications of intratumoral heterogeneity on drug response and the implications of residual cells dispersed within in the resection cavity with respect to tumor recurrence. It was concluded that future studies must focus on interrogating the clinical consequences of the latter two phenomena on outcome together with the development of models for the currently not covered GCIMP / IDH mutated subtype.

Chapter 5 provides an overview of the literature that is available on oncolytic adenovirus therapy for malignant glioma. Oncolytic virotherapy for GBM provides an attractive alternative treatment for several reasons. For one, viruses can be modified to selectively infect and lyse tumor cells, introduce therapeutic genes through viral replication and induce a bystander immunological response by shedding tumor antigens that would otherwise remain shielded from detection. In addition, much can be learned from the study of viruses with regard to tumor treatment. As the virus implements similar strategies as tumor cells to interact with the cell cycle to effectively replicate or prevent apoptosis, one may study these mechanisms to adapt them to oncology-oriented problems. Indeed, the study of the adenoviral infection cycle has provided substantial insight into nuclear transcription factors, cell death pathways, protein translation and cellular stress pathways. For instance, several viral proteins seem specifically designed to alter the function of known tumor suppressor genes such as p53, Rb1, BCL-2 and p21. For these reasons, it is my personal opinion that oncolytic virotherapy bypasses many limitations of single protein targeted tumor therapies since these viruses are actually evolutionarily driven for thousands of years to circumvent problems like pathway inhibitor resistance.

Chapter 6 focuses on the identification of compounds that enhance oncolytic virotherapy for malignant glioma in GSCs. Four compounds out of a library of over 450 individual agents were validated to significantly enhance Delta24-RGD therapy. These agents (Fluphenazine, Indirubin, Lofepramine and Ranolazine) interacted with either infection, viral progeny production and/or programmed cell death machinery significantly. All four compounds share a favorable toxicity profile, for which the FDA has approved these drugs for other indications than malignant glioma. In addition, these samples are known to pass the blood brain barrier, suggesting a high likelihood of intracranial dosing at an adequate concentration for therapeutic success. We demonstrated that the sensitization of cells to Delta24-RGD by combination treatment with these compounds is shared by oncolytic herpes virus and Newcastle Disease virus. Follow up studies are planned to reproduce this effect in animal models.

In chapter 7, it is demonstrated that Delta24-RGD administration can be enhanced by trafficking of cells within, or attached to, lymphocytes. Delta24-RGD is demonstrated to replicate within a T-cell-model and is effectively transferred to GSCs in vitro and in xenografts. In addition, these cellular vehicles were able to facilitate delivery of Delta24-RGD into invasive clusters of tumor cells. However, the distribution of cellular vehicles after systemic injection was limited to sporadic cells and therefore deserves further development of the concept. All in all, this chapter provides a proof of concept and feasibility for enhancing oncolytic adenoviral delivery by T-cells, which provides a window to combination therapy with autologous tumor targeted T-cells for adoptive immune therapy.

Chapter 8 focuses on two oncolytic reoviruses, which are assessed (and compared) for their ability to effectively infect, replicate and lyse a panel of GSCs. The results are illustrative for the potential of reovirus based oncolytic virotherapy as demonstrated by others in different models of GBM. Indeed, the oncolytic efficacy of reovirus in GSCs was shown to vary significantly between separate cultures, similar to Delta24-RGD as shown in chapter 6. This effect was not entirely dependent on the expression of known entry receptors, and furthermore, the ability of reovirus to kill tumor cells does not necessarily lead to a fruitful viral replication cycle. Indeed, the distribution of reovirus within spheroid bodies of GSCs was demonstrated to be heterogeneous as well, which suggests a role of tumor-specific induced matrix molecules that influences the ability of reovirus to disperse into the tumor core.

General conclusions and discussion

The following paragraphs will shed light on the questions addressed within this thesis. Since the main purpose of the thesis was to improve insight into (novel) therapeutic options for GBM, the evaluation of this thesis should be focused around this goal. As mentioned before in the introduction, we chose to investigate these novel therapeutic alternatives in the context of a novel patient derived model. The validation of this model is of pivotal concern to the later derived insight into the therapeutic strategies investigated with the model. As such, we will first discuss the improvements of limitations of scientific method derived through utilizing the GSC model.

The patient derived glioma stem cell model

The ability to selectively propagate patient derived tumor cells that are proposed to be the driving population of the tumor is a very attractive feature of the GSC model. Whether this selection is achieved through culture medium composition remains to be elucidated. As mentioned in chapter 4, the definitive markers for specific isolation of glioma stem cells remain to be identified. Therefore, it remains a matter of definition, as to whether these cells are truly all glioma stem cells. The likelihood that out of millions of cells within the bulk of resection tissue, more than thousands of cells may truly be considered the initiating cells seems counterintuitive. The ability to discern the initiating cell may be of more fundamental (pathophysiological) importance than of direct therapeutic consequence. At the moment, no evidence exists of therapeutic consequences of directly targeting the stem cell compartment of a tumor apart from in vitro studies with cells derived from this same assay[1], which is a biased approach for multiple reasons such as the lack of definitive markers of bona fide glioma stem cells, the inability to reliably assess the viability of these cells within their specific microenvironment, and the inability to assess for therapeutic specificity for GSCs apart from other tumor cells.

The main (and in our opinion most urgent) incentive for us to work with this culture model is the ability to more adequately recapitulate molecular and histological traits of the disease (chapter 2). The following questions however remain open for debate with regard to the interpretation of GSC model derived data; 1) what is the driving molecular feature that differentiates between tumors that can and cannot be cultured under GSC-conditions? 2) How predictive of therapeutic response in humans are drug-screening data obtained through GSC models?

With regard to the first question, the data in this thesis are finger pointing towards the extracellular domain of the tumor cells for clues. Others have demonstrated the interaction between tumor cells and the surrounding stroma as pivotal to survival and proliferation[2]. It is reasonable to hypothesize that the extracellular cues that are required for cells to proliferate in vitro may differ between glial subgroups and therefore may dictate culture outcome. It remains to be determined which factors are crucial in the failure of the subgroup of tumors that remain a challenge to culture to date. Specifically the development of in vitro models for IDH mutant/ GCIMP tumors would have significant impact.

The second question has been touched upon to some extent by this thesis, but still remains to be prospectively addressed in parallel with a clinical trial. We, amongst others, have determined GSCs to adequately mirror TMZ response in vitro, retrospectively (chapter 3). However, this is just one therapeutic agent, while the future may be dictated by combination therapies, based on molecular testing of multiple parameters acquired from surgical sampling. With respect to intratumoral heterogeneity, and inter-individual heterogeneity, it is hard to imagine that future clinical decision-making on chemotherapeutic dosing will be based on preclinical data derived from cell lines that are not derived from the same patient. To have a predictive in vitro screening tool will be paramount, and prospective studies will deliver the final answer to this question.

Oncolytic virotherapy and GSCs

The aforementioned concerns on GSCs are equally vital to OV as to any other therapeutic agent. In addition, the use of viruses for the treatment of diseases remains a brow-raising strategy to many clinicians and researchers to date. Especially when the viruses are not genetically manipulated to be replication deficient. The safety-concerns with regard to local or systemic infection resulting in significant adverse events have to date not been justified in toxicity studies[3, 4]. However, long-term effects have not been studied, although this concern is of less relevance to GBM patients.

Fortunately we have found the GSC model to work conveniently with the testing of the OVs Delta24-RGD (chapter 6), reovirus (chapter 7), NDV (chapter 6) and herpes simplex virus (chapter 6). It was demonstrated that individual cultures harbor a unique response profile to OVs, which was dependent on known mechanisms (e.g. the expression of cell-surface receptors that are known to facillitate viral entry) and more elusive mechanisms that should be the focus of future studies. These results are congruent with multiple publications on other OVs. These individual GSCs response profiles can be tackled by combination therapy (such as viral sensitizers identified in chapter 6), or the genetic manipulation of the OV (as discussed in chapter 5 and demonstrated in chapter 7 for reovirus). The major hurdles for OV in the coming decades will be similar to other compounds with regard to patient selection and toxicity studies. In this respect, the testing of OV on GSCs is convenient and repro-

ducible and could therefore provide leads into patient selection, methods of resistance and how to bypass these hurdles through combination therapy.

Future studies are expected to shed significant light on the immune response to OVs and therefore the GSC model is more or less redundant since patient derived material can only be grafted into immune compromised animals. To take this problem into account, one could possibly imagine the application of fundamental research into the pathophysiology of malignant glioma subtypes and reconstitute glioma subtypes by driver gene editing through novel gene-manipulation methods such as the CRISPR system[5]. Another approach may be the use of humanized mouse models[8]. In conclusion, this thesis has provided the opportunity to further investigate viral sensitizers that are expected to broaden the therapeutic response in GBM patients when compared to mono-therapy.

Oncolytic virotherapy administration

A separate hurdle for OV remains the administration of the virus, for which multiple strategies have been explored in the past. In this thesis one chapter was designed to address the ability of Delta24-RGD to be packaged and delivered within cellular vehicles, as a molecular version of a Trojan horse. This strategy was found to be effective locally (by intracranial administration) and to lesser degree systemically. As a proof of concept study, the ability to deliver oncolytic adenovirus by packaging in a model of T-cells could provide a so-called double-edged sword. For one, OVs are able to replicate and burst, which results in a local amplification of Delta24-RGD within the tumor. In addition, T-cells can be manipulated to boost the immune response to tumor antigens, as well as provide a cytolytic function to tumor cells in parallel of the OV. Furthermore, the ability to deliver these cells systemically through a venous/central line makes repeated administration possible which significantly limits the invasiveness of the treatment. Obviously, this could also boost the process of clinical validation of these OVs. Similar studies have been undertaken with reovirus, vesicular stomatitis virus, varicella viruses and measles[6, 7]. In conclusion, the presented data has opened a window for more studies into the systemic administration of OVs in combination with immune modulating strategies. In the end, this strategy may capitalize on the ability of both therapies to induce a lasting anti-tumor response against the individual patients' specific tumor antigens.

The author's future perspectives

As a neurosurgery resident in a large academic center, brain tumors will remain a significant portion of my daily practice. While neurosurgery is not likely to provide a definitive cure to malignant glioma, the first strike against the disease by adequate decompression, representative tissue biopsies and most importantly achieving this without the induction of new neurological deficits, puts the neurosurgeon in the front seat to drive the outcome of glioma patients. The neurosurgeon is in the unique position to experience the three-dimensional structure of malignant glioma in situ. This renders neurosurgeons with an opportunity to hypothesis generation for scientific research. In line with this, together with physicians from multiple specialties, a shared responsibility exists towards patients to push the limits with respect to optimal treatment under safe circumstances while inquiring for options to always improve current standards.

In the end, I foresee that malignant glioma patients will, similar to other solid tumors, capitalize on the enhanced treatment options provided by the scientific community. Based on the little steps that have been made in the last decades, in spite of large efforts, it is also anticipated that fundamental, translational and clinical research into this disease will remain a humbling experience. In the near future, patient trials will probably be stratified based on driving molecular features, combined with upfront laboratory tests on samples gathered through surgery and routine blood samples in advance to adjuvant therapy. As a result of this, the identification of the best drug for the specific individual will potentially lead to durable response and most importantly the circumvention of off-target treatment with possibly preventable adverse effects. In line with that, routine MRI imaging months after the initiation of therapy to inquire for therapeutic response is likely to be replaced by synchronous imaging and blood assessment of markers that implicate local therapeutic efficacy. Similar to this, it is feasible to predict the undertaking of clinical trials that will investigate the impact of gross total versus subtotal resection in certain cases (for instance IDH and/or 1p19q altered low grades) that may warrant safety to prevail instead of maximal debulking since adjuvant therapy could be able to provide a durable stable disease condition, a situation that already exists for the treatment of medulloblastoma.

In anticipation of these significant steps that are foreseeable in the near future, the end of this thesis should at least conclude the following: although the body of the thesis delivers answers to previously generated hypothesis, as with all scientific progress the end result is new hypothesis generation and the humble conclusion that all our work remains ahead of us.

Samenvatting en conclusies proefschrift

Het maligne glioom zal de komende decennia een catastrofale diagnose voor patiënten en significante uitdaging voor de betrokken artsen blijven. Terwijl de klinische vooruitzichten voor patiënten met andere solide tumoren, zoals borst- of prostaatkanker, behoorlijk verbeterd zijn de afgelopen decennia (waarbij zelfs een subgroep genezen of chronisch in remissie kan verblijven), blijft dit voor patiënten met een kwaadaardige hersentumor een vergezicht.

Dit proefschrift onderzocht potentiele therapeutische behandelingen voor het maligne glioom in de context van een nieuw in vitro modelsysteem van deze ziekte. Er werden meerdere strategieën verkend voor het combinatie-effect met de huidige standard chemotherapie (TMZ) ofwel een alternatieve behandeling genaamd Delta24-RGD (virotherapie). De volgende alinea's zullen de belangrijkste bevindingen samenvatten, gevolgd door een beschouwing van de auteur met betrekking tot de toekomstperspectieven van de behandelde onderwerpen.

In hoofdstuk 2 werd er op prospectieve wijze onderzoek gedaan naar de distributie van moleculaire afwijkingen in het genoom en transcriptoom van patiënten plus de van hen verkregen in vitro Gliomen-Stam-Celkweken (GSCs). Er werd geconstateerd dat het GSC model een goede representatie waarborgt van de moleculaire afwijkingen als gevonden in de patiënt. Echter, het lijkt erop dat niet iedere patiënt zijn tumor zich leent voor propagatie middels deze kweekmethode. Tevens blijkt er een verrijking plaats te vinden voor tumoren met een bepaalde genetische constitutie welke gekenmerkt wordt door chromosoom 7p amplificaties en chromosoom 10q deleties. Verder valt op dat tumoren met een IDH mutatie niet langdurig in kweek gehouden kunnen worden. Qua transcriptoom werd er een verrijking voor het Classical subtype geconstateerd. Voorts werd er op basis van de eerdergenoemde resultaten het vermoeden aannemelijk gemaakt dat G-CIMP tumoren, bestaande uit een prognostisch relatief faveure subgroup, mogelijk niet binnen dit model kweekbaar zijn. Dit is belangrijk omdat G-CIMP/IDH1 tumoren een belangrijke overlap hebben, en deze tumoren voornamelijk gediagnosticeerd worden bij patiënten die jongvolwassen zijn en een relatief goede prognose hebben.

In hoofdstuk 3 werd aangetoond dat het GSC-model zich praktisch goed leent voor het identificeren van response profielen voor het testen van combinatietherapie. Hierbij werd aangetoond dat het huidige gouden standard chemotherapeuticum (TMZ) een voorspelbaar respons profiel heeft in GSCs wanneer de expressie van het eiwit MGMT in acht wordt genomen. Dit is een wel bekend klinisch gegeven, wat ook maatgevend is voor de therapeutische respons in patiënten. Vervolgens werd aangetoond dat remming van PARP, een eiwit met een cruciale rol in de DNA-schade respons cascade, middels de stof ABT-888 (merknaam Veliparib) in een groot panel GSCs leidde tot een verruiming van het vermogen van deze beide stoffen om celdood te bewerkstelligen. Deze potentiering is specifiek interessant omdat het optreedt onafhankelijk van de a priori gevoeligheid van een GSC voor TMZ. Gezien het te verwachten is dat de standard adjuvante behandeling voor patiënten met een maligne glioom voorlopig zal blijven bestaan uit het geven van TMZ, is een additief zoals PARP een potentieel zeer welkome stof, mede gezien TMZ in de huidige setting niet bij iedere patiënt effectief is. Vervolgstudies zullen nodig zijn voor het vertalen van deze resultaten naar dier- en patiëntstudies. Hierbij zal ook specifieke aandacht nodig zijn voor biomarkers die therapeutisch effect kunnen vervolgen, zodat er gericht gedoseerd en gecombineerd kan worden op basis van het susceptibiliteitsspectrum van de individuele patiënt.

In hoofdstuk 4 vindt de lezer een literatuuroverzicht (review) van beschikbare publicaties waarbij gekeken is naar de moleculaire karakterisatie van GSCs. In lijn met de bevindingen in hoofdstuk 2, wordt er geconstateerd dat GSCs in het algemeen een correcte reflectie van het tumorprofiel blijken te hebben wanneer gekeken wordt naar het genoom, transcriptoom en epigenoom. Tevens worden er in dit review een aantal uitzonderingen op deze regel besproken, en wordt er dieper ingegaan op de consequenties van deze uitzonderingen op de interpretatie van de data verkregen middels dit model. Hierbij wordt de grote intratumorale heterogeniteit van mutaties, de variabele behandelingsrespons van individuele tumorcellen en de invloed van lokalisatie van tumorcellen binnen de tumorperiferie voor kweekbaarheid besproken. Er werd geconcludeerd dat er ruimte is voor vervolgstudies waarbij het wenselijk is deze knelpunten verder te verkennen voor oplossingen.

Hoofdstuk 5 voorziet de lezer van een vergelijkbare literatuurstudie echter ditmaal over oncolytische virotherapie. In dit hoofdstuk wordt de huidige stand van zaken omtrent adenovirus-gebaseerde virotherapie voor patiënten met een maligne glioom besproken. Oncolytische virotherapie is een interessante optie voor patiënten met een glioom om meerdere redenen. Allereerst is het mogelijk om met virussen selectief tumorcellen te infecteren (zonder gezond weefsel te beschadigen), hier therapeutische genen in tot expressie te brengen, en daarnaast door de infectie het (door de tumor actief gehinderde) immuunsysteem te reactiveren tegen de tumor. Verder kan er veel van virussen geleerd worden met betrekking tot het pathologisch functioneren van tumorcellen. Dezelfde machinerie die tumorcellen gebruiken om het immuunsysteem te ontwijken, de celdeling in het voordeel te gebruiken, en de grootschalige productie van eiwitten voor groei aan te jagen worden door het virus tijdens een infectie ook mis/gebruikt. In lijn met deze theorie zijn er in het verleden meerdere zogenaamde tumor-supressorgenen (eiwitten die als functie hebben het ontwikkelen van tumoren te voorkomen) ontdekt na het constateren van een adenoviraal interacterend eiwit (bijvoorbeeld p53, BCL-2, p21 en Rb). Het bestuderen van deze interacties kan ons derhalve aanwijzingen opleveren voor het gericht frustreren van deze mechanismen om tumorcellen te remmen/doden. Dit hoofdstuk geldt voorts als een introductie op de hoofdstukken die hierna volgen.

In hoofdstuk 6 wordt een drug-screening uitgevoerd ter identificatie van stoffen die oncolytische virotherapie effectiever maken. Hierbij wordt een grootschalige test uitgevoerd op GSCs met een medicatie-bank van 450 separate stoffen (door de Amerikaanse voedsel en medicijnen warendienst, FDA, gekeurde medicamenten) getest op een positieve interactie met Delta24-RGD. Uiteindelijk werden er 4 potentieel zeer interessante

stoffen gevonden, wetende Fluphenazine, Indirubine, Lofepramine en Ranolazine. Deze stoffen waren in staat om, via meerdere afzonderlijke mechanismen, Delta24-RGD als oncolytische virotherapie synergistisch te versterken. Tevens werd er aangetoond dat dit effect ook voor 2 andere virussen (Herpes Zoster en Newcastle Disease Virus) gold, en in kweekmodellen van 2 andere solide tumoren gereproduceerd kon worden. Vervolgstudies worden gepland in dieren om deze virusmodulerende stoffen te valideren.

In hoofdstuk 7, werd een bekende limitatie van virotherapie (distributie in bloedbaan en brein) geprobeerd te verhelpen door het virus (Delta24-RGD) verpakt in lymfocyten toe te dienen. Door gebruik te maken van een model voor T-cellen (Jurkats) konden buiten het lichaam geïnfecteerde cellen na injectie in het brein, of via de perifere bloedcirculatie, virus in de tumor brengen. Echter, het effect van deze strategie binnen de gebruikte methodiek was minder groot dan gehoopt. Deze studie toont evenwel de “principiële bruikbaarheid” van deze strategie voor adenovirus en lymfocyten, en kan derhalve worden gezien als een kans om op latere termijn oncolytische virotherapie te combineren met autologe gerichte t-celtherapie zoals al gebruikt wordt voor een aantal hematologische maligniteiten.

Hoofdstuk 8 heeft betrekking op het testen van de effectiviteit van twee oncolytische reovirussen, waarbij specifiek is gekeken naar infectiviteit, replicatie en lysis in een panel GSCs. Hierbij werd het eerder gevonden potentieel van reovirus voor de behandeling van gliomen (zoals in andere modellen) bevestigd in GSCs. Tevens werd er een belangrijke variatie in effectiviteit geconstateerd tussen verschillende GSCs, wat een reële reflectie zou kunnen zijn van de interindividuele heterogeniteit tussen patiënten voor deze virussen. Opvallend genoeg werd deze variatie niet veroorzaakt enkel door verschillen in zogenaamde intrede-receptoren die op de celwand aanwezig moeten zijn om infectie te faciliteren. Hierbij lijkt het derhalve dat infectie op zichzelf niet altijd leidt tot effectieve virusreplicatie en lysis. Verder bleek de mogelijkheid van het virus om te penetreren door tumor sferoïden variabel is tussen GSCs, wat suggereert dat er mogelijk een rol is weggelegd voor specifieke door de tumor uitgescheiden matrix moleculen ten aanzien van de verspreiding van het virus buiten de cel.

Discussie

In de volgende paragrafen zal dieper ingegaan worden op de hoofdvragen waarnaar onderzoek is gegaan in dit proefschrift. Het voornaamste doel van deze thesis is het verbeteren van de efficiëntie van behandelingsopties voor het maligne glioom, en derhalve zal de evaluatie van het proefschrift ook in het teken staan hiervan. Zoals genoemd in de introductie werd er met name onderzocht of het gebruik van een nieuw model voor deze ziekte, wetende zogenaamde glioma stam cellen ontleend aan de primaire tumor, een betere predictieve waarde zou kunnen hebben voor het effect van deze (nieuwe) medicijnen. Er werd dus validatie betracht, en vanuit deze validatie gekeken naar de eventuele verbetering die nieuwe middelen op de huidige standaardbehandeling zouden kunnen hebben. Gezien deze tweeledige opzet zullen we beide onderwerpen separaat, en in het licht van elkaar, bespreken in de volgende uiteenzetting.

Primaire patient-gederiveerde glioma stamcelkweken

De mogelijkheid om selectief tumor initiërende (en onderhoudende) cellen te kweken om hierop medicatie gevoeligheid te onderzoeken, is een van de grootste potentiele voordelen van het GSC-model. In dit proefschrift wordt onderschreven dat dit model voordelen heeft ten opzichte van de modellen die voorheen werden aangewend ten aanzien meerdere aspecten van het maligne glioom zowel op moleculair als histopathologisch niveau. Of de huidige constitutie van het kweekmedium werkelijk selectief stamcellen includeert in de kweken, en hierbij niet a priori een subgroep (IDH mutant) excludeert valt nog definitief te bewijzen. Anderszins moet nog aangetoond worden in prospectieve studies dat tumorstamcel gerichte therapie an sich zijn grote preklinische belofte voor patiënten in kan lossen[1].

Het voornaamste (en in mijn opinie meest urgente) doel voor onderzoekers werkende met dit model was het onderschrijven van de in vitro betrouwbaarheid van dit model om moleculaire diversiteit gevonden in individuele samples te bestuderen in kweken. De volgende kwesties staan echter nog open voor definitieve oplossingen en antwoorden; 1) Wat zijn de sturende moleculaire afwijkingen verantwoordelijk voor het wel of niet kweekbaar zijn van individuele tumoren? 2) Hoe voorspellend voor therapeutische respons in patiënten is het responseprofiel van medicatie getest op GSCs?

Met betrekking tot de eerste vraag; de data in dit proefschrift wijst richting het extracellulaire domein van de tumor, waar mogelijk aanwijzingen liggen met betrekking tot de vele eiwitten en receptoren die daar in samenspel de configuratie van de tumorcel binnen zijn niche organiseert. Meerdere studies hebben aangetoond dat deze interacties van groot belang zijn voor overleving en proliferatie van tumorcellen[2]. Het is goed voorstelbaar dat verschillende subgroepen van het glioom op variërende wijze afhankelijk zijn van lokaal beschikbare extracellulaire signalen die in meer of mindere mate aanwezig moeten zijn in het kweekmedium om gepropageerd te kunnen worden in vitro. Vervolgstudies zijn geïndiceerd om te onderzoeken waar wat deze kwestie betreft aanpassingen gedaan moeten worden om de IDHmutant/G-CIMP tumoren binnen het model te kunnen vatten.

Wat betreft de tweede kwestie is er in dit proefschrift enige progressie geboekt ten aanzien de voorspellende waarde van het GSC-model. Allereerst is er in hoofdstuk 3 aangetoond dat het biologisch substraat van TMZ-responseprofielen zoals gekend in patiënten door het GSC-model adequaat vertaald wordt in vitro. Echter, dit betreft slechts monotherapie, waarbij het in de lijn de verwachting ligt dat de toekomst gekenmerkt zal worden door combinatietherapieën, waarbij het aantonen van deze translationele vertaling door de meerdere variabelen die combinatietherapie inherent met zich meebrengt als gevolg moeilijker zal worden. Apart van laatstgenoemde rest dan nog het probleem dat intratumorale heterogeniteit een vertekend beeld kan geven medicatiegevoeligheid wanneer een tweede sample wellicht resistente cellen zou kunnen bevatten waar in

kweek de gevoelige cellen zijn gepropageerd. Om deze reden ligt het in de lijn der verwachting dat toekomstige trials enkel nog gebruik zullen maken van patiënt gederiveerde kweken (liefst meerdere samples) waarbij, na in vitro testen op responseprofiel, in klinische setting het therapeutisch effect middels biomarkers al gedurende de behandeling wordt geobjectiveerd. Om deze reden zal een robuust predictief model zoals het gebruikte GSC-model van groot belang zijn voor initiële screening voorafgaand aan geïndividualiseerde behandelingen.

Oncolytische virotherapie en GSCs

De eerdergenoemde knelpunten met betrekking tot GSCs zijn van gelijkwaardig belang voor het testen van virotherapie bij het maligne glioom. Bijkomend is het gebruik van een virus om een ziekte te behandelen op zichzelf, voor zowel medische geschoolden als het grote publiek, top op heden een enigszins verontrustende strategie. Dit geldt in het bijzonder voor virale vectoren die hun capaciteit om hun viraal genoom te repliceren en hiermee een (gelokaliseerde) infectie te bewerkstelligen, zoals de vectoren die in dit proefschrift werden aangewend. Het valt ten aanzien van deze terechte zorgen te vermelden dat toxiciteitstudies van meerdere oncolytische virussen voor hersentumoren tot dusver geen significante (levensbedreigende) bijwerkingen aan het licht hebben gebracht [3, 4]. Hoewel langetermijneffecten nog niet onderzocht zijn, hebben deze mogelijk in de nabije toekomst minder relevantie voor patiënten. Dit argument gaat echter niet op voor de medewerkers die met deze medicatie in contact komen.

Met betrekking tot de vragen geadresseerd in het proefschrift valt te vermelden dat het GSC-model praktisch zeer handzaam is gebleken voor het testen van OVs; Delta24-RGD (hoofdstuk 6), reovirus (hoofdstuk 7), NDV (hoofdstuk 6) en herpes simplex virus (hoofdstuk 6). Deze resultaten zijn vergelijkbaar met andere studies gepubliceerd met OV voor GBM. Net als voor andere medicijnen hebben individuele kweken een bijpassend responseprofiel wat afhankelijk blijkt te zijn van verschillende variabelen. Interessant is dat hierbij meerdere combinatiestrategieën de effectiviteit van OV kunnen verbreden (in de populatie) en verstevigen (op individueel niveau). De significante hordes die OV de komende decaden zal nemen zijn georiënteerd rondom patiënten selectie en (langere) toxiciteitsstudies. Hierbij zou het GSC-model een rol kunnen spelen.

Toekomstige studies zullen naar verwachtingen de interacties van OV met het immuun systeem beter adresseren. Hierbij is het GSC-model minder aantrekkelijk omdat de cellen die men hierbij gebruikt doorgaans exclusief gebruikt kunnen worden in immuun gecompromitteerde proefdieren. Een oplossing van dit probleem zou kunnen worden gevonden in selectieve gen manipulatie strategieën om de ontstaanswijze van het maligne glioom te kopiëren in diermodellen middels het CRISPR systeem [5]. Ook het gebruik van gehumaniseerde muizen (m.b.t het immuunsysteem) zou een oplossing kunnen blijken.

Tot slot valt te concluderen dat dit proefschrift meerdere kansen heeft benut en opgeleverd om het gebruik van combinatie strategieën om OV te potentiëren voor de behandeling van het maligne glioom.

Toediening van oncolytische virotherapie

Een extra horde voor OV blijft de toediening van vectoren, in het bijzonder bij adenovirus. In dit proefschrift werd hier in het bijzonder aandacht aan besteed in hoofdstuk 7. Hierbij werd middels het gebruik van T-cellen de vector Delta24-RGD verpakt en zowel lokaal als systemisch toegediend in muizen met een maligne glioom in cerebro. Dit bleek in beide gevallen effectief (alhoewel systemisch in mindere mate). Als bewijs van "principiële bruikbaarheid" kan deze strategie op zichzelf een gecombineerde behandeling betekenen. Enerzijds werkt het virus op zijn gekende wijze door selectief tumorcellen te infecteren en te presenteren voor het immuunsysteem. Tegelijkertijd worden de noodzakelijke effector lymfocyten zelf gebruikt als de bezorgmedewerkers om de virussen ter plekke te verkrijgen. Hierdoor vergoot men wellicht de immuunrespons ter plekke. Het primaire doel, herhaalde toediening waarbij het virus niet opgemerkt wordt door het immuunsysteem tot het via de bloedbaan in de tumor wordt afgeleverd, is an sich al een grote stap vooruit. Vervolgstudies zullen aandacht schenken aan de optimale tijdspanne, verhoudingen in virus incubatie van de T-cellen en targeting van lymfocyten richting specifieke receptoren die de tumor herbergt ter herkenning. Er zijn vergelijkbare studies gepubliceerd waarbij deze strategie voor andere virale vectoren effect sorteert in meerdere vormen van kanker[6, 7]. Concluderend kan gesteld worden dat de gepresenteerde data kansen biedt voor vervolgstudies naar deze behandelingsstrategie in patiënten, zodra het effect van Delta24-RGD middels lokale therapie verder ontwikkeld is.

De auteurs toekomstperspectief

Als neurochirurg in opleiding in een groot academisch centrum blijft de behandeling van patiënten met een maligne hersentumor deel van mijn dagelijkse praktijk. Alhoewel curatie van het maligne glioom niet middels een chirurgische interventie mogelijk zal blijken, is het wel degelijk de neurochirurg die aanvankelijk een belangrijke rol speelt in de behandeling van de patiënt. De eerste klap lijkt ook in de context gliomen wel degelijk een daalder waard te zijn met betrekking tot adequate weefseldiagnose en, zo mogelijk, een zo ruim mogelijke decompressie van de tumor. Beide bepalen het verdere behandelplan en mogelijk het eventuele effect van dit plan. Gezien het belang van het testen van patiëntmateriaal staat de neurochirurg in het middelpunt van hypothesegeneratie in een unieke positie. In de multidisciplinaire behandeling van patiënten met een maligne glioom in de 21ste eeuw is derhalve (nog steeds) een rol van importantie weggelegd voor de neurochirurg.

Er valt te voorzien dat patiënten de komende decaden de vruchten zullen plukken van de toegenomen kennis van de moleculaire constitutie van deze ziekte. Op die manier zal de klinische vooruitgang zoals geboekt bij andere maligniteiten ook bij gliomen gezien worden. Op basis van de kleine stapjes zoals gemaakt in de laatste jaren, ondanks de grote financiële en immateriële investeringen, zal deze tak van wetenschap de onderzoeker nederig houden ten aanzien van de grote stappen die nog te maken zijn voor onze patiënten.

Ik verwacht dat binnen afzienbare tijd patiënten trials zullen includeren en stratificeren op basis van moleculaire markers, in combinatie met responseprofielen verkregen uit laboratorium onderzoek op patiëntmateriaal. Therapeutisch effect zal geobjectiveerd worden tijdens de behandeling middels beeldvorming en bloedtesten. Als gevolg zal de beste behandeling, met zo min mogelijk bijwerkingen, snel te identificeren blijken wat een enorme vooruitgang op meerdere niveaus zal blijken (zowel qua effectiviteit als kosten).

In anticipatie op deze vooruitzichten valt naar aanleiding van dit proefschrift te concluderen dat, na weer een aantal kleine stappen vooruit, er nog significante inspanningen noodzakelijk zullen blijken om het perspectief voor onze patiënten te verbeteren.

References

1. Lathia, J.D., et al., Cancer stem cells in glioblastoma. Genes Dev, 2015. 29(12): p. 1203-17.

2. Cooper, L.A., et al., The tumor microenvironment strongly impacts master transcriptional regulators and gene expression class of glioblastoma. Am J Pathol, 2012. 180(5): p. 2108-19.

3. Piccioni, D.E. and S. Kesari, Clinical trials of viral therapy for malignant gliomas. Expert Rev Anticancer Ther, 2013. 13(11): p. 1297-305.

4. Parker, J.N., et al., Oncolytic viral therapy of malignant glioma. Neurotherapeutics, 2009. 6(3): p. 558-69.

5. Kim, H. and J.S. Kim, A guide to genome engineering with programmable nucleases. Nat Rev Genet, 2014. 15(5): p. 321-34.

6. Russell, S.J. and K.W. Peng, The utility of cells as vehicles for oncolytic virus therapies. Curr Opin Mol Ther, 2008. 10(4): p. 380-6.

7. Kranzler, J., et al., Stem cells as delivery vehicles for oncolytic adenoviral virotherapy. Curr Gene Ther, 2009. 9(5): p. 389-95.

8. Ito, R.; Takahashi, T.; Katano, I.; Ito, M. (2012). "Current advances in humanized mouse models". Cellular & molecular immunology 9 (3): 208–214. doi:10.1038/cmi.2012.2.

10

PhD Profile
Curriculum vitae

Phd Profile

Rutger K Balvers,

Dept. of Neurosurgery, Brain Tumor Center, Erasmus Medical Center Rotterdam

Phd School; Molecular Medicine Post-graduate School (MolMed)

	Activity	Year	Workload (ECTS)
Courses/Seminars/ Workshops			
	Animal handling and ethics (Art.14) (NL)	2008	1
	Animal handling and ethics (Art.14) (USA)	2011	1
	Molmed Partek course	2011	1.3
	Molmed In Vivo Imaging course	2010	1.8
	Departmental Lab-meetings / Journal Clubs >20, incl. >5 oral presentations in NL/USA	2009-2013	4
	Molmed Conference (posters)	2010-2011	0.6
International Conferences	SNO (posters)	2010	1
	SNO (posters)	2012	1
	EANO (posters)	2010	1
	EANO (oral/posters)	2012	2
	OVT (posters)	2011	1
Teaching			
	Gene therapy Course for medical students	2009/2010	1
	Animal Bioluminescence Imaging for Molmed Master students	2011	1
	Supervising Molmed and medicine master students	2009/2010	8
Organizing skills / Grants			
	LWNO-i secterary	2012-2013	3
	Stop hersentumoren resource grant (incucyte FLR)	2010	2
	Travel grants (KWF / Rene Vogels Stichting)	2012	2

Curriculum Vitae

Rutger K. Balvers was born in Rotterdam, the Netherlands, on June 28th, 1983. He completed secondary education (Atheneum) in 2001 at the Sint-Laurenscollege in Rotterdam. In 2001, he started studying Biomedical Sciences at the Free University (VU) Amsterdam. In 2003 he enrolled into medical school at the Erasmus University Rotterdam. During his medical studies he successfully obtained a research masters degree in Neuroscience in the group of prof. Chris de Zeeuw. He graduated on the thesis " Intra-operative mapping of functional cortical regions during awake low grade glioma surgery" in 2008. Directly after completing his research masters in neuroscience and clinical masters in medicine, in the autumn of 2008, he started his PhD studies at the dept. of Neurosurgery at the Erasmus MC Rotterdam. In 2011 he travelled to Houston as a research fellow to join the Brain Tumor Center at the MD Anderson Cancer Center. Here he investigated the role of cell death pathways in adenovirus mediated oncolysis under the guidance of Juan Fueyo. After this fellowship he returned to the Erasmus MC to complete his clinical rotations in order to successfully obtain his medical degree in 2013. The same year he started his residency in Neurosurgery at the Erasmus Medical Center. At the time of completing this thesis he is happily engaged with his future spouse, Emma Jane, with whom he has a son named Ezra. The family happily resides in The Hague.

Author Publications

1. Eva Klijn · Hester C Hulscher · Rutger K Balvers · Wim P J Holland · Jan Bakker · Arnaud J P E Vincent · Clemens M F Dirven · Can Ince*Laser speckle imaging identification of increases in cortical microcirculatory blood flow induced by motor activity during awake craniotomy*. J Neurosurg, 2013. 118(2): p. 280-6.

2. Linda B C Bralten · Nanne K Kloosterhof · Rutger Balvers · Andrea Sacchetti · Lariesa Lapre · Martine Lamfers · Sieger Leenstra · Hugo de Jonge · Johan M Kros · Erwin E W Jansen · Eduard A Struys · Cornelis Jakobs · Gajja S Salomons · Sander H Diks · Maikel Peppelenbosch · Andreas Kremer · Casper C Hoogenraad · Peter A E Sillevis Smitt · Pim J French*IDH1 R132H decreases proliferation of glioma cell lines in vitro and in vivo.* Ann Neurol, 2011. 69(3): p. 455-63.

3. Rutger Balvers · Hong Jiang · Sujan Piya · Candelaria Gomez-Manzano. Juan Fueyo *Adenovirus, autophagy and lysis: ecstasies and agonies.* Future Virology 10/2011; 6(10):1161-1164. DOI:10.2217/fvl.11.93

4. Rutger K. Balvers, Zineb Belcaid, Sanne K. van den Hengel, Jenneke Kloezeman, Jeroen de Vrij, Hiroaki Wakimoto, Rob C. Hoeben, Reno Debets, Sieger Leenstra, Clemens Dirven and Martine L.M. Lamfers *Locally-delivered T-cell-derived cellular vehicles efficiently track and deliver adenovirus delta24-RGD to infiltrating glioma.* Viruses, 2014. 6(8): p. 3080-96.

5. Rutger K. Balvers, Anne Kleijn, Jenneke J. Kloezeman, Pim J. French, Andreas Kremer, Martin J. van den Bent, Clemens M. F. Dirven, Sieger Leenstra and Martine L. M. Lamfers, *Serum-free culture success of glial tumors is related to specific molecular profiles and expression of extracellular matrix-associated gene modules.* Neuro Oncol, 2013. 15(12): p. 1684-95.

6. SK van den Hengel, RK Balvers, IJC Dautzenberg, DJM van den Wollenberg, JJ Kloezeman, ML Lamfers, PAE Sillivis-Smit and RC Hoeben, *Heterogeneous reovirus susceptibility in human glioblastoma stem-like cell cultures.* Cancer Gene Ther, 2013. 20(9): p. 507-13.

7. Rutger Balvers, Candelaria Gomez-Manzano, Hong Jiang, Sujan Piya, Sarah R. Klein, Martine L.M. Lamfers, Clemens M.F. Dirven, Juan Fueyo: *Advances in Oncolytic Virotherapy for Brain Tumors.* Gene Therapy of Cancer, 3rd edited by E.C. Lattime, S.L. Gerson, 01/2014: chapter 10: pages 137-151; Elsevier., ISBN: 978-0-12-394295-1

8. Rutger K Balvers, Martine LM Lamfers, Jenneke J Kloezeman, Anne Kleijn, Lotte ME Berghauser Pont, Clemens MF Dirven and Sieger Leenstra, *ABT-888 enhances cytotoxic effects of temozolomide independent of MGMT status in serum free cultured glioma cells.* J Transl Med, 2015. 13: p. 74.

9. Lotte M.E. Berghauser Pont, Rutger K. Balvers, Jenneke J. Kloezeman, Michal O. Nowicki, Wouter van den Bossche, Andreas Kremer, Hiroaki Wakimoto, Bernadette G. van den Hoogen, Sieger Leenstra, Clemens M.F. Dirven, E. Antonio Chiocca, Sean E. Lawler, Martine L.M. Lamfers ; *In vitro screening of clinical drugs identifies sensitizers of oncolytic viral therapy in glioblastoma stem-like cells.* Gene therapy, 07/2015; DOI:10.1038/gt.2015.72

10. Rutger K Balvers, Clemens MF Dirven, Sieger Leenstra and Martine LM Lamfers *Malignant glioma in vitro models: on the utilization of stem-like cells and the recapitulation of molecular subtypes.* Current Cancer Drug Therapeutics; Glioblastoma Multiforme (accepted for publication)

Dankwoord / Acknowledgements

Als je begint aan een promotietraject en andermans thesis zo nu en dan onder ogen krijgt, heb je bepaalde voorstellingen over het schrijven van een dankwoord na een waanzinnige periode (jaartje of 3-4) waarin je het onderwerp van jouw thesis wetenschappelijk volledig op zijn kop hebt gezet met je publicaties, presentaties en discussies. Bijna 7 (!) jaar later na; vreselijk veel geleerd te hebben, veel plekken gezien te hebben, en meer meegemaakt te hebben dan in de 25 jaar ervoor (bij wijze van spreken), kan ik nu me maar moeilijk voorstellen dat de komende 2-3 pagina's mijn dank en waardering aan de onderstaande mensen daadwerkelijk recht zullen doen. Hoe dan ook ga ik een poging wagen.

Allereerst wil ik via deze weg, omdat het op schrift toch ook iets tastbaars is en blijft, mijn waardering en dank uitspreken voor (en naar) mijn overleden vader. Het gemis wordt er nooit minder op, de waardering (voor alles) alleen maar meer.

Prof.dr. Dirven, Beste Clemens; als promotor, hoogleraar en afdelingshoofd ben ik jou ontzettend veel dank verschuldigd. Ik kan me als jonge wetenschapper en arts geen betere omgeving wensen dan degene die jij voor ons in het lab en op de afdeling hebt georkestreerd. Heel veel dank voor alle mogelijkheden die je mij tot dusver hebt gegund.

Prof.dr. Leenstra, Beste Sieger, dank voor de bergen aan onmisbare input, plus de originele en nuancerende beschouwingen van de neuro-oncologie. Ook je (niet zeldzame) correcties van mijn hoogdravende schrijfwijzen werpen inmiddels min of meer reflexmatig bij mij hun vruchten af wanneer ik weer in de pen klim. (Ik vermoed dat je deze zin ook al over het randje zal vinden). Het is bewonderenswaardig met hoeveel toewijding je Tilburg, Rotterdam en het vele reizen tussen deze twee plaatsen al die tijd bolwerkt. Ik kijk ernaar uit over enkele jaren zelf dagelijks naar Tilburg te forenzen.

Dr. Lamfers, Beste Martine; waar te beginnen? Als copromotor ben je wat mij betreft de stuwende kracht achter het leeuwendeel van dit proefschrift geweest. Dank voor alle feedback (honderden emails, vele werkbesprekingen, koffiebreaks, metroritten etc etc). Dank voor de ruimte om af en toe een zijspoor te kunnen nemen. Ik heb er ontzettend veel van geleerd om onder jouw hoede te mogen werken. Heel veel geluk en gezondheid gewenst voor jou en je 4 helden.

De leescommissie;

Prof.dr. Sillevis Smitt; dank voor de plezierige samenwerking zowel binnen het Hersentumorcentrum als tijdens mijn neurologie stage. Hartelijk dank voor het beoordelen van deze thesis.

Prof.dr. Van der Spek; hartelijk dank voor de input en goede gesprekken ten aanzien van de thesis en een eventueel vervolg.

Prof.dr. Kros; Dank voor de goede gesprekken, goede raad en de altijd open deur. Hartelijk dank voor uw deelname in mijn leescommissie.

De data in deze thesis is grotendeels ontstaan vanuit experimenten met restweefsel van patienten. Het is niet triviaal of banaal stil te staan bij het feit dat wij als wetenschappers, en als toekomstige patienten, van wat voor medisch probleem dan ook, schatplichtig zijn aan talloze mensen die zich belangenloos voor wetenschappelijk onderzoek willen inzetten op wat voor manier dan ook. Hetzelfde geldt voor de mogelijkheid om dier experimenteel onderzoek te doen. Het feit dat wij als NLse samenleving het huidige klimaat hanteren met betrekking tot bovengenoemde peilers van deze beschaving kan niet vaak genoeg onderstreept worden als groot gemeengoed. Dank hiervoor.

Collega's van het lab neurochirurgie;

Jenneke, Anne, Lotte, Mariëlle, Jan Willem, Zineb, Mani, Wouter. Hartelijk dank voor de vele avonturen in binnen en buitenland maar vooral op de 22ste. Toen ik begon was er nog niet zoveel (in het JNI te gast bij de neurologie), nu ik weg ben beginnen we net lekker op stoom te komen. Go figure! In alle serieusheid wens ik jullie allen het allerbeste in privé- en carrièresfeer. Heb een hoop van jullie geleerd, al kennen jullie mij natuurlijk vooral als iemand die het zelf goed denkt te weten.

Collega's uit Leiden;

Prof. Hoeben: dank voor uw deelname aan de oppositie tijdens mijn verdediging. Nog meer dank voor de goede samenwerking tussen Rotterdam en Leiden en de inspirerende werkbesprekingen.

Sanne van den Hengel dank voor de goede samenwerking in Leiden en Rotterdam. Niet alles is uiteindelijk even goed gelukt voor ons beider promotietraject, maar dat maakt het niet minder waardevol. Heel veel succes met je verdediging binnenkort! **Jeroen de Vrij:** eigenlijk collega uit overal; Leiden, Rotterdam, Utrecht en nu weer Rotterdam! Dank voor je hulp bij de virusproeven, sparren voor de juiste opzet en de goede gesprekken over weetiknietwatallemaal. Het allerbeste bij de NEMO en vanzelfsprekend veel gezondheid voor je jonge gezin!

Collega's van het hersentumorcentrum:

Pim French, altijd in voor een scherpe discussie over waar het nou heen gaat/moet in Gliomenland. Dank voor alle hulp en input.

Prof.dr. Martin van den Bent: beste Martin, veel dank voor de input tijdens vele werkbesprekingen!

Lonneke en Linda; Blijft leuk elkaar nog steeds op vrij frequente basis te treffen in de kliniek, altijd goede gesprekken. Cheers op de goede herinneringen in het Nefkens!

Collega's van de afdeling neurochirurgie;

Alle stafleden, en in het bijzonder **Arnaud Vincent en Joost Schouten**, voor het beschikbaar stellen van potentieel kweekweefsel.

Alle assistenten van de afdeling neurochirurgie; **Hazem, Elianne, Jochem, Lesley, Eelke, Victor, Herjan en Anne. Dafna en Nadine**. Ik had 7 jaar geleden niet gedacht dat ik dit nu zou schrijven maar ik meen oprecht dat wij het mooiste beroep hebben wat je maar kunt wensen. Iedere dag ga ik benieuwd naar het EMC. Een groter voorrecht kan ik me niet wensen. Dit alles voor een groot deel ook dankzij jullie!

Alle **operatieassistenten** (ik noem expres geen namen want het zijn er zoveel) van OK-zuid en SKZ ben ik veel dank verschuldigd voor de logistieke hulp bij inzamelen van kweekmateriaal en zeker tegenwoordig in de hulp en bereidwilligheid een jonge assistent op weg te helpen.

De afdeling Neurochirurgie in het **Elizabeth Ziekenhuis Tilburg** voor het beschikbaar stellen van weefsel en helpen met de logistiek om deze samples in Rotterdam beschikbaar te krijgen.

Fueyo lab and MD Anderson Brain Tumor Center friends;

Juan, Cande, Helen, Sujan, Belayat, Nahir, Sarah, Konrad, Joy, Felix and Tal. It has been such an invaluable experience to have been visiting Houston. When I went, I could not have imagined how profound (and lasting) an impression you guys, and the whole of MD Anderson, would leave on me. I cherish having been able to learn from all of you.

Vrienden van Erasmus Anatomy Research Project; **Gert Jan Kleinrensink, Hilco Theeuwes, Jan Willem Potters, Jan Willem Dijk, Joost ten Brinke, Joris Harlaar.**

Paranimfen

John Soria van Hoeve: Vriend! Altijd daar! Niks dan respect! De wereld en nog een stuk!

Mario de Jonge; Vriend! Dank voor de wederdienst :) Vraag me af wie ons destijds in de Kempenaarstraat ervan zou kunnen hebben overtuigen dat een promotietraject (laat staan de wetenschap) iets voor ons zou zijn. Nee, we komen niet uit een ei.

Vrienden!

Gerard, Guido, Remko, Olivier, Jochem, Han, Joost, Roel, Onno, Chris, Dieuwer, Eef, Lot, Kim, Tim, Hanna en iedereen die hier zeker ook tussen hoort maar me nu niet te binnen schiet ; ook al zien we elkaar steeds minder doordat we allemaal "ergens heen moeten" jullie zitten allemaal in mijn hoofd en ik gun jullie de wereld!

Joel en Clara Shapiro; niks dan liefde en dank voor alle gezelligheid, wijsheid en blijheid!. Veel gezondheid en geluk gewenst voor jullie gezin en (extended) fam!!

Veel dank aan mijn schoonfamilies; **Marie Sophie en Joscha, Reinier en Anne Kee, Anne Irene, Koos en Anneke, Jaap en Yvonne**. Het is altijd een feest om langs te komen en met jullie bij te praten. Dank voor de steun en gezelligheid door de jaren heen.

Ruud, Jolise, Sweder en Witte: veel dank voor de gezelligheid, de opbeurende gesprekken en de fijne tijden in Zeeland. Een significant deel van dit boek is in Noordwelle geboren!

Evalien en Dick: heel veel dank voor alle hulp en gezeliigheid door de jaren heen in Delft, Delfgauw en waar niet allemaal nog meer. Heel veel gezondheid en geluk gewenst.

Vafeas Family:

Nan and Costas; Thank you so much for all the fun and enlightening trips in and around FL. We love being around and love to see you over here in NL. So many memories. **Dimitri, Nancy, Neil and Tracy;** we wish you all the health and joy in the world! Thank you for all the golden moments over in Sarasota.

Mijn familie

Thannée; dank voor al je hulp de afgelopen jaren. Ik ben heel trots op je. Daan vanzelfsprekend ook bedankt voor alle hulp. Voor je het weet zitten we in San Gimignano.

Mama; al mijn respect en bewondering voor hoe je jezelf de afgelopen jaren herpakt hebt. Namens mijn gezin: we houden allemaal ontzettend van je en zijn je nog dankbaarder voor al je onmisbare hulp.

Emma Jane en Ezra: lieve Emma jij bent van Mijendel tot MD Anderson altijd mijn referentiepunt, bron van relativering, geruststelling en ontspanning geweest. Dank voor al je geduld, begrip en vermogen om soms toch ook een *lichtpunt* te kunnen benoemen in gebeurtenissen die ik enkel als zwart herken. Samen komen we er altijd wel uit. Lieve Ezra; op en dag gaan we voor dit boek zitten. Tot die tijd lezen we alles van Winnie de Pooh tot Asterix tot de GVR tot wat je maar wilt, want wie leest die komt verder in de wereld. Veel liefs, papa!